CAST-METAL RESIN BONDED BRIDGES:

A LABORATORY AND CLINICAL STUDY

This thesis, based on an original study by the author,
is submitted to the University of Sydney in fulfilment
of the requirements for
the degree of Master of Dental Surgery

UNIVERSITY
OF SYDNEY
DENTAL LIBRARY

DAVID SYKES
B.D.S.(London), L.D.S., R.C.S.(Eng.), F.R.A.C.D.S.

Presented in two volumes

Volume II

November 1986

TABLE OF CONTENTS

	Page
Table of contents	ii
Tables	2 - 25
Figures	27 - 190

The tables are placed in consecutive order
from Table 3.1
to Table 10.9

The figures are placed in consecutive order
from Figure 2.1
to Figure 11.2

TABLES

TABLE 3.1

Tensile bond strengths of some resin materials to acid-etched enamel

Resin type	Tensile bond strength (MPa)	
Direct filling resin*	2.5	(Lee et al, 1971)
	1.8	(Muira et al, 1971)
Composite resin	13.9	(Short et al, 1976)
	16.9	(Soetopo et al, 1978)
Modified acrylic resin	3.9	(Muira et al, 1971)
	4.3	(Faust et al, 1978)
Epoxy resin	8.0	(Retief, 1974b)

* Methyl methacrylate based resin.

TABLE 4.1

Electrolytic etching conditions for various nickel–chromium and cobalt–chromium prosthodontic alloys

Alloy	Conditions
Etching conditions for Ni–Cr–Be alloys	
Rexillium III [i]	10% H_2SO_4 — 300 mA/cm^2 - 3 min
Bak-On NP [ii]	10% H_2SO_4 — 300 mA/cm^2 - 3 min
Litecast B [iii]	10% H_2SO_4 + Methanol 9:1 — 200 mA/cm^2 - 6 min
Unitbond [iv]	10% H_2SO_4 — 300 mA/cm^2 - 3 min
Ticonium 100 [v]	10% H_2SO_4 — 300 mA/cm^2 - 5 min
Etching conditions for Ni–Cr alloys	
Biobond C & B [vi]	0.5 N HNO_3 — 250 mA/cm^2 - 5 min
Microbond NP^2 [vi]	0.1 HNO_3 + 2% glacial acetic acid — 400 mA/cm^2 - 5 min (Pretreat with 5% NH_4OH in ultrasonic bath for 5 min)
Etching conditions for Co–Cr alloys	
Biocast [i]	0.5 N HNO_3 — 250 mA/cm^2 - 5 min
Cobond [vi]	36% HCL:Me OH (4:6) — 300 mA/cm^2 - 2 min then 100 mA/cm^2 - 7 min (samples rinsed in tap water after etching)
Vitallium [vii]	18% HCL — 400 mA/cm^2 - 10 min

All alloys cleaned in 18% HCL following etching

---

i Jeneric Industries, Wallingford, Connecticut, USA
ii Johnson and Johnson, East Brunswick, New Jersey, USA
iii Williams Gold Co, Buffalo, New York, USA
iv Jensen Industries, New Haven, New York, USA
v Ticonium Inc, Albany, New York, USA
vi Dentsply, York, Pennsylvania, USA
vii Howmedica Inc, Chicago, Illinois, USA

Table 4.1: adapted from Simonsen et al (1983) and Thompson (1985)

TABLE 4.2

Tensile bond strengths of various electrolytically etched nickel-chromium and cobalt-chromium prosthodontic alloys bonded to composite resin

Author	Alloy	Alloy type	Cement	Bond strength (MPa)
Simonsen et al, 1983	Rexillium III	Ni-Cr-Be	Comspan	22.0
Thompson and Sangtaek, 1983	Rexillium III	Ni-Cr-Be	Comspan	20.0
Dhillon et al, 1983	Rexillium III	Ni-Cr-Be	Miradapt [i]	15.0
Mee et al, 1985	Rexillium III	Ni-Cr-Be	Resin bonded bridge cement	20.0
Zidan, 1985	Rexillium III	Ni-Cr-Be	Comspan	64.0
Simonsen et al, 1983	Litecast B	Ni-Cr-Be	Comspan	32.0
Koelbl et al, 1985	Litecast B	Ni-Cr-Be	Comspan	14.0
Zidan, 1985	Litecast B	Ni-Cr-Be	Comspan	46.0
Zidan, 1985	Biobond II	Ni-Cr-Be	Comspan	55.0
Simonsen et al, 1983	Bak-On NP	Ni-Cr-Be	Comspan	20.0
	Unitbond	Ni-Cr-Be	Comspan	21.0
	Ticonium	Ni-Cr-Be	Comspan	25.0
	Biobond C & B	Ni-Cr	Comspan	18.00
Ullo et al, 1984	Biobond C & B	Ni-Cr	Comspan	18.00
Zidan, 1985	Biobond C & B	Ni-Cr	Comspan	33.00
Simonsen et al, 1983	Microbond NP[2]	Ni-Cr	Comspan	18.00
Simonsen et al, 1983	Biocast	Co-Cr	Comspan	9.0
Thompson, 1985	Vitallium	Co-Cr	Comspan	18.0
Zidan, 1985	Vitallium	Co-Cr	Comspan	40.0
Zidan, 1985	Cobond	Co-Cr	Comspan	23.0
Thompson, 1985	Cobond	Co-Cr	Comspan	25.0
Dhillon et al, 1983	Rochette type retention		Miradapt [i]	5.0

i Johnson and Johnson, East Brunswick, N.J., USA.

TABLE 4.3

Shear bond strengths of various electrolytically etched nickel-chromium alloys bonded to composite resin

Author	Alloy	Alloy type	Bond strength (MPa)
Ballesteros et al, 1985	Rexillium III	Ni-Cr-Be	14.0
McLaughlin and Masek, 1985	Rexillium III	Ni-Cr-Be	25.0
Koelbl et al, 1985	Litecast B	Ni-Cr-Be	6.0
Querens et al, 1984	Stainless steel orthodontic buttons		17.0 (etched) 8.0 (mesh controls)
Brady et al, 1985	Biobond C & B	Ni-Cr	26.0 (etched) 6.0 (perforated)

TABLE 4.4

Commercial composite resin luting cements mentioned in Chapter 4

Product	Manufacturer
Comspan	Dentsply, York, Pennyslvania, USA
Conclude	3M Co., St Paul, Minnesota, USA
Resin bonded bridge cement	Kerr, Romulus, Michigan, USA
Retain	Pentron Corp, Wallingford, Connecticut, USA

TABLE 4.5

Tensile bond strengths of electrolytically etched nickel-chromium alloys in relation to the various test methods

Author	Alloy	Test machine	Cross head speed (mm/minute)	Bond strength (MPa)
Simonsen et al, 1983*	Rexillium III	[i]Thwing-Albert	1.0	22.0
Thompson and Sangtaek, 1983*	Rexillium III	Thwing-Albert	1.0	20.0
Dhillon et al, 1983*	Rexillium III	[ii]Instron	1.0	15.0
Mee et al, 1985**	Rexillium III	not reported	0.5	20.0
Zidan, 1985**	Rexillium III	[iii]MTS	1.0	64.0
Simonsen et al, 1983*	Litecast B	Thwing-Albert	1.0	32.0
Koelbl et al, 1985**	Litecast B	Instron		14.0
Zidan, 1985**	Litecast B	MTS	1.0	46.0
Zidan, 1985**	Biobond II	MTS	1.0	55.0
Simonsen et al, 1983*	Bak-On NP	Thwing-Albert	1.0	20.0
	Unitbond	Thwing-Albert		21.0
	Ticonium	Thwing-Albert		25.0
	Biobond C & B	Thwing-Albert		18.00
Ullo et al, 1984*	Biobond C & B	not reported	2.0	18.00
Zidan, 1985**	Biobond C & B	MTS	1.0	33.00
Simonsen et al, 1983*	Microbond NP[2]	Thwing-Albert	1.0	18.00
Simonsen et al, 1983*	Biocast	Thwing-Albert	1.0	9.0
Thompson, 1985*	Vitallium	Thwing-Albert	2.0	18.0
Zidan, 1985**	Vitallium	MTS	1.0	40.0
Zidan, 1985**	Cobond	MTS	1.0	23.0
Thompson, 1985*	Cobond	Thwing-Albert	2.0	25.0
Dhillon et al, 1983*	Rochette type retention	Instron	1.0	5.0

* Column of cement bonded to casting.
** Two castings cemented together.

i Model 65 TM, Thwing-Albert Instrument Co., Philadelphia, Pennyslvania, USA
ii Instron Corp., Canton, Massachussetts, USA
iii 812-Series, MTS Corp., Eden Prairie, Minnesota, USA

TABLE 6.1

Some commercial examples of restorative composite resins

Composite resin	Classification*	Type of particle	Method of cure
Command[i]	Conventional	Barium + $LiAlSiO_2$	Photo
Adaptic[ii]	Conventional	Quartz	Chemical
Concise[iii]	Conventional	Quartz	Chemical
Prismafil[iv]	Intermediate	Barium glass	Photo
P10[iii]	Intermediate	Quartz	Chemical
P30[iii]	Intermediate	Zinc glass	Photo
Miradapt[ii]	Intermediate	Colloidal silica + Quartz	Chemical
Silar[iii]	Microfill	Colloidal silica	Chemical
Durafil[v]	Microfill	Colloidal silica	Photo

i Kerr Sybron, Romulus, Michigan, USA
ii Johnson & Johnson, East Brunswick, New Jersey, USA
iii 3M Co., St Paul, Minnesota, USA
iv Dentsply, York, Pennsylvania, USA
v Kulzer, Friedrichsdorf, West Germany

* According to Leinfelder (1985)

TABLE 6.2

Some commercially-available composite resin luting cements

Composite resin luting cement	Presentation	Bonding resin included	Colour
Comspan[i]	Two paste	No	Tooth coloured and Opaque
Conclude[ii]	Two paste	Yes	Opaque
Resin bonded bridge cement[iii]	Two paste	Yes	Tooth coloured and Opaque
Duralingual[iv]	Syringe paste and liquid	No	Opaque
Retain[v]	Two paste	Yes	Tooth coloured
Maryland bridge cement[vi]	Two paste	Yes	Two Opaque colours
Micropont[vii]	Two paste (has light-curing ability)	No	Tooth coloured and Opaque

i Caulk/Dentsply, York, Pennsylvania, USA
ii 3M Co., St Paul, Minnesota, USA
iii Kerr Sybron, Romulus, Michigan, USA
iv Unitek, Monrovia, California, USA
v Den-Mat Corp., Santa Maria, California, USA
vi Dentron Corp., Wallingford, Connecticut, USA
vii Kulzer and Co., Friedrichsdorf, W. Germany

TABLE 6.3

Comparison of the commercial products Concise (conventional restorative composite resin) and Conclude (composite resin luting cement).

	Concise*	Conclude*
Resin	BIS-GMA/TEG-DMA	Same
Catalyst/Accelerator	Amine/peroxide	Same
Filler	Ground quartz	Same
Silane coupling agent	Methacrylate type	Same
Filler distribution		
Average size (micrometres)	9	1
Maximum size (micrometres)	75	25
Filler loading		
Coated filler (weight %)	79	72

* Both materials manufactured by 3M Co., St Paul, Minnesota. Information supplied by 3M Co. (1983).

TABLE 6.4

Filler loading and setting time for some luting cements for use with resin bonded bridges*

Cement	Filler Loading (weight %)	Set time (min)
Concise	79	2:30
Conclude	72	2:40
Comspan	63	2:50
Retain	65	2:12
Maryland bridge cement	79	3:05

* Information supplied by 3M Co. (1983)

TABLE 6.5

Commercial adhesive resin luting cements

Product	Manufacturer
Panavia Ex	Kuraray Co. Ltd., Osaka, Japan
ABC - Cement	Vivadent, Schaan, Lichtenstein
Chemiace	Sun Medical Co., Kyoto, Japan
Superbond C&B	Sun Medical Co., Kyoto, Japan

TABLE 7.1

Mean lingual enamel thickness (mm) of maxillary anterior teeth

	Incisal third	Middle third	Gingival third
Maxillary central	.65	.60	.40
Maxillary lateral	.70	.60	.40

from Gratton et al, 1983

TABLE 8.1

Reported success rates for Rochette bridges from definite clinical studies

Author	No of Cases	Success rate[i] (%)	Maximum functioning period (months)	Mean functioning period (months)	Period for[ii] majority of failures (months)
Shaw and Tay (1982)	46	80	44	20	0 - 7
Bergendal et al (1983)	100	71	59	35	no pattern
Gratton et al (1983)	95	76	36	not stated	0 - 6
Eshelman et al (1984)	39	75	32	24	no pattern
Williams et al (1984)	63	84	84	36	0 - 12
Chew (1985)	10	100	24	24	-
Creugers et al (1985)	31	90	12	12	-

i Success is defined as total lack of bond failure.

ii Failure is defined as the first bond failure of any retainer.

TABLE 8.2

Clinical reports of the success rates of Maryland bridges

Author	No of Cases	Success[i] rate (%)	Observation[ii] period (months)
Thompson and Livaditis (1982)	140	98	24
Gratton et al (1983)	79	91	12
Simonsen et al (1983)	45	100	36
La Barre and Ward (1984)	45	91	12
Hamada et al (1985)	57	74	14
Creugers et al (1985)	39	100	12

i Success is defined as total lack of bond failure.

ii None of these studies state the range of functioning periods. The maximum observation period is the only information provided.

TABLE 9.1

Rochette bridges

Bridge position	Number placed	Number failed (%)	Mean period to failure (months) (range)	Mean observation period of success (months) (range)
Maxillary anterior	3	2 (66)	3 (2 - 4)	9
Maxillary posterior	1	1 (100)	3	-
Mandibular anterior	1	1 (100)	16	-
Total	5	4 (80)	8 (2 - 16)	9

Table 9.2

Maryland Bridges

Bridge position	Number placed	Number failed (%)	Mean period to failure (months) (range)	Mean observation period of success (months) (range)
Maxillary anterior	17	10 (59)	6 (2 - 21)	7 (1 - 35)
Maxillary posterior	2	1 (50)	2	4
Mandibular anterior	3	0	-	12 (4 - 21)
Mandibular posterior	2	1 (50)	1	23
Total	24	12 (50)	5 (1 - 21)	10 (1 - 35)

TABLE 9.3

Other resin bonded bridges

Bridge position	Number placed	Number failed (%)	Mean period to failure (months)	Mean observation period of success (months)
Combination bridges				
Maxillary posterior	2	0	-	30
Duralingual bridges				
Maxillary anterior	1	0	-	1
Lost-salt bridges				
Maxillary anterior	1	0	-	11
Maxillary posterior	1	0	-	5
Total	2	0	-	8
Silicoater technique bridges				
Maxillary anterior	1	0	-	11
Maxillary posterior	1	0	-	4
Total	2	0	-	8

TABLE 9.4

Rebonding of Maryland bridges

Number of failures	Number of successful rebonds (%)	Mean rebond observation period (months) (range)	Number of multiple rebonds
12	8 (66)	4 (1-9)	4

TABLE 10.1

Range of errors in surface area estimation

	True area (cm^2)	Mean estimated area (cm^2) for ten evaluators (SD)*	Percentage error at two standard deviations**	Number of errors relative to true area Below	Above
Bridge A	0.70	0.89 (0.22)*	± 49.4	8	2
Bridge B	0.52	0.46 (0.09)	± 39.0	7	3
Bridge C	0.97	1.09 (0.14)	± 29.2	6	4

* SD — value for one standard deviation in parentheses.
** — refer text (10.3.1).

TABLE 10.2

Range of errors in surface area estimation by dental surgeons and dental technicians

	True area (cm^2)	Mean estimated area (cm^2) for five evaluators (SD)	Percentage error at two standard deviations	Number of errors relative to true area Below	Above
Dental Surgeons					
Bridge A	0.70	0.80 (0.17)	± 42.5	1	4
Bridge B	0.52	0.49 (0.06)	± 24.5	3	2
Bridge C	0.97	0.96 (0.09)	± 18.8	2	3
Dental Technicians					
Bridge A	0.70	0.97 (0.24)	± 49.5	1	4
Bridge B	0.52	0.43 (0.09)	± 41.9	5	0
Bridge C	0.97	0.97 (0.19)	± 39.2	4	1

TABLE 10.3

Solutions of nitric acid and acetic acid investigated in the etching solution preparatory study

Amount of concentrated nitric acid (ml)	Normality of nitric acid solution	Amount of glacial acetic acid (%)
3.5	0.06 N	2
6.0	0.09 N	2
7.0	0.11 N	2
8.0	0.13 N	2
10.5	0.17 N	2
7.0	0.11 N	0
7.0	0.11 N	4
7.0	0.11 N	10

TABLE 10.4

Code letter/number designating the various electrolytic etching conditions that were tested

Etching solution	Current density mA/cm^2	Time (minutes)
A = 0.09 N HNO_3	1 = 280 mA/cm^2	I = 4
B*= 0.11 N HNO_3	2*= 400 mA/cm^2	II*= 5
C = 0.13 N HNO_3	3 = 520 mA/cm^2	III = 6

* Conditions B,2,II are the recommended etching conditions.

TABLE 10.5

Tensile bond strengths of specimens cast in Microbond NP[2] and electrolytically etched under various conditions

Mean tensile bond strength in decreasing order (MPa)	No of samples that could be tested	Etching conditions*
7.76	4	A,1,I
7.45	3	A,2,III
7.29	4	B,2,III
5.67	2	B,3,I
5.58	5	A,3,III
4.74	5	C,3,III
4.06	3	B,3,III
3.73	4	C,3,II
3.46	2	B,3,II
3.32	4	B,2,II
11.61	1	B,2,I
3.87	1	A,3,I
2.53	1	C,2,I
1.89	1	A,1,III
0.83	1	A,3,II
0.69	1	B,1,III

Note: 1 Specimens etched under all other test conditions failed to survive thermal-cycling and could not be tensile tested.

2 Five specimens prepared for each etching condition.

* A,B,C = Etching solution
1,2,3 = Current density
I,II,III = Time

TABLE 10.6

Total number of etching conditions that provided various numbers of specimens that could be tested

No of specimens tested	Total number of etching conditions
5	2
4	4
3	2
2	2
1	6
0	11
	27

TABLE 10.7

Tensile bond strengths for individual specimens etched under various etching conditions

Etching conditions	Tensile* bond strength (Specimen No)	Tensile bond strength after first retest (MPa)	Tensile bond strength after second retest** (MPa)
A,1,I	8.85 (1) 8.43 (3) 7.46 (5) 6.36 (4) 0.00 (2)		
B,3,III	6.91 (2) 4.15 (3) 1.11 (1) 0.00 (4) 0.00 (5)		
A,3,III	10.09 (5) 7.32 (2) 7.19 (4) 1.93 (3) 1.38 (1)	4.01 (4) 2.35 (1) 2.35 (5) 0.00 (3) 0.00 (4)	6.63 (5) 0.00 (1) 0.00 (2) 0.00 (3) 0.00 (4)
B,2,II	5.11 (2) 2.76 (3) 2.76 (1) 2.63 (3) 0.00 (4)	4.84 (1) 0.00 (2) 0.00 (3) 0.00 (4) 0.00 (5)	5.53 (3) 2.07 (2) 0.00 (1) 0.00 (2) 0.00 (3)

* Arranged in decreasing strength.

** Following an additional set of simulated porcelain firings.

Etching conditions B,2,II are the manufacturer's recommended conditions

TABLE 10.8

Tensile strengths of specimens cast in Rexillium III

Tensile strength of specimens[i] that failed within the composite resin (MPa)	Tensile strength of specimens[ii] that failed at the resin/metal interface (MPa)
24.88	17.42
23.49	
21.15	
18.66	
13.82	
20.40	

i These five specimens failed within the column of composite resin at some distance from the resin/metal interface. These are, therefore, NOT actual bond strengths.

ii One specimen failed at the resin/metal. The tensile bond strength was 17.42 MPa.

Note: The one specimen of Rexillium III was bonded a total of six times. Each prepared specimen survived thermal-cycling and was able to be tested.

TABLE 10.9

Etching conditions listed against the number of specimens each condition provided for testing

No of specimens that could be tested	Etching condition
5	A,3,III C,3,III
4	A,1,I B,2,II B,2,III C,3,II
3	A,2,III B,3,III
2	B,3,I B,3,III
1	A,1,III A,3,I A,3,II B,1,III B,2,I C,2,I
0	A,1,II A,2,I A,2,II B,1,I B,1,II B,1,II C,1,I C,1,II C,1,III C,2,II C,2,II C,2,III C,3,I

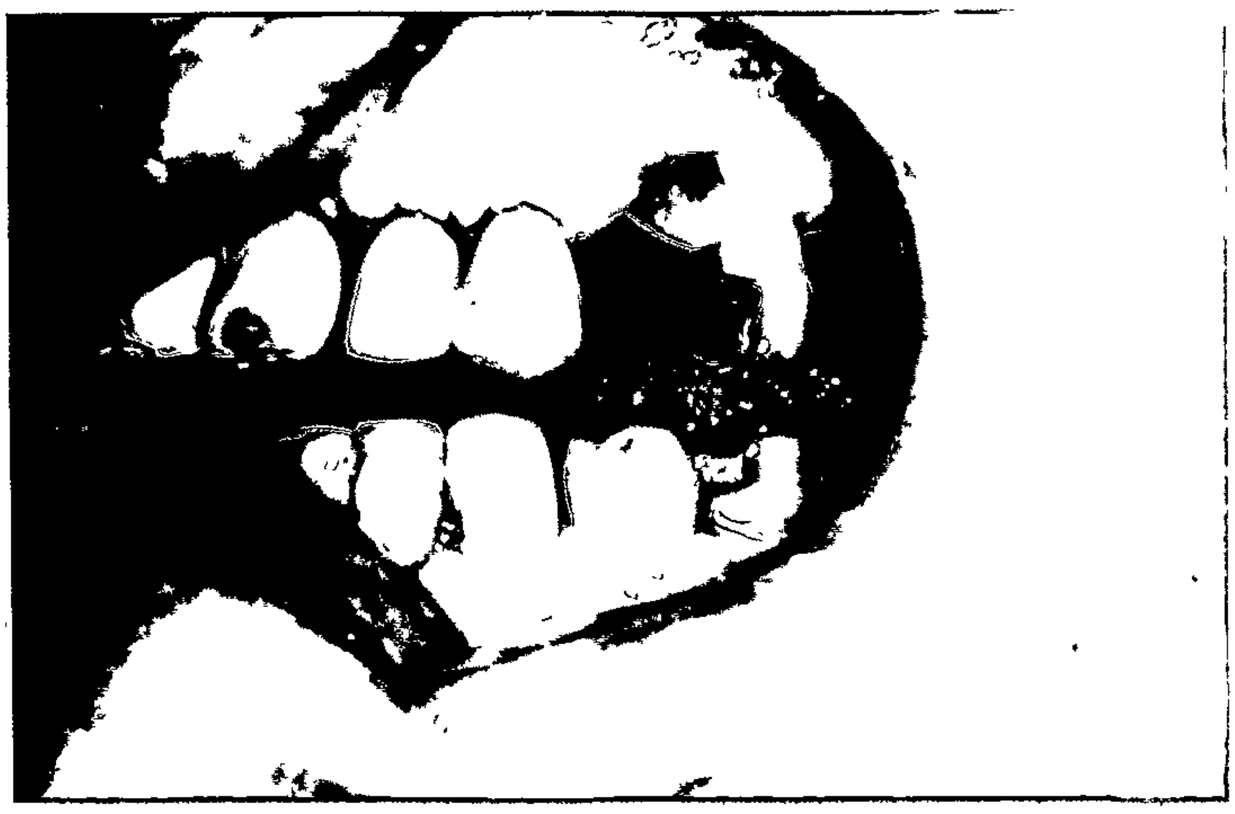

Figure 2.1a
An edentulous space created by the emergency extraction of an upper left first premolar for periodontal reasons (courtesy Dr T.R. Walton).

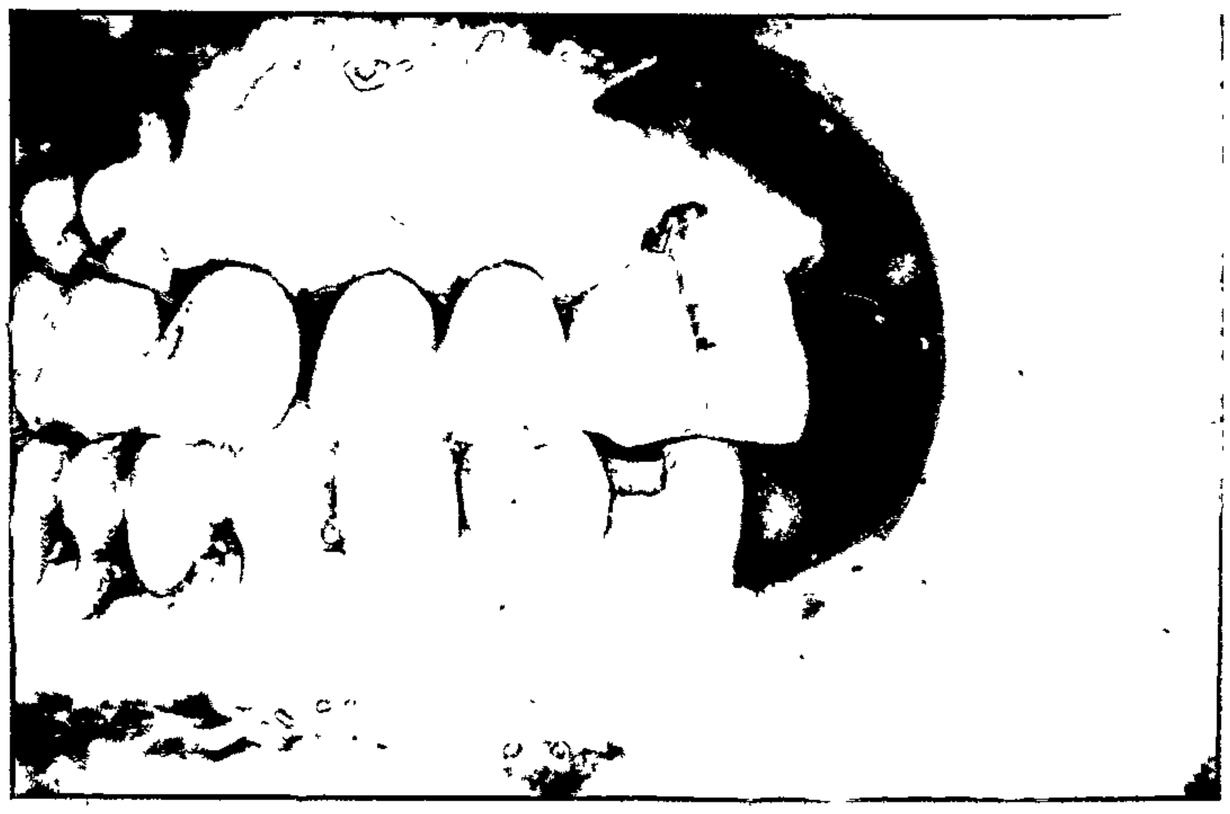

Figure 2.1b
The crown of the upper left first premolar subsequently bonded in position as a temporary prosthesis using the acid-etch technique (courtesy Dr T.R. Walton).

Figure 2.2
A temporary fixed prosthesis using a composite resin pontic replacing the upper left central incisor bonded to the adjacent abutments using the acid-etch technique.

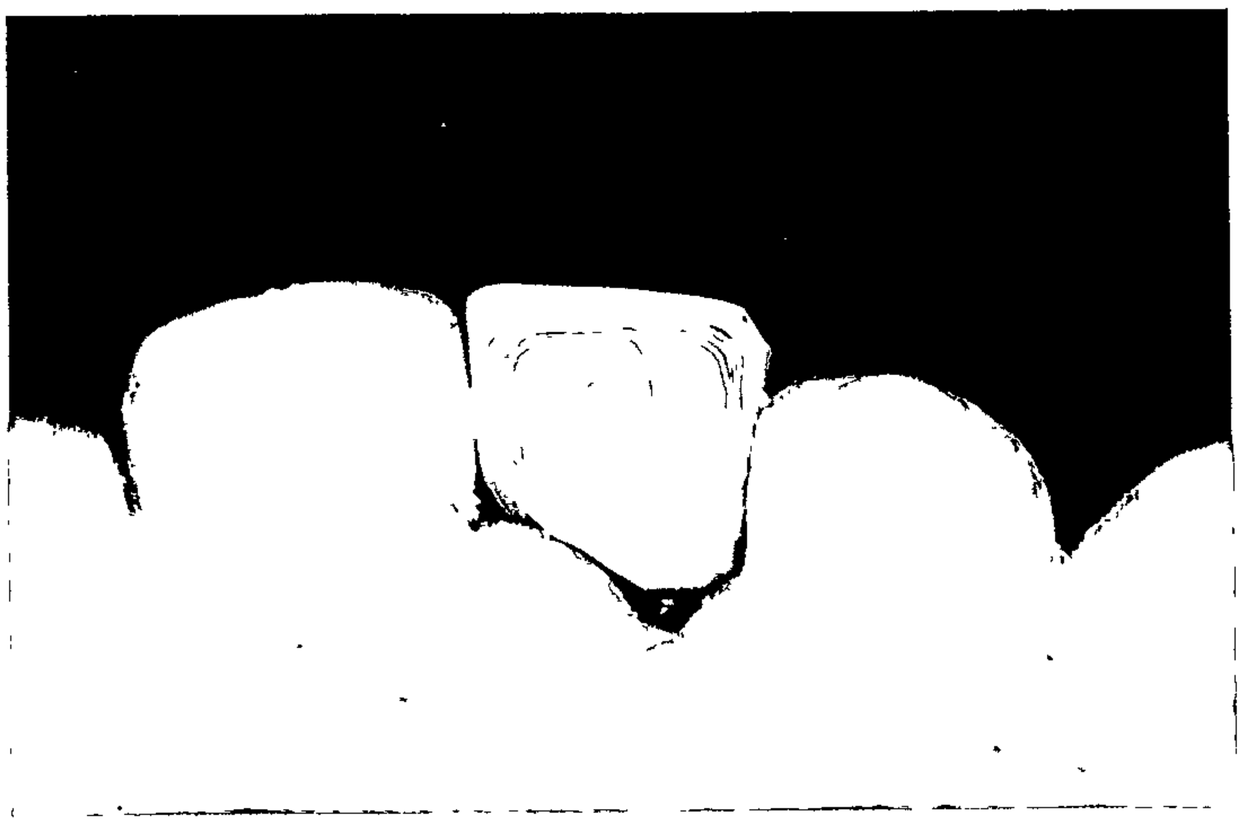

Figure 2.3
An acrylic resin denture tooth adapted to fit an edentulous space and prepared with retentive cavities for use as a resin bonded bridge pontic.

Figure 2.4
An acrylic resin denture tooth adapted to fit an edentulous space and fitted with a stainless steel strengthening wire.

Figure 2.5
A cast-metal periodontal splint similar to the original design of Rochette (1973) with retentive perforations to obtain a bond between the composite resin cement and the casting.

Figure 2.6
A Rochette type cast-metal resin bonded bridge similar in design to that described by Howe and Denehy(1977),(courtesy Dr. Barry Reid).

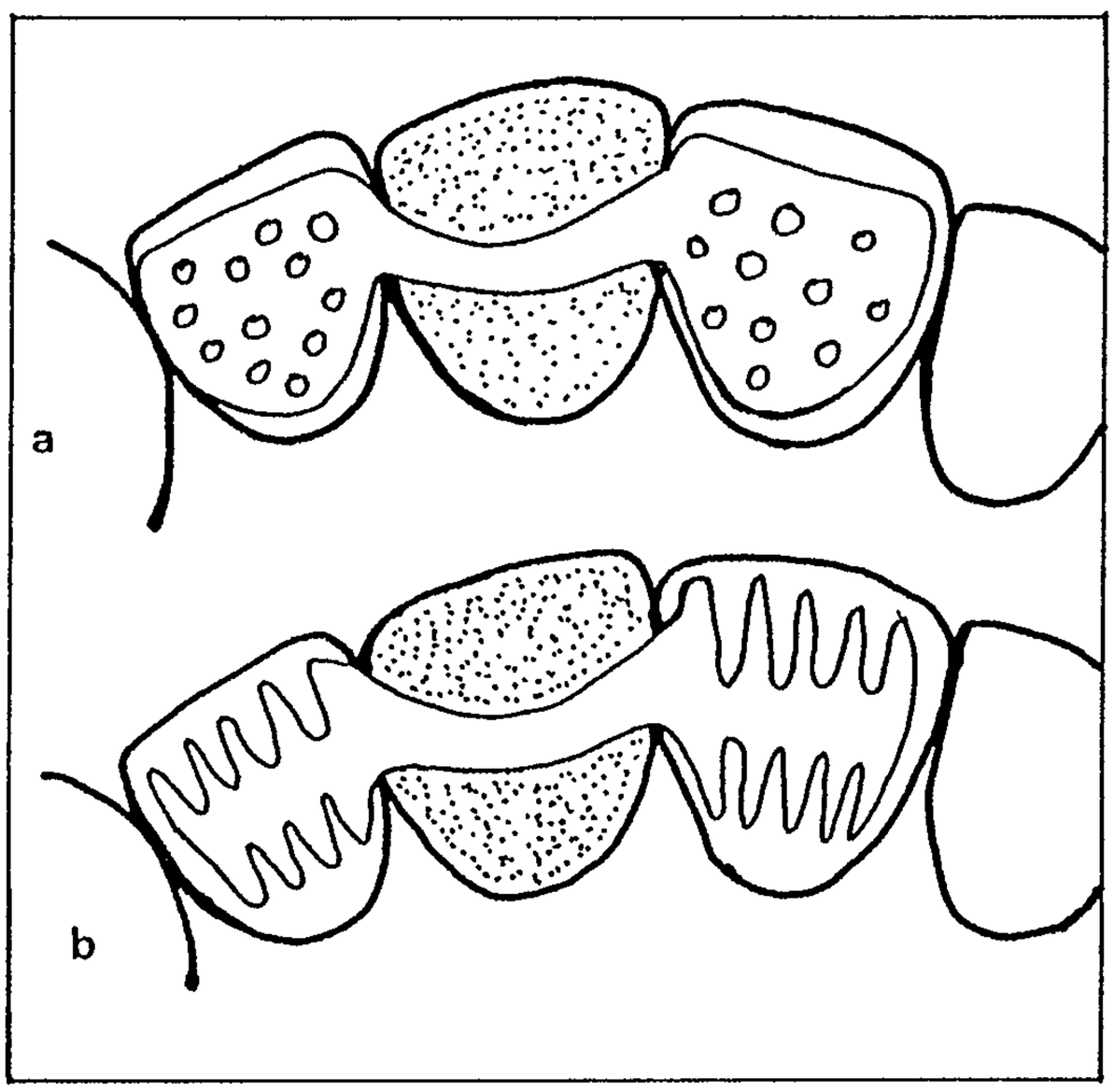

Figure 2.7
Diagrammatic representation of two variations in Rochette bridge retainer design (from Peck et al, 1981).

Figure 2.8
A Maryland type cast-metal resin bonded bridge showing the lack of retentive perforations on the retaining flanges.

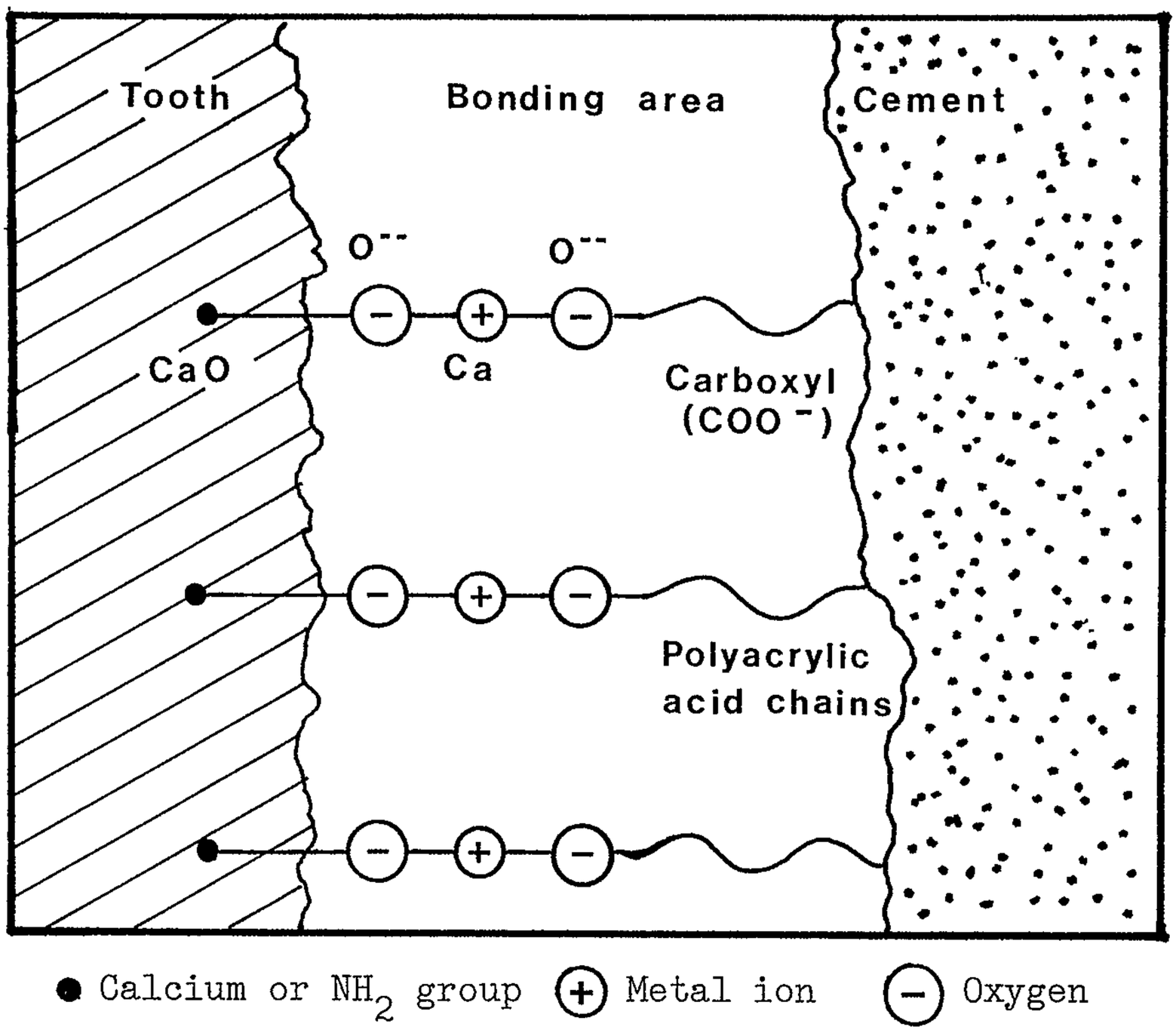

Figure 3.1a
Diagrammatic representation of physicochemical adhesion involving polyacrylic acid cement (from McLean, 1977).

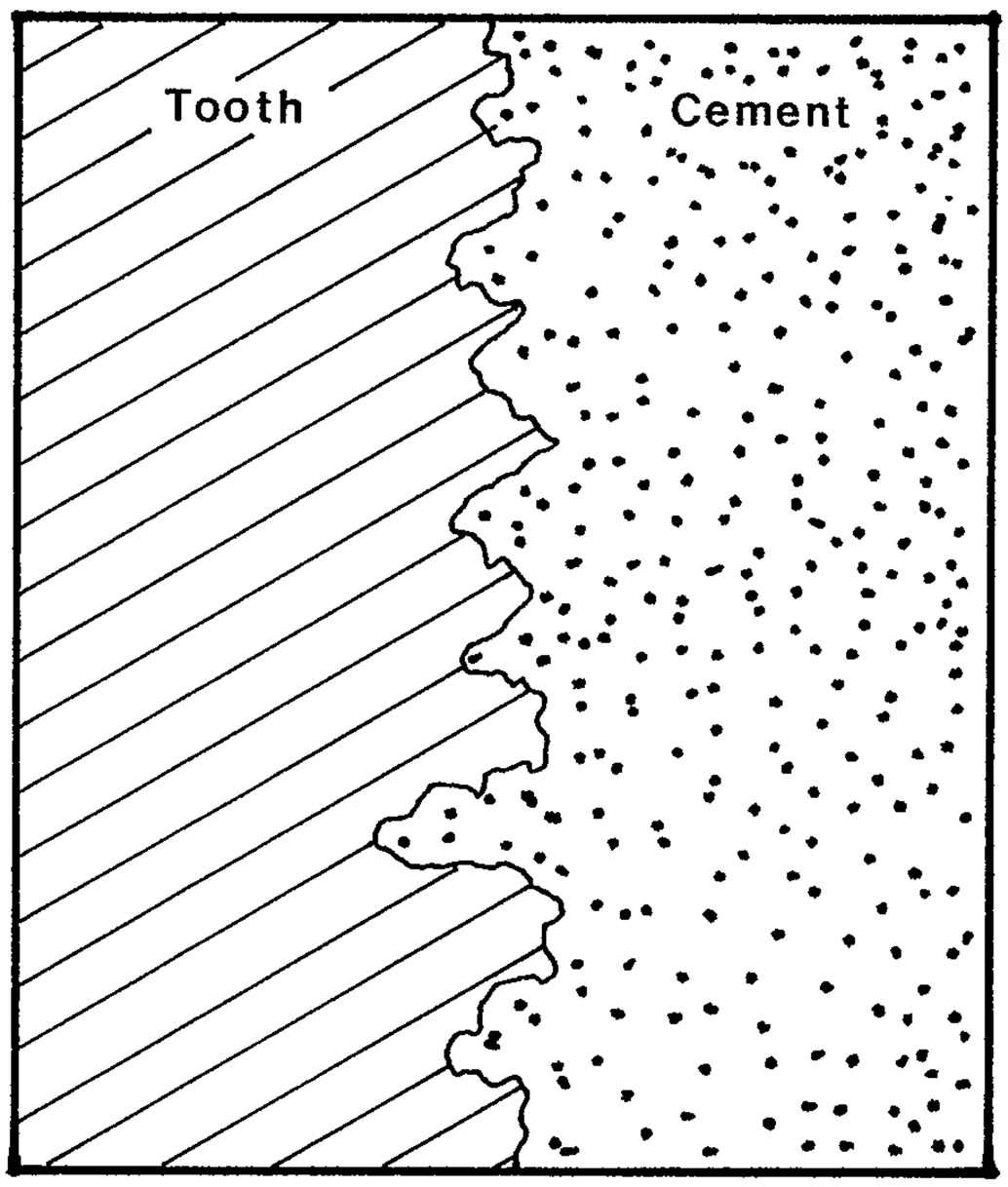

Figure 3.1b
Diagrammatic representation of mechanical interlocking (from McLean, 1977).

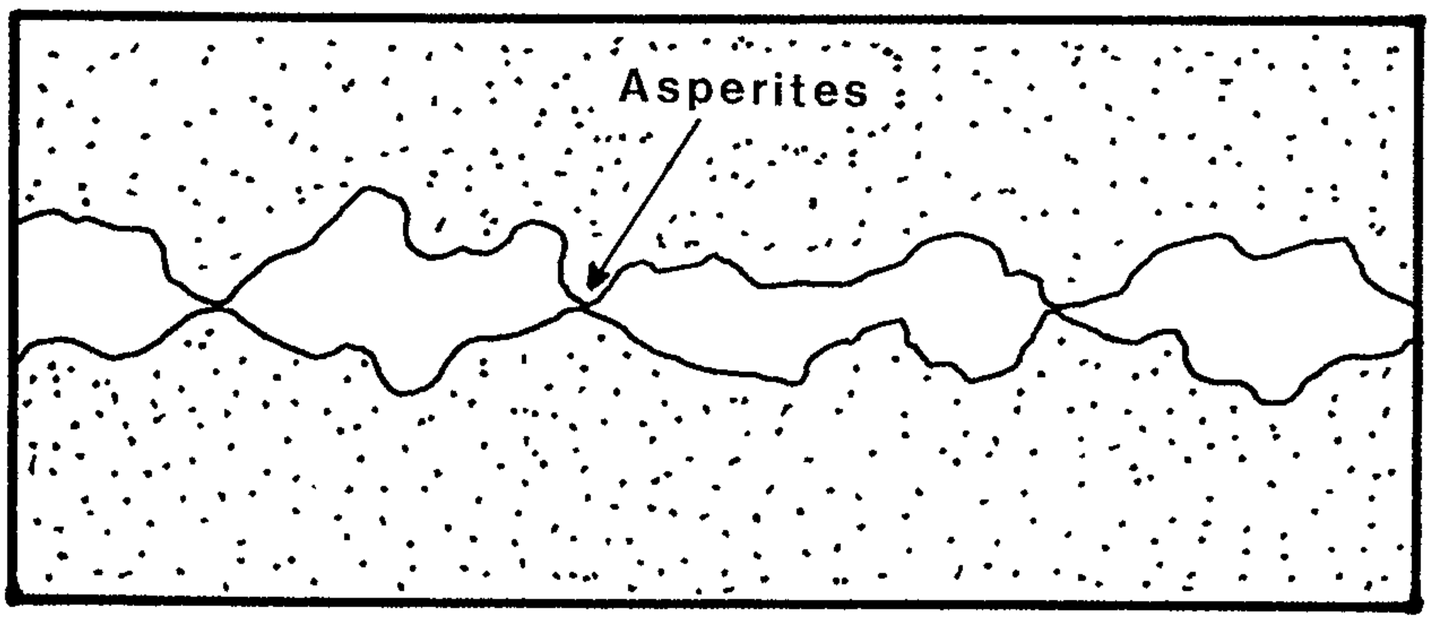

Figure 3.2
Diagrammatic representation of two bonding surfaces, at high magnification, showing the points of contact known as the asperites (from Buonocore, 1975).

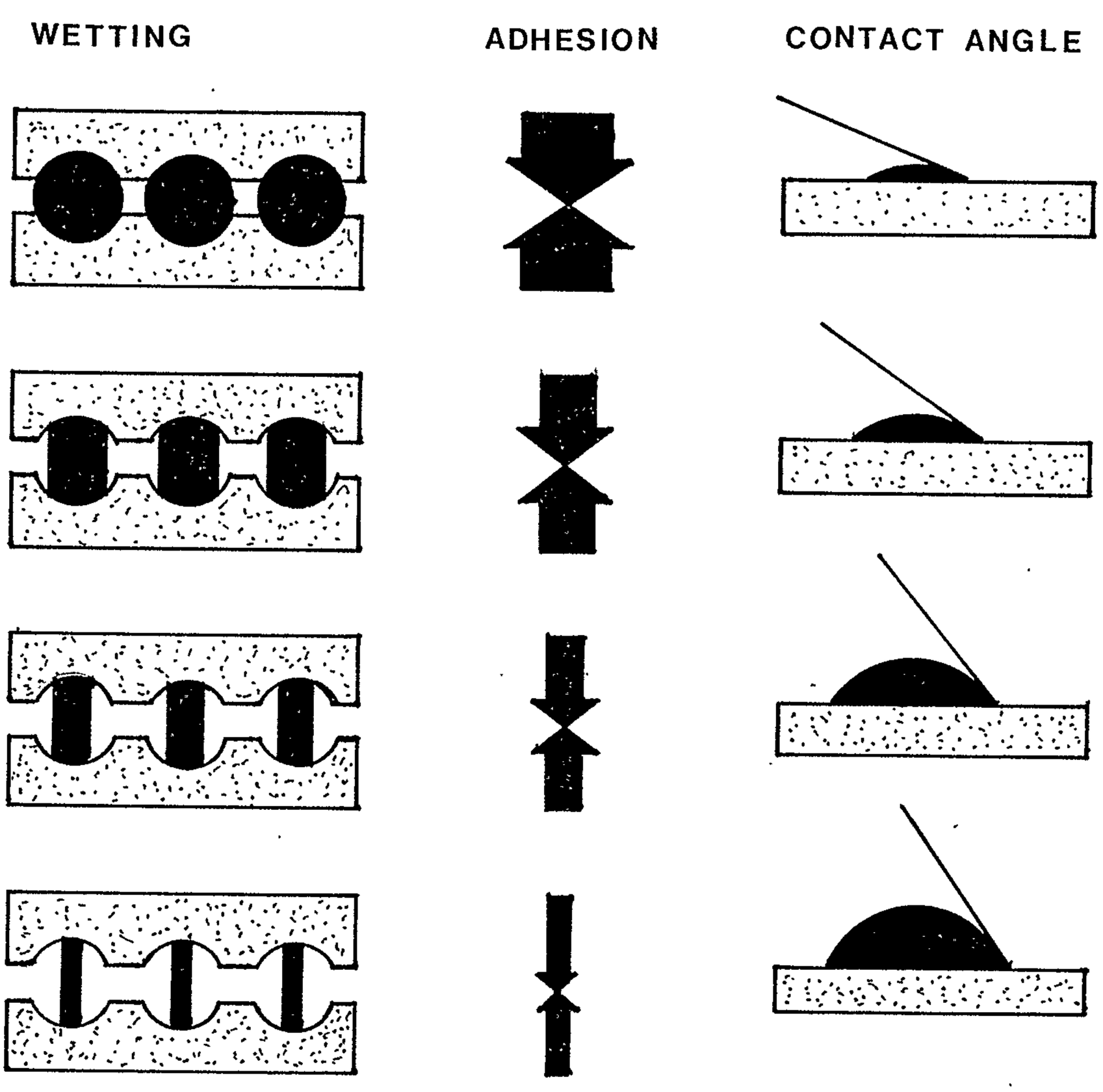

Figure 3.3
Diagrammatic representation of the relationship between contact angle, wetting and adhesion (from Retief, 1973a).

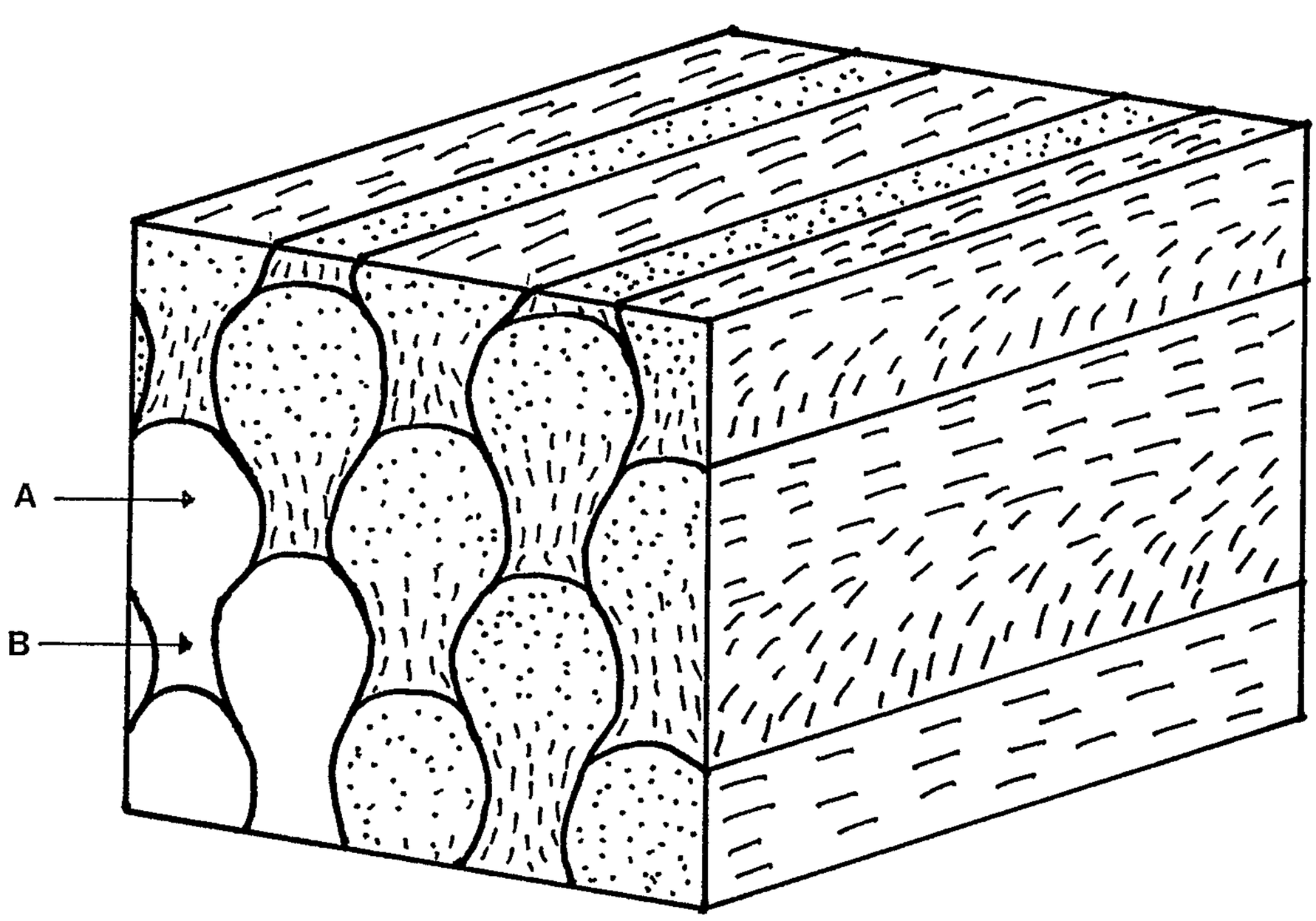

Figure 3.4
Diagrammatic representation of enamel prisms showing their arrangement and that of the crystallites as found commonly in human permanent teeth. 'A' denotes the 'head' region of the prism and 'B' denotes the 'tail' region (from Meckel et al, 1965).

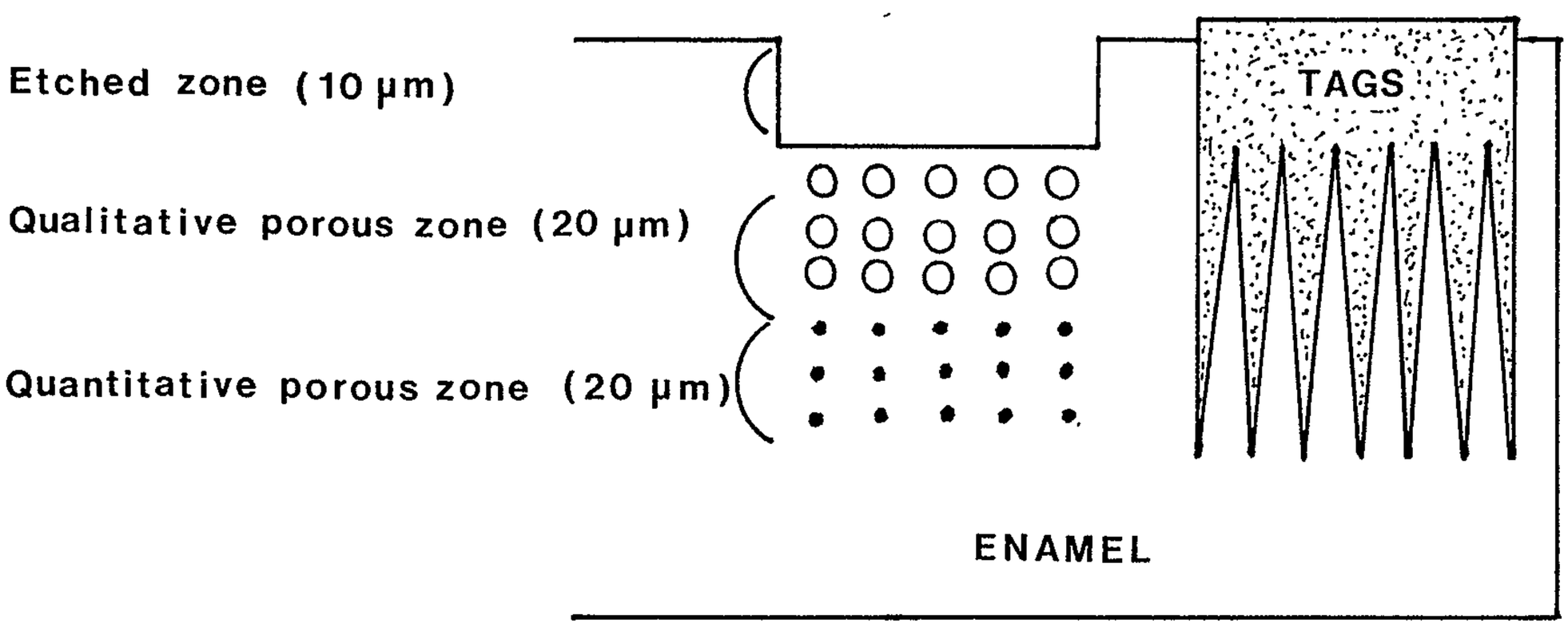

Figure 3.5
Diagrammatic representation of an etched and porous enamel surface showing three distinct zones and the subsequent penetration of tags of resin (from Silverstone, 1975).

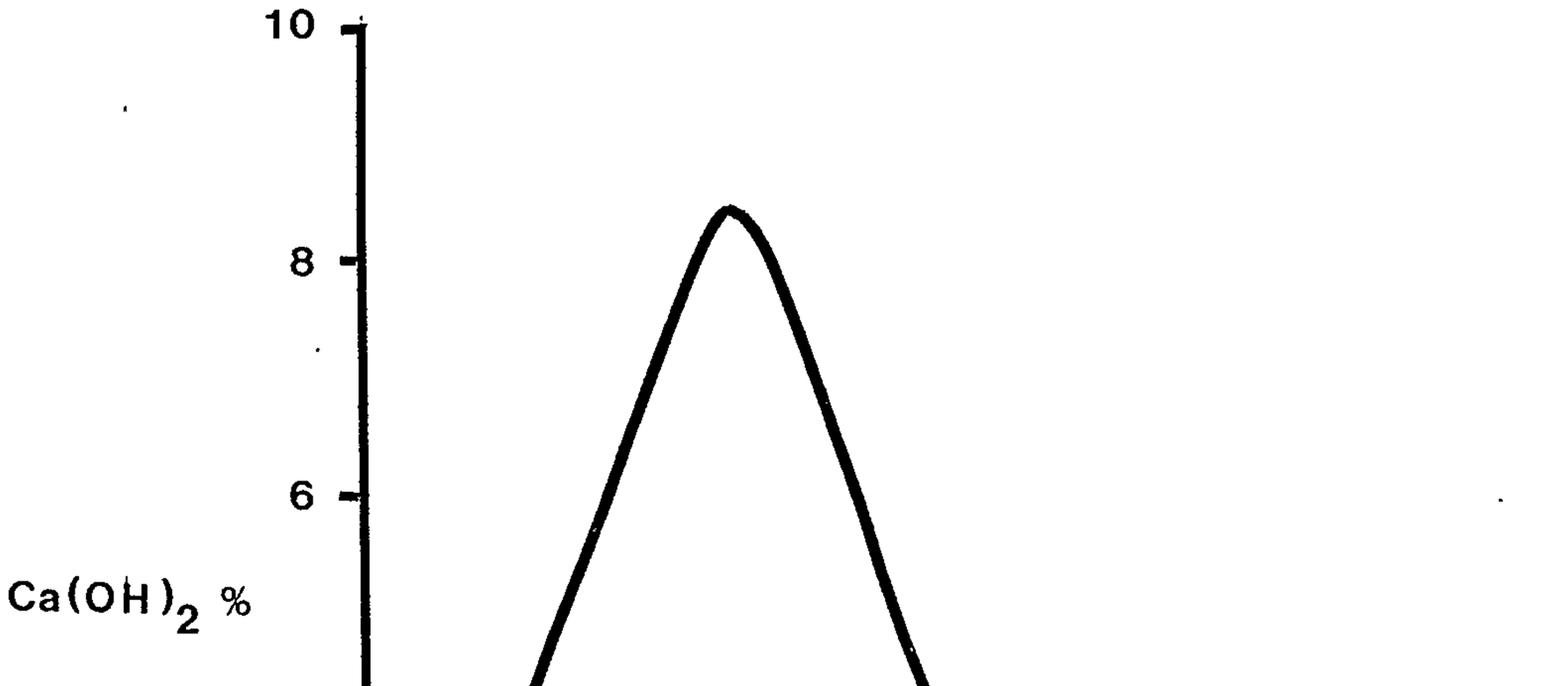

Figure 3.6
The solubility phase diagram for the $Ca(OH)_2/H_3PO_4/H_2O$ system at 25°C (from Chow and Brown, 1973).

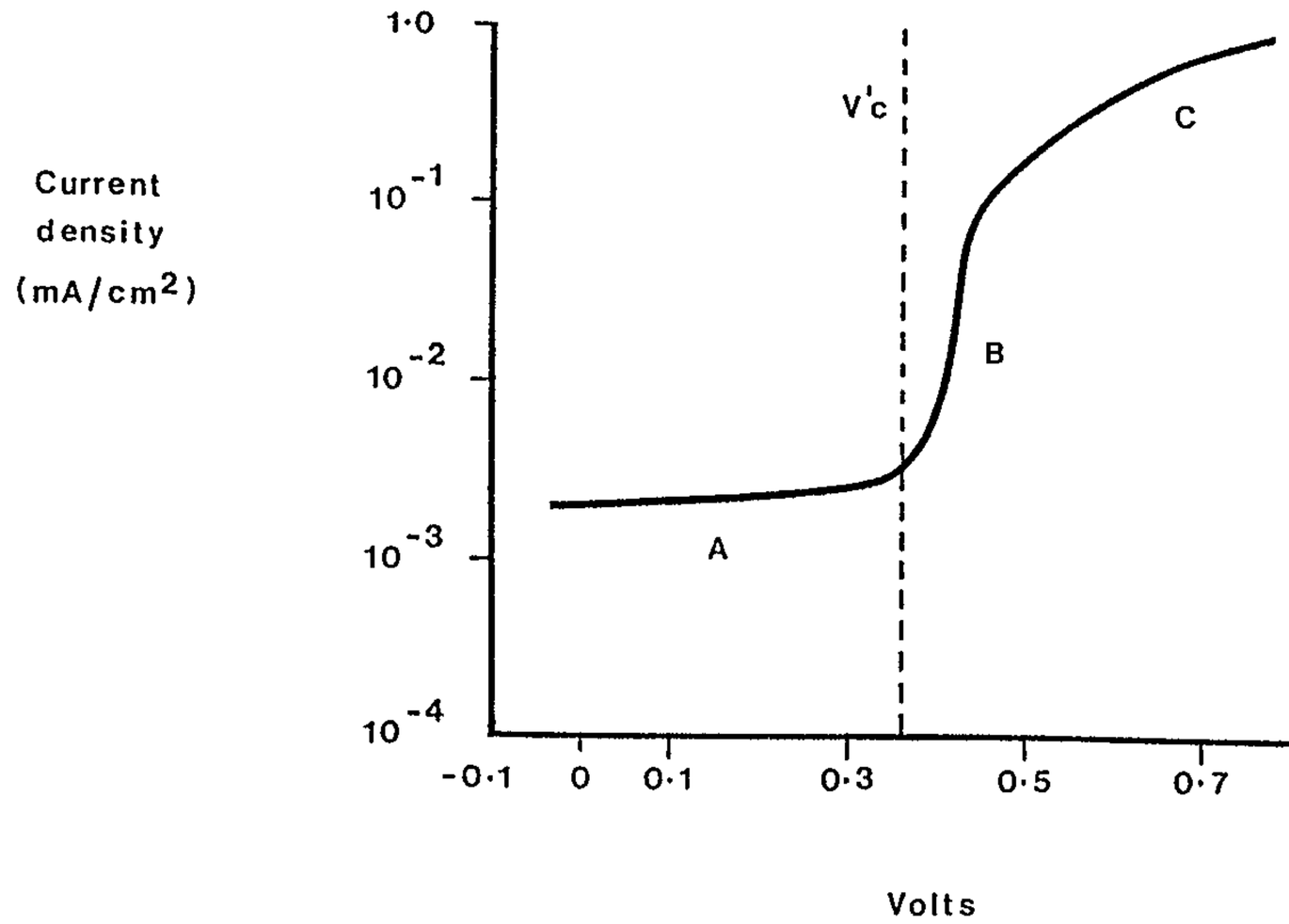

Figure 4.1
Potentiostatic polarization curve for 18-8 stainless steel in 0.1N sodium chloride. Region 'A' is below the critical potential, V'c, where no corrosion pits occur. Region 'B', above the critical potential V'c, is where rapid pit growth occurs. The current density curve levels out in region 'C' due to polrization effects within the pit (from Leckie and Uhlig, 1966).

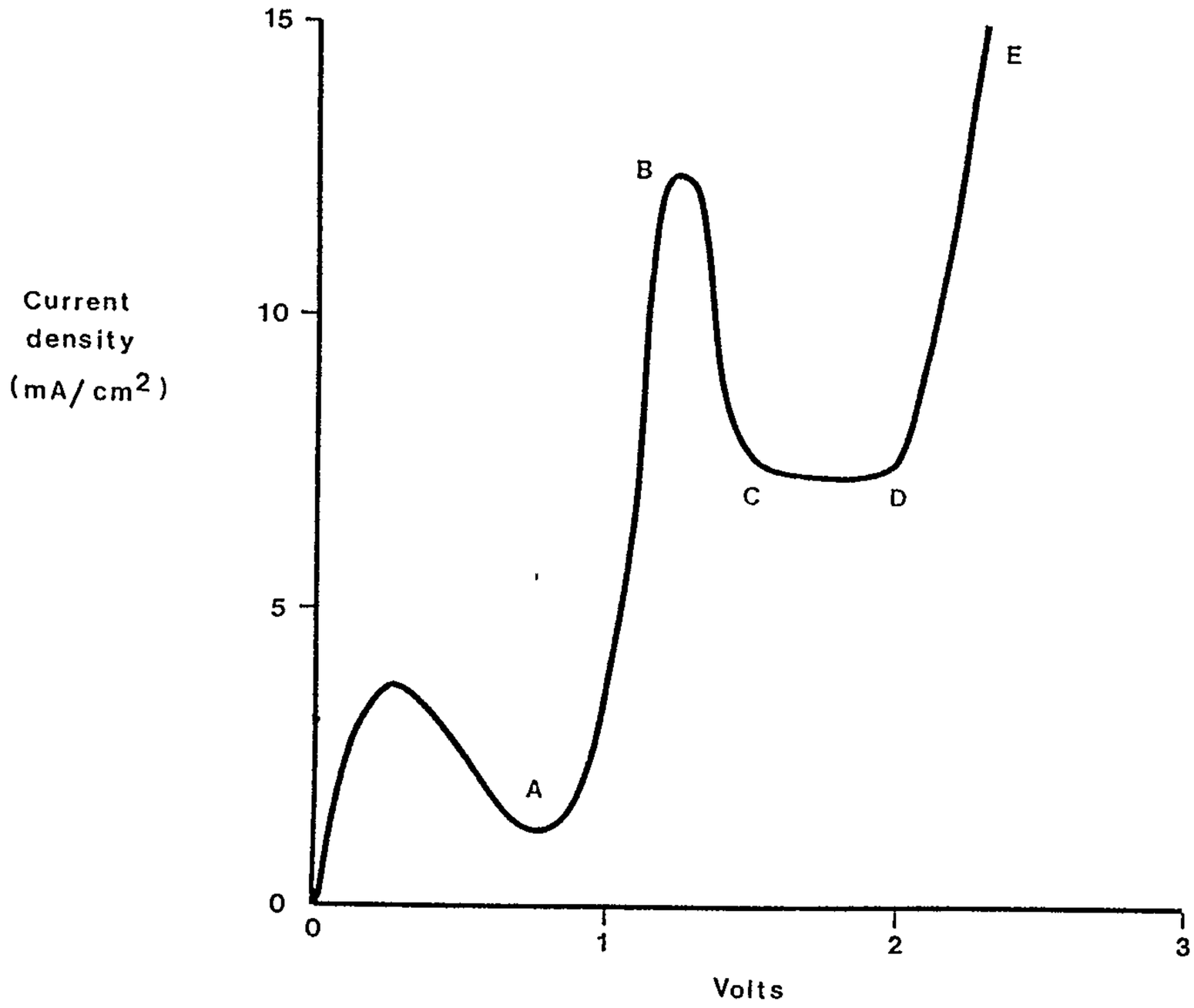

Figure 4.2
The curve of voltage as a function of current density for copper in phosphoric acid. Between 'A' and 'B' etching occurs. Between 'C' and 'D' there is a stable plateau at which polishing occurs. Between 'D' and 'E' there is slow gas evolution with pitting of the metal surface (from Tegart, 1956).

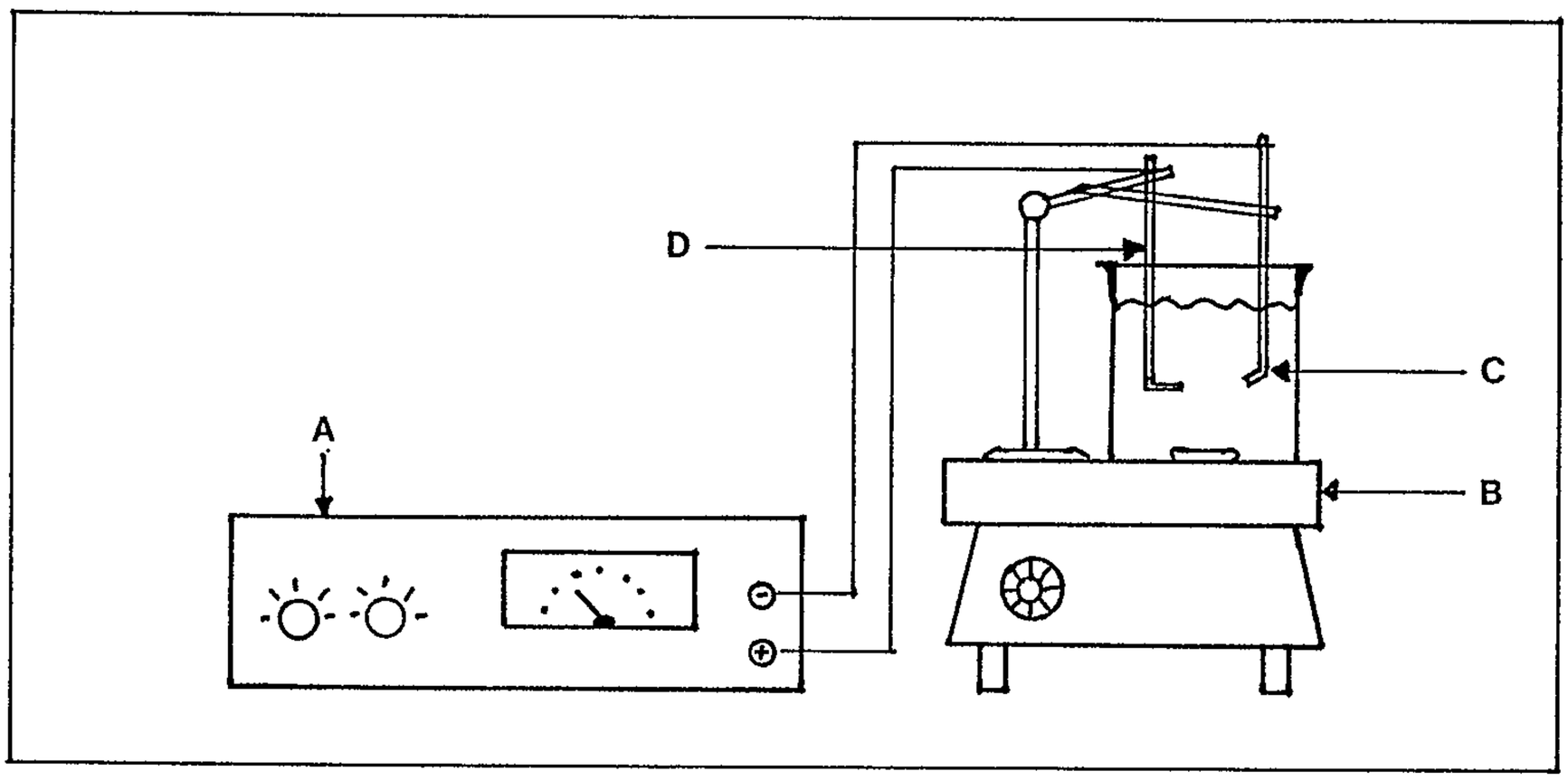

Figure 4.3
Diagrammatic representation of the etching apparatus used at the University of Maryland to develop the electrolytic etching process. A: Power supply, B: Magnetic stirrer, C: Anode/Specimen, D: Cathode (from Del Castillo and Thompson, 1982).

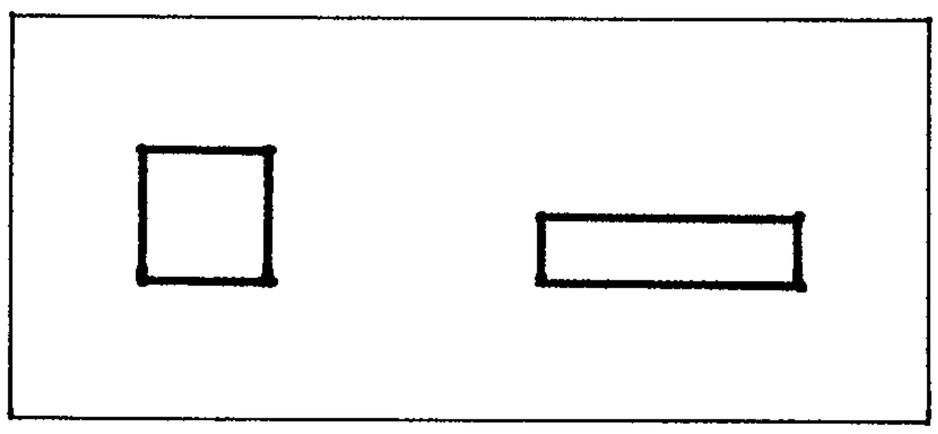

Figure 4.4
Diagrammatic representation of the one centimetre square standards used to aid Maryland bridge retainer surface area estimation (Actual size).

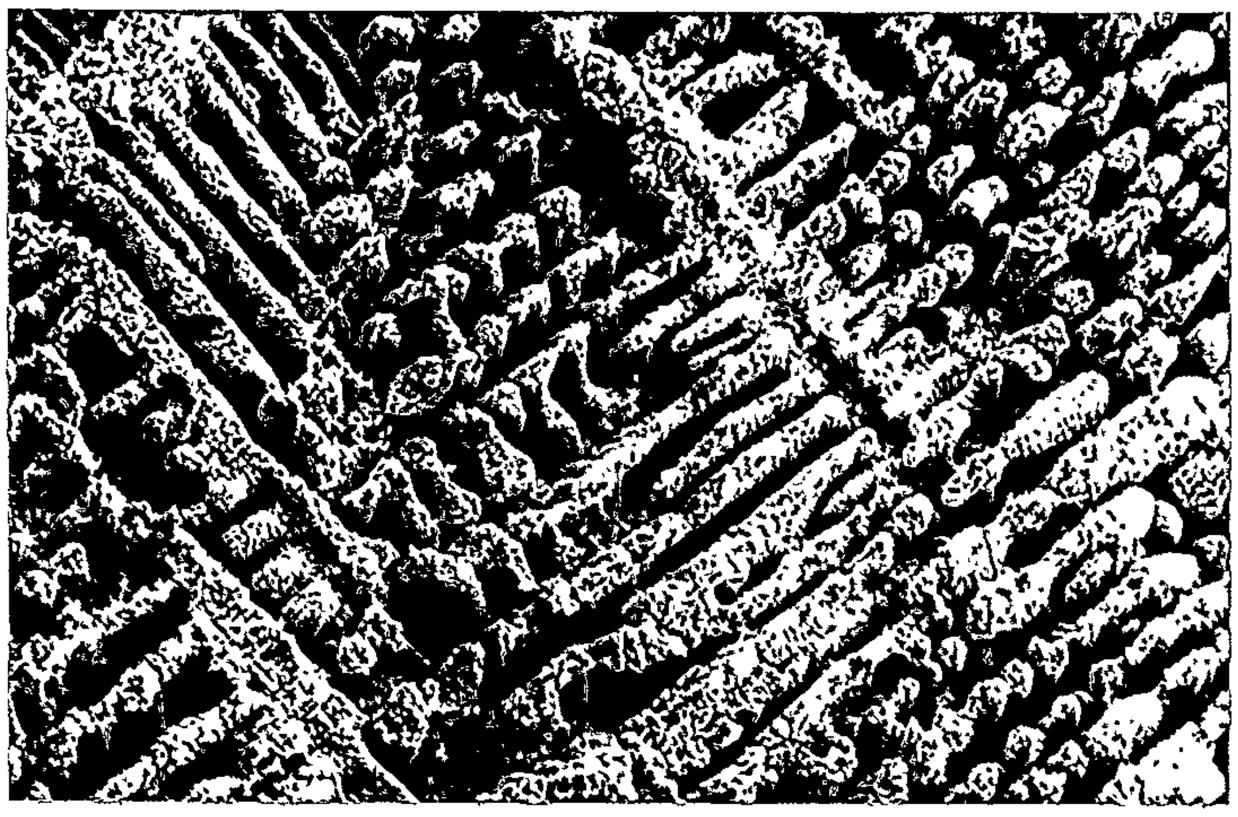

Figure 4.5
SEM of Rexillium III alloy surface electrolytically etched under recomended conditions (Table 4.1). Note that the dendritic arms have been left intact and the high Be content interdendritic eutectic has been removed creating extensive three dimensional relief. Magnification X 500 (from Simonsen et al, 1983).

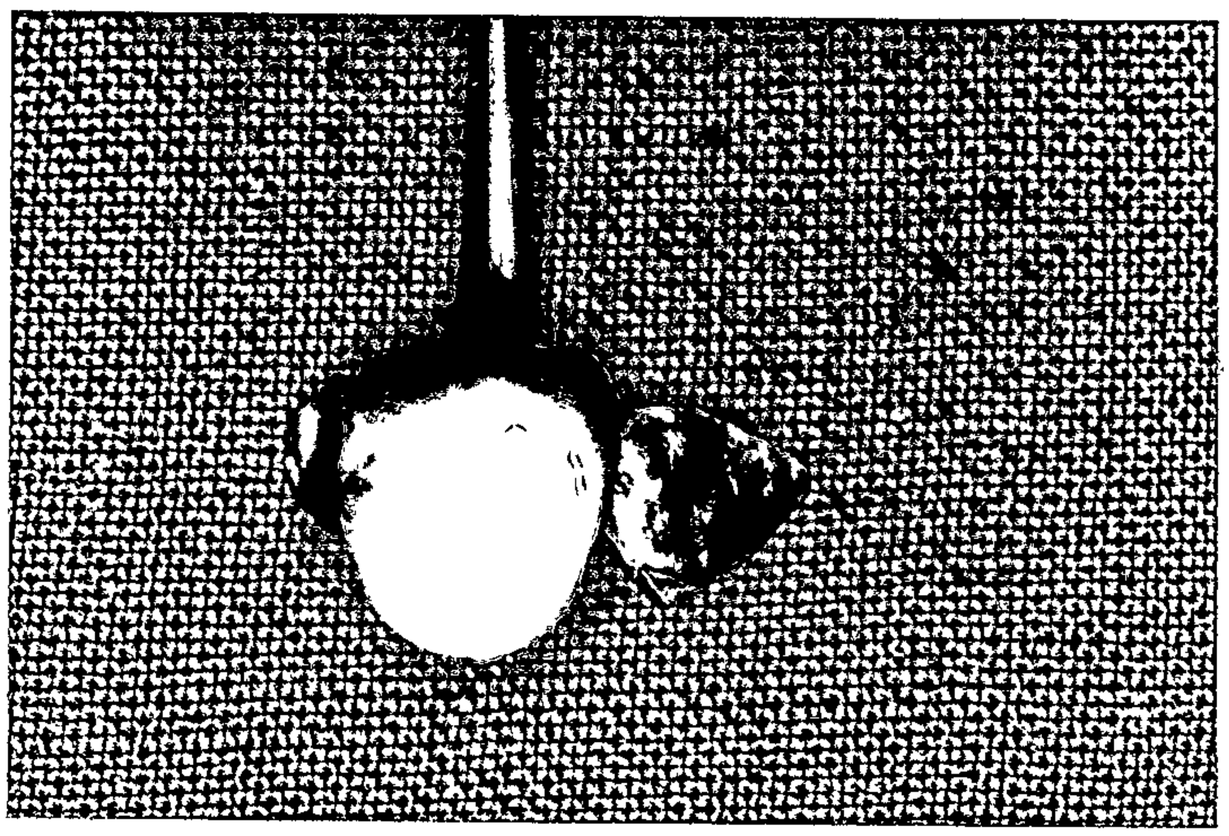

Figure 4.6a
A Maryland bridge attached to a copper electrode with sticky wax so that all but the bonding surfaces of the retainers are masked.

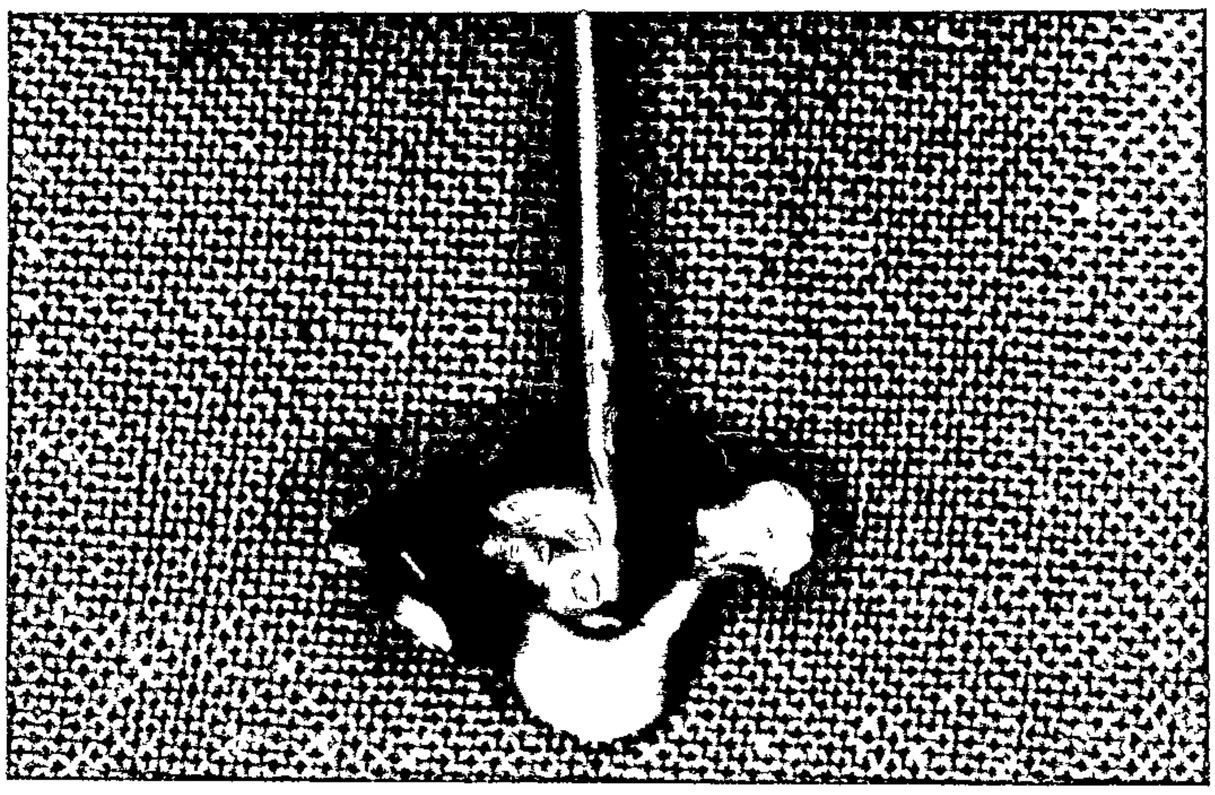

Figure 4.6b
Another view of the Maryland bridge depicted in Figure 4.6a showing masking with sticky wax complete.

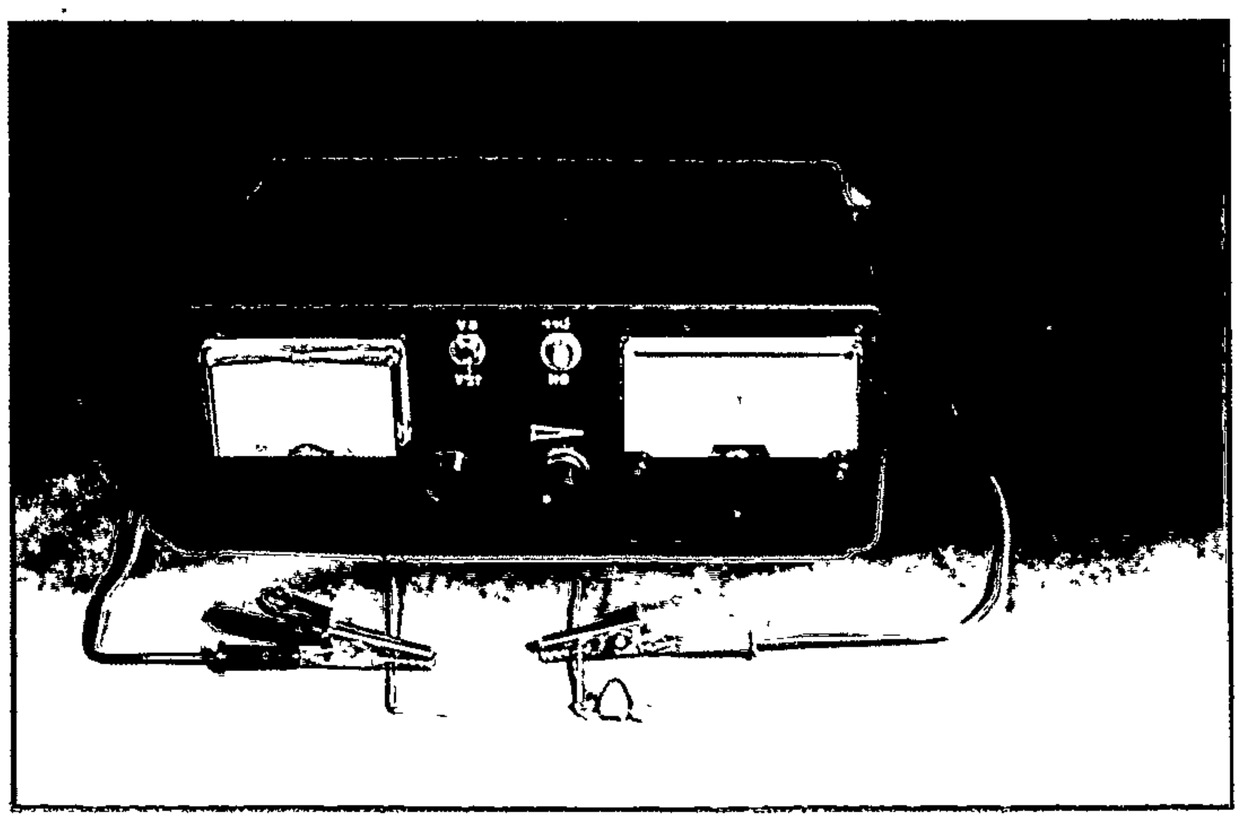

Figure 4.7
An electrolytic etching apparatus power supply showing connections to a Maryland bridge.

Figure 4.8
A Maryland bridge in an electrolytic etching bath showing the yellow discoloration that forms around the bridge and the evolution of gas bubbles around the cathode.

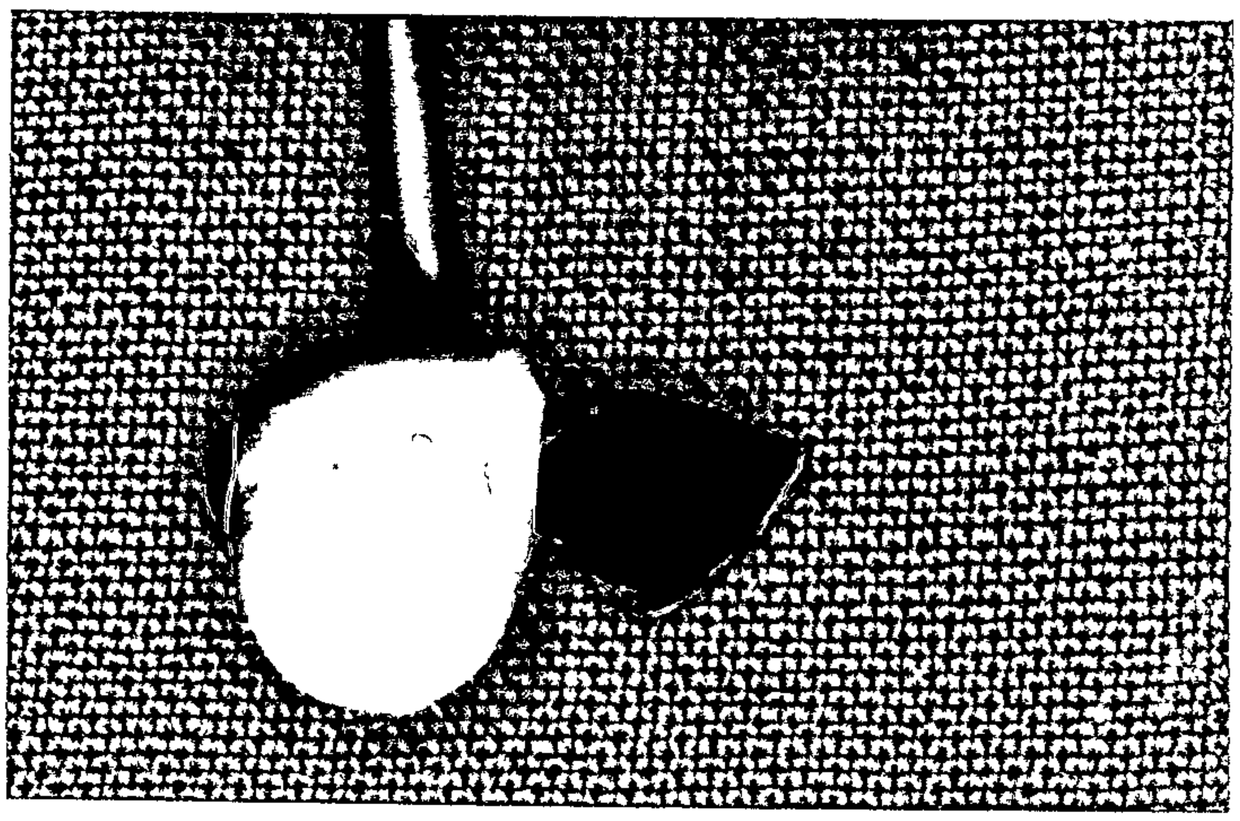

Figure 4.9
A Maryland bridge subsequent to electrolytic etching showing the black deposit formed as a result of the etching process.

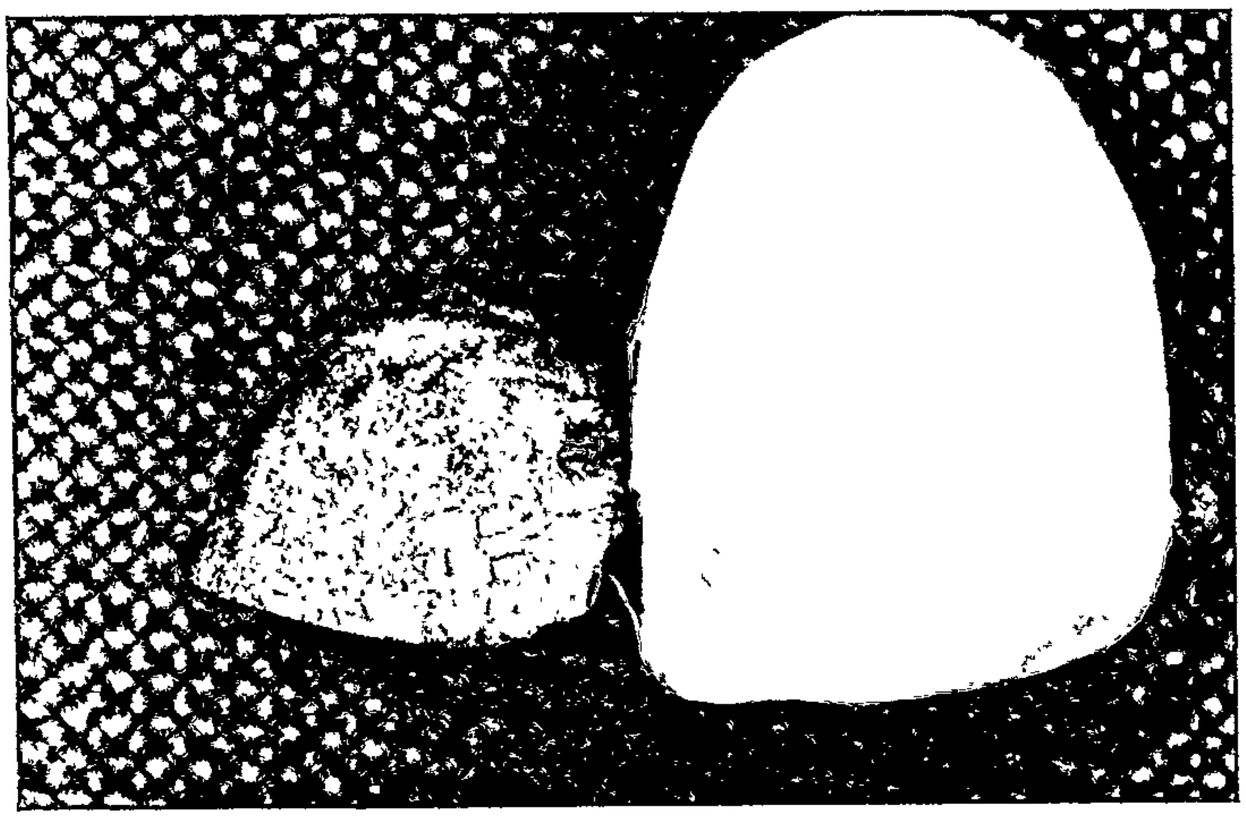

Figure 4.10
The Maryland bridge depicted in Figure 4.9 subsequent to cleaning in 18 per cent HCL. The electrolytic etching process is complete.

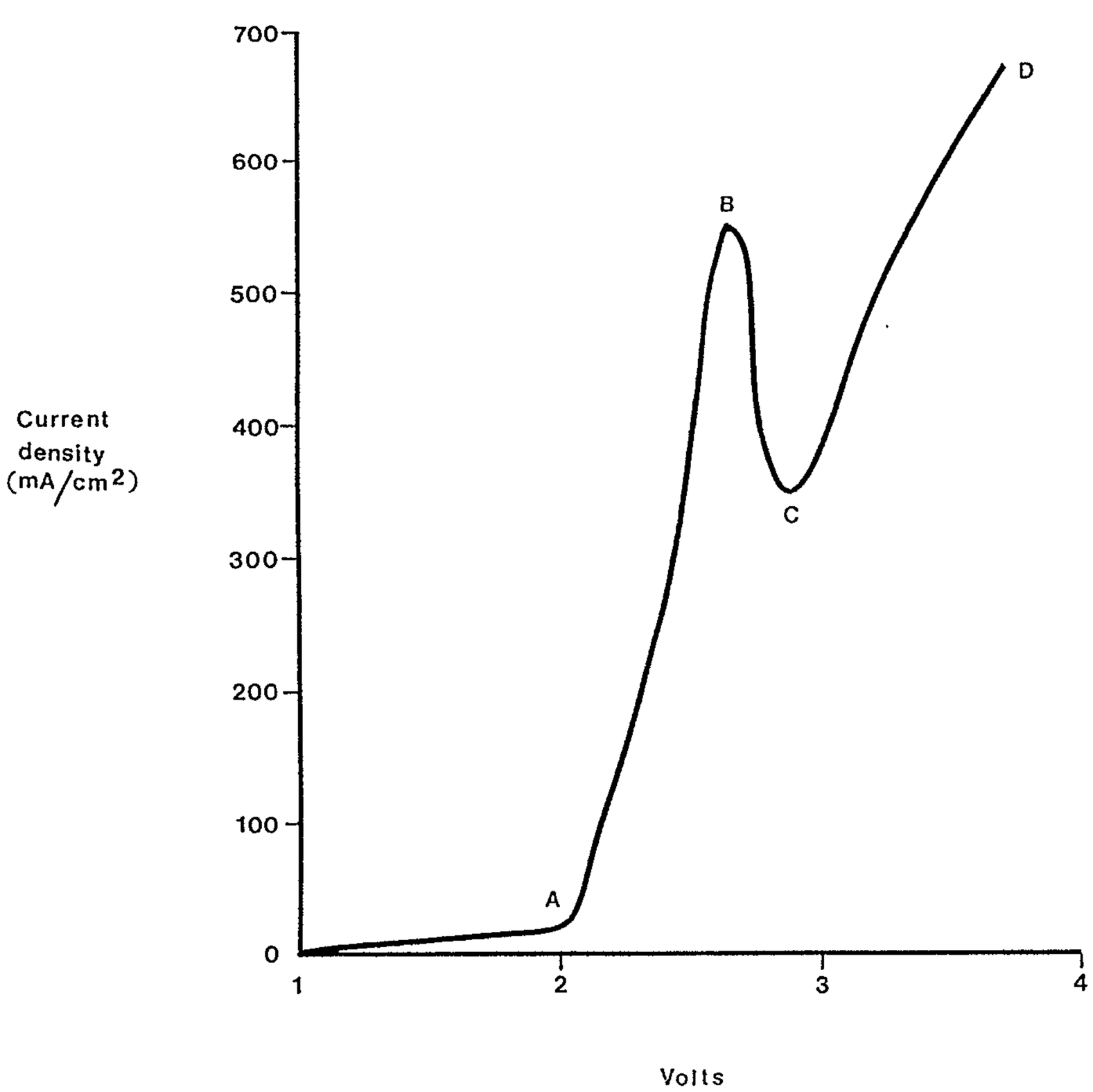

Figure 4.11

Potentiostatic-anodic-current density (PACD) curve for the alloy Rexillium III in 10 per cent H_2SO_4 solution. Etching of the alloy surface occurs between 'A' and 'B'. Between 'C' and 'C' electropolishing occurs (from Simonsen et al, 1983).

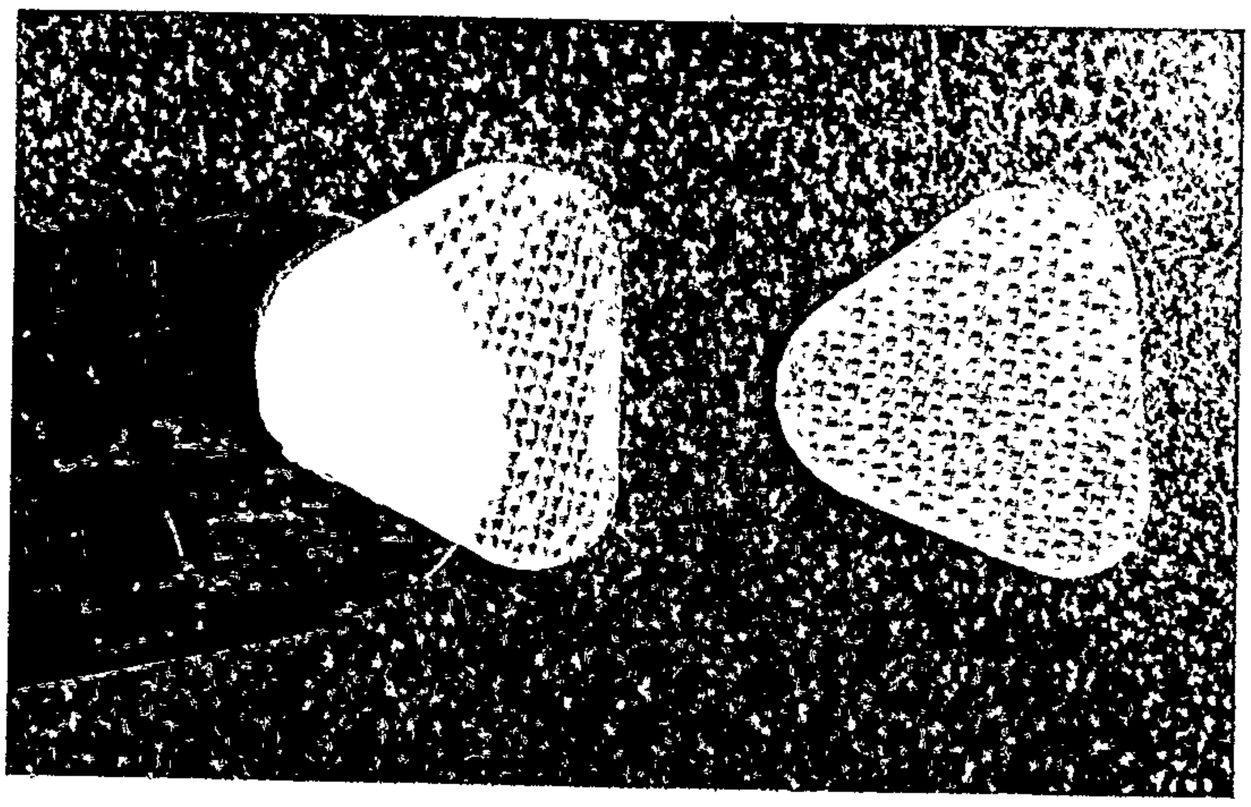

Figure 5.1
Plastic mesh profiles used to construct Maryland bridges (Duralingual, Unitek Corp., Monrovia, California).

Figure 5.2
Duralingual profiles being cut to conform to the lingual surfaces of abutment teeth on a die-stone model.

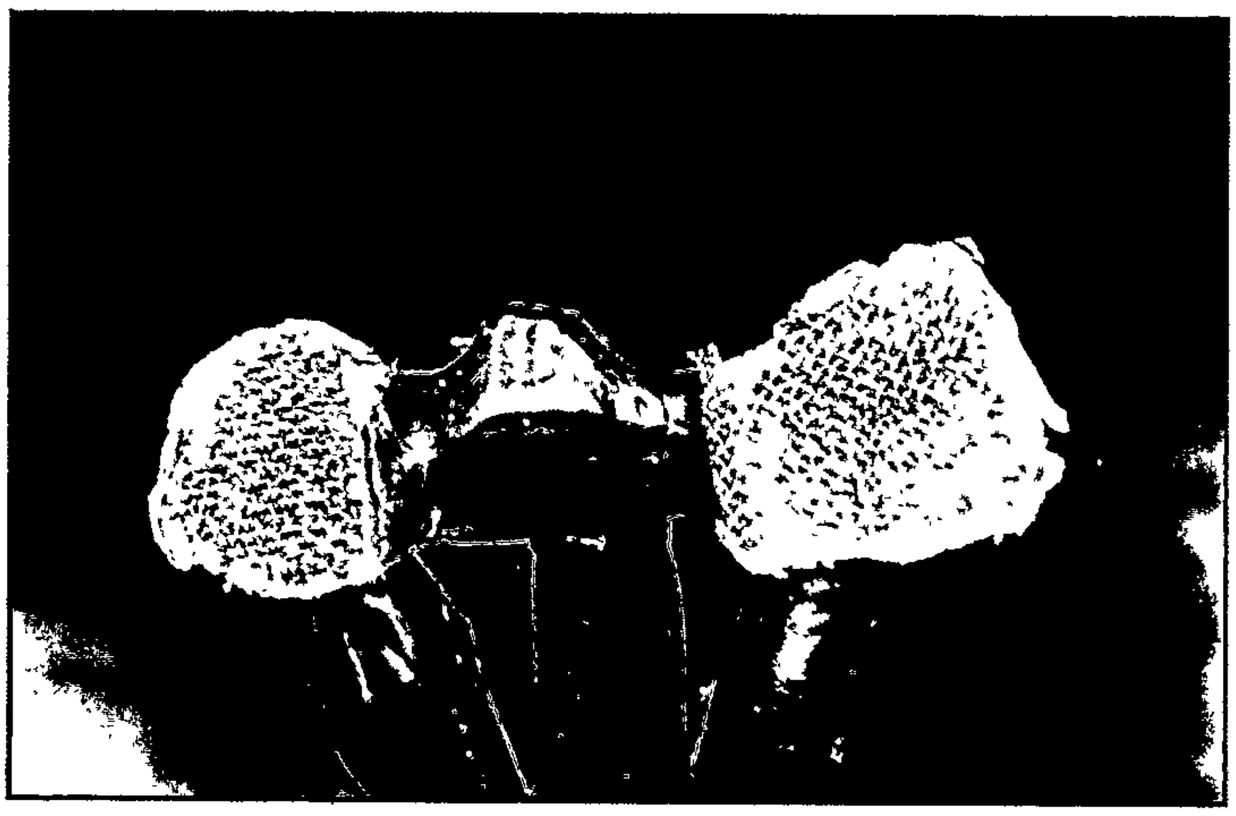

Figure 5.3
A wax pattern for the Maryland bridge for which the die-stone model is depicted in Figure 5.2.

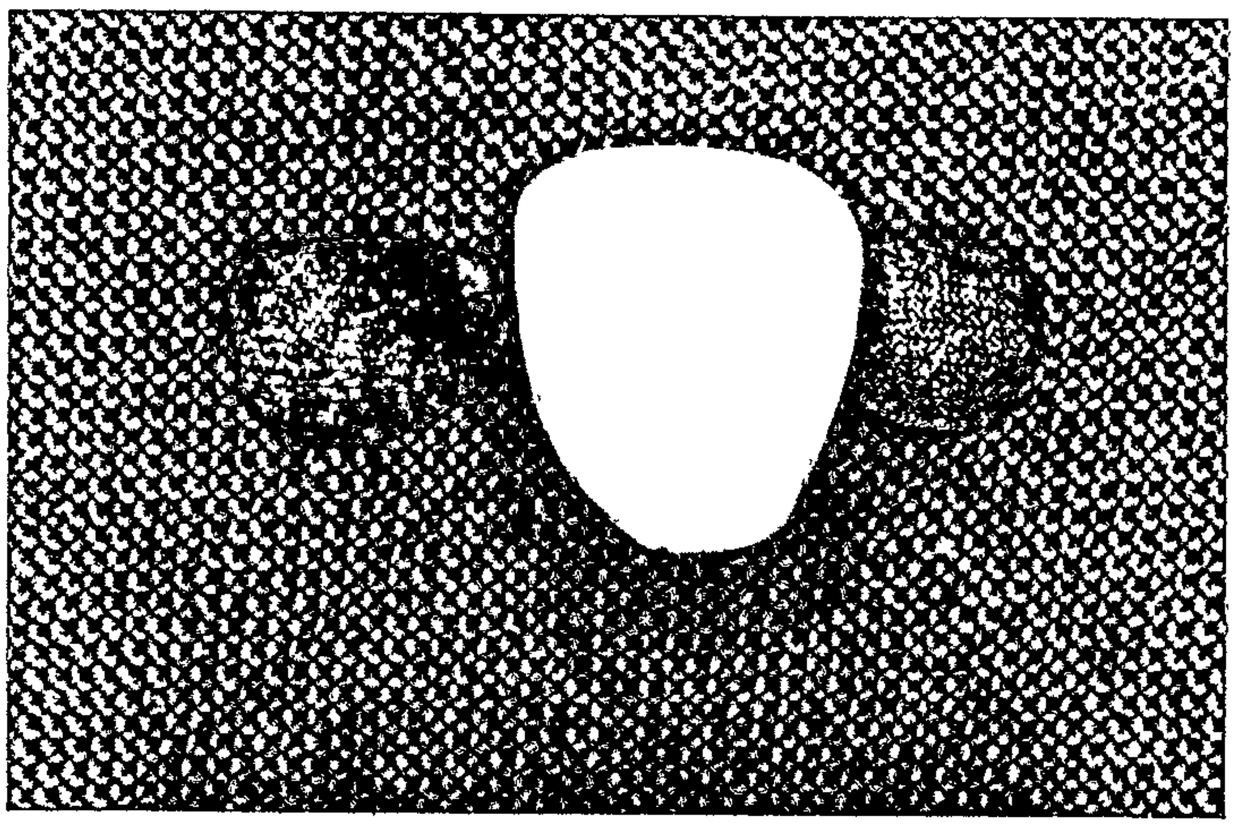

Figure 5.4
The Maryland bridge whose wax pattern is depicted in Figure 5.3. The surface morphology on the bridge retainer produced by the Duralingual profiles can be seen.

Figure 5.5
The Maryland bridge depicted in Figure 5.4 cemented in the mouth.

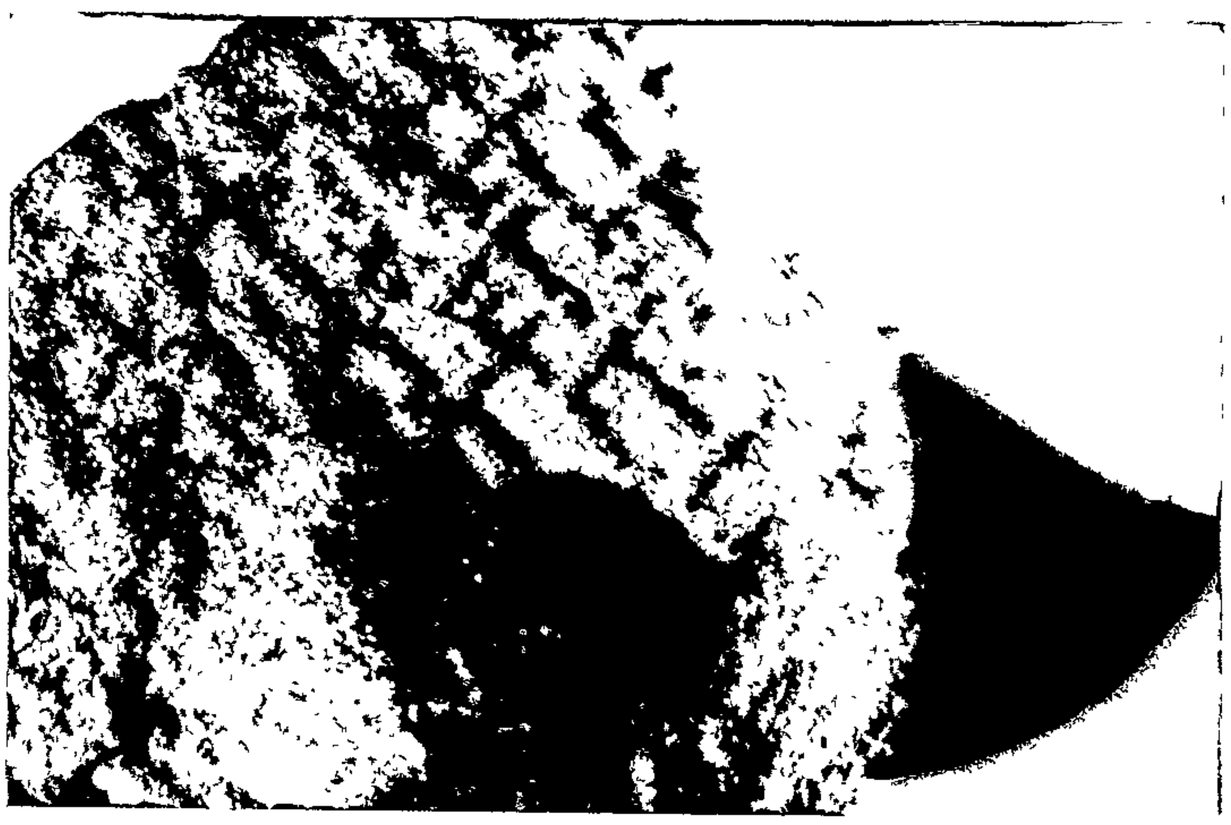

Figure 5.6
A magnified view of a Maryland bridge retainer constructed using Duralingual profiles. The surface morphology does not appear to have been reproduced well during the casting process and does not appear very retentive. In addition, the area of the cingulum rest seat does not contain a retentive surface.

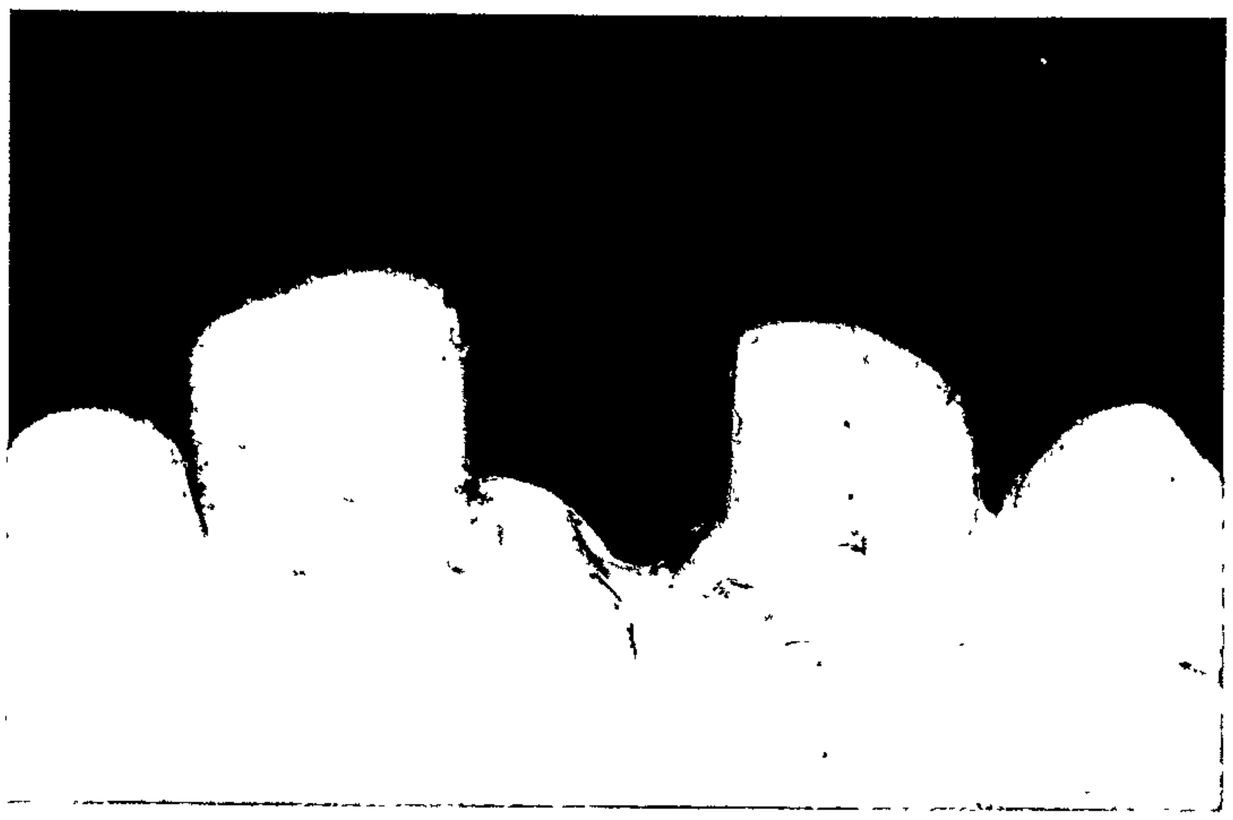

Figure 5.7
A die-stone model of a clinical case where a Maryland bridge is to be constructed using the Lost-salt technique. The abutment teeth have been coated with petroleum jelly.

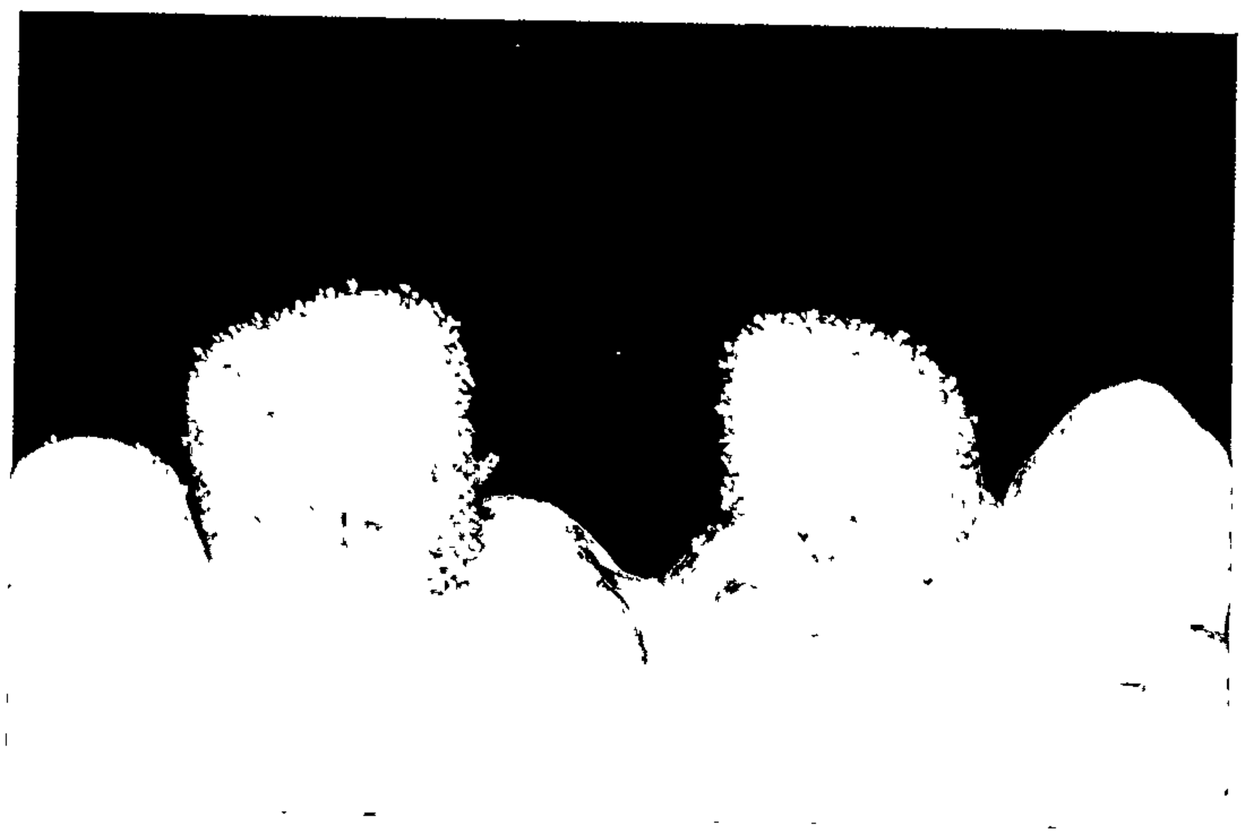

Figure 5.8
The model depicted in Figure 5.7 with salt crystals applied to the abutment teeth. The crystals adhere to the petroleum jelly.

Figure 5.9
The model depicted in Figure 5.8 showing an acrylic pattern material (Duralay, Reliance Dental Manufacturing Co., Worth, Illinois, USA) applied on and around the salt crystals.

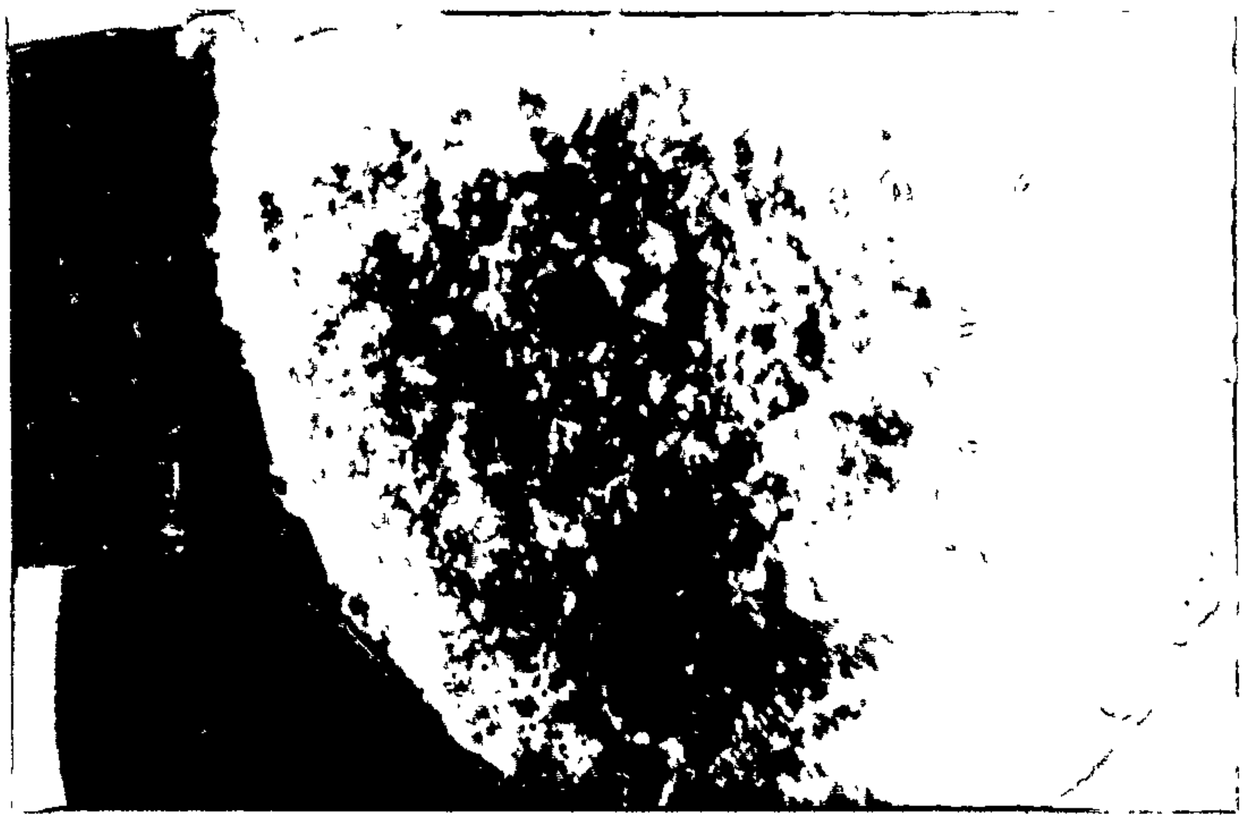

Figure 5.10
A magnified view of an acrylic pattern of one of the retainers from the bridge depicted in Figure 5.9. The salt crystals have been washed out in an ultrasonic bath. A mechanically retentive surface has been produced.

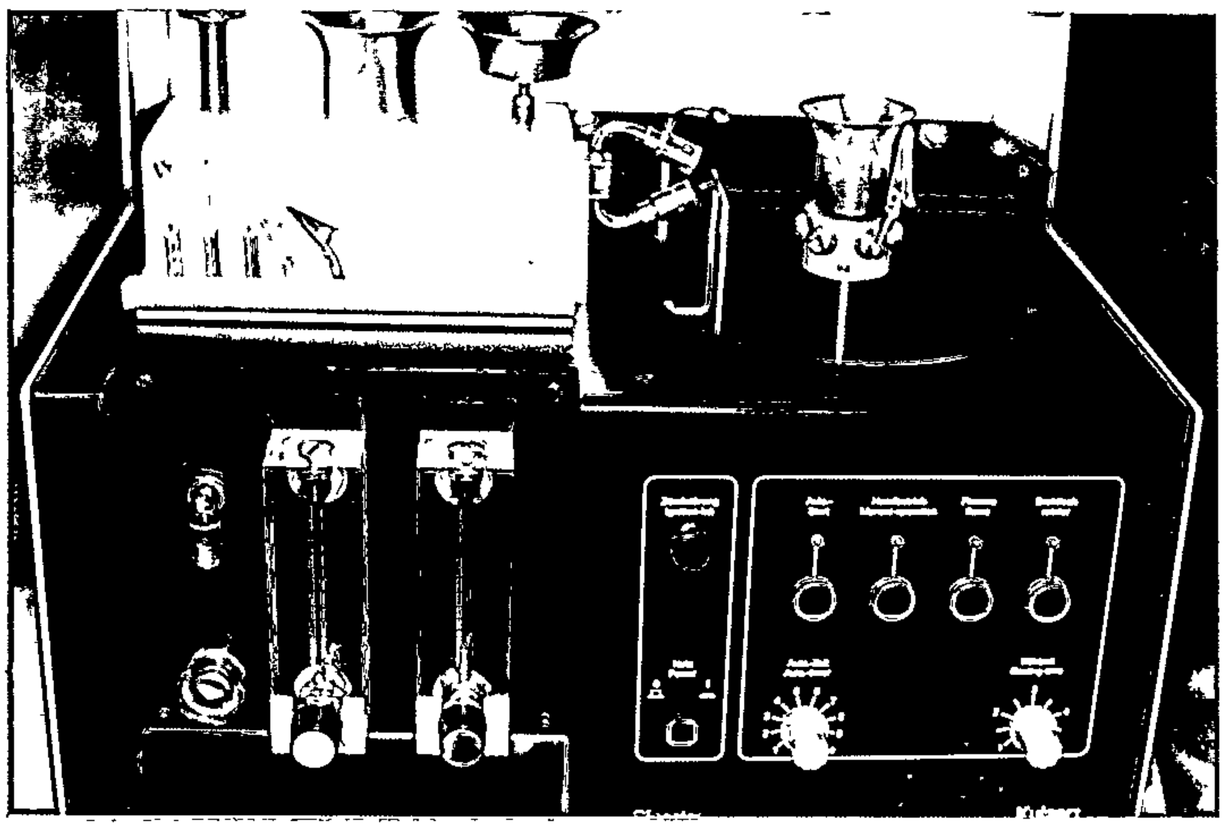

Figure 5.11
The Kulzer Silicoater machine.

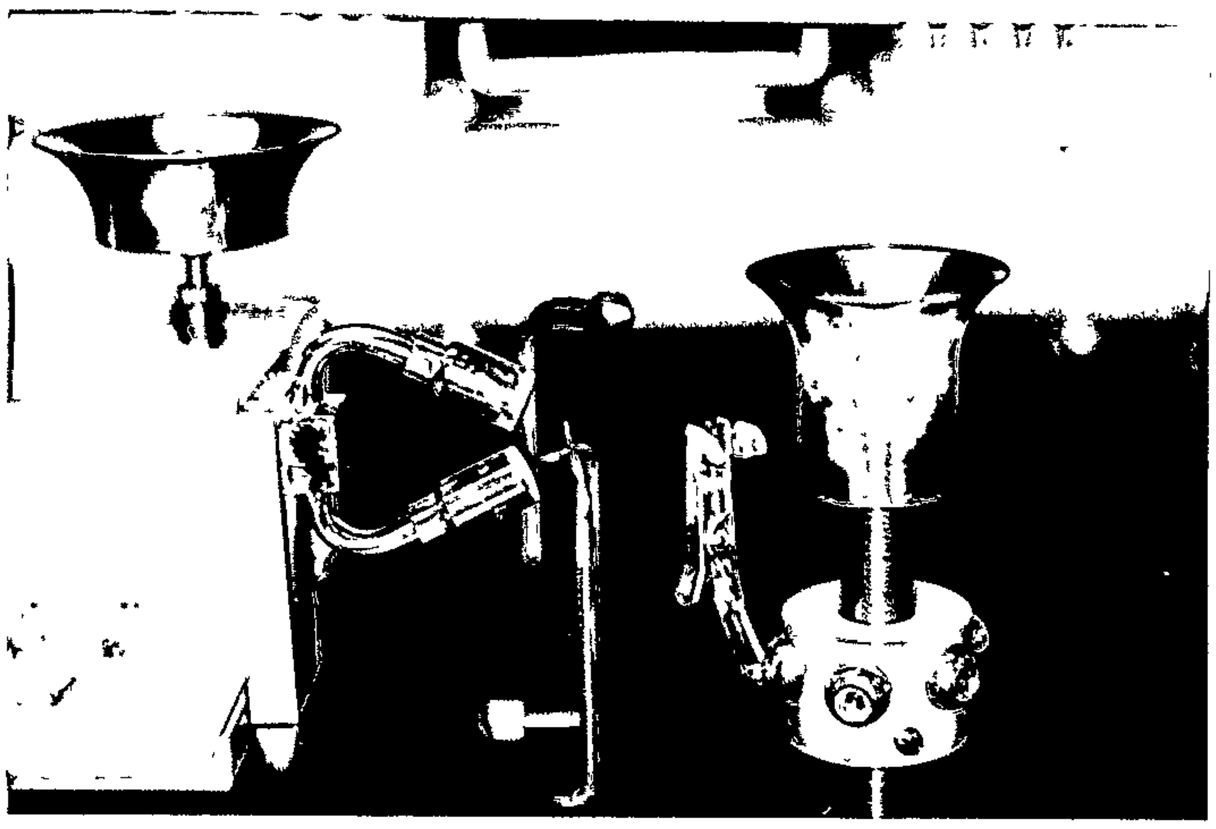

Figure 5.12
A close-up view of the Kulzer Silicoater machine showing the gas flame nozzles and the rotating spindle that holds the bridge and passes it successively through the gas flame.

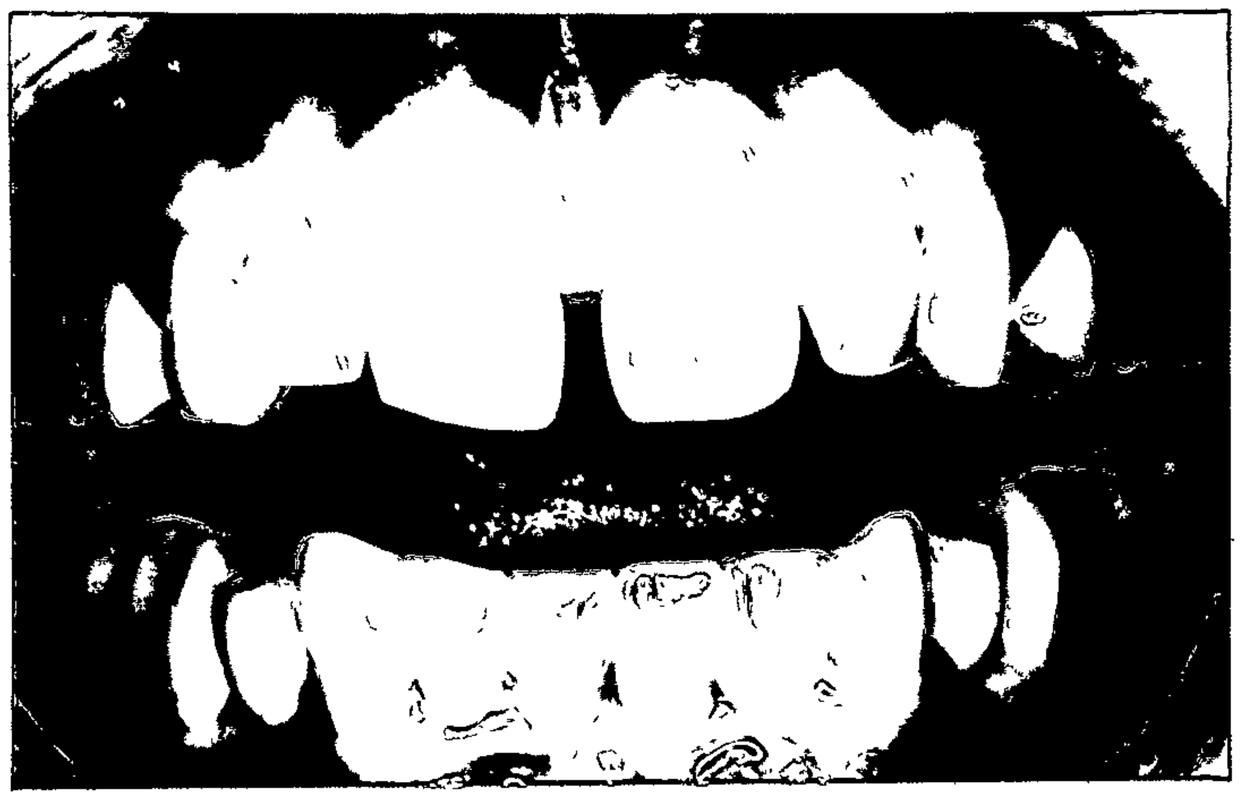

Figure 7.2a
A Maryland bridge replacing four mandibular anterior teeth in one span together with two mandibular premolars. This bridge has been successfully retained for two years.

Figure 7.2b
The lingual view of the Maryland bridge depicted in Figure 7.2a.

Figure 7.3a
A patient with a Class II division 1 anterior occlusal relationship with incomplete overbite. There is a more than adequate space for the lingual retainers of a cast-metal resin bonded bridge.

Figure 7.3b
A patient with a Class II division 2 anterior occlusal relationship where the deep overbite precludes the placement of a lingual resin bonded retainer.

Figure 7.4
A Maryland bridge originally designed with a retainer on the upper lateral incisor abutment. However, this retainer failed within two months of cementation. It was sectioned from the bridge which has continued to function as a cantilevered design for three and a half years.

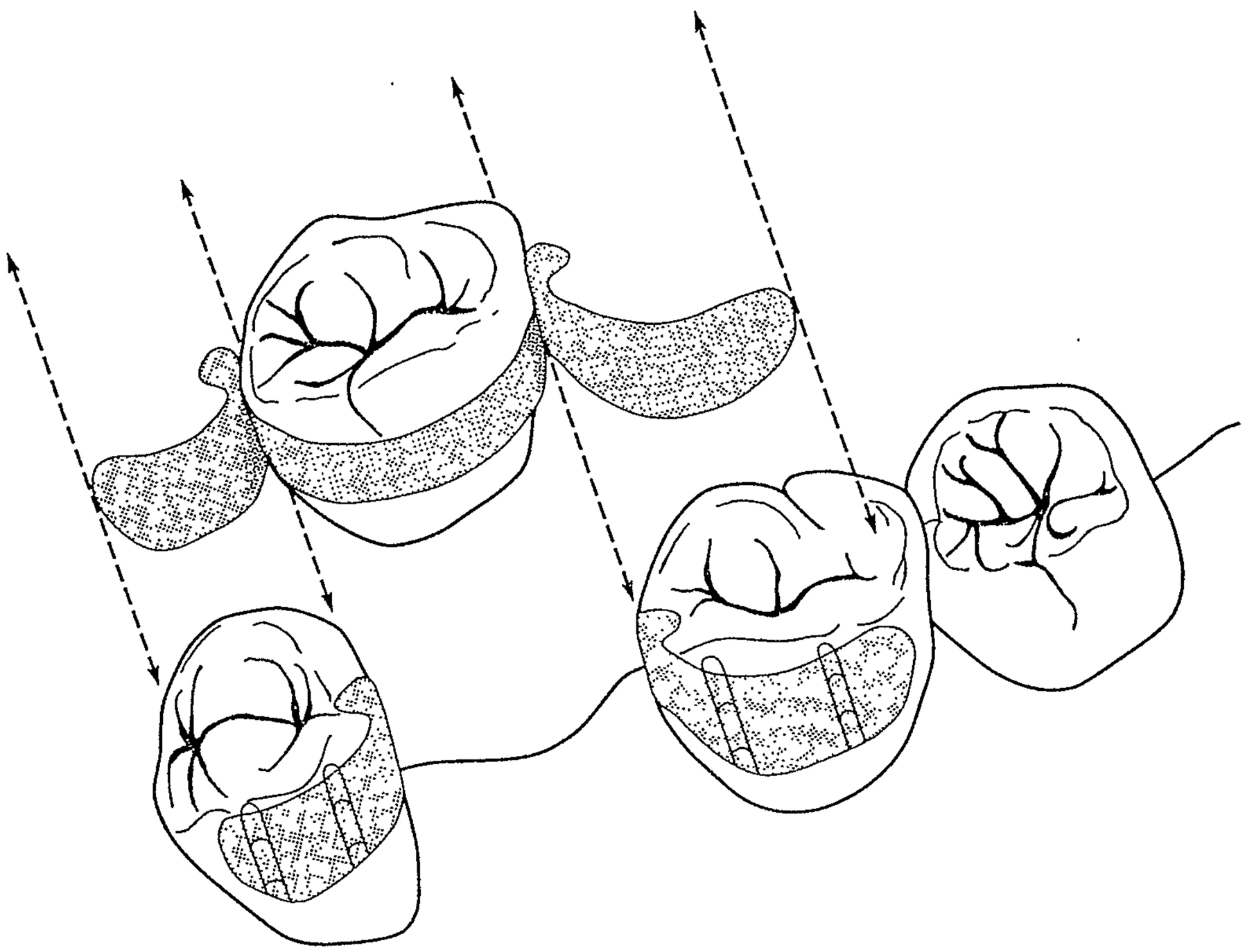

Figure 7.5
Diagrammatic representation of guide plane preparation on cast-metal resin bonded bridge abutment teeth. Note the limited path of insertion and the accessory retentive grooves (from Simonsen et al, 1983).

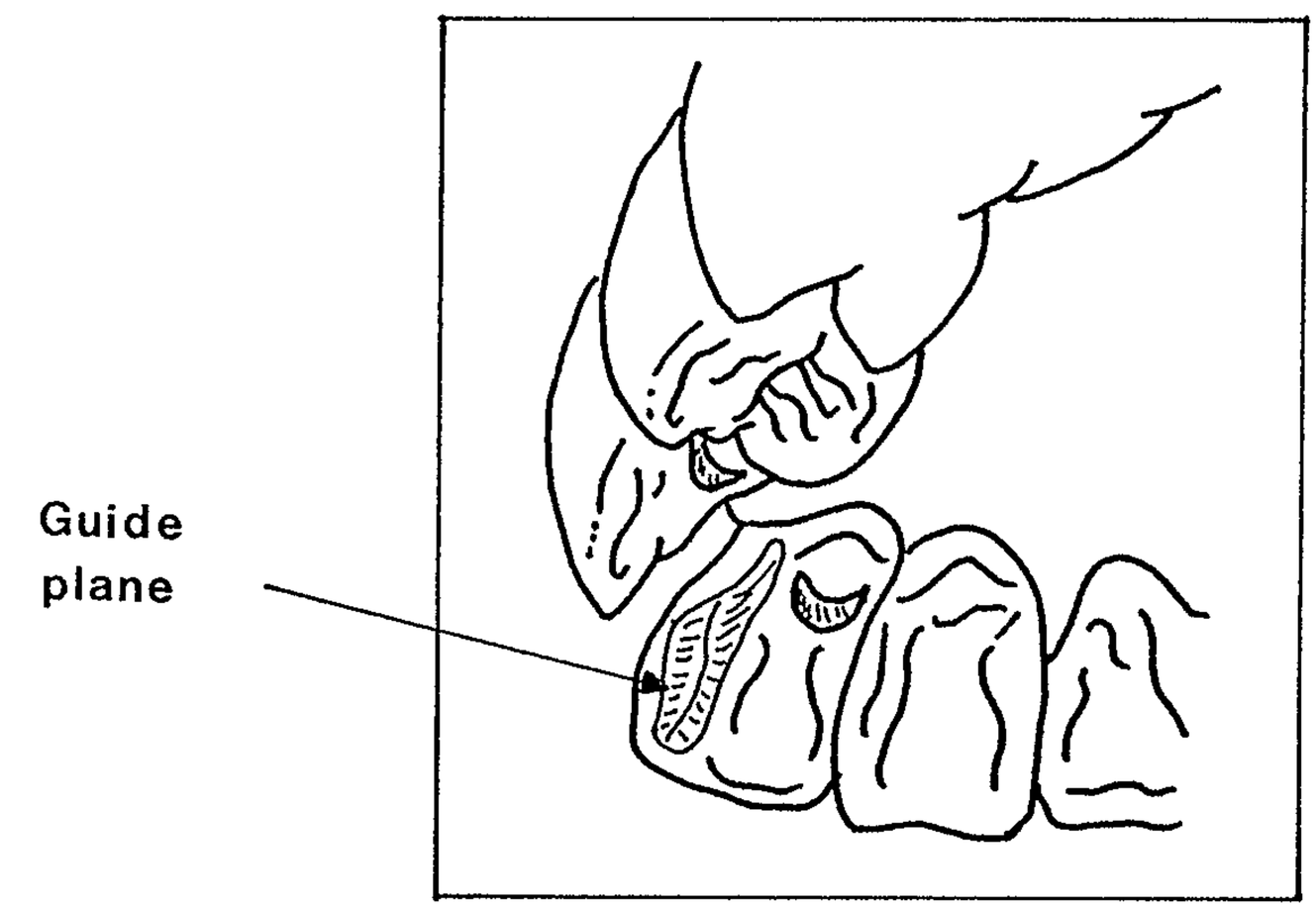

Figure 7.6
Diagrammatic representation of guide plane and cingulum rest seat preparation in anterior abutment teeth for cast-metal resin bonded bridges (from Simonsen et al, 1983).

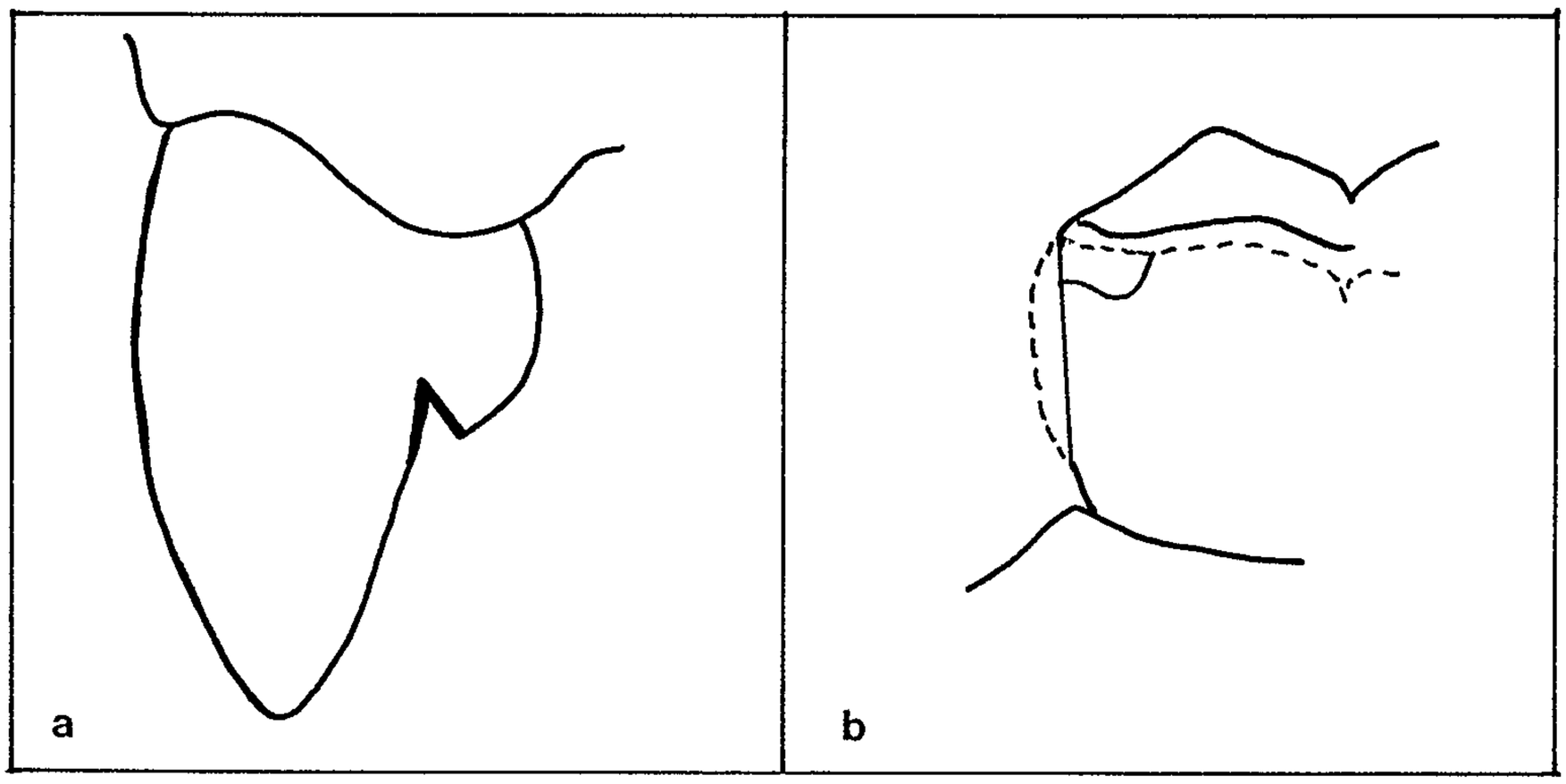

Figure 7.7a
Diagrammatic representation of the V-shaped cingulum rest prepared in anterior cast-metal resin bonded bridge abutments (from Simonsen et al, 1983).

Figure 7.7b
Diagrammatic representation of the occlusal rest prepared in the marginal ridge area of posterior cast-metal resin bonded bridge abutments (from Simonsen et al, 1983).

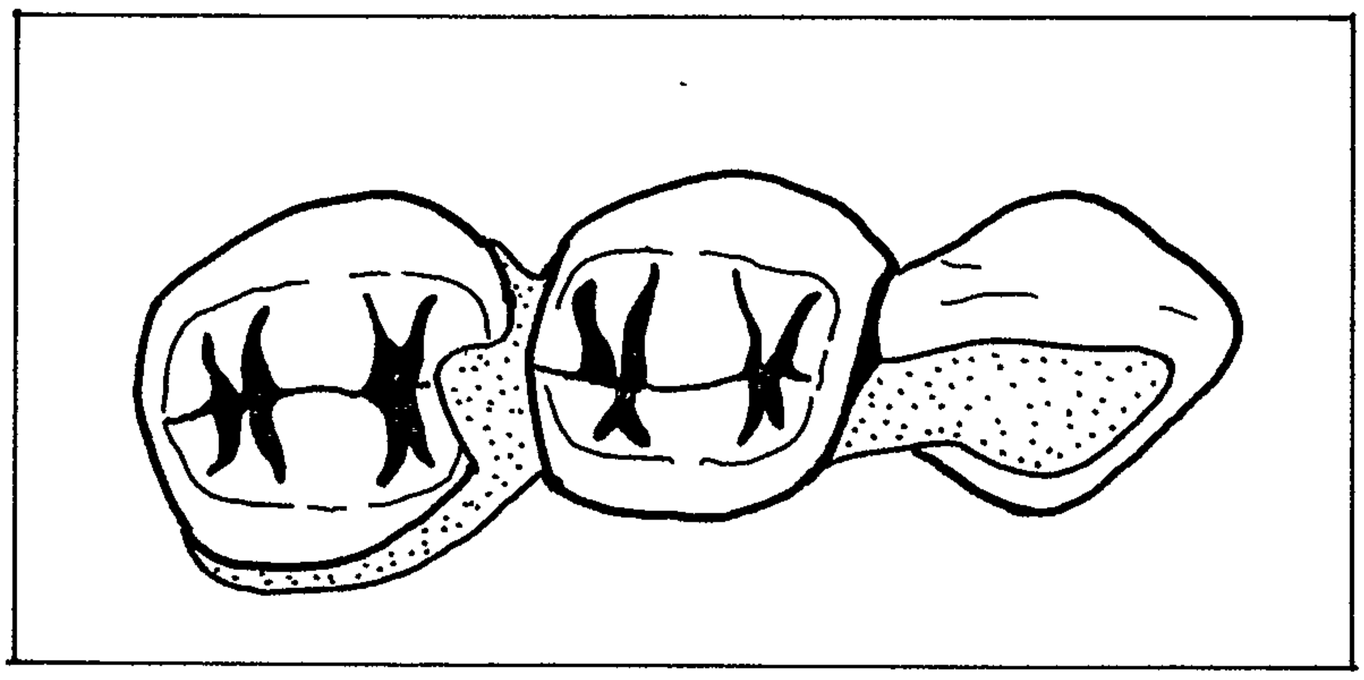

Figure 7.8
Diagrammatic representation of the concept of proximal wrapping. The distal abutment has an extension of the casting around the buccal aspect of the tooth. On the anterior abutment, where aesthetics are a consideration, the pontic has been extended onto the buccal surface of the tooth (from Sykes and Walton, 1983).

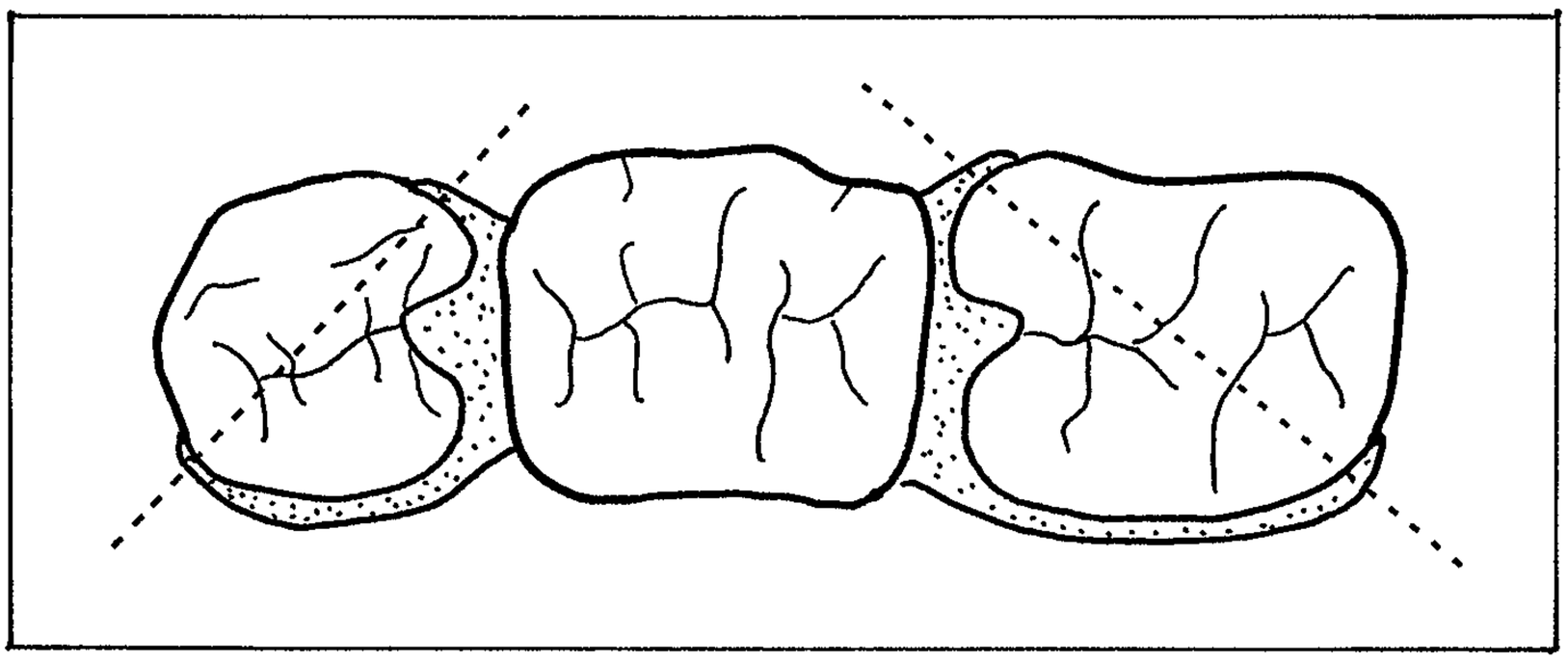

Figure 7.9
Diagrammatic representation of the concept of 180° wrap-around in which the abutment tooth is mechanically engaged by the casting (from Simonsen et al, 1983).

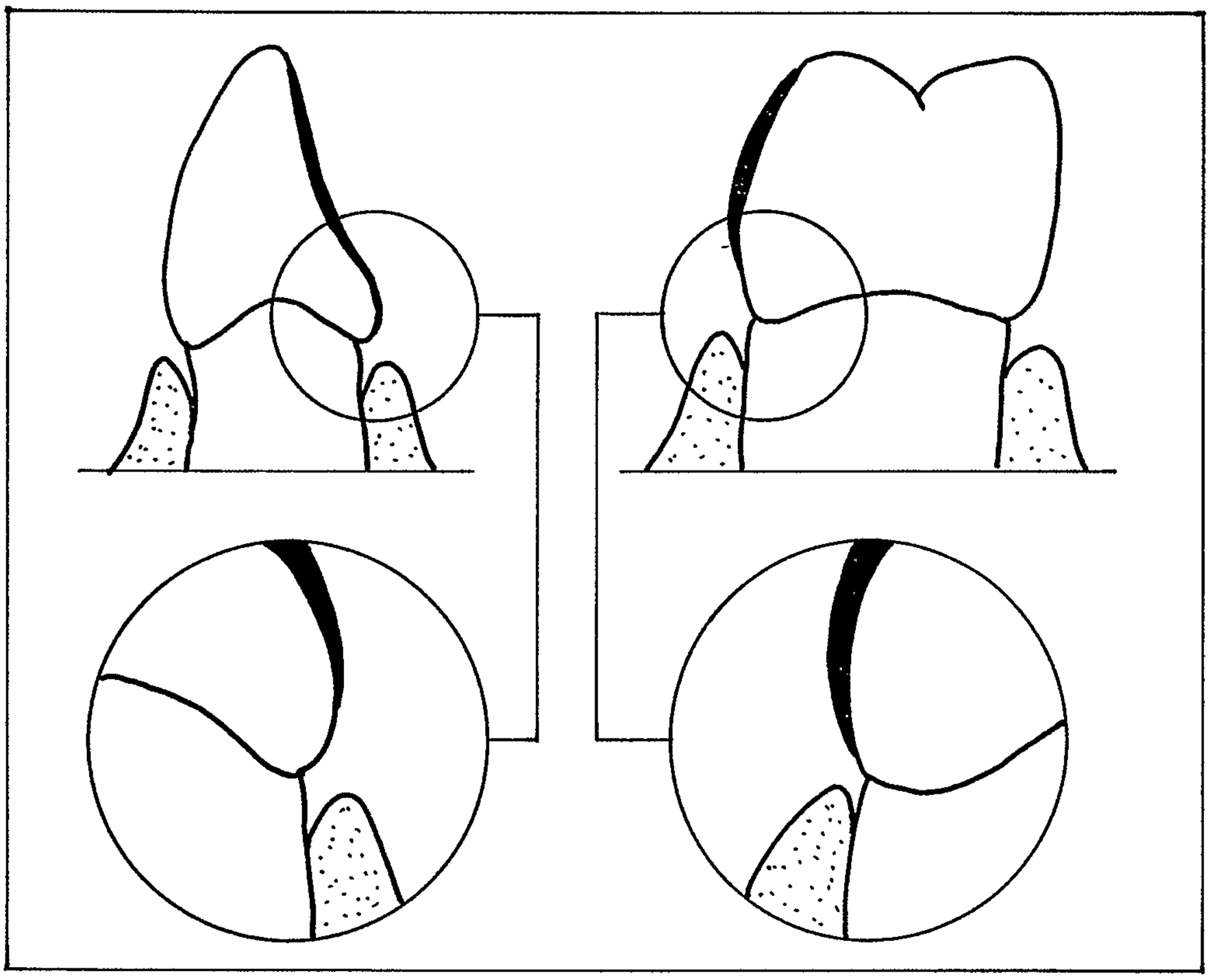

Figure 7.10
Diagrammatic representation of knife-edged margin configurations for resin bonded retainers on anterior and posterior abutment teeth (from Wood, 1982).

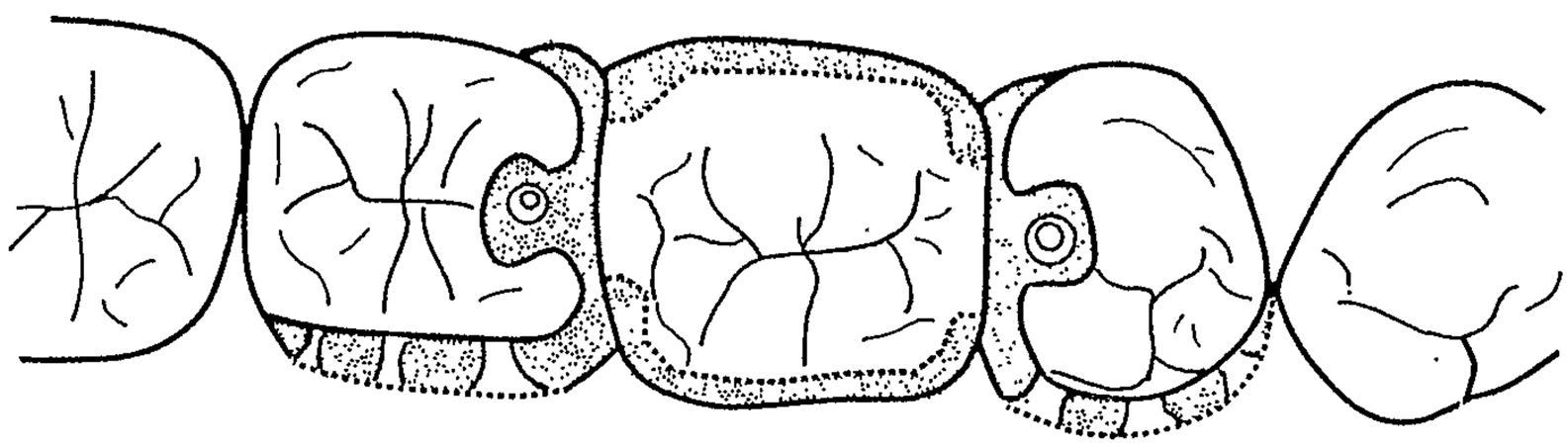

Figure 7.11a
Diagrammatic representation of a posterior Rochette bridge (from Livaditis, 1980).

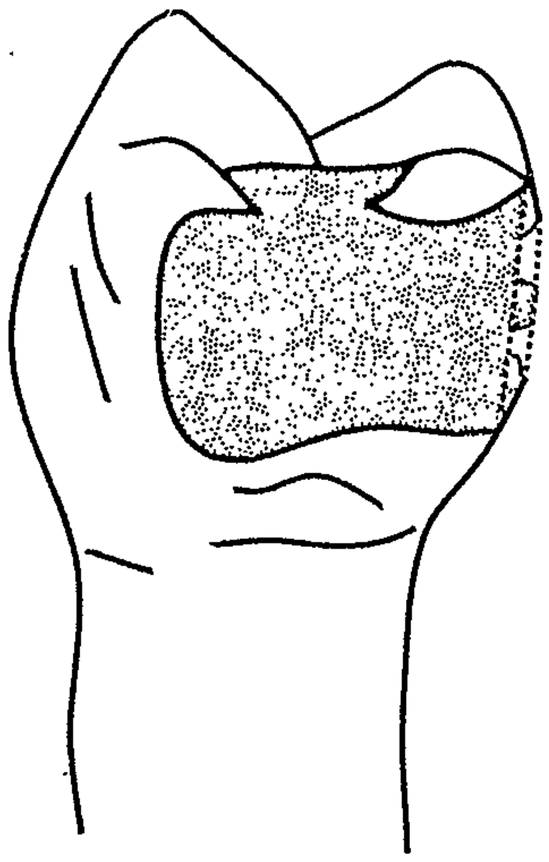

Figure 7.11b
Diagrammatic representation of a posterior Rochette bridge abutment tooth (from Livaditis, 1980).

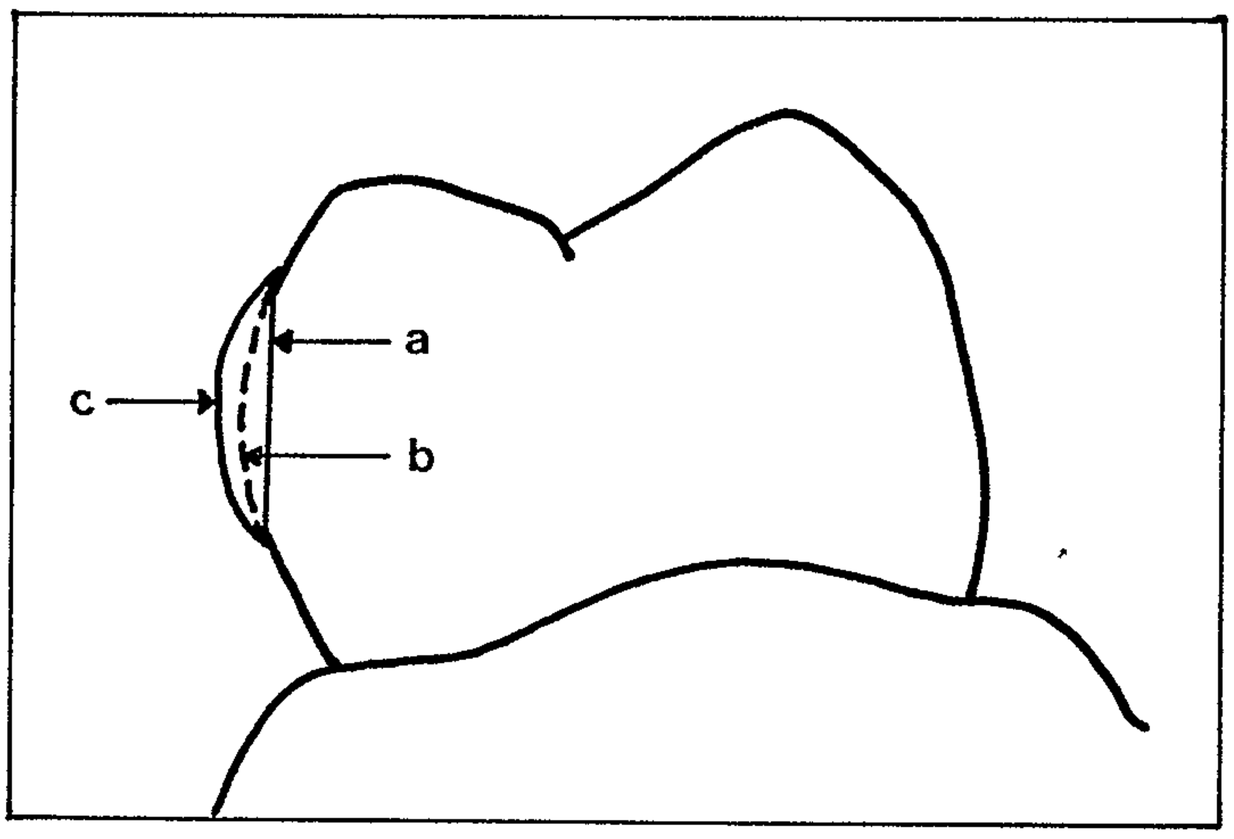

Figure 7.12
Diagrammatic representation of the eventual thickness of a resin bonded retainer after guide plane preparation. If 0.2mm of enamel is removed (a) and the retainer is 0.5mm thick (c) there will be only 0.3mm added to the original contour (b) of the tooth (from Simonsen et al, 1983).

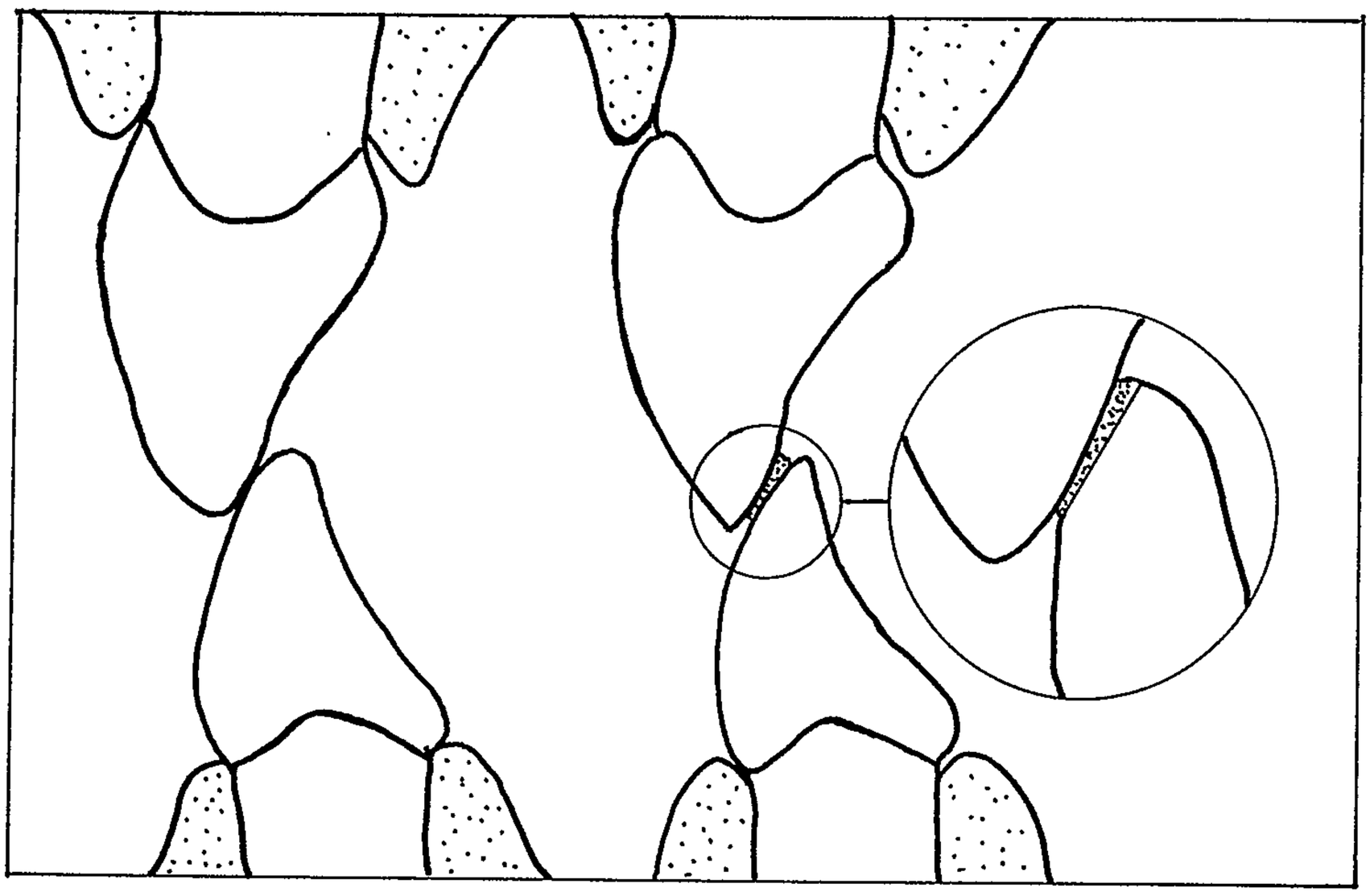

Figure 7.13
Diagrammatic representation of the use of composite resin bonded to the opposing tooth of a cast-metal resin bonded bridge in order to hold the occlusal contacts after the tooth has been adjusted to provide occlusal clearance for lingual retainer (from Wood and Halpern, 1983).

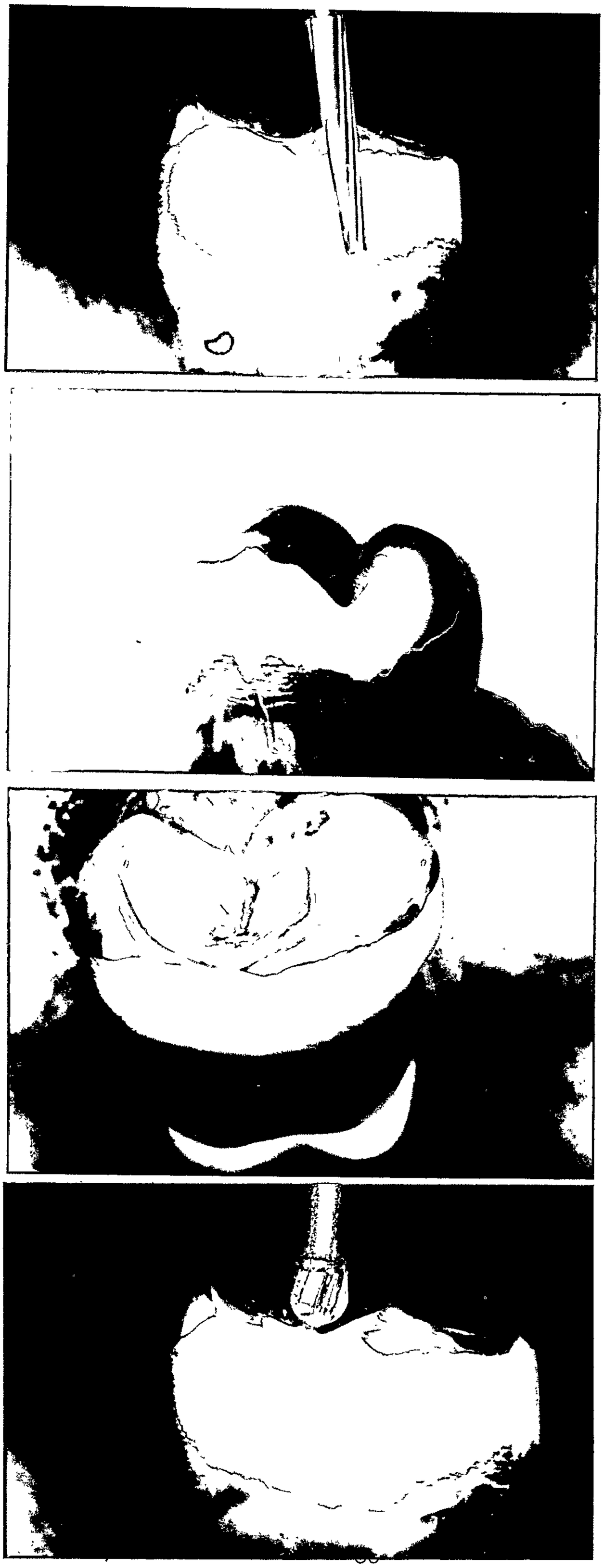

Figure 7.14
Preparation of a posterior abutment for a resin bonded retainer.

a) A guide plane is prepared on the proximal and lingual surface.

b) Supplemental vertical retention grooves.

c) The guide plane is extended onto the buccal surface of the abutment to gain proximal wrapping.

d) Preparation of the occlusal rest seat.

Figure 7.15
Preparation sequence for an anterior cast-metal resin bonded bridge.

a) Preparation of the cingulum rest seat.

b) Preparation of the proximal guide planes.

c) The prepared guide planes showing their extension onto the facial surfaces of the abutments.

d) A further view of the prepared guide planes.

Figure 7.15 cont.
Preparation sequence for an anterior cast-metal resin bonded bridge.

e) Adjustment of the occlusal contact areas to provide occlusal clearance for the retaining flange.

f) Occlusal clearance prepared.

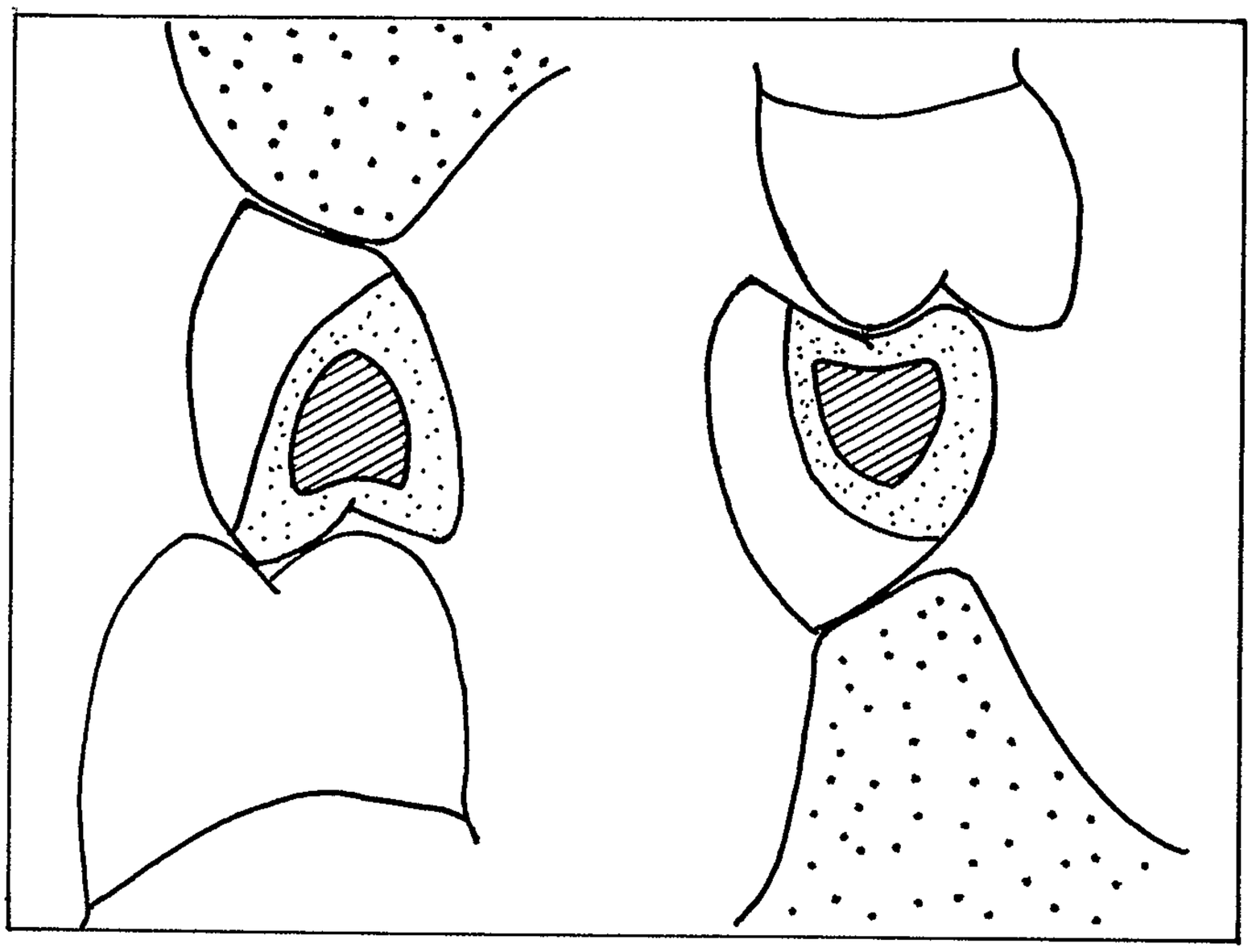

Figure 7.16
Diagrammatic representation of ridge-lap designs of maxillary and mandibular pontic teeth (from Shillingburg et al, 1981).

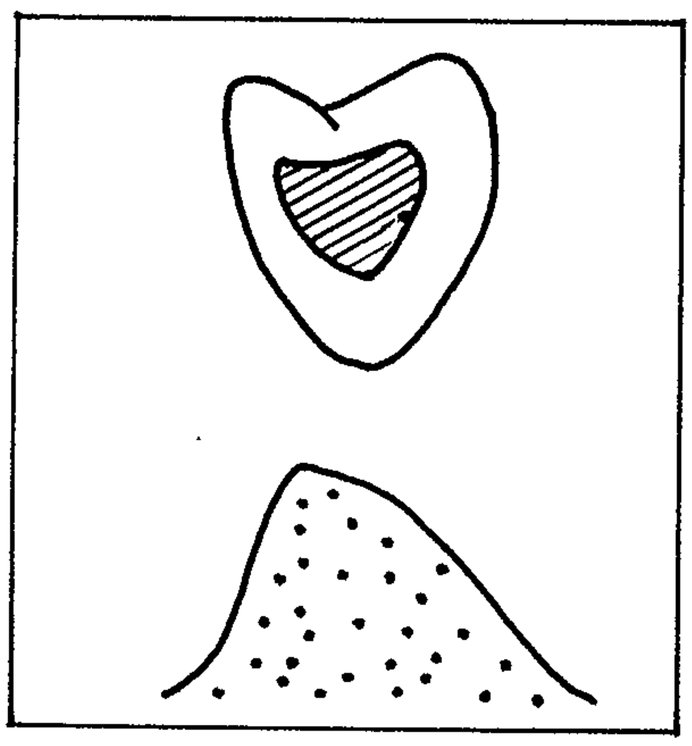

Figure 7.17
Diagrammatic representation of a hygienic pontic design (from Shillingburg et al, 1981).

Figure 7.18
A clinical case where rubber dam has been placed, the abutment teeth ligated with dental floss, and mylar strips placed distal to the abutments prior to cementation of a cast-metal resin bonded bridge.

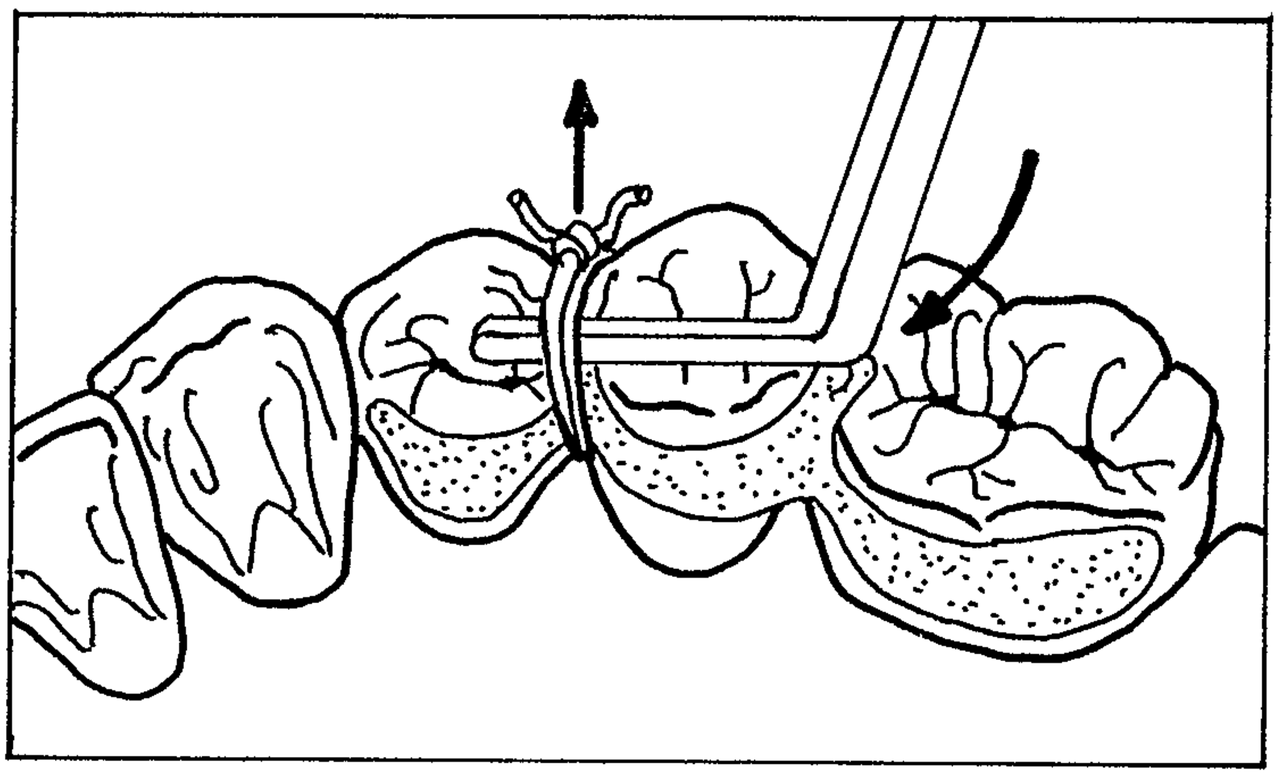

Figure 8.1
Diagrammatic representation of a method of Maryland bridge removal. See text for explanation (from Wood and Halpern, 1983).

Figure 9.1a
An anterior Maryland bridge replacing an upper lateral incisor. The bridge has been successfully retained for one year.

Figure 9.1b
Lingual view of the Maryland bridge depicted in Figure 9.1a

Figure 9.2a
A patient with a missing upper lateral incisor showing caries, periodontal inflammation and denture stomatitis as a result of wearing an acrylic removable partial denture.

Figure 9.2b
The same patient as depicted in Figure 9.2a after the placement of a Maryland bridge showing the improvement in soft tissue health. The bridge has been successfully retained for two years.

Figure 9.3a
A Maryland bridge replacing an upper canine.

Figure 9.3b
Lingual view of the Maryland bridge depicted in Figure 9.3a. The retainer on the distal abutment has been extended to encompass the available enamel surface. A conventional prosthesis would probably have required full veneer crown preparations on both abutments.

Figure 9.4
A Maryland bridge whose failure is depicted in Figure 9.8.

Figure 9.5
Two cast-metal resin bonded bridges replacing upper first molar teeth. The one on the right has been constructed using the Lost-salt technique. The one on the left has been constructed using the Silicoater technique. Both bridges have been successfully retained for one year.

Figure 9.6a
A Rochette bridge constructed from a cobalt-chromium framework with an acrylic pontic.

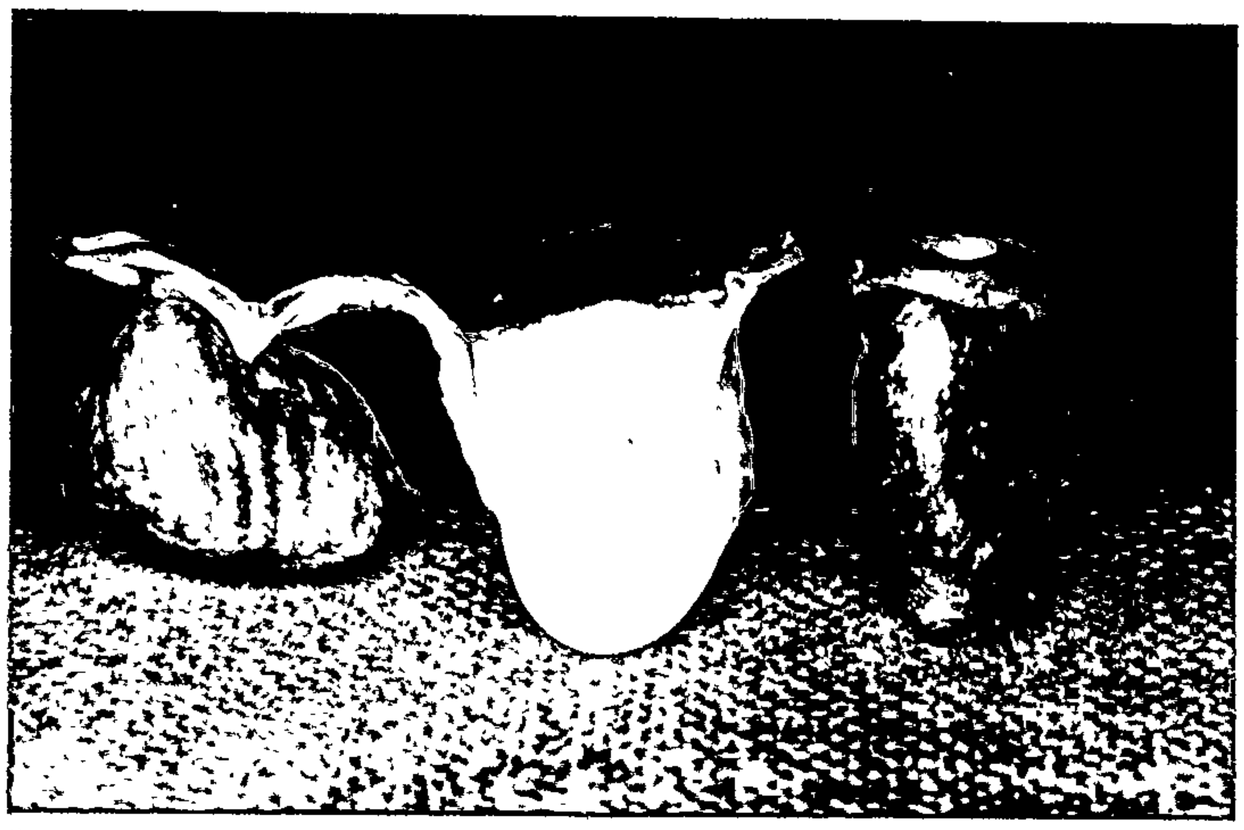

Figure 9.6b
The Rochette bridge depicted in Figure 9.6a after failure through a retentive perforation. The perforations were too large and seriously weakened the structure.

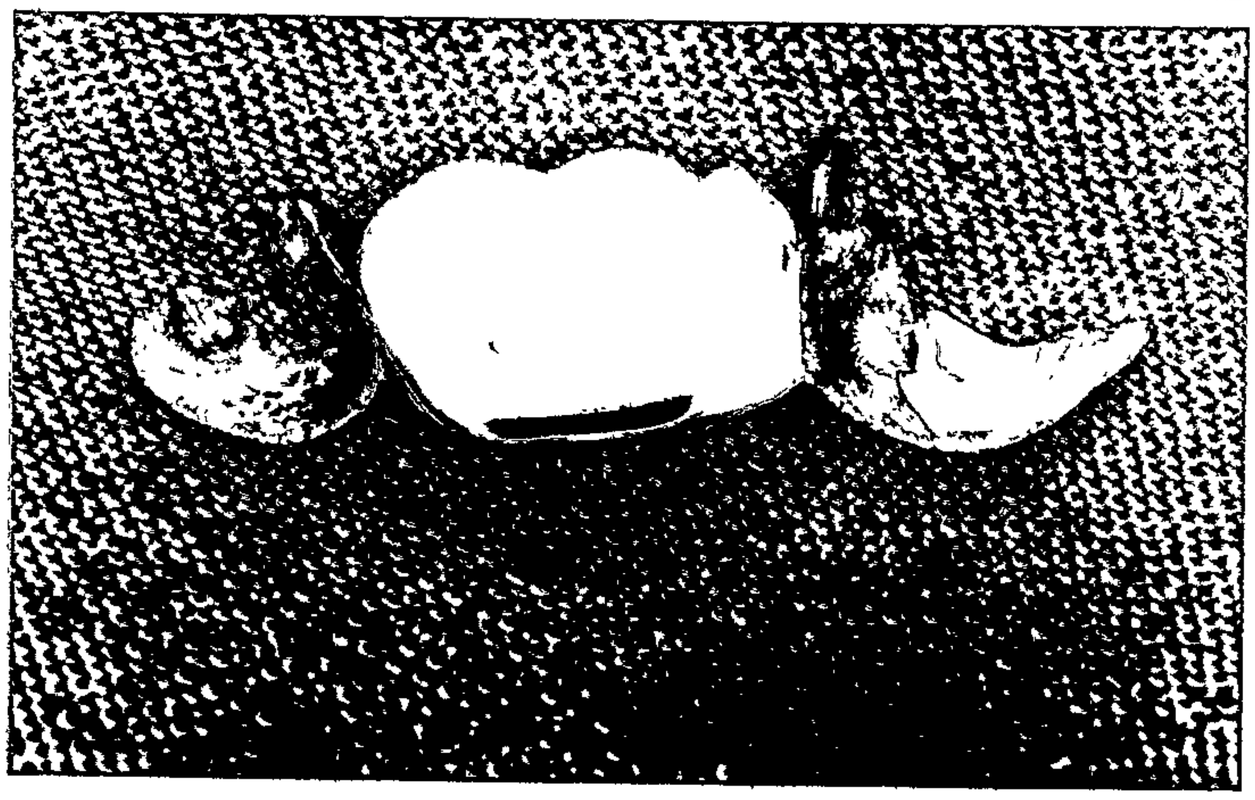

Figure 9.7a
A failed posterior Maryland bridge with some composite resin luting cement retained on the distal retainer.

Figure 9.7b
The abutments for the bridge depicted in Figure 9.7a after bridge failure. Note the absence of composite resin luting cement on these abutments. This suggests that the enamel etching was inadequate and the lack of rubber dam placement at cementation was suspected. The bridge was subsequently rebonded, successfully, under rubber dam.

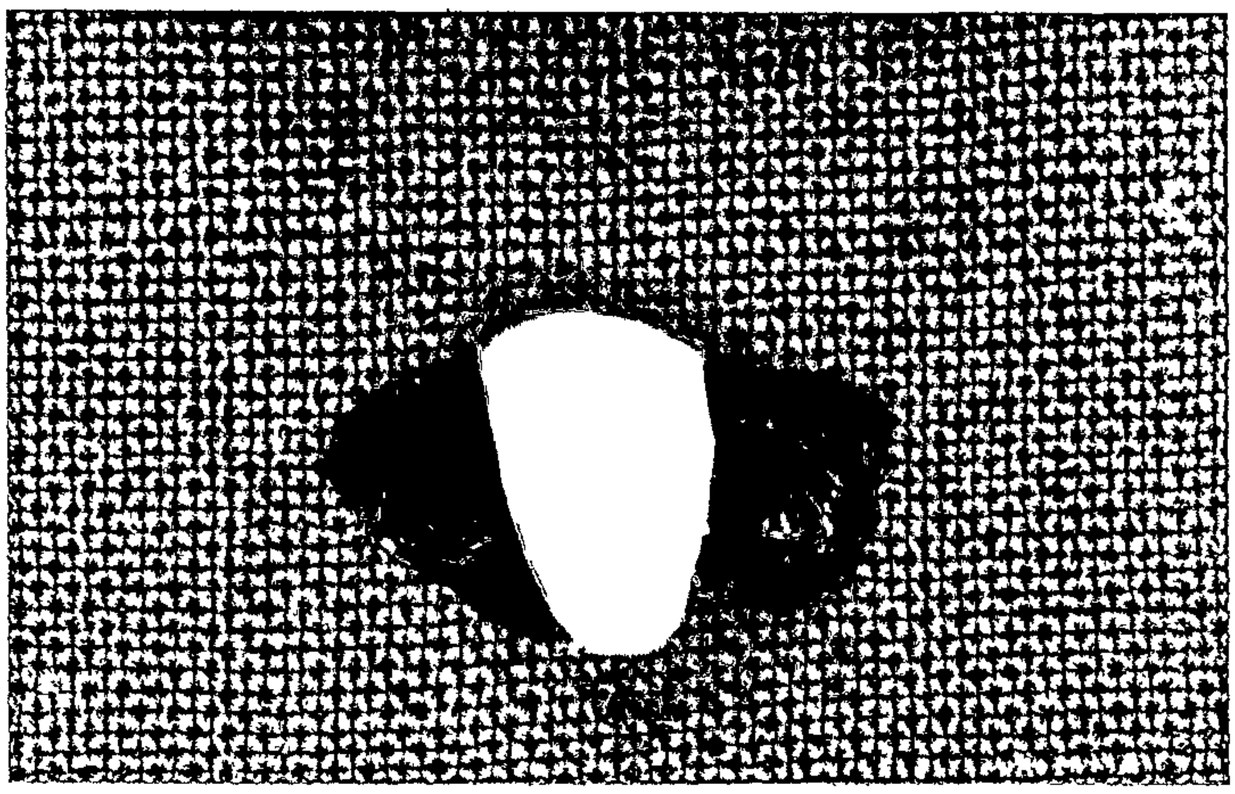

Figure 9.8a
A Maryland bridge replacing a lower lateral incisor after bridge failure. Note the lack of composite resin luting cement adhering to the bridge retainers.

Figure 9.8b
The Maryland bridge depicted in Figure 9.8a. Note the composite resin luting cement retained on the abutment teeth. This patient was a heavy smoker and only reported the bridge failure some time after it had occurred.

Figure 9.9a
A Maryland bridge replacing an upper canine where the mesial retainer has been extended onto the central incisor since the lateral incisor had been considered inadequate as a sole abutment.

Figure 9.9b
The Maryland bridge depicted in Figure 9.9a. after failure through an excessively thin portion of the casting. Note that the composite resin luting cement is retained on the enamel surface.

Figure 9.10
An anterior Maryland bridge showing separation of the smallest retainer from its abutment tooth whilst the larger retainer is still bonded successfully.

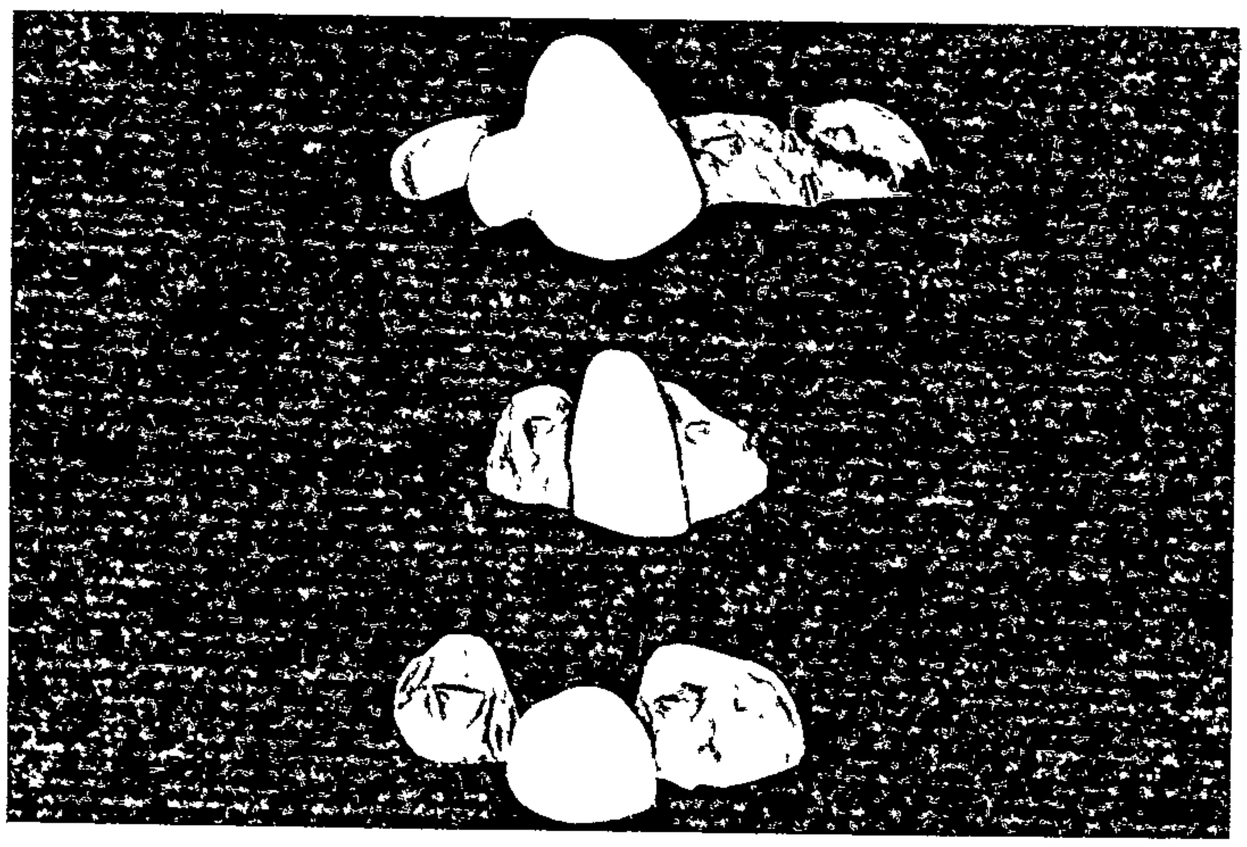

Figure 10.1
The three Maryland bridges used in the pilot study to determine the most common degree of error in the surface area estimation.

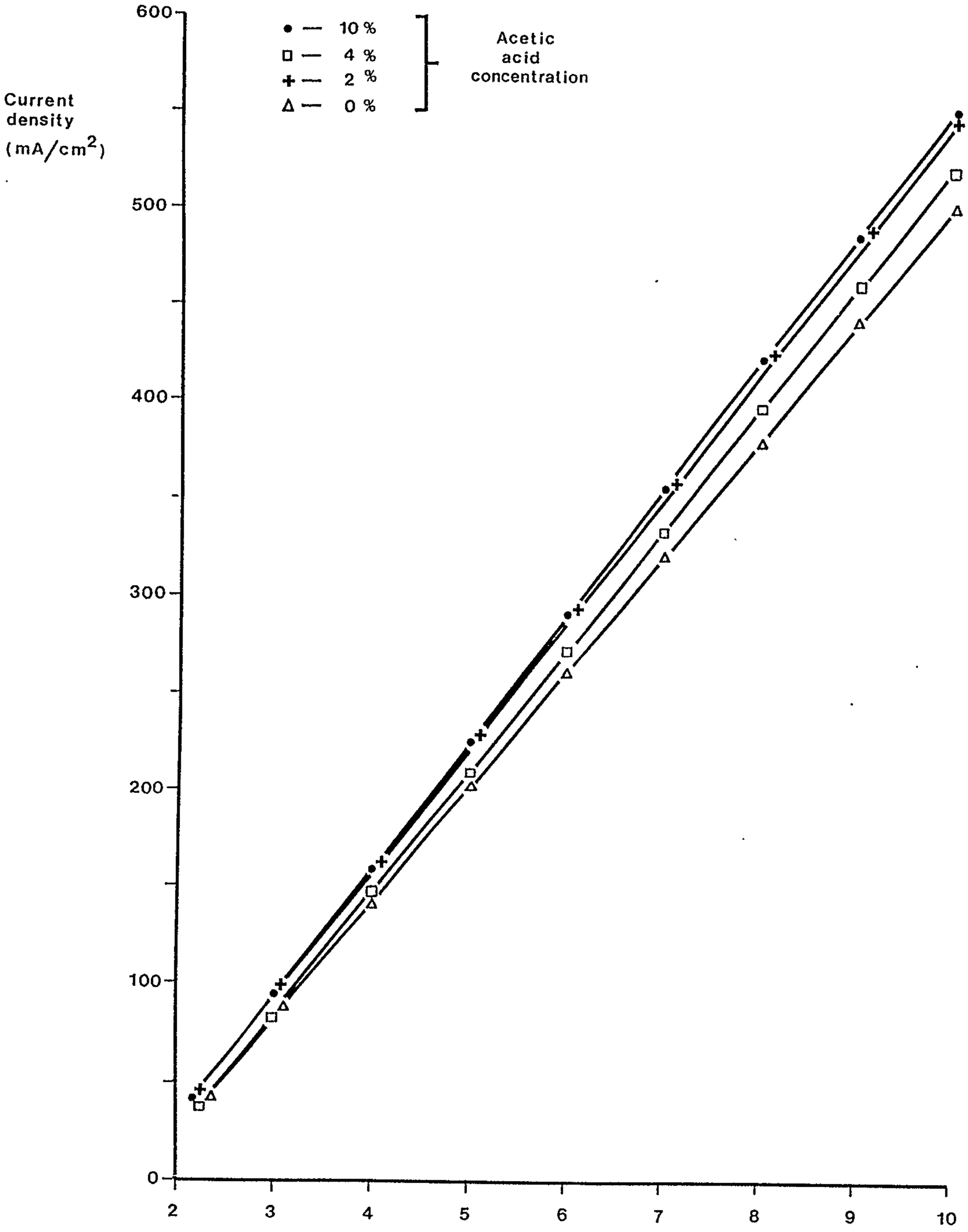

Figure 10.2
Potentiostatic-anodic-current density (PACD) curves for etching solutions with variations in acetic acid concentration. All solutions contained 0.11N nitric acid.

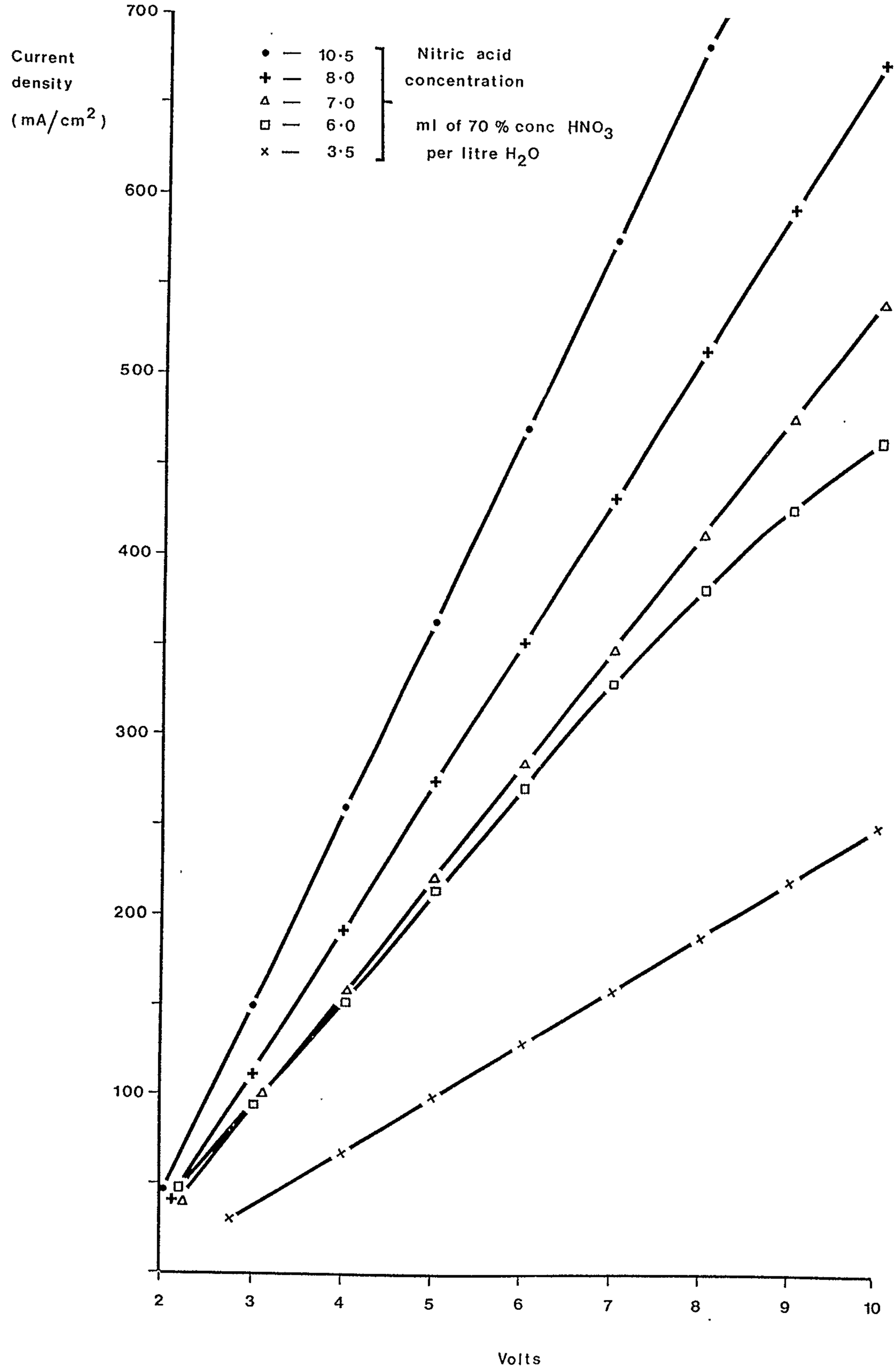

Figure 10.3
Potentiostatic-anodic-current density (PACD) curves for etching solutions with variations in nitric acid concentration. All solutions contained 2 per cent acetic acid.

10.4a
(X 50)

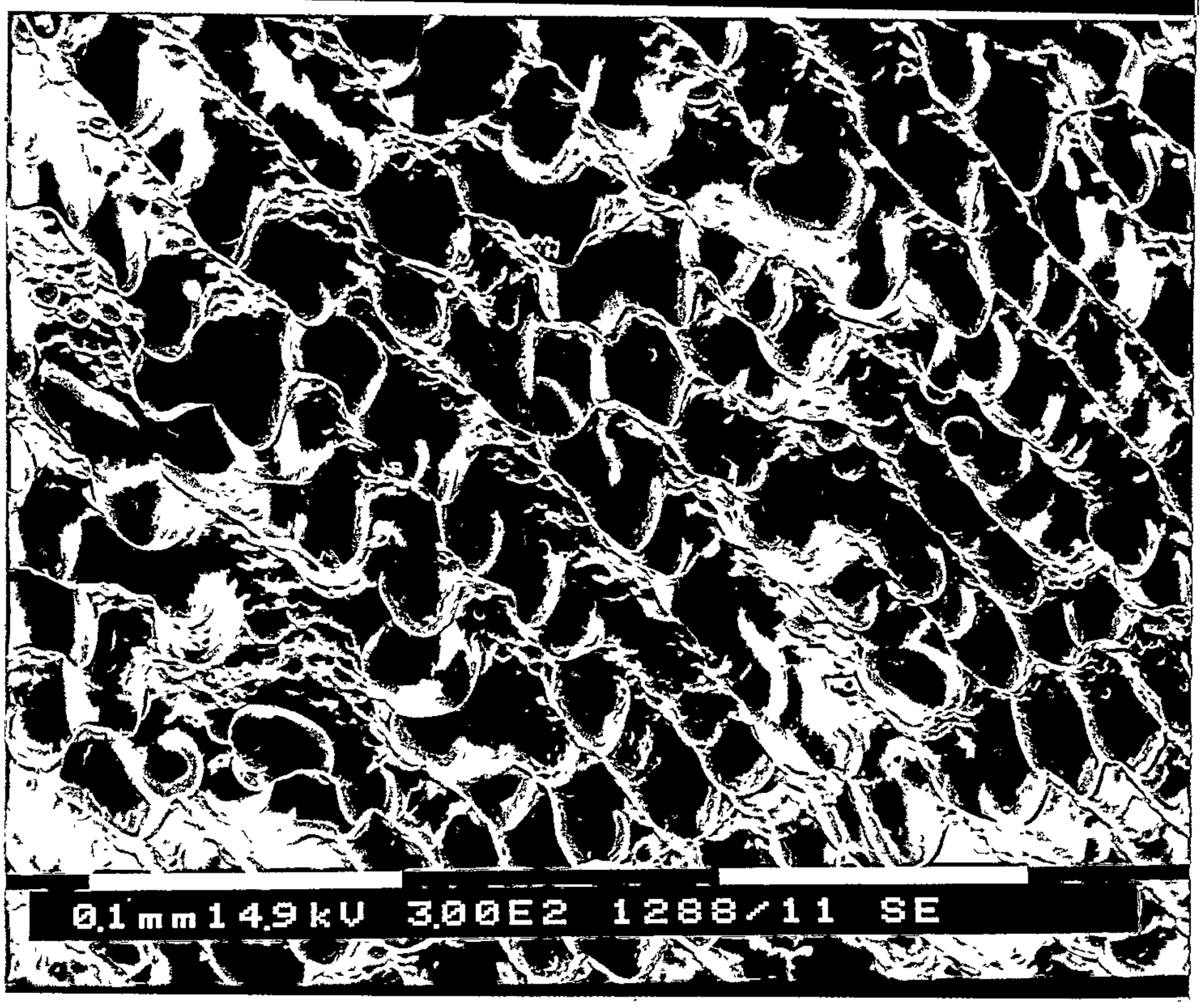

10.4b
(X 300)

Figure 10.4a,b

SEM of a Microbond NP^2 specimen electrolytically etched in a solution containing .0.17N HNO_3 and 2 per cent acetic acid for the preparatory study.

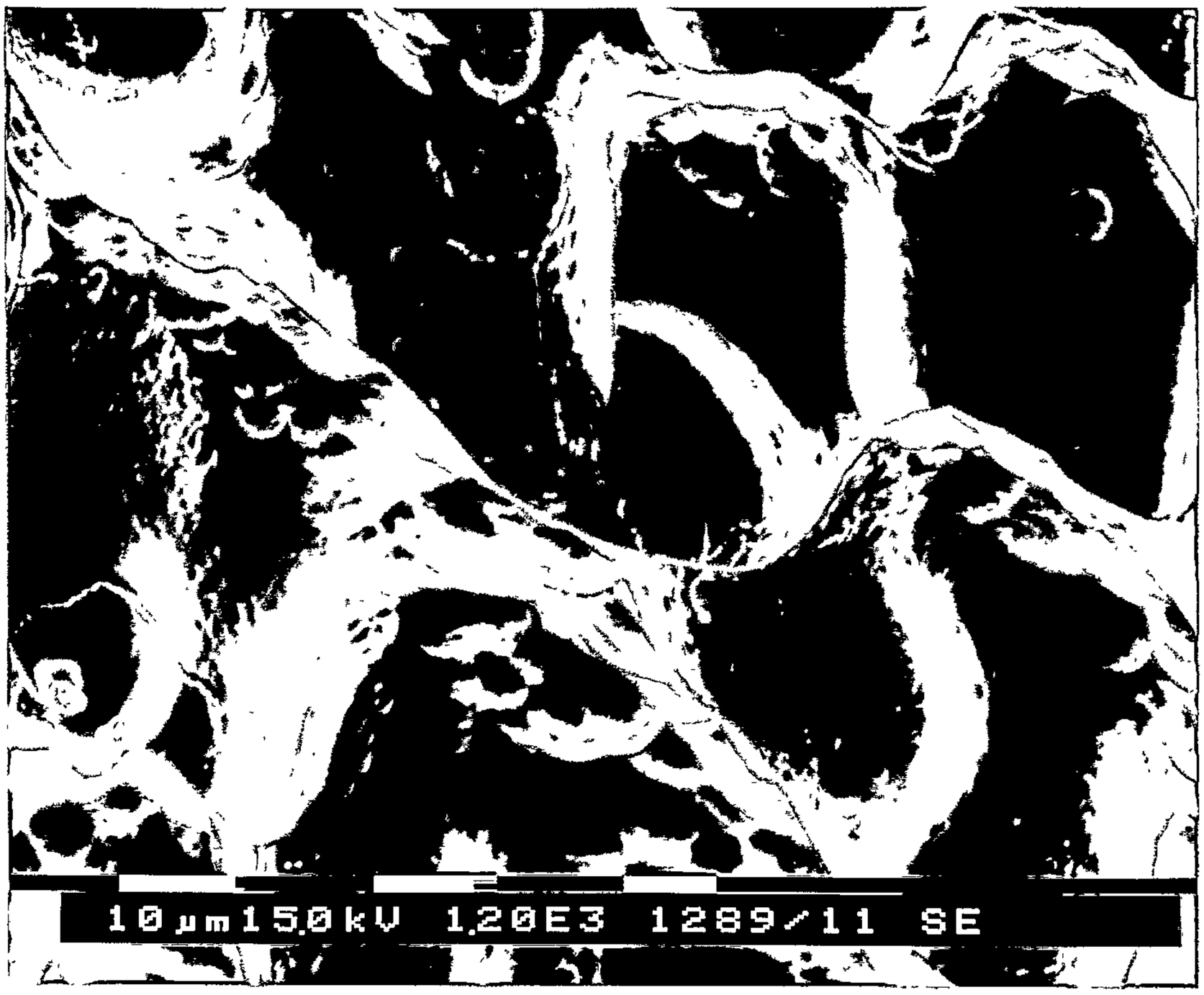

Figure 10.4c
SEM of the Microbond NP^2 specimen depicted on Figure 10.4a,b at higher magnification (X 1200).

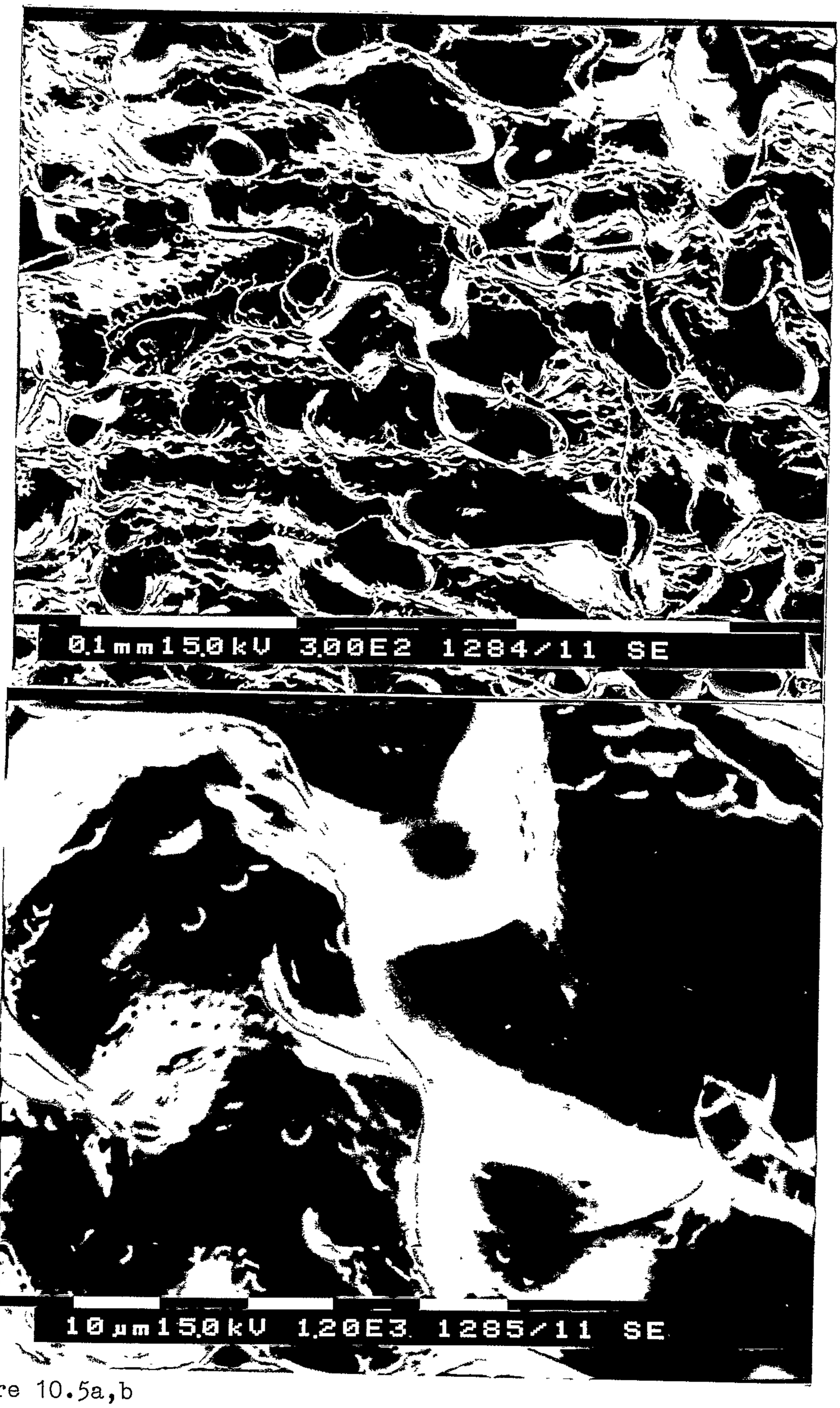

10.5a
(X 300)

10.5b
(X 1200)

Figure 10.5a,b

SEM of a Microbond NP^2 specimen electrolytically etched in a solution containing 0.06N HNO_3 and 2 per cent acetic acid for the preparatory study.

10.6a
(X 50)

10.6b
(X 1200)

Figure 10.6a,b

SEM of a Microbond NP^2 specimen electrolytically etched in solution containing 0.11N HNO_3 and 0 per cent acetic acid for the preparatory study.

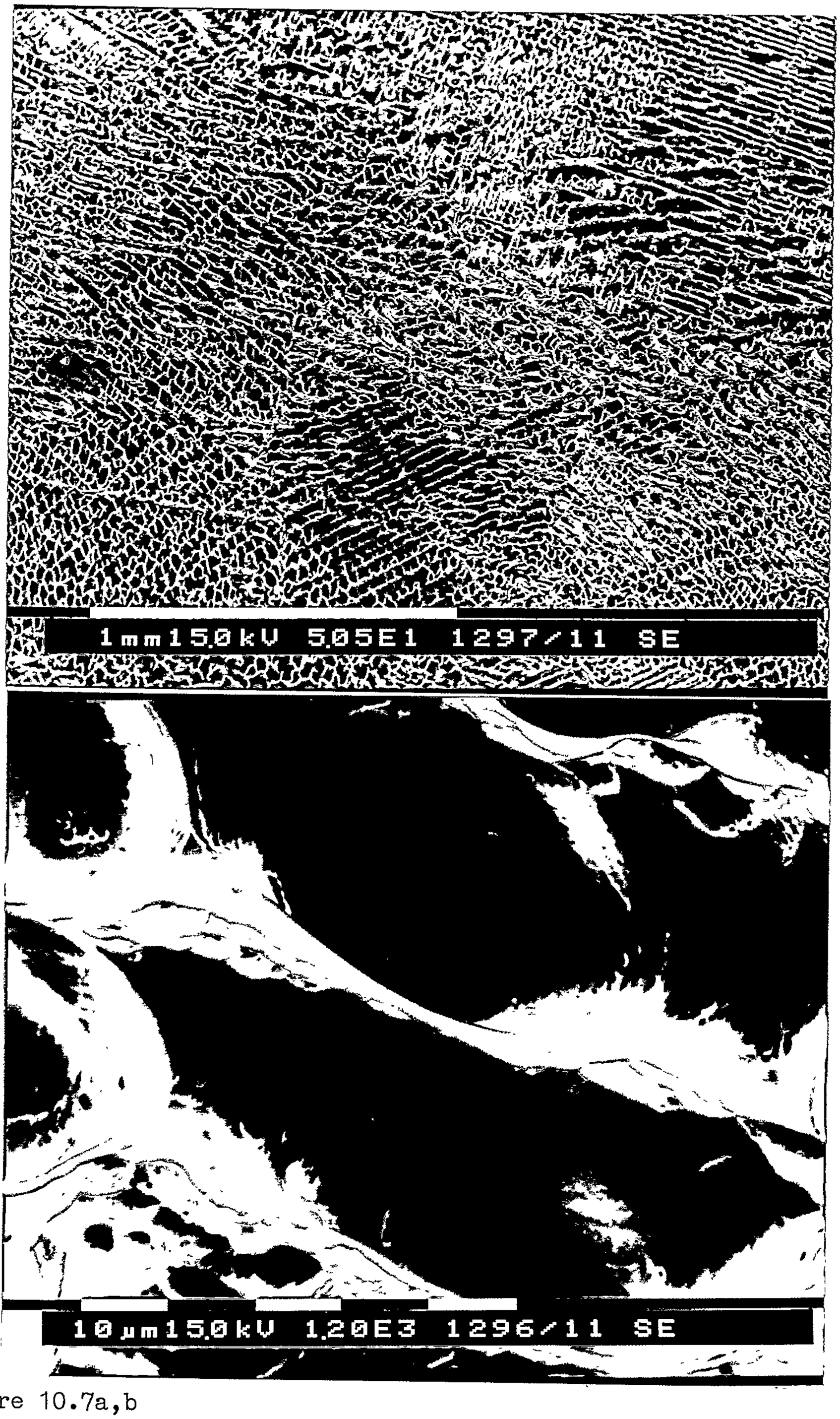

10.7a
(X 50)

10.7b
(X 1200)

Figure 10.7a,b
SEM of a Microbond NP^2 specimen electrolytically etched in a solution containing 0.11N HNO_3 and 2 per cent acetic acid for the preparatory study.

Figure 10.8
SEM of a Microbond NP^2 specimen electrolytically etched in a solution containing 0.11N HNO_3 and 4 per cent acetic acid for the preparatory study (X 1200).

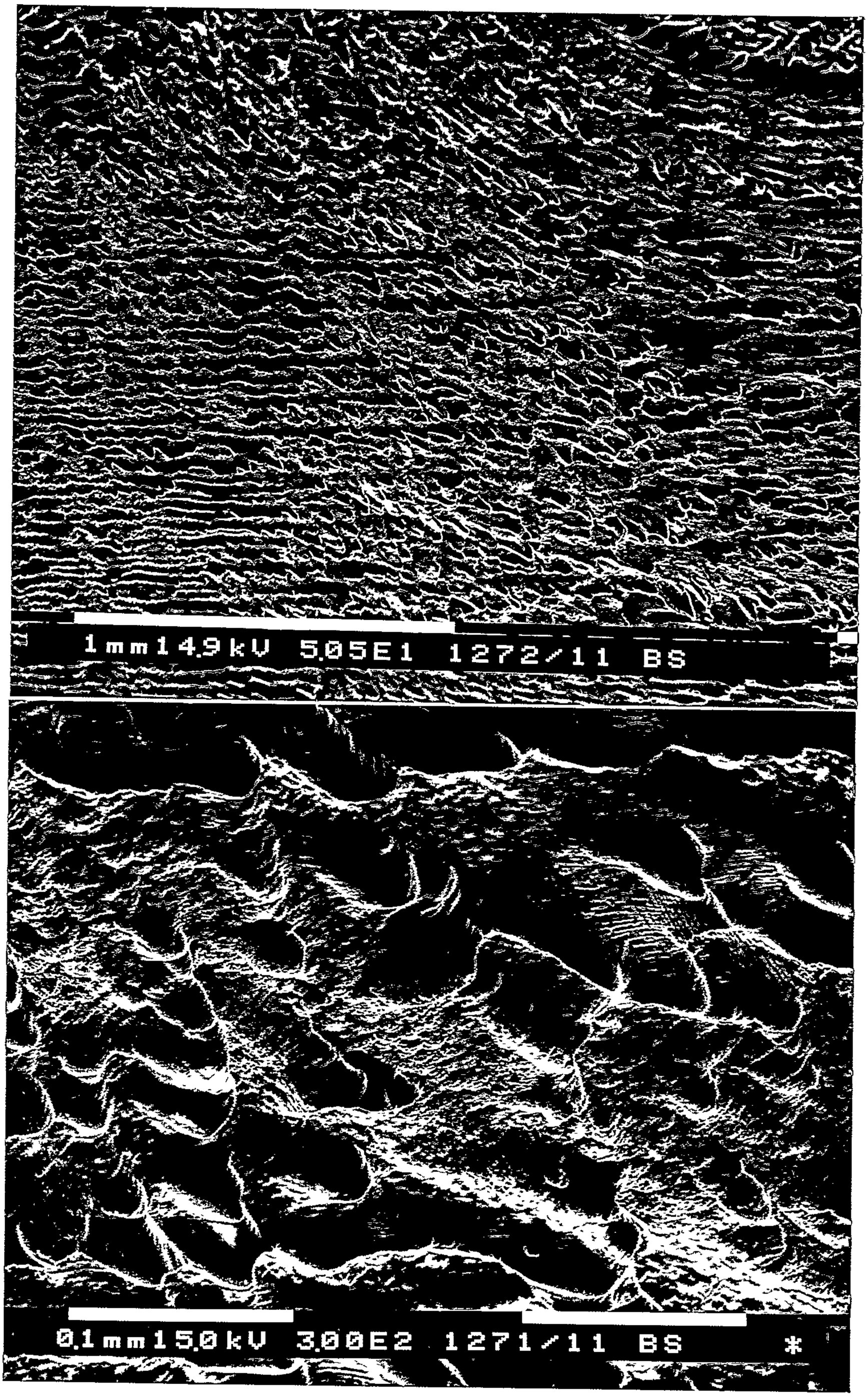

10.9a
(X 50)

10.9b
(X 300)

Figure 10.9a,b
SEM of a Microbond NP^2 specimen electrolytically etched in a solution containing 0.11N HNO_3 and 10 per cent acetic acid for the preparatory study.

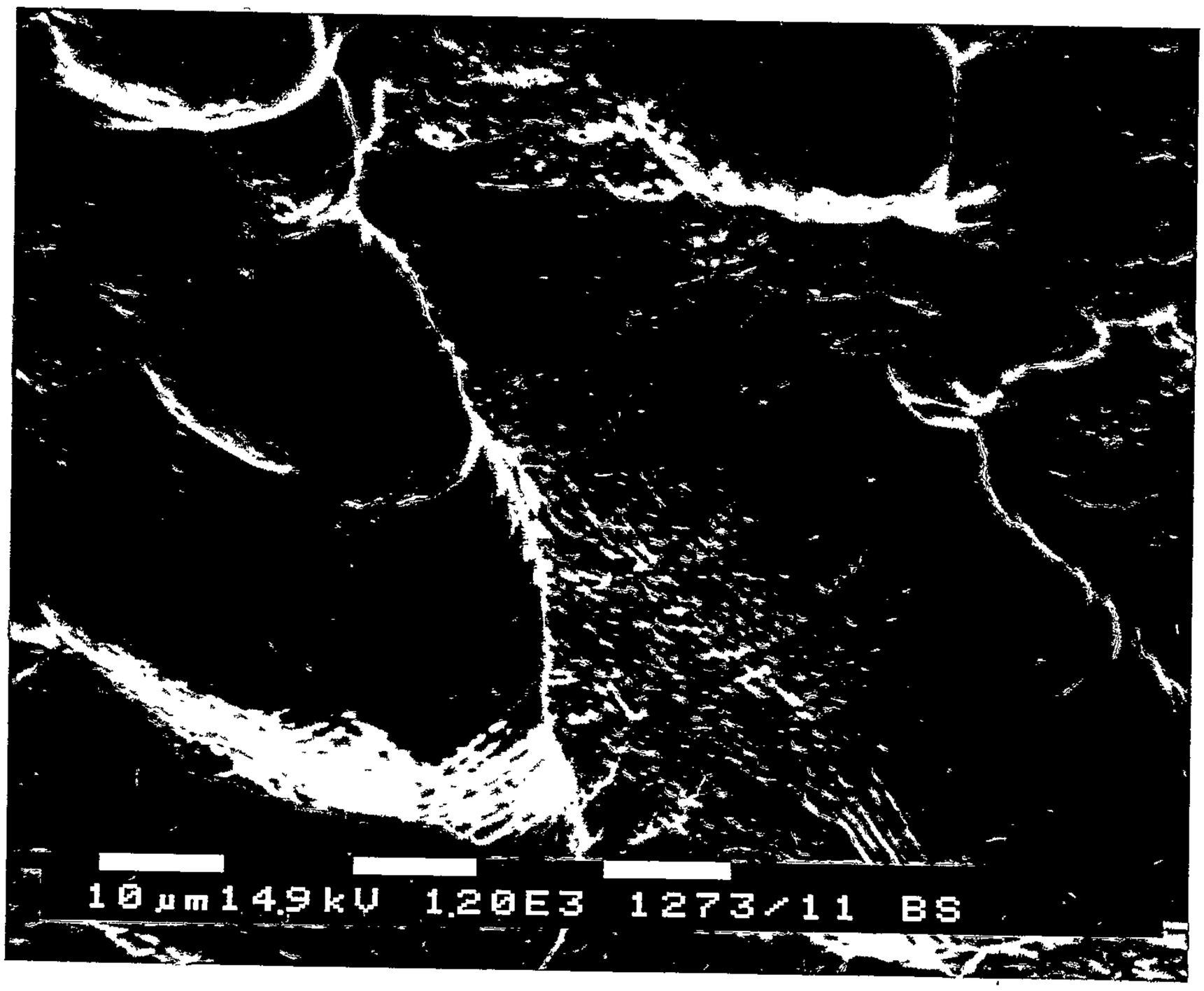

Figure 10.9c
SEM of the Microbond NP^2 specimen depicted in Figure 10.9a,b at higher magnification (X 1200).

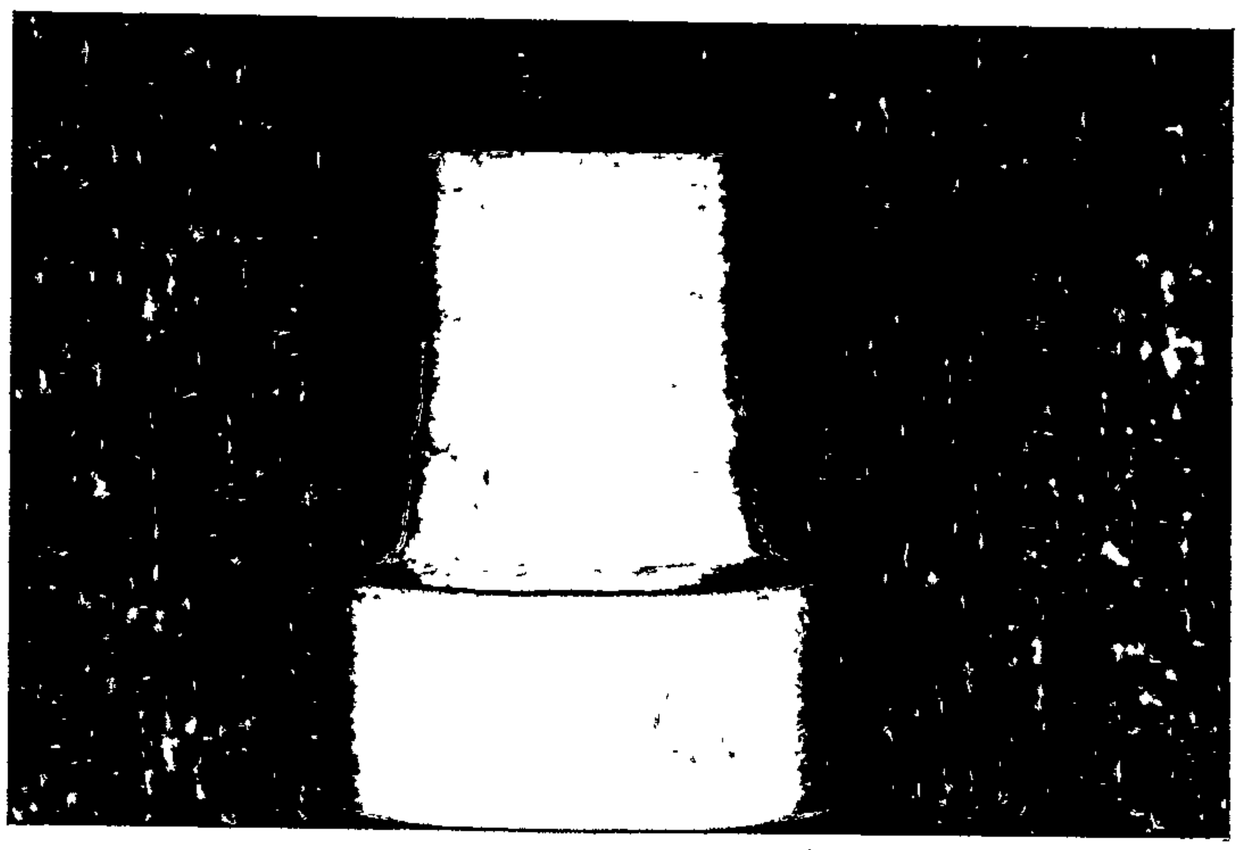

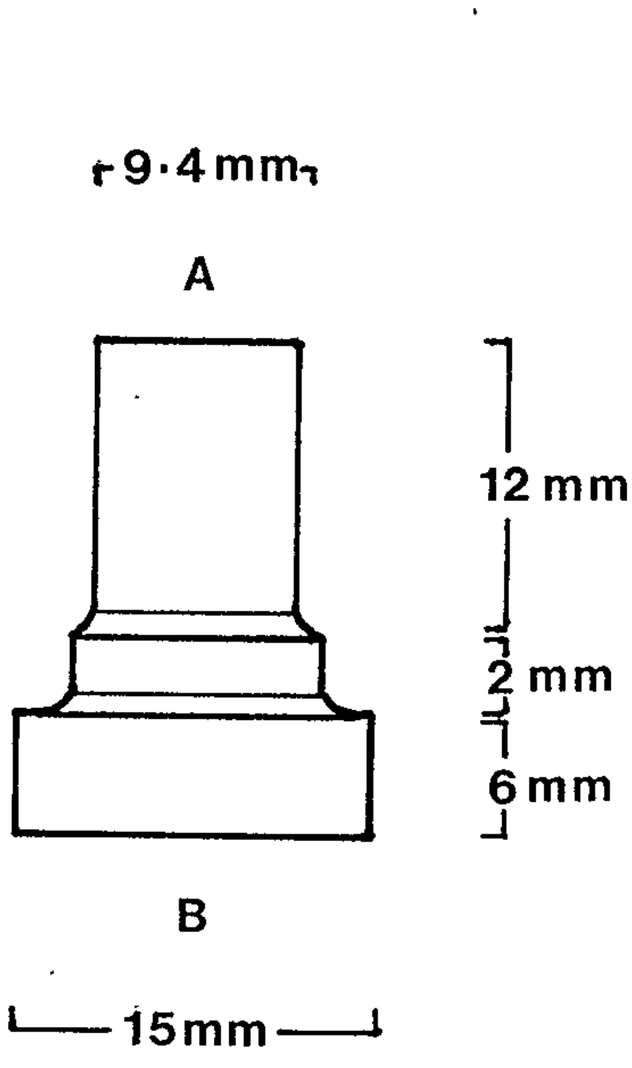

Figure 10.10
Photograph and diagrammatic representation, with dimensions, of a test specimen cast in Microbond NP^2.

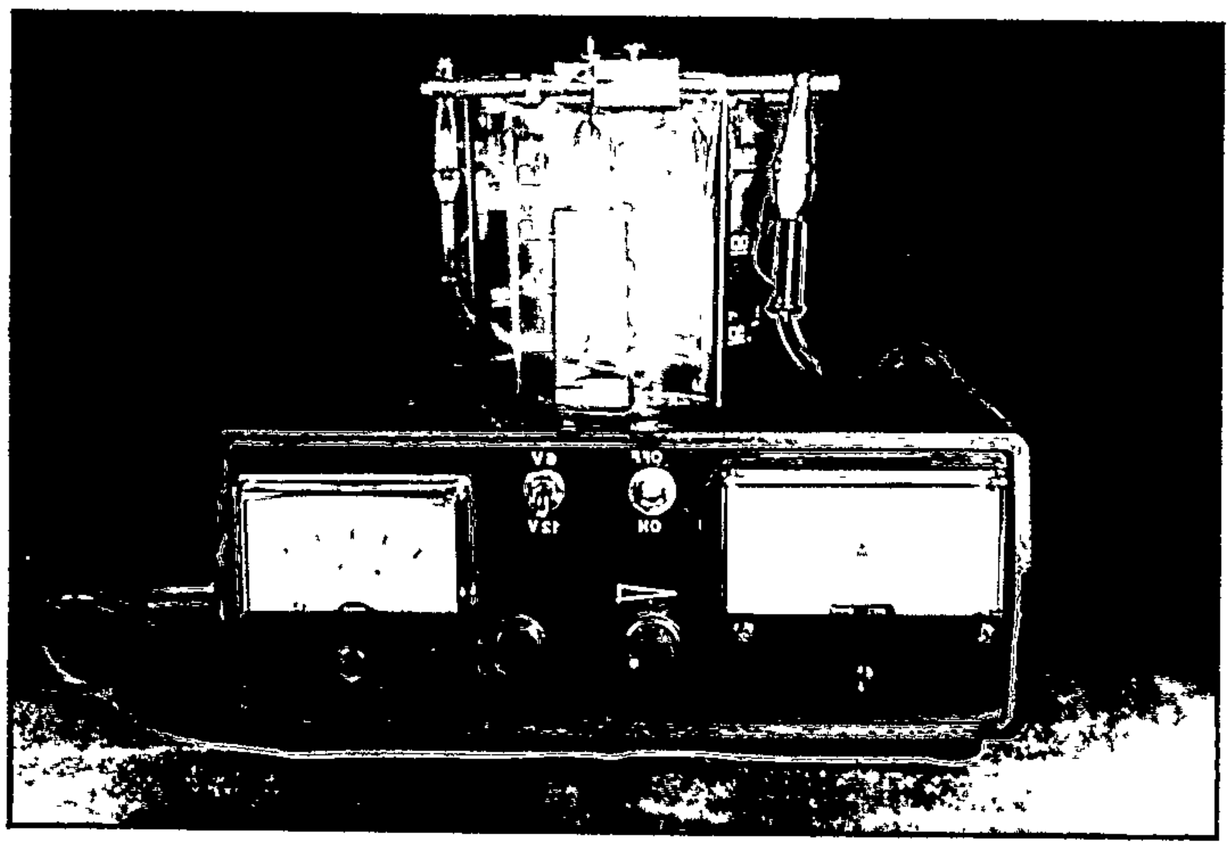

Figure 10.11
The electrolytic etching apparatus used to etch the specimens in the laboratory study.

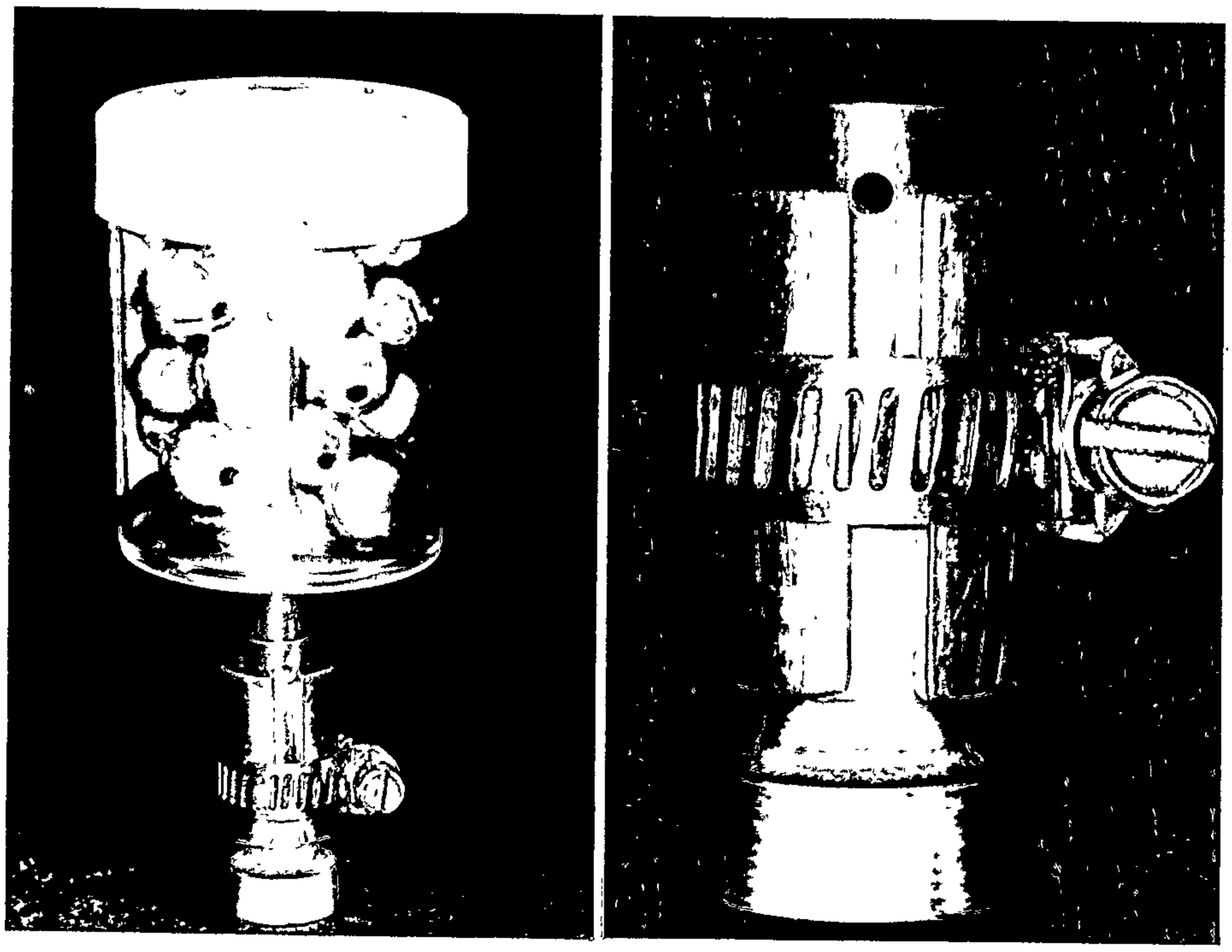

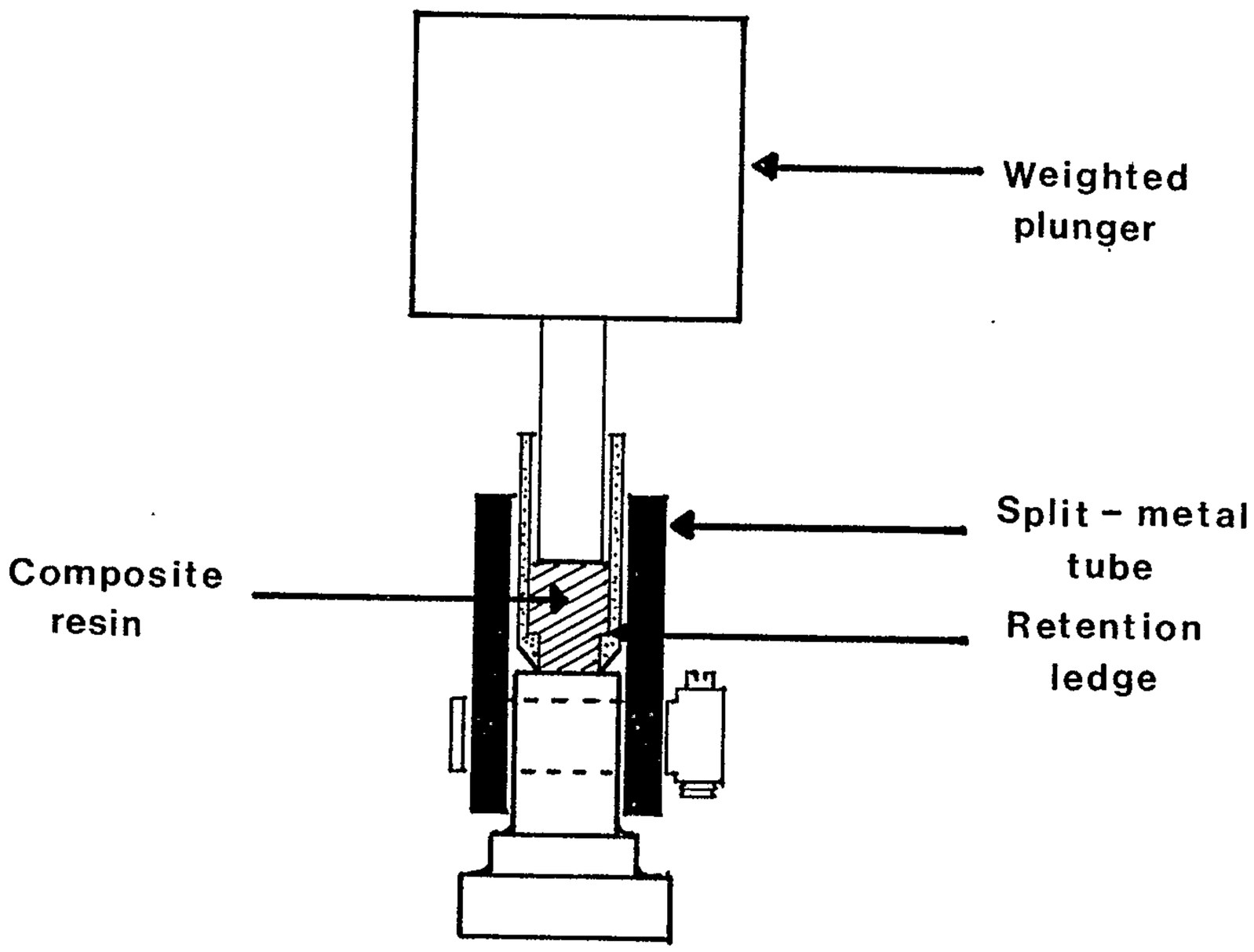

Figure 10.12
Photographs and diagrammatic representation of the apparatus used during the bonding of the test specimens to a column of composite resin luting cement.

Figure 10.13a

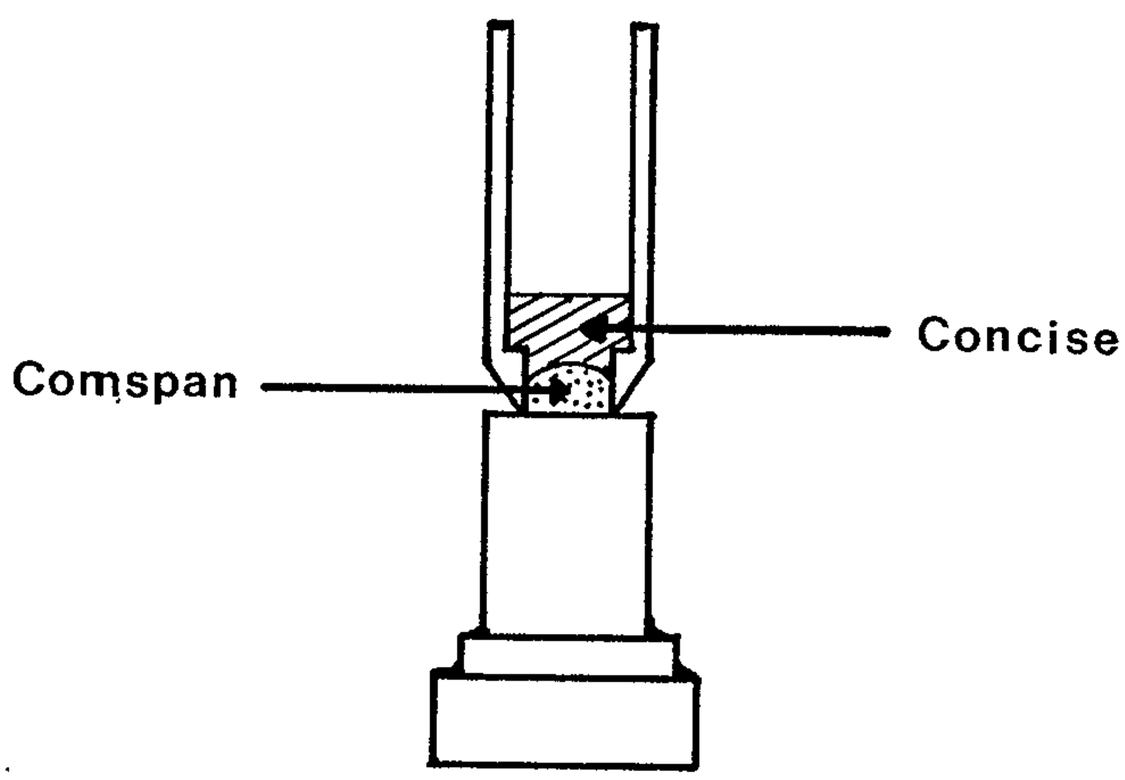

Figure 10.13b

Figure 10.13 a,b
Photograph and diagrammatic representation of the distribution of composite resin materials used to bond to the test specimens. Figure 10.13a shows a cross-section of a column of composite resin removed from its retaining metal tube.

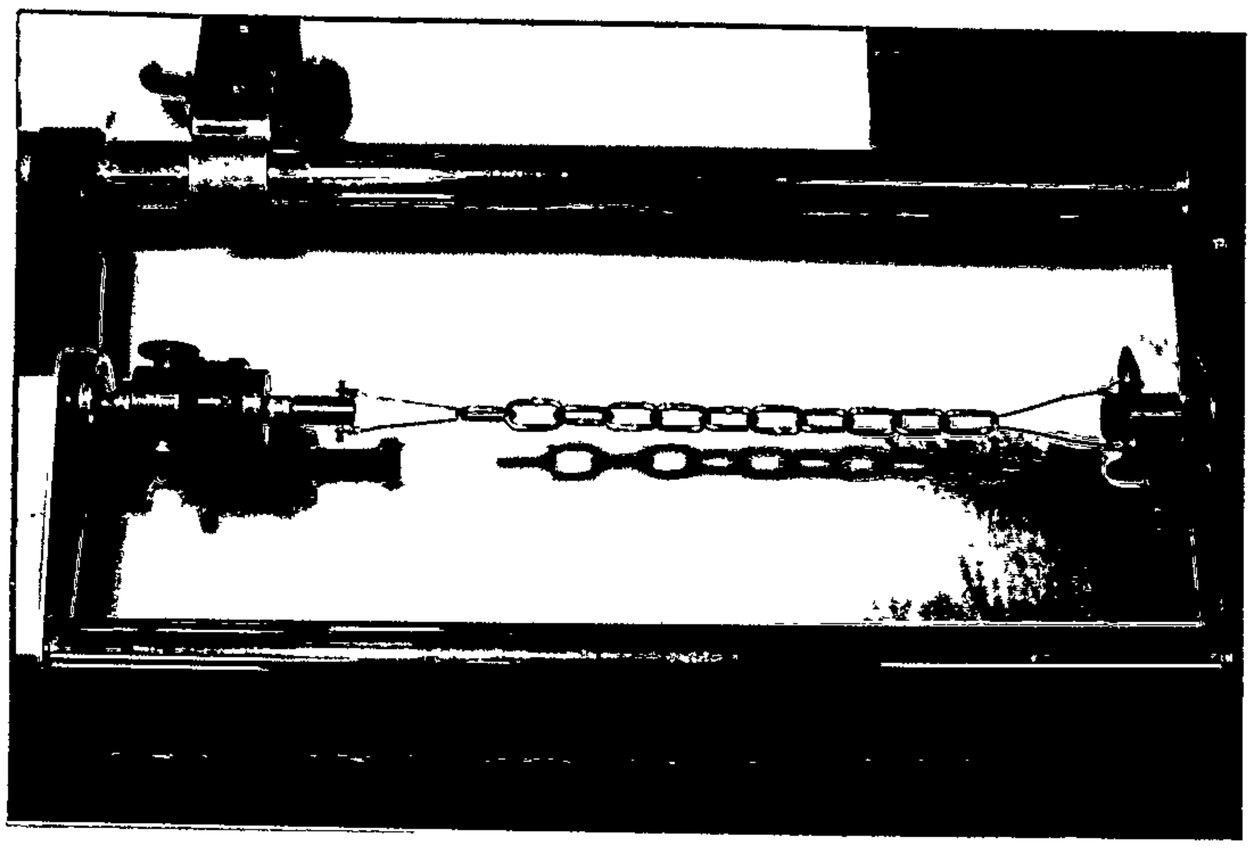

Figure 10.14a
The specimen testing apparatus showing the bonded specimen placed in the Hounsfield Tensometer ready for tensile bond testing.

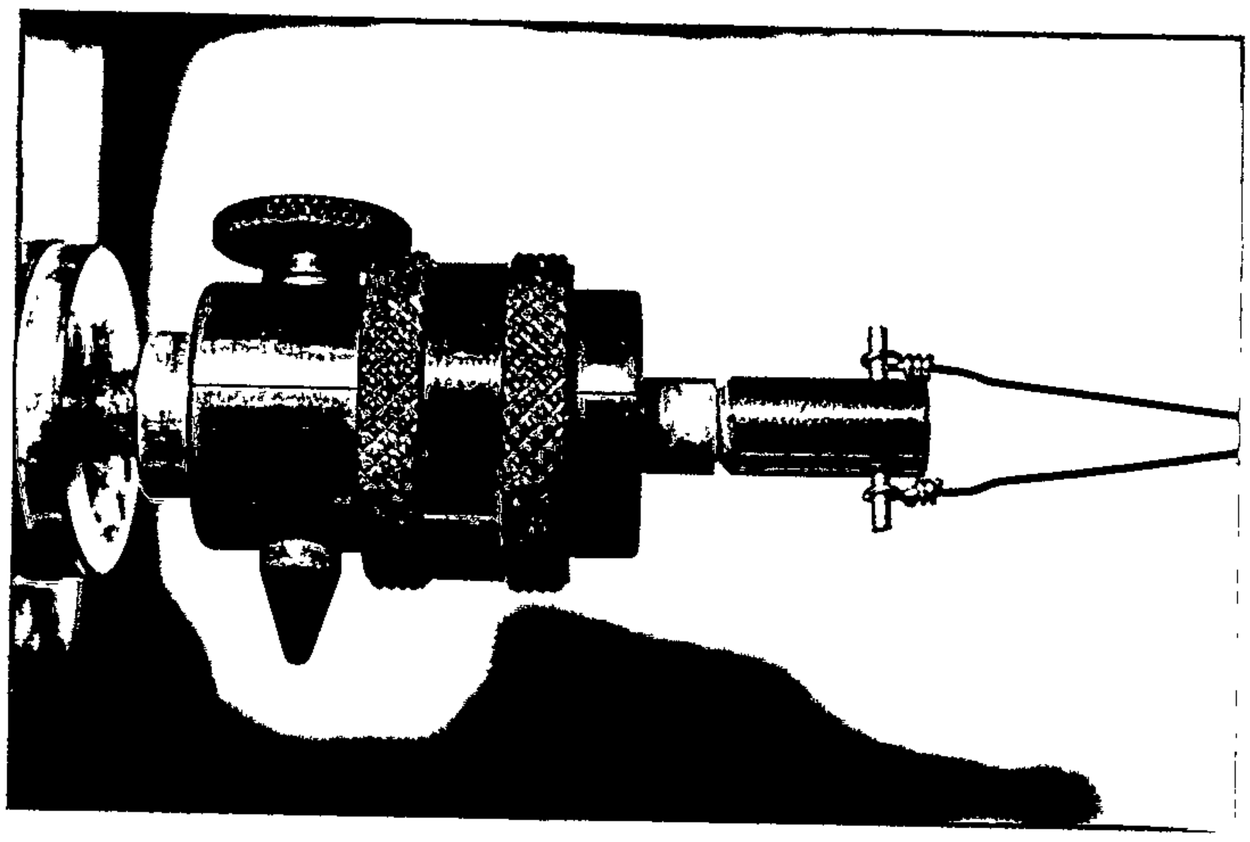

Figure 10.14b
A close-up of the attachment of the bonded specimen to one end of the Hounsfield Tensometer.

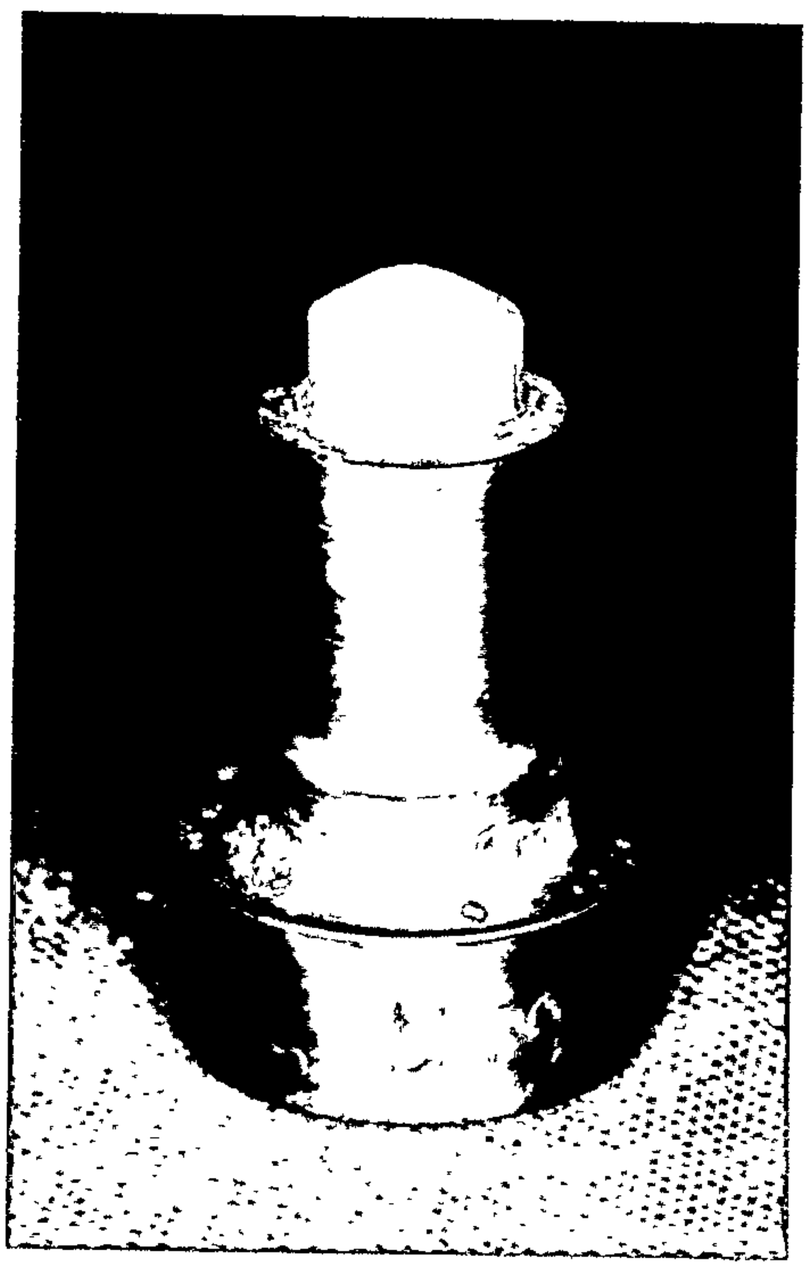

Figure 10.15
A specimen of Rexillium III showing the point of failure after bond testing. The specimen has failed through the column of cement leaving a sustantial amount of cement still bonded to the electrolytically etched metal surface.

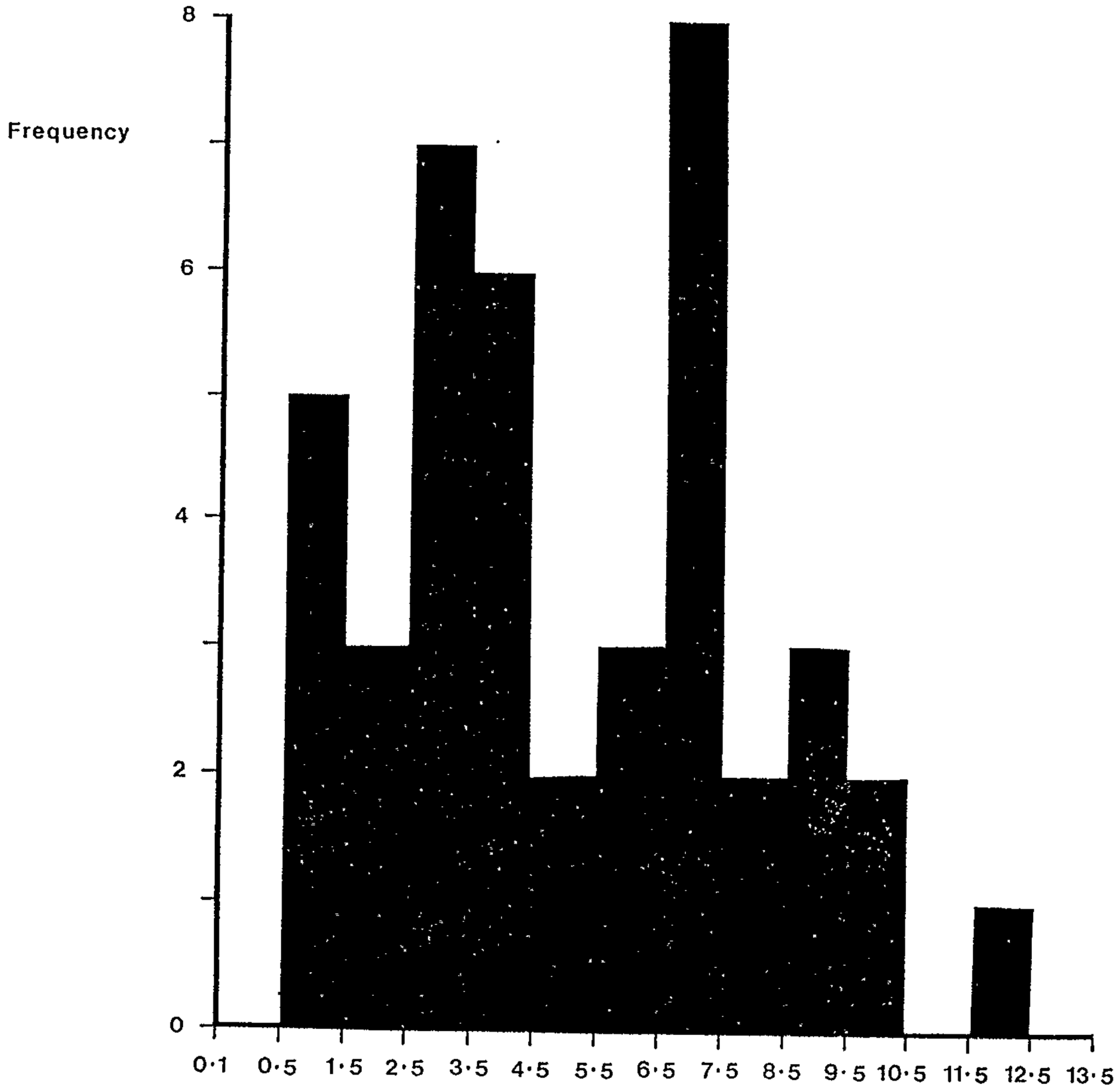

Figure 10.16
The frquency with which various tensile bond strengths were found from specimens that survived thermal-cycling. 93 specimens failed on thermal-cycling, 43 specimens could be tensile bond tested.

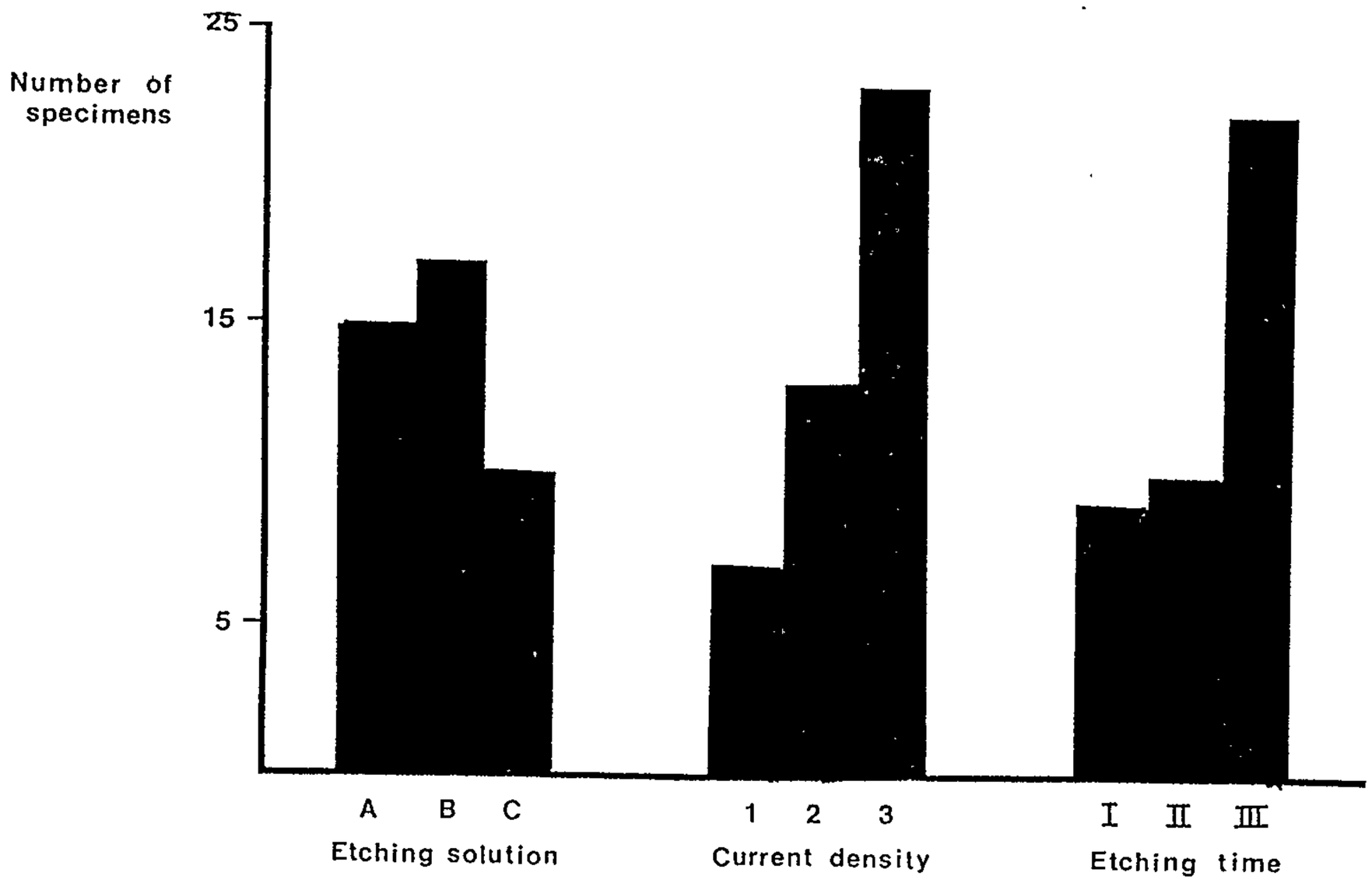

Figure 10.17
The total number of specimens that survived thermal-cycling and were tensile bond tested in relation to individual etching conditions (maximum possible number of specimens for a particular etching condition = 45).

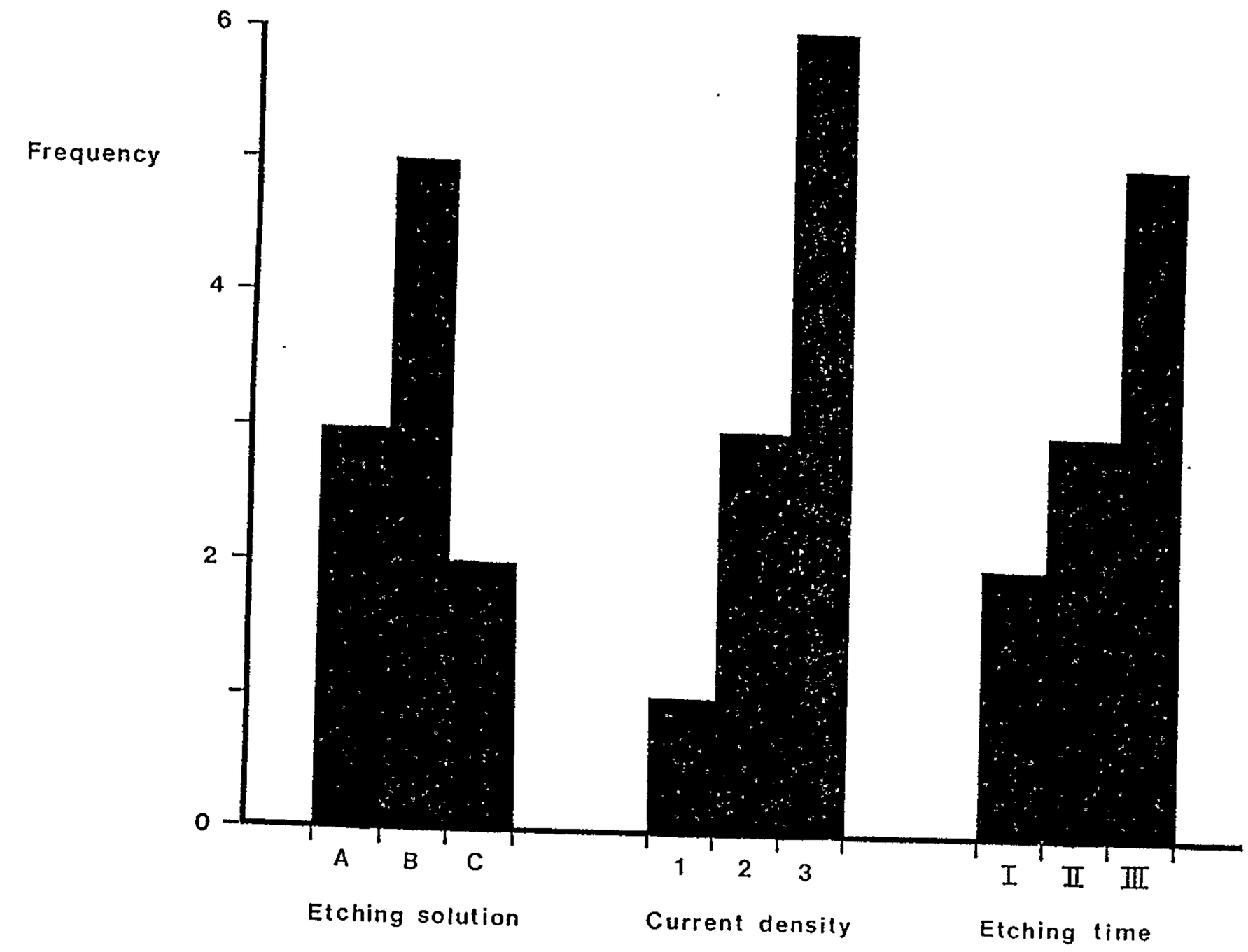

Figure 10.18
The frequency with which particular etching conditions provided two or more specimens that survived thermal-cycling (maximum possible frequency = 9).

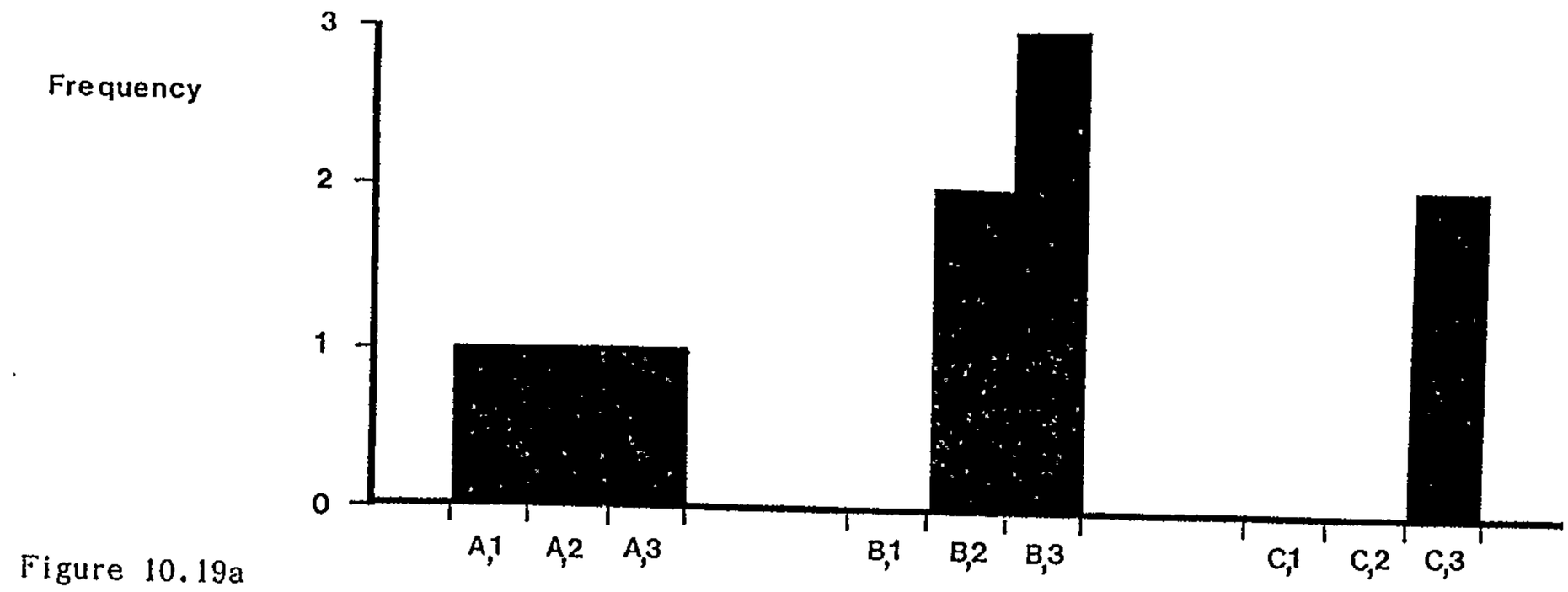

Figure 10.19a

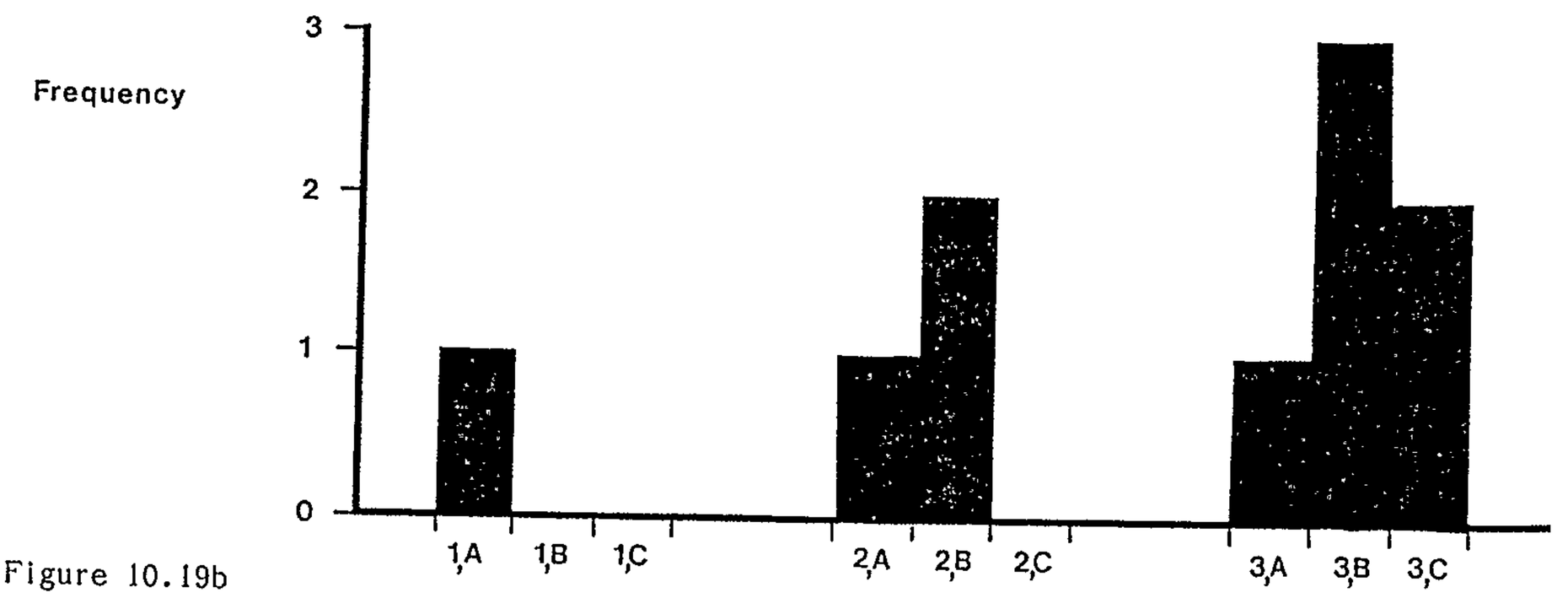

Figure 10.19b

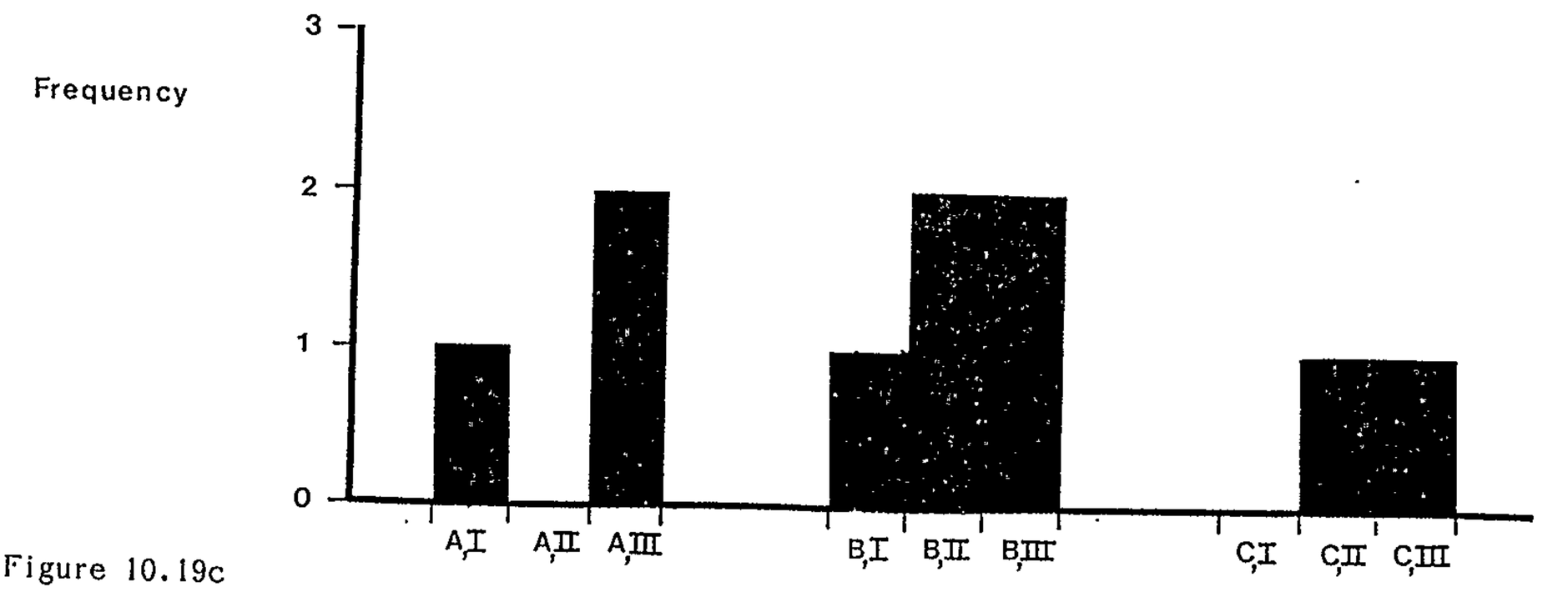

Figure 10.19c

A,B,C = Etching solution

1,2,3 = Current density

I,II,III = Etching time

Figure 10.19 a,b,c
The frequency with which various etching conditions, in combinations of two, produced two or more specimens that survived thermal-cycling (maximum possible frequency = 3).

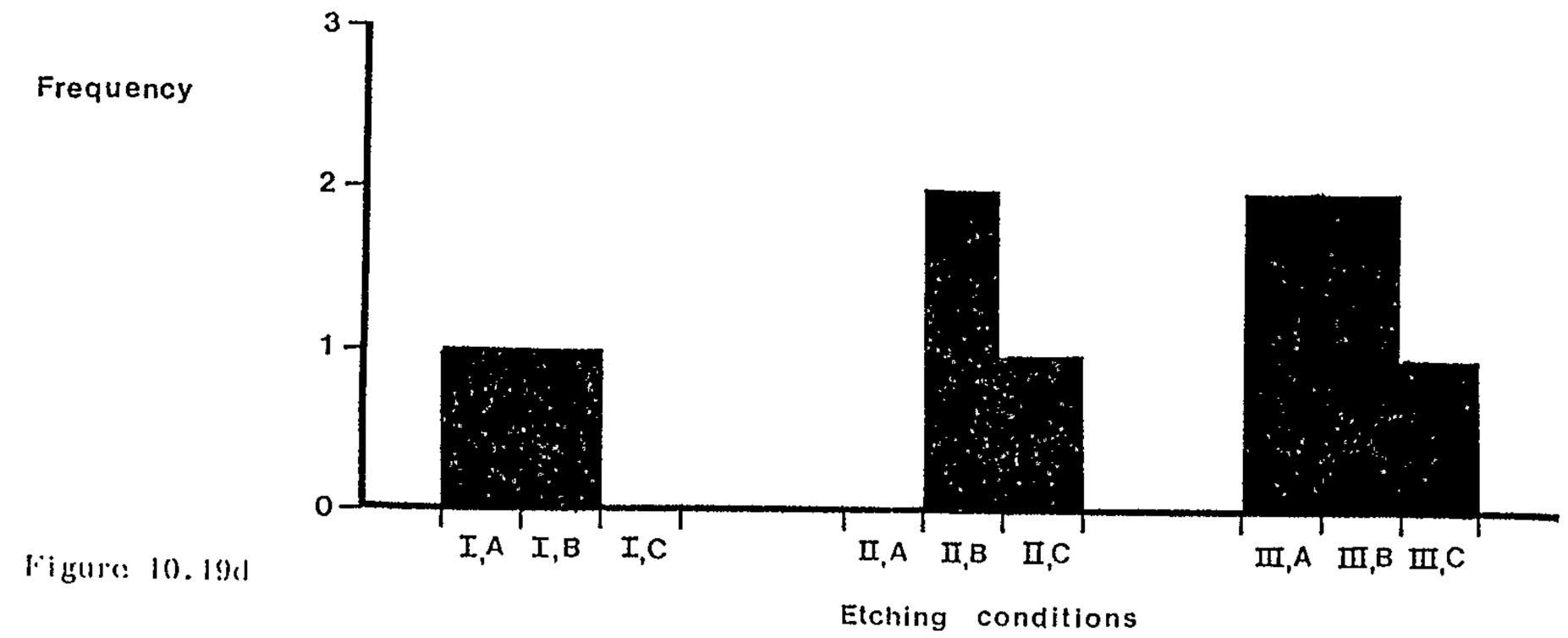

Figure 10.19d

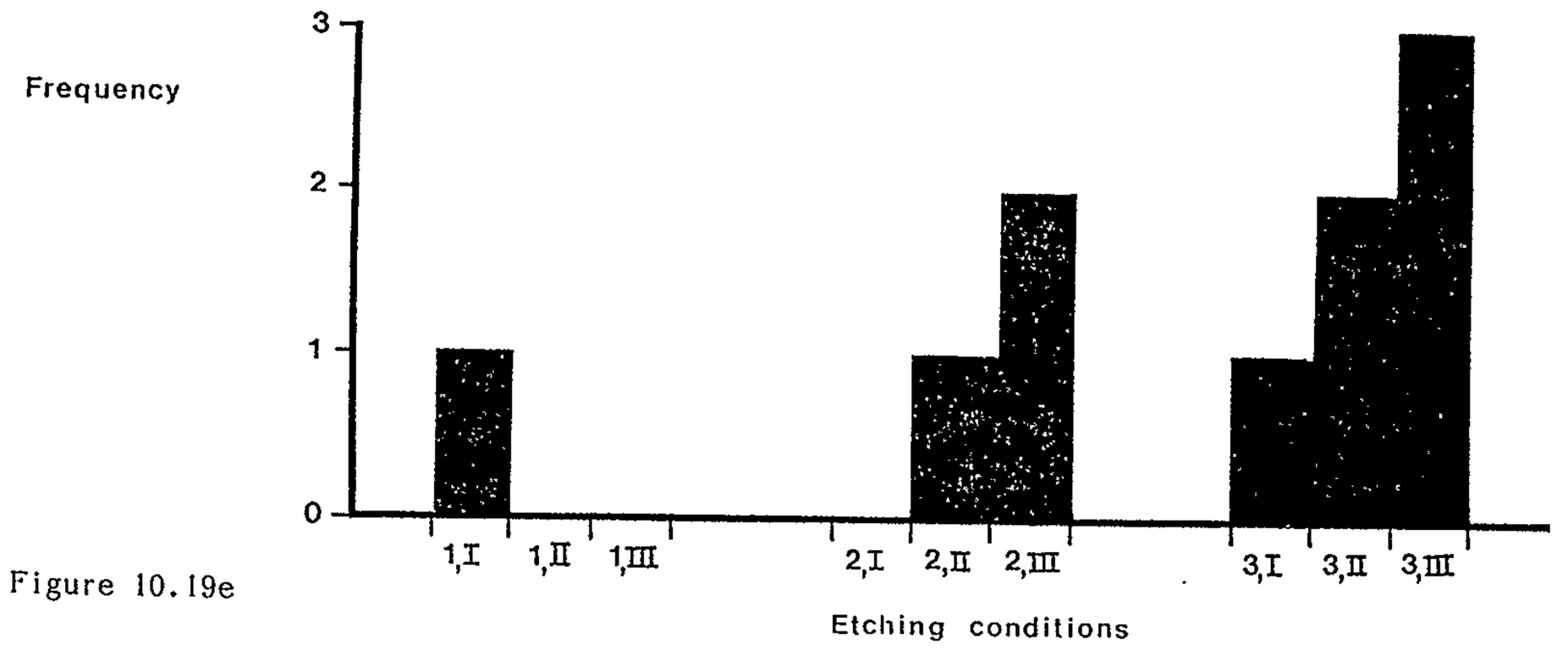

Figure 10.19e

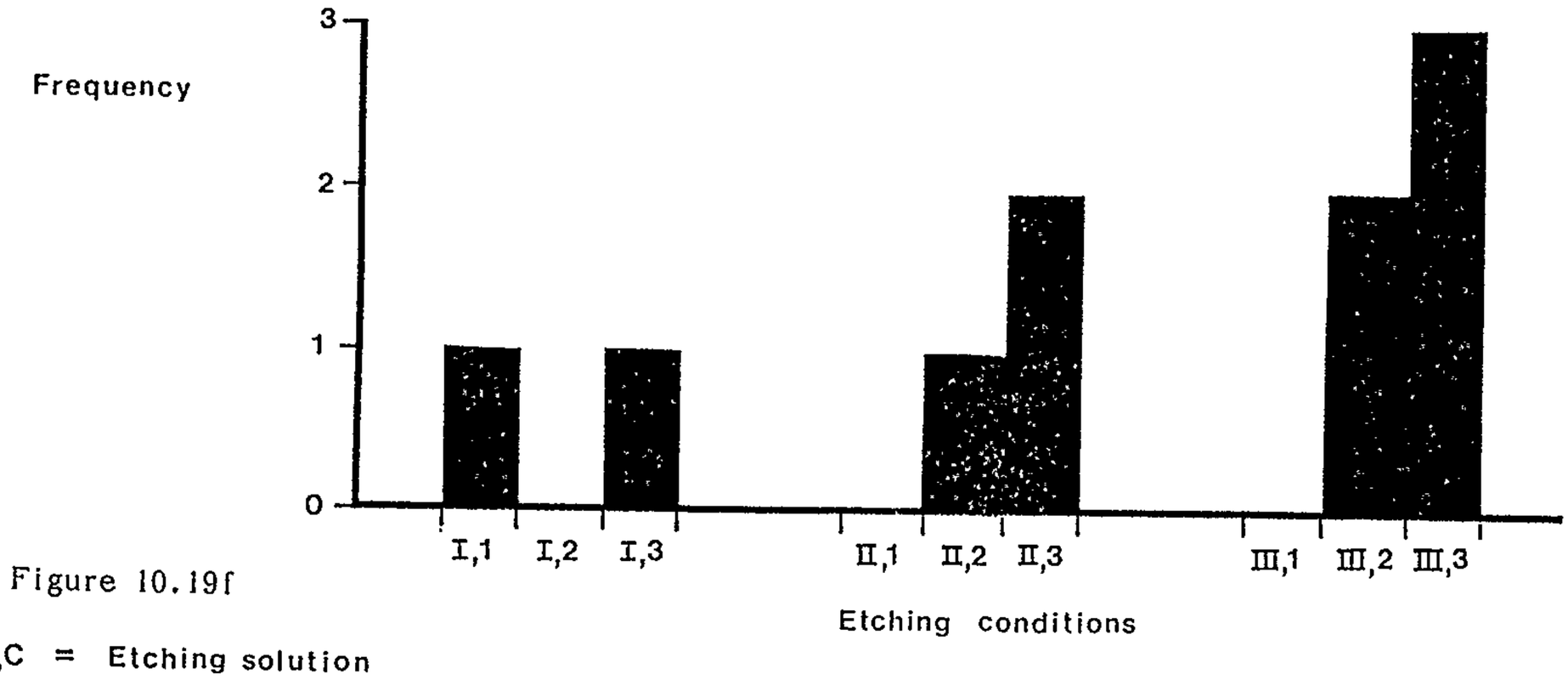

Figure 10.19f

A,B,C = Etching solution
1,2,3 = Current density
I,II,III = Etching time

Figure 10.19 d,e,f
The frequency with which various etching conditions, in combinations of two, produced two or more specimens that survived thermal-cycling (maximum possible frequency = 3).

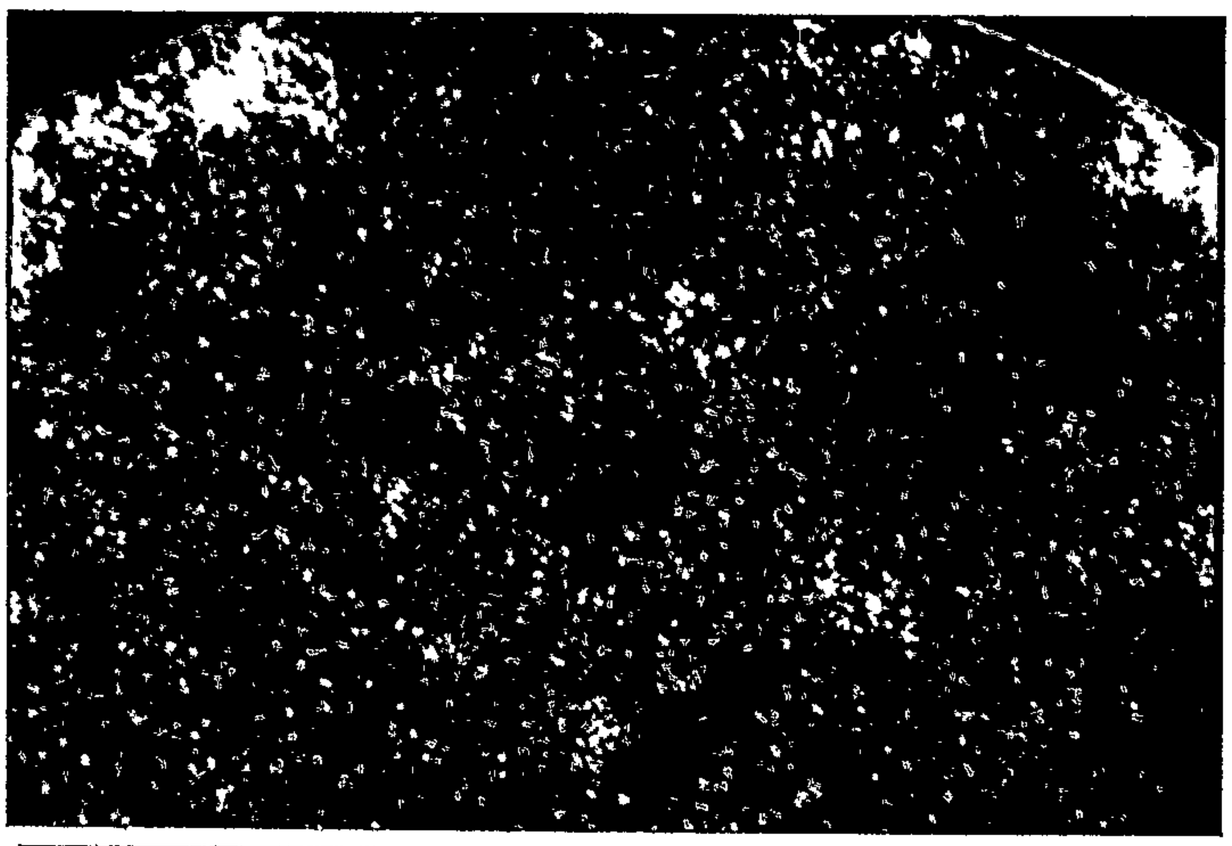

Figure 10.20a
Photomicrograph of a Rexillium III specimen electrolytically etched under the recommended etching conditions (X 34).

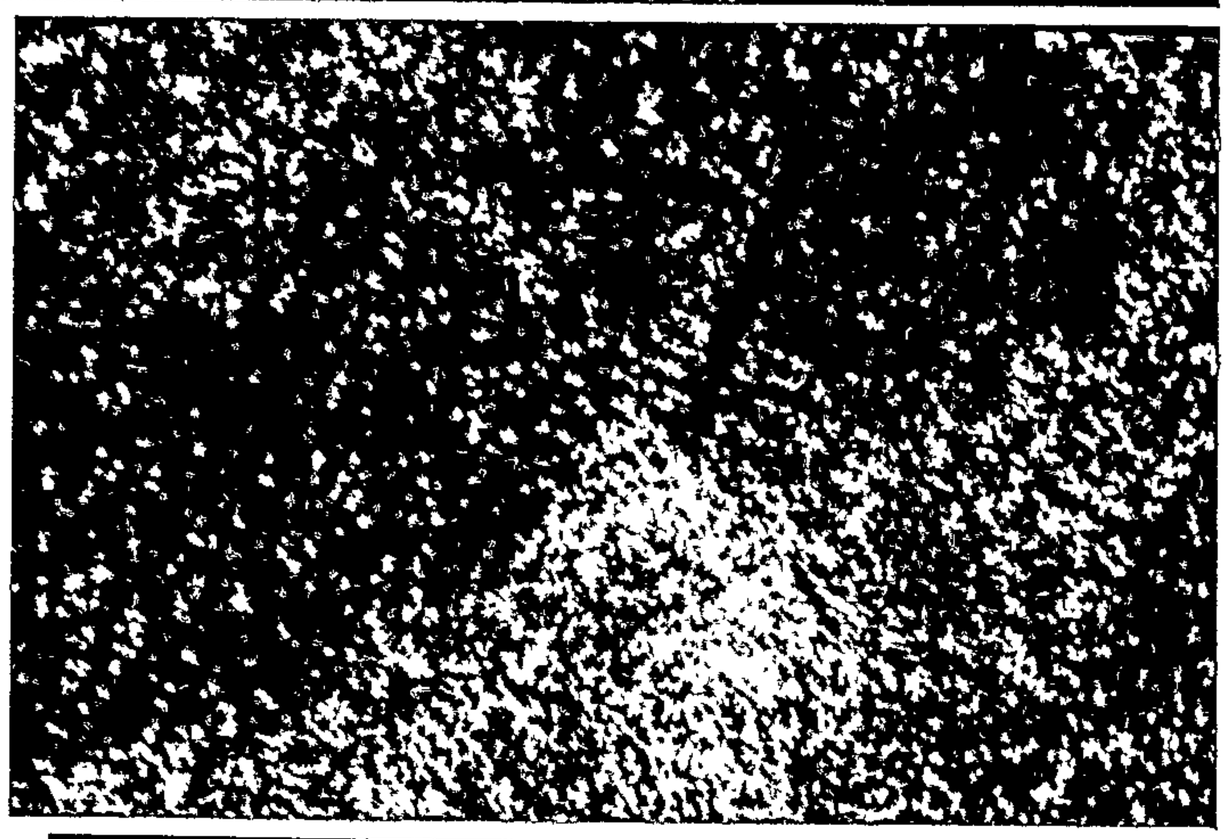

Figure 10.20b
Photomicrograph of the Rexillium III specimen depicted in Figure 10.20a at higher magnification (X 168).

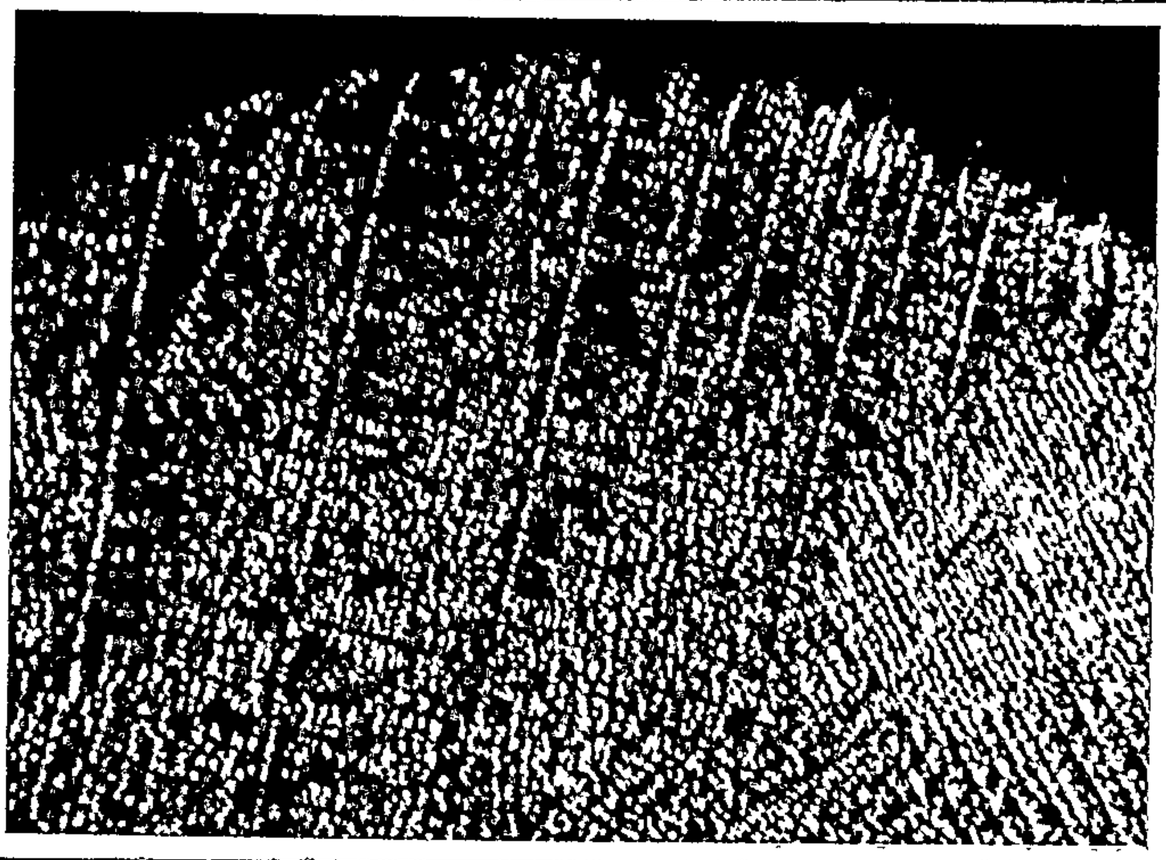

Figure 10.21a
Photomicrograph of a Microbond NP^{2} specimen electrolytically etched under the recommended etching conditions (X 34).

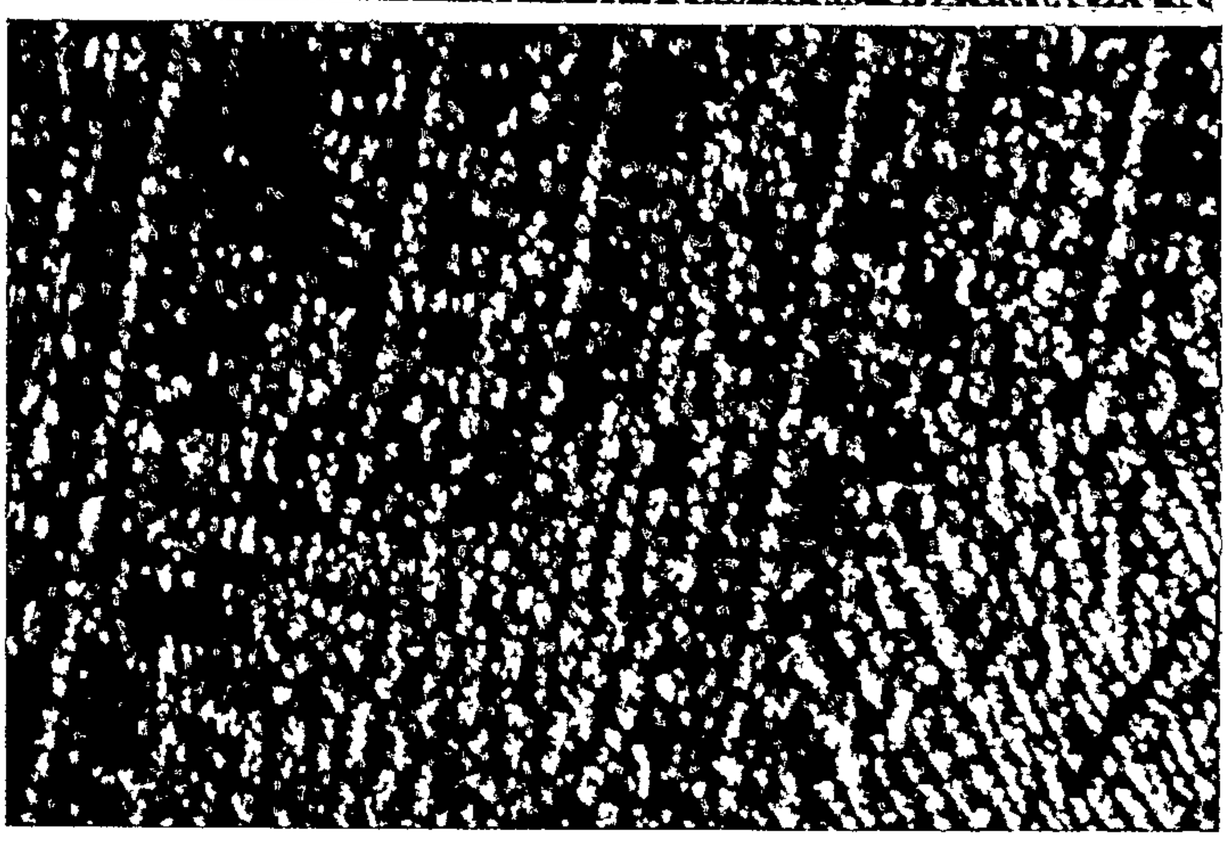

Figure 10.21b
Photomicrograph of the Microbond NP^{2} specimen depicted in Figure 10.21a at higher magnification (X 168).

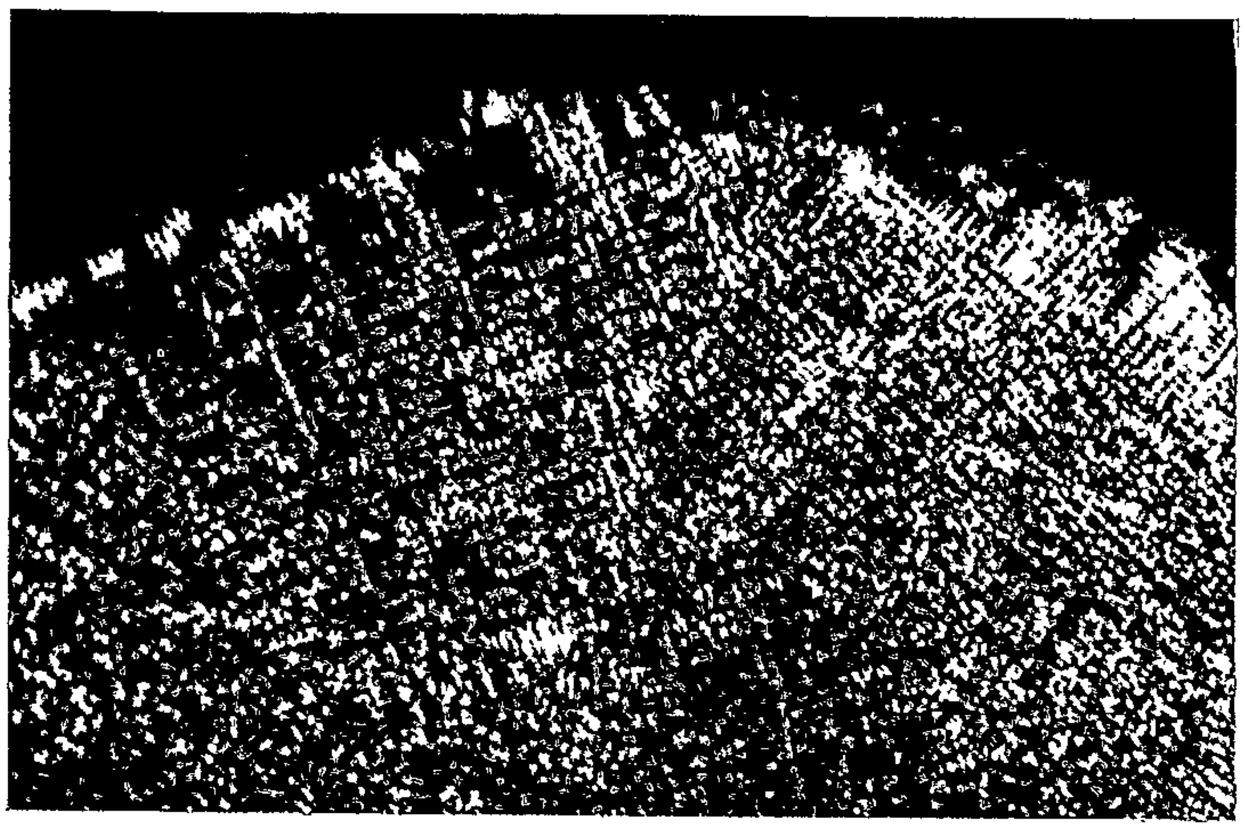

Figure 10.22a
Photomicrograph of the edge of a Microbond NP^2 specimen showing the ditching at the periphery of the specimen after the specimen was electrolytically etched (X 34).

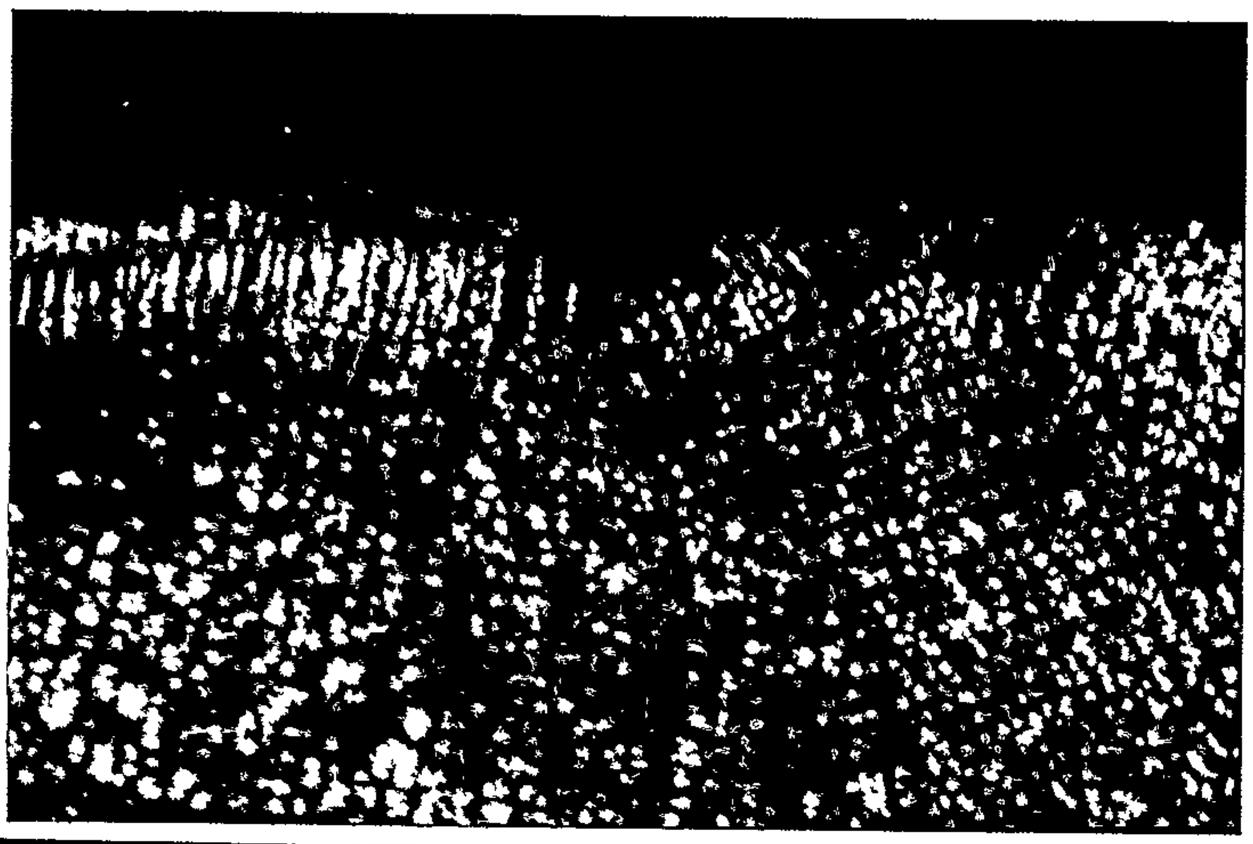

Figure 10.22b
Photomicrograph of the Microbond NP^2 specimen depicted in Figure 10.22a at higher magnification (X 168).

Figure 10.23a
Photomicrograph of the bonding surface of a Microbond NP^2 specimen after sandblasting with 50 µm aluminium oxide particles (X 34).

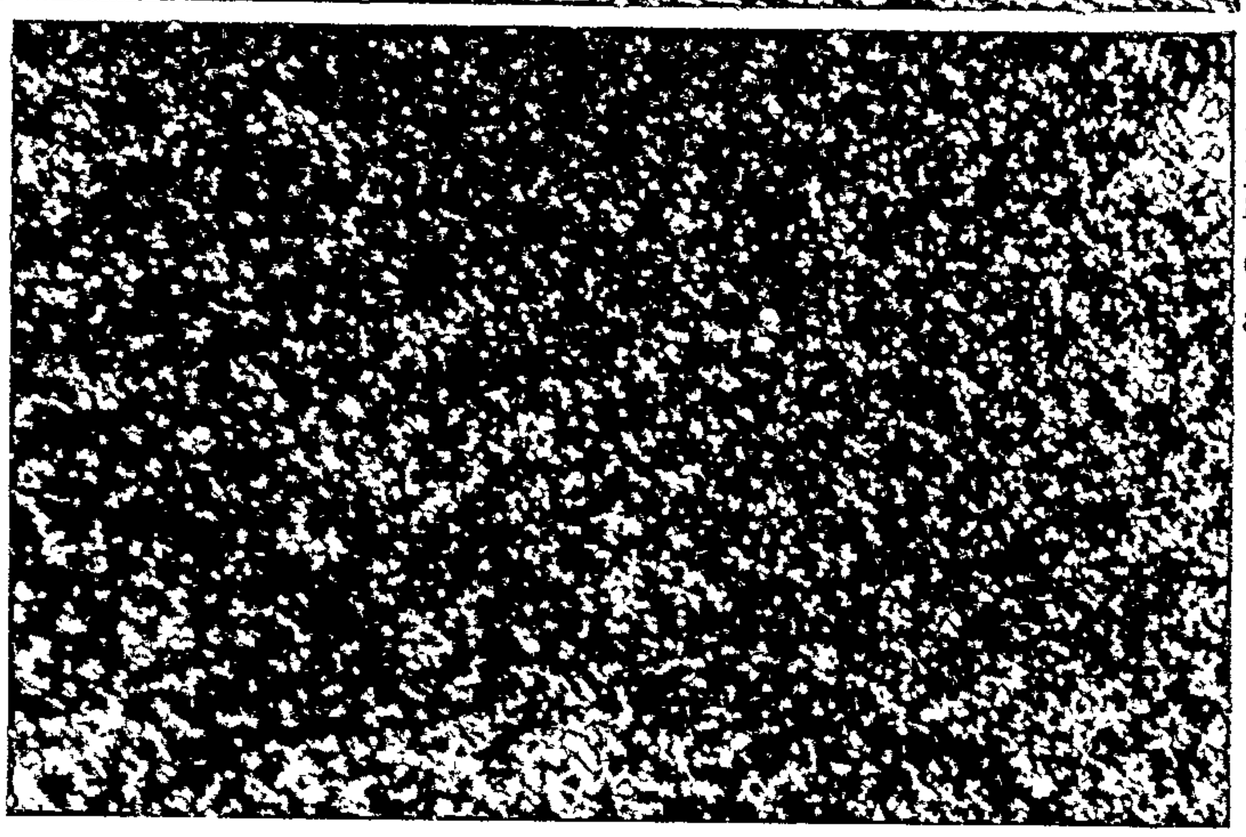

Figure 10.23b
Photomicrograph of the Microbond NP^2 specimen depicted in Figure 10.23b at higher magnification (X 168).

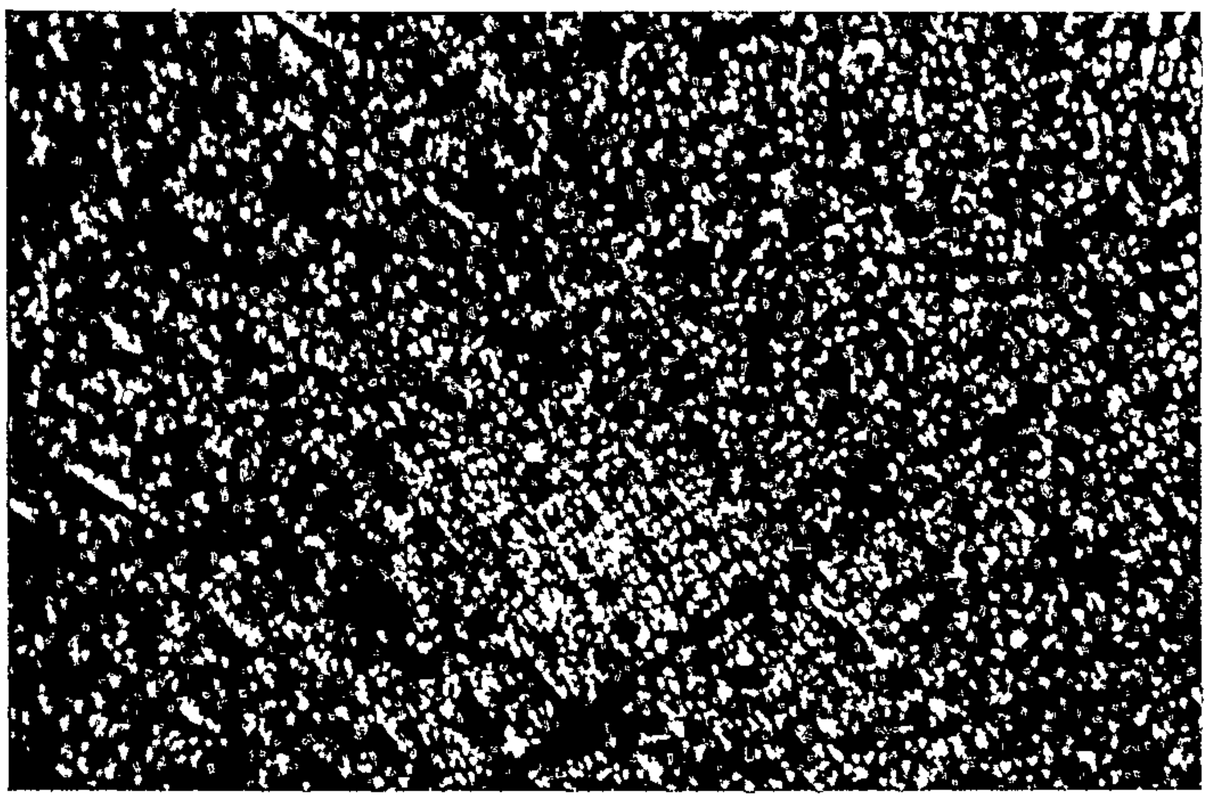

Figure 10.24a
Photomicrograph of a Microbond NP^2 specimen electrolytically etched under the etching conditions B,3,I. Specimen coded No. 4. This specimen was judged as the worst in the group of five (X 168).

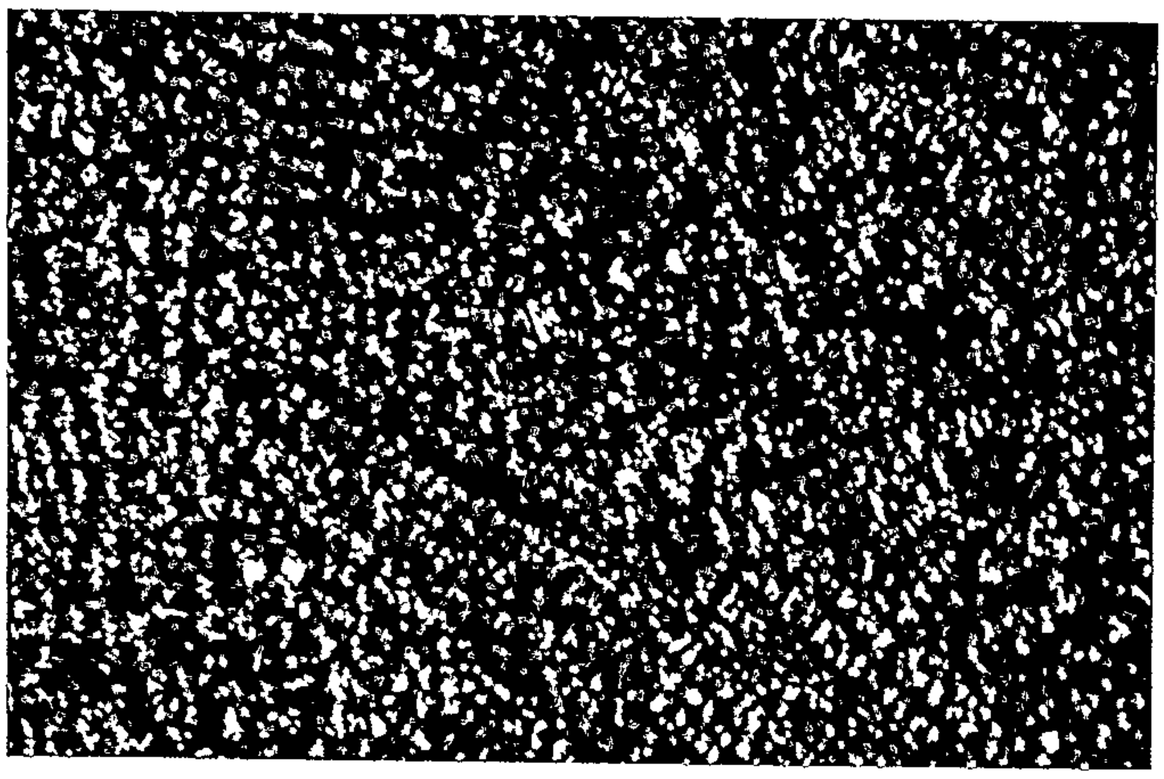

Figure 10.24b
Photomicrograph of a Microbond NP^2 specimen electrolytically etched under the same etching conditions as the specimen depicted in Figure 10.24a (B,3,I). Specimen coded No. 5. This specimen was judged as the best in the group of five (X 168).

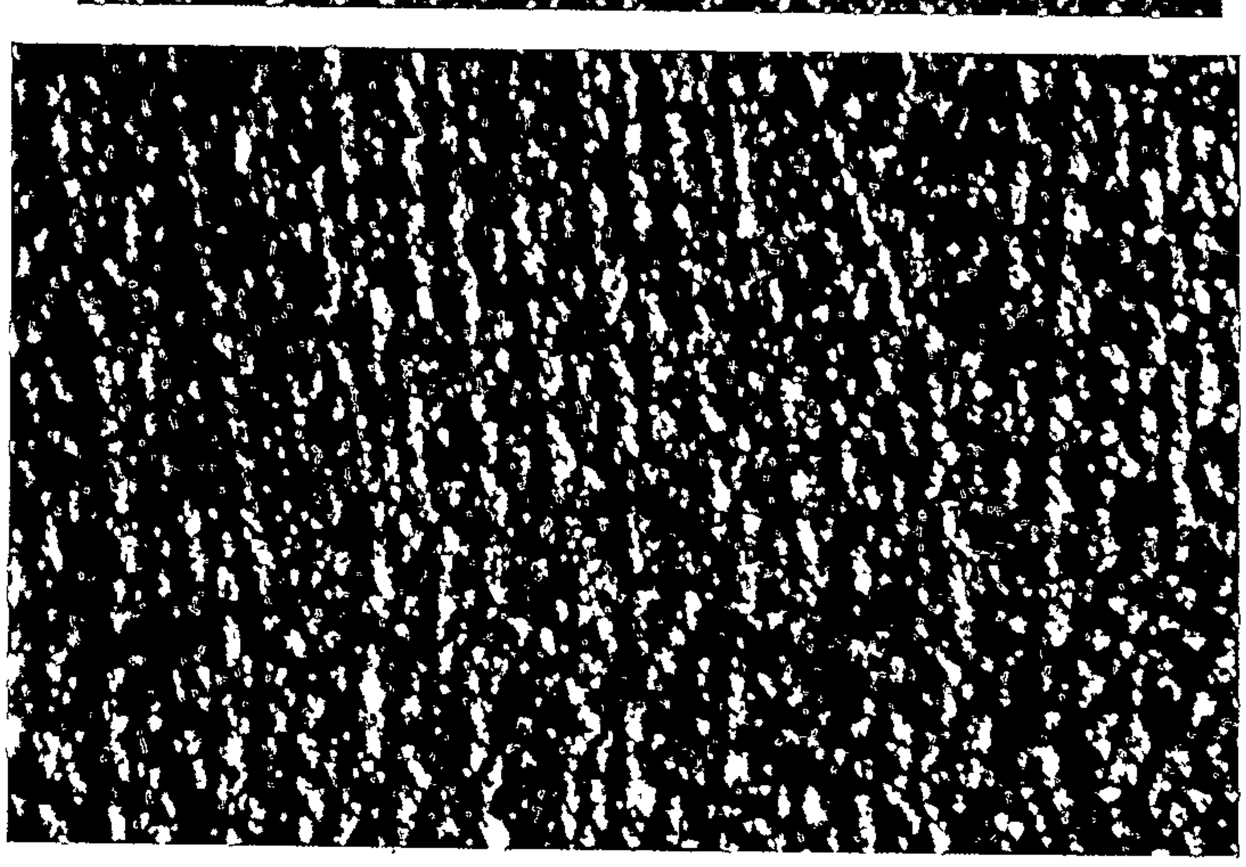

Figure 10.24c
Photomicrograph of a Microbond NP^2 specimen electrolytically etched under the etching conditions A,2,I. Specimen coded No. 3. This specimen was judged as the worst in the group of five (X 168).

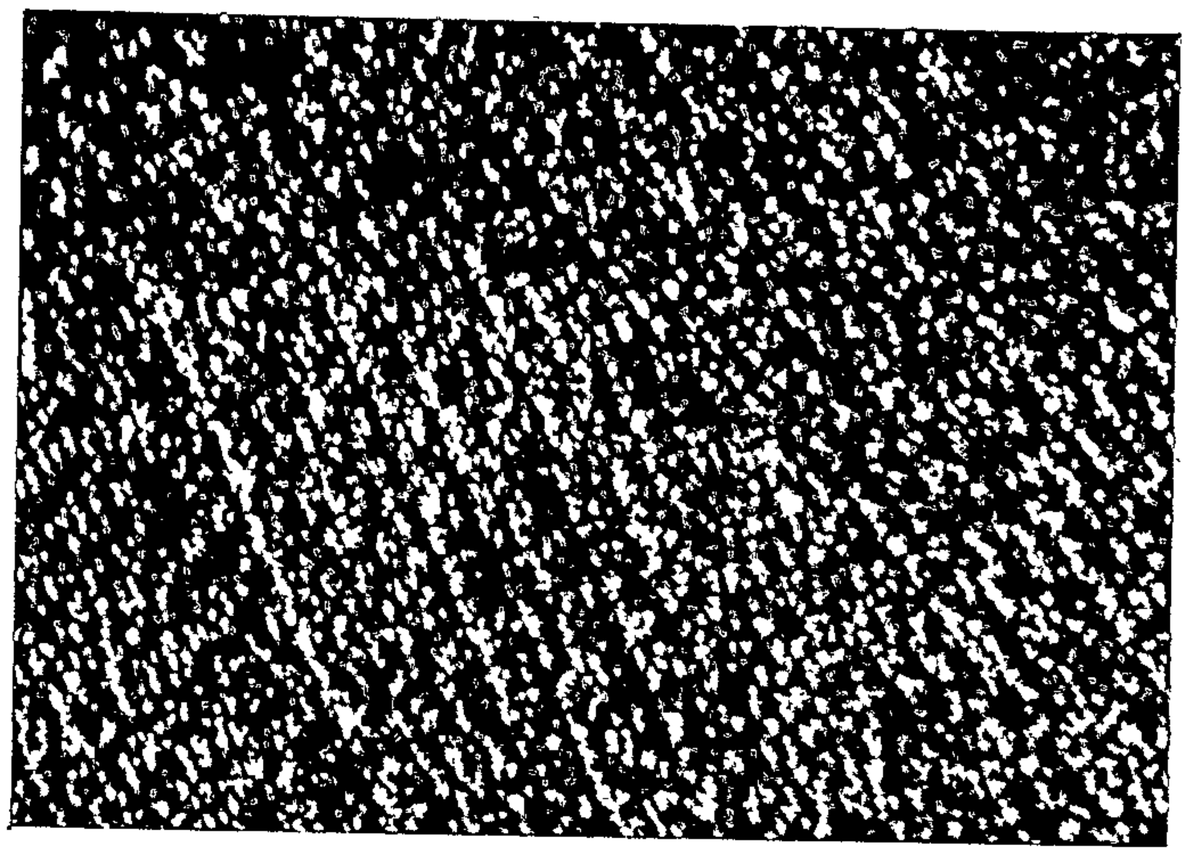

Figure 10.24d
Photomicrograph of a Microbond NP^2 specimen electrolytically etched under the same etching conditions as the specimen depicted in Figure 10.24c. Specimen coded No. 1. This specimen was judged as the best in the group of five (X 168).

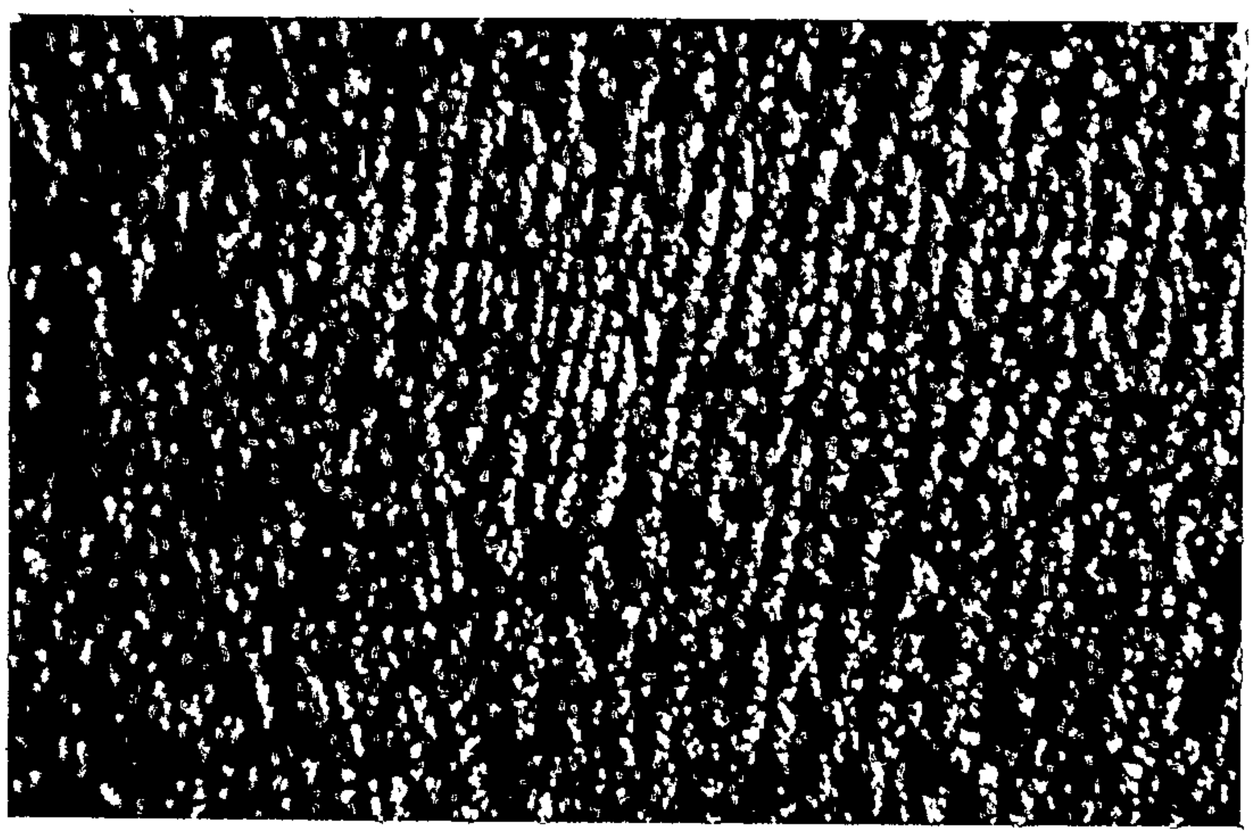

Figure 10.25a
Photomicrograph of a Microbond NP^2 specimen electrolytically etched under the etching conditions B,1,I (recommended etching solution concentration, decreased current density and etching time) (X 168).

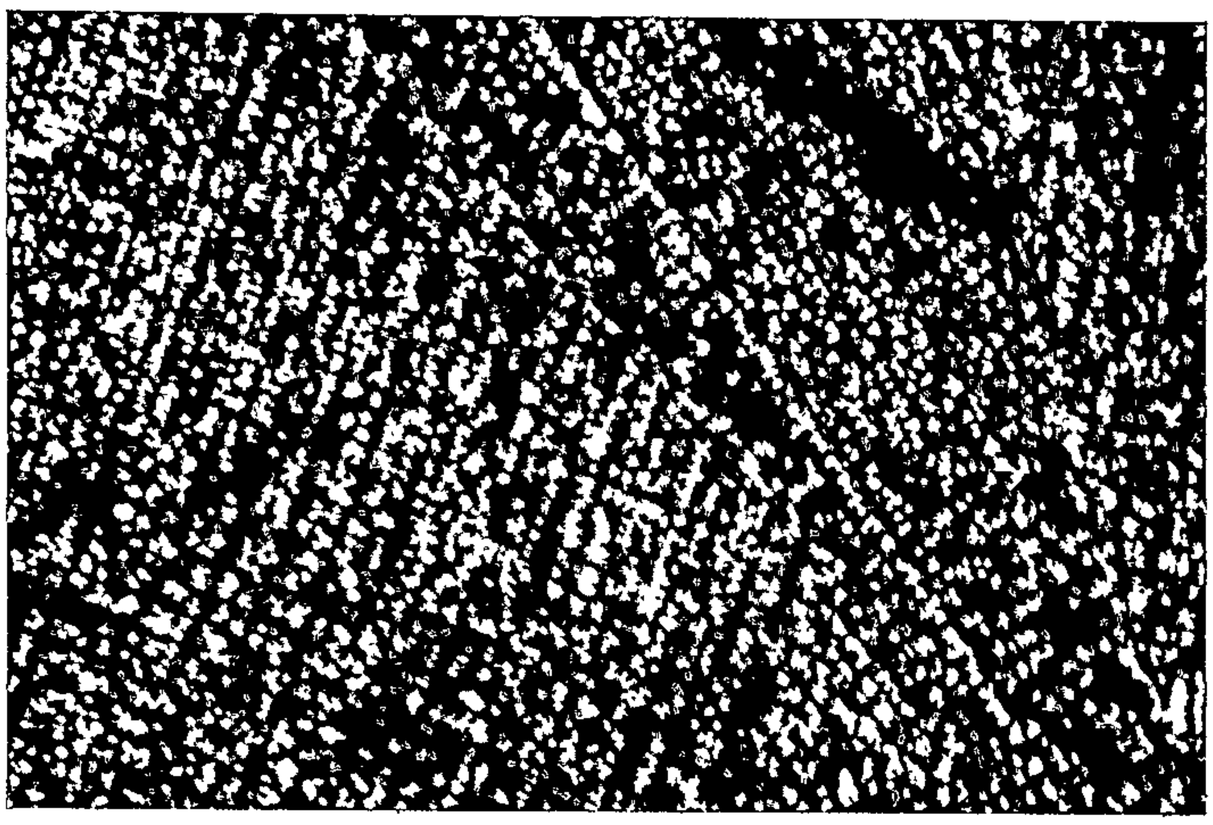

Figure 10.25b
Photomicrograph of a Microbond NP^2 specimen electrolytically etched under the etching conditions B,2,II (recommended etching solution concentration, current density and etching time) (X168).

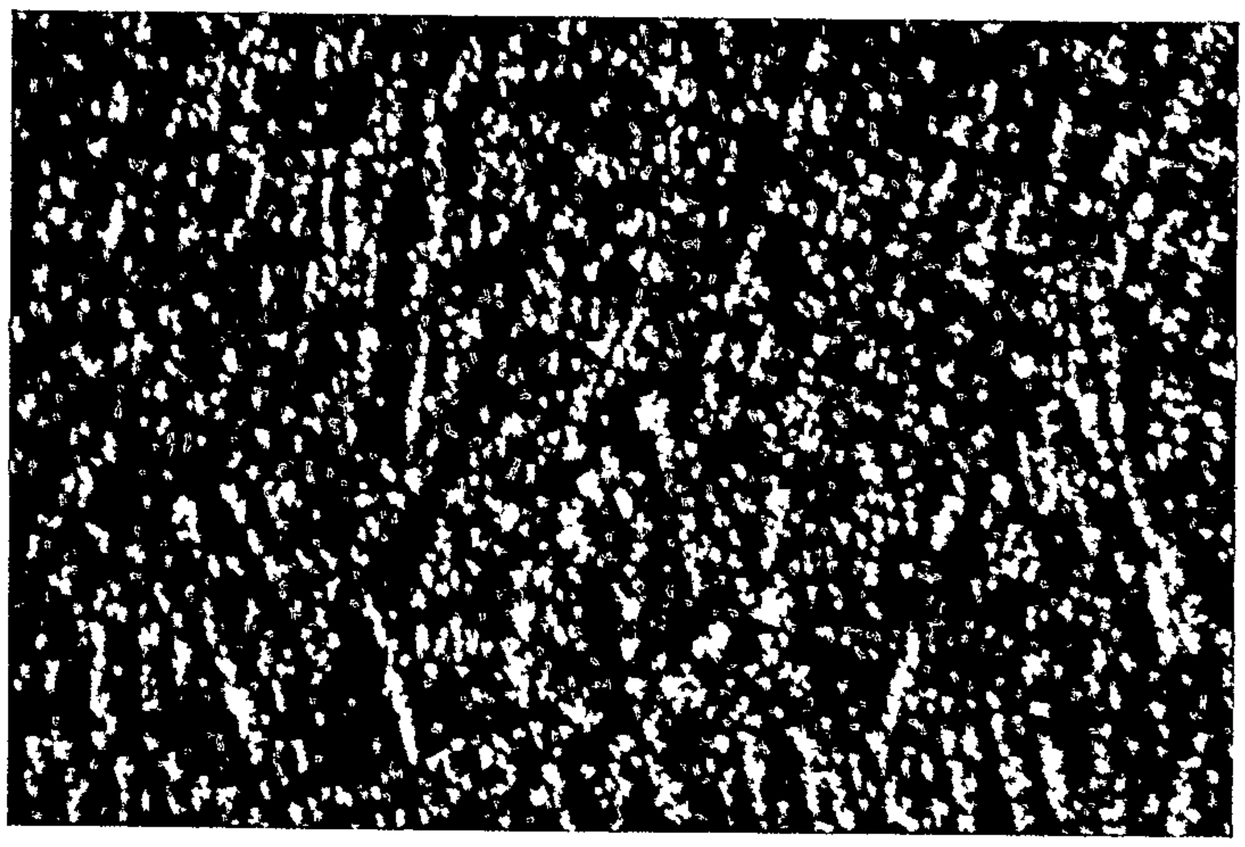

Figure 10.25c
Photomicrograph of a Microbond NP^2 specimen electrolytically etched under the etching conditions B,3,III (recommended etching solution concentration, increased current density and etching time) (X 168).

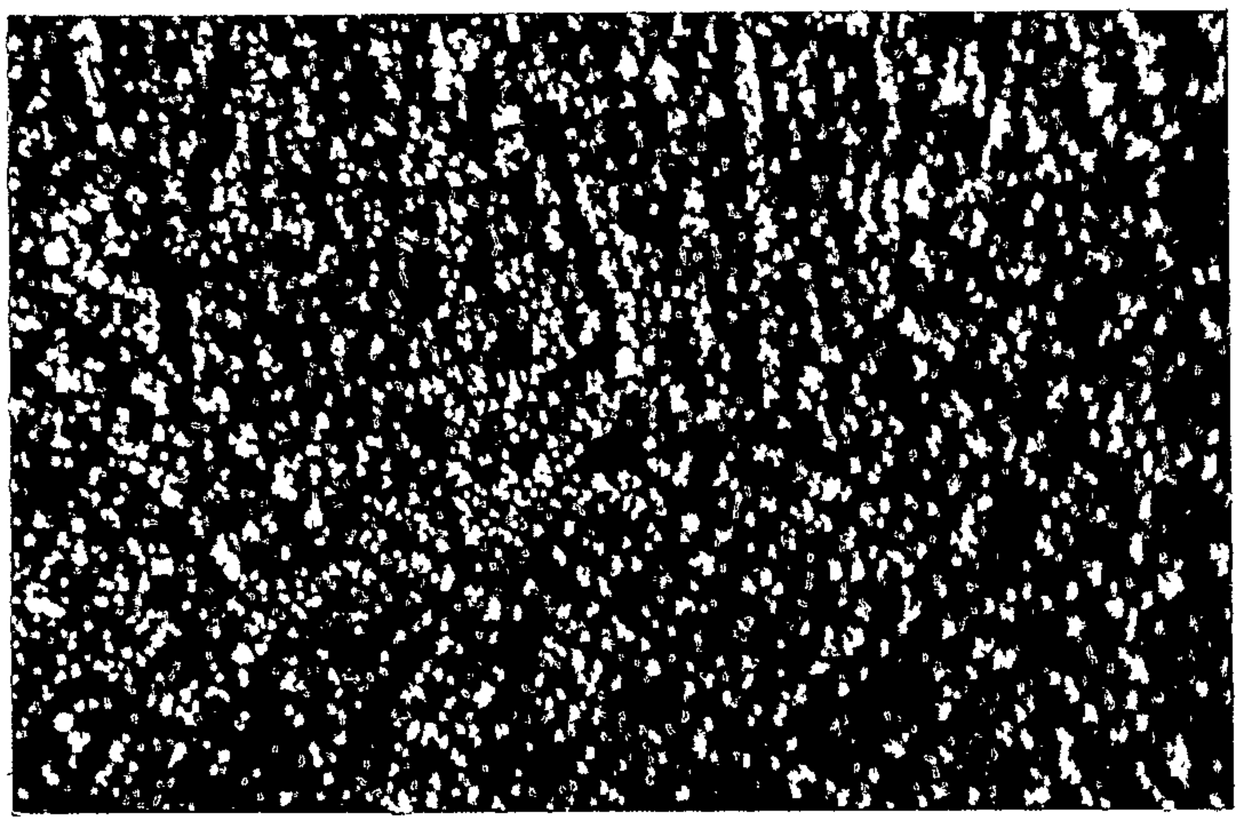

Figure 10.26a
Photomicrograph of a Microbond NP^2 specimen electrolytically etched under the etching conditions B,3,II. Specimen coded No. 1. This specimen was judged to be the best in the group of five but failed to survive thermal-cycling (X 168).

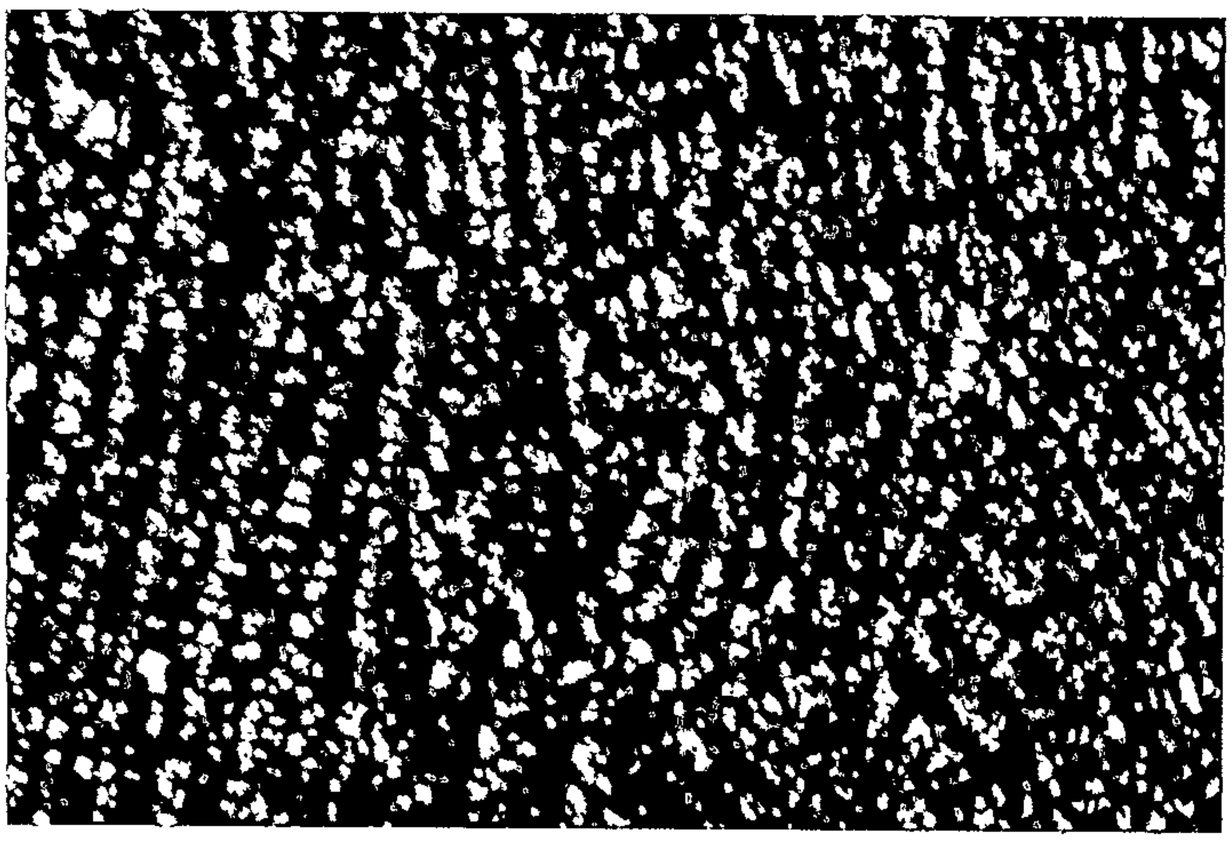

Figure 10.26b
Photomicrograph of a Microbond NP^2 specimen from the same group as that depicted in Figure 10.26a. Specimen coded No. 4. This specimen was judged to be the worst in the group of five but provided a tensile bond strength of 3.32 MPa (X 168).

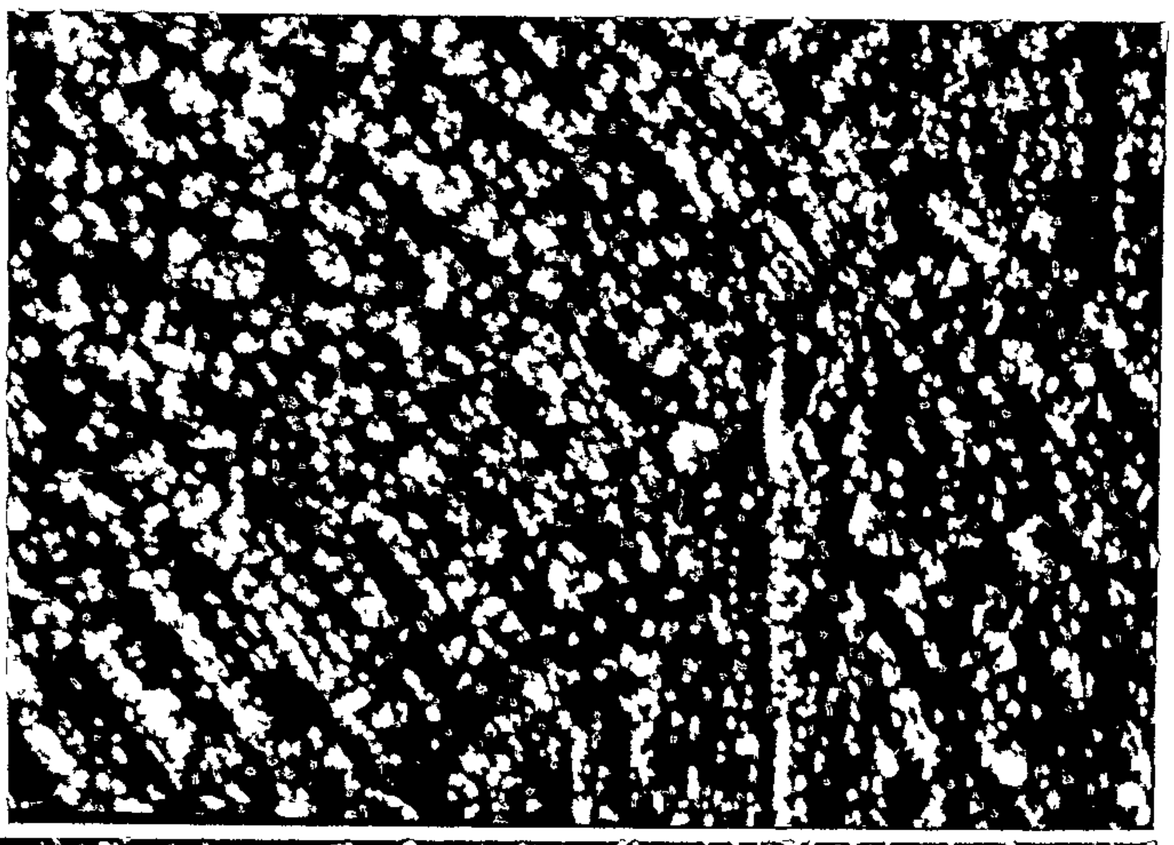

Figure 10.26c
Photomicrograph of a Microbond NP^2 specimen electrolytically etched under the etching conditions C,3,III. Specimen coded No. 1. This specimen was judged the best in the group of five and produced a tensile bond strength of 5.53 MPa (X 168).

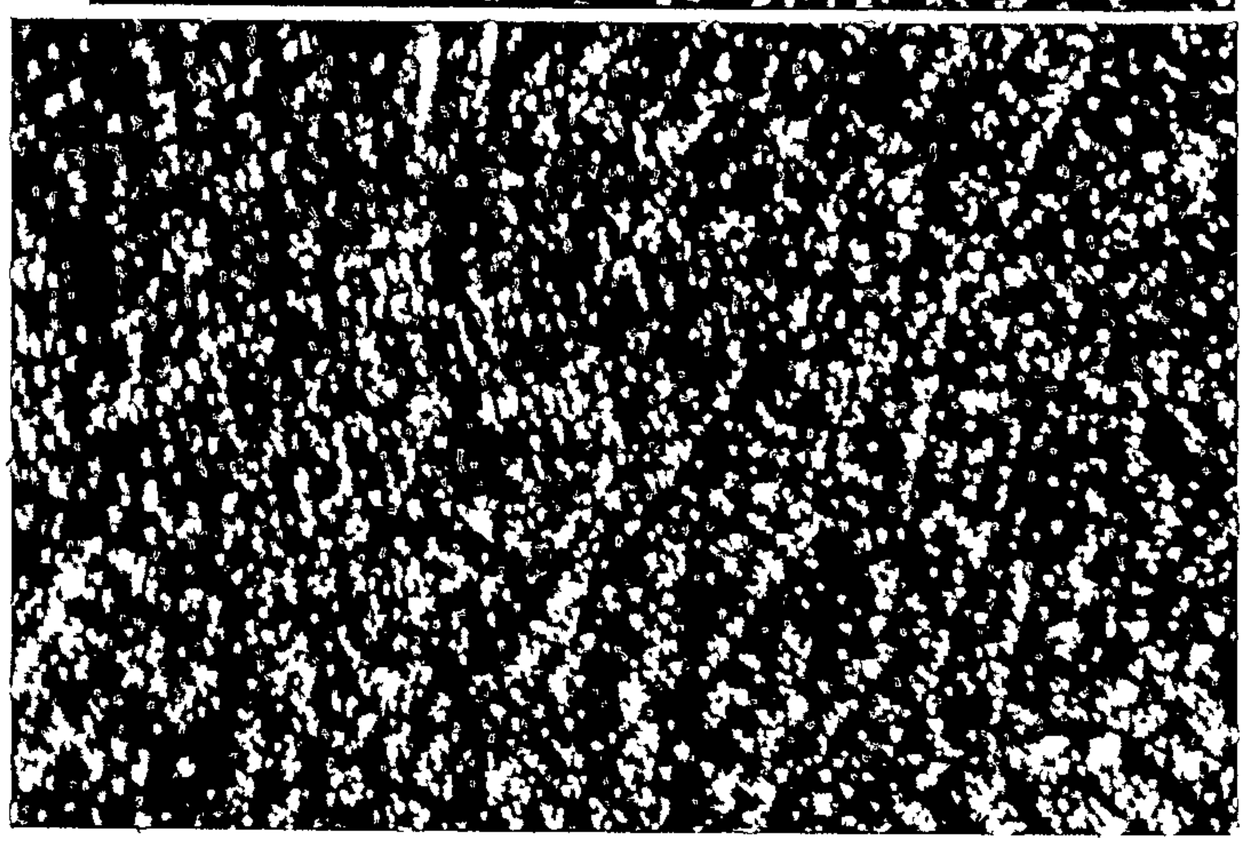

Figure 10.26d
Photomicrograph of a Microbond NP^2 specimen from the same group as that depicted in Figure 10.26c. Specimen coded No. 2. This specimen was judged the worst in the group of five and produced a tensile bond strength of 1.38 MPa (X 168).

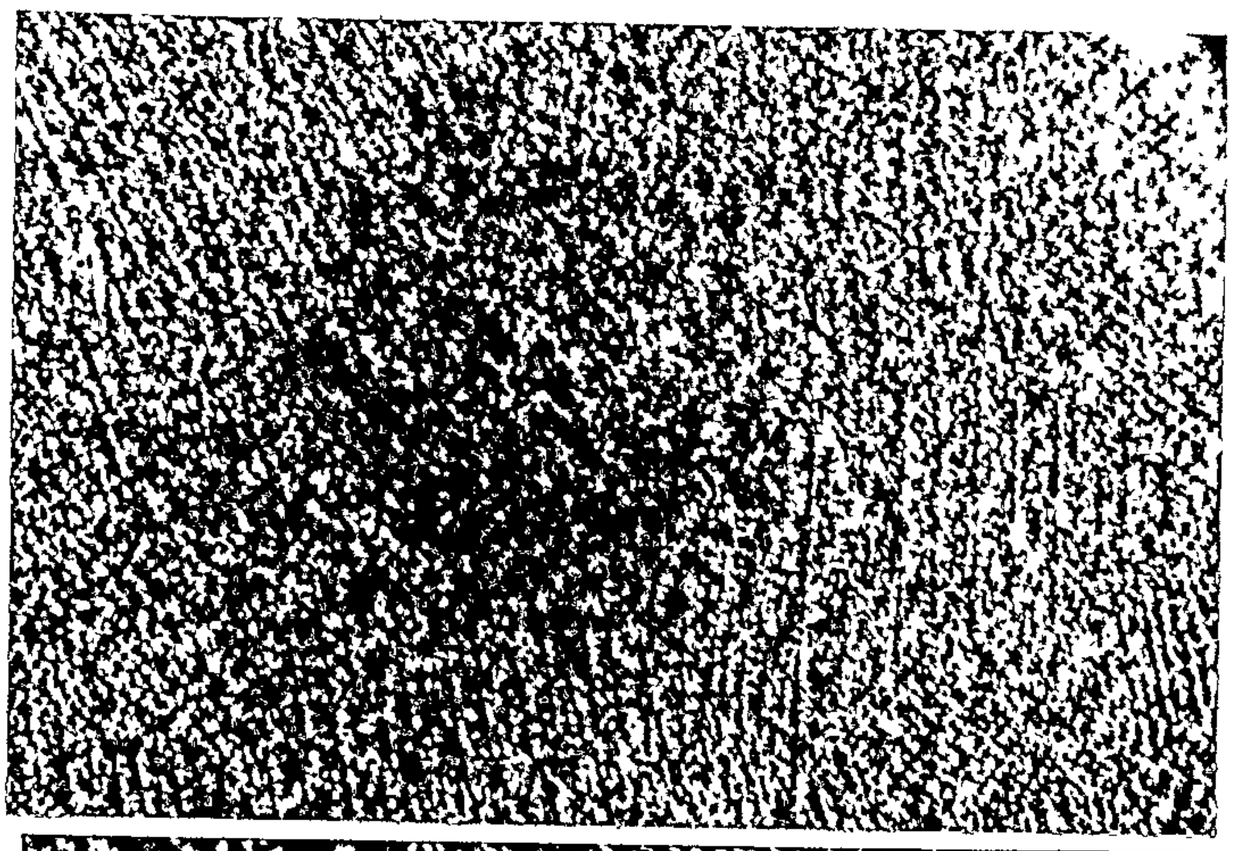

Figure 10.27
Photomicrograph of a Microbond NP^2 specimen electrolytically etched under the etching conditions B,2,II immediately after the specimen had been subjected to a simulated porcelain firing. Note the dark grey area in the centre of the specimen which is a retained layer of oxide (X 34).

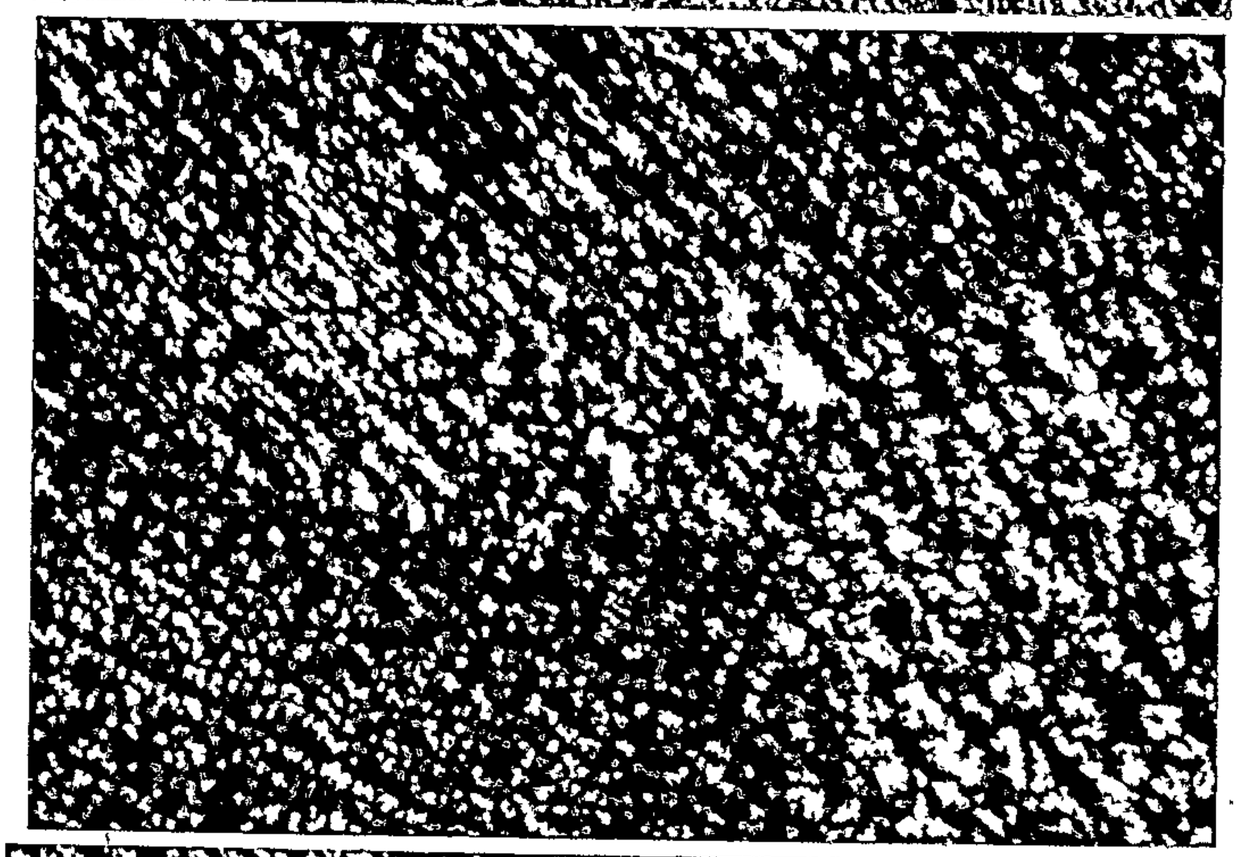

Figure 10.28a
Photomicrograph of a Microbond NP^2 specimen electrolytically etched under the etching conditions B,2,III. Specimen coded No. 1. Tensile bond strength was 6.91 MPa. Note the scattered areas of composite resin retained after bond testing (X 168).

Figure 10.28b
Photomicrograph of the Microbond NP^2 specimen No.3 from the group mentioned in Figure 10.28a. This specimen failed to survive thermal-cycling and there are no areas of retained composite resin (X 168).

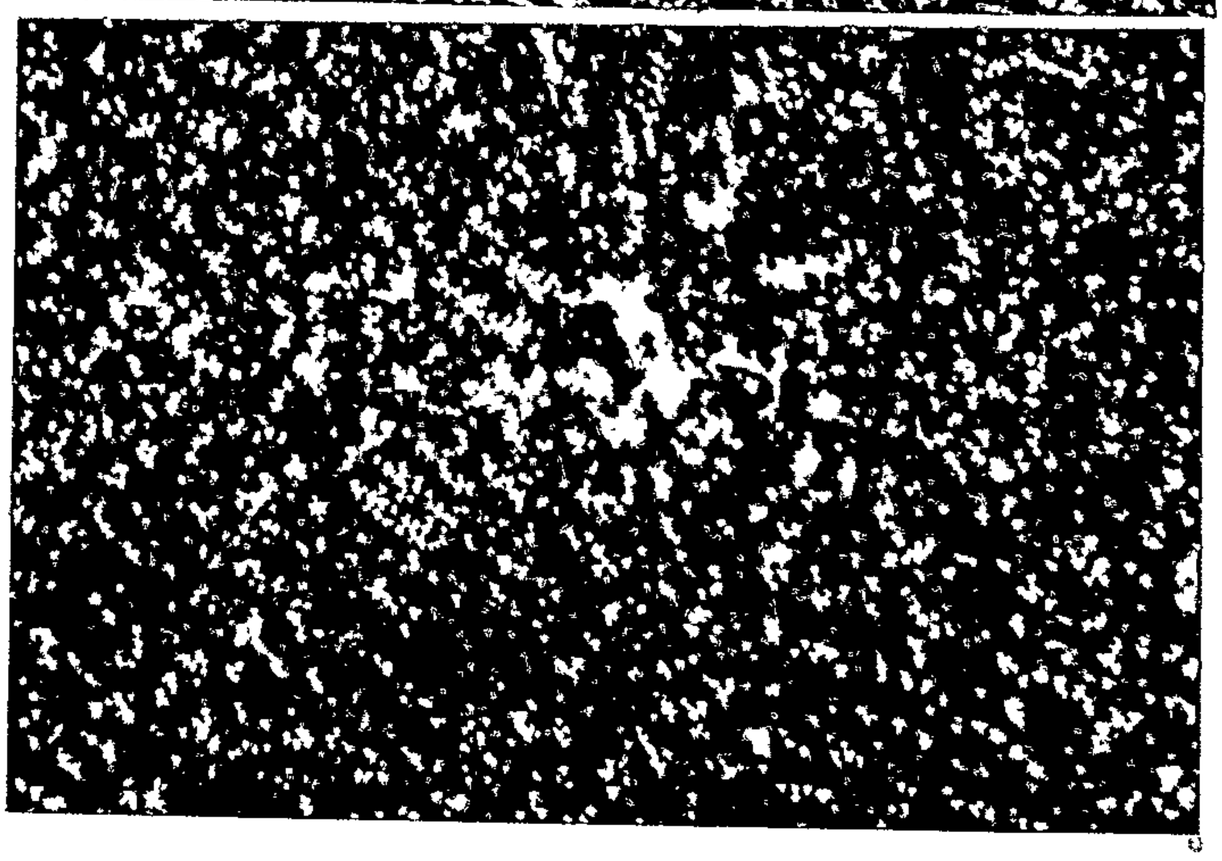

Figure 10.28c
Photomicrograph of a Microbond NP^2 specimen electrolytically etched under the etching conditions A,2,II. Specimen coded No. 4. Tensile bond strength = 9.85 MPa. Many areas of composite resin retained after bond testing can be seen (X 168).

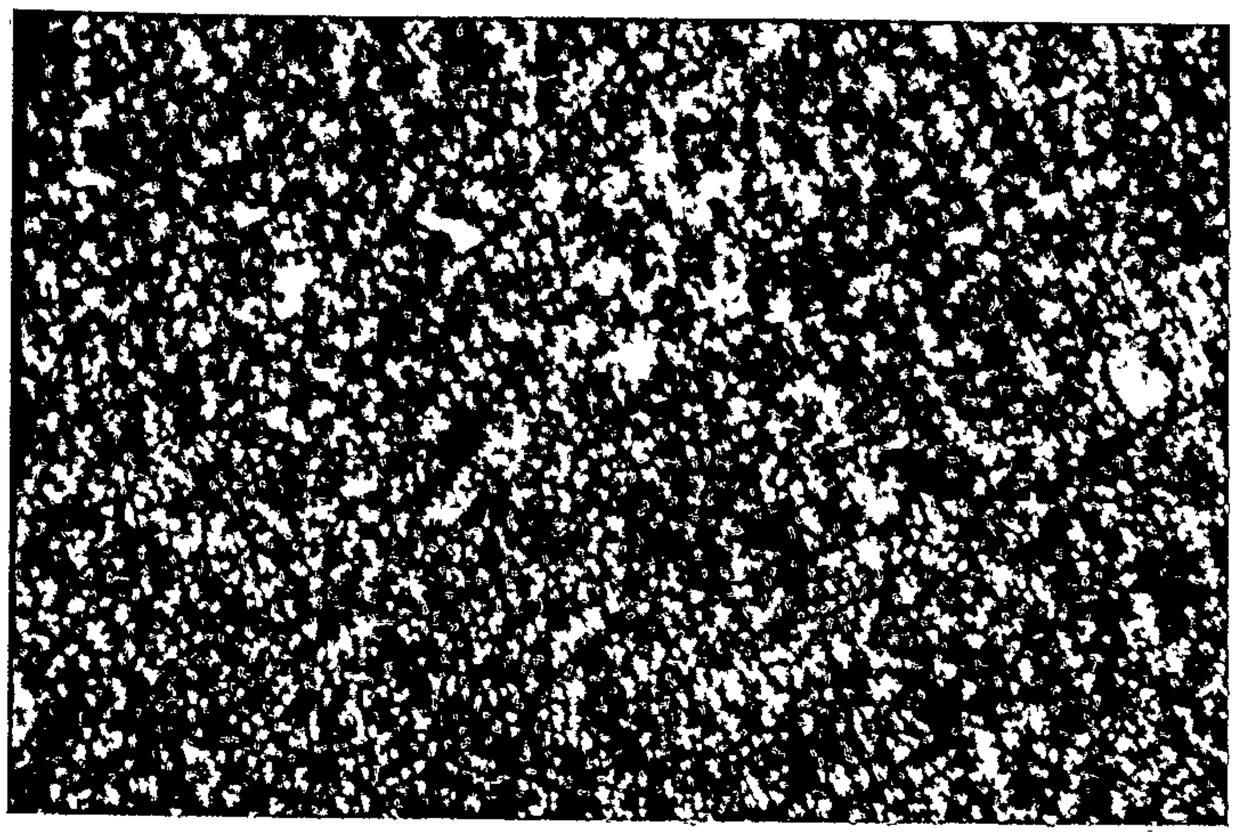

Figure 10.28d
Photomicrograph of a Microbond NP^2 specimen from the same group as that mentioned in Figure 10.28c. Specimen coded No. 1. Tensile bond strength = 4.98 MPa. Only a few areas of composite resin retained after bond testing can be seen (X 168).

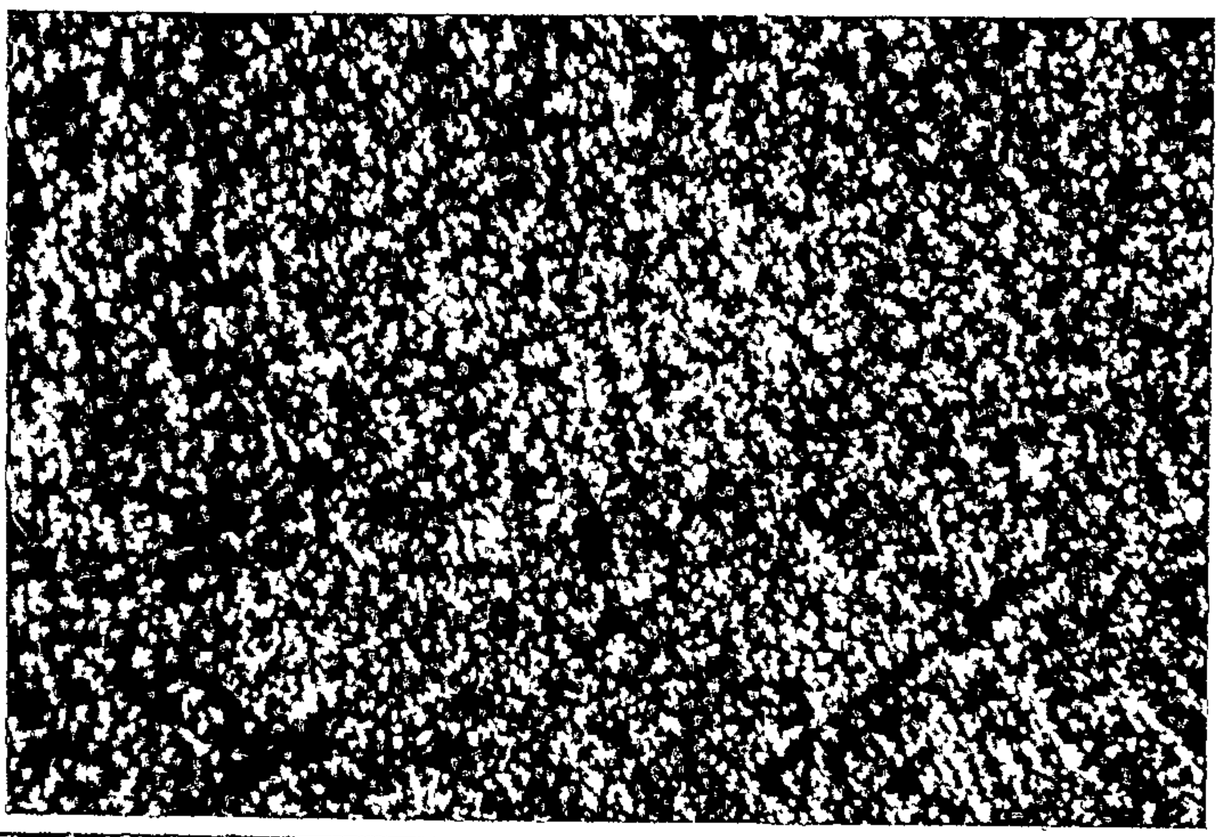

Figure 10.28e
Photomicrograph of a Microbond NP^2 specimen from the same group as that mentioned in Figure 10.28c. Specimen coded No. 2. This specimen failed to survive thermal-cycling and no areas of retained composite resin can be seen (X 168).

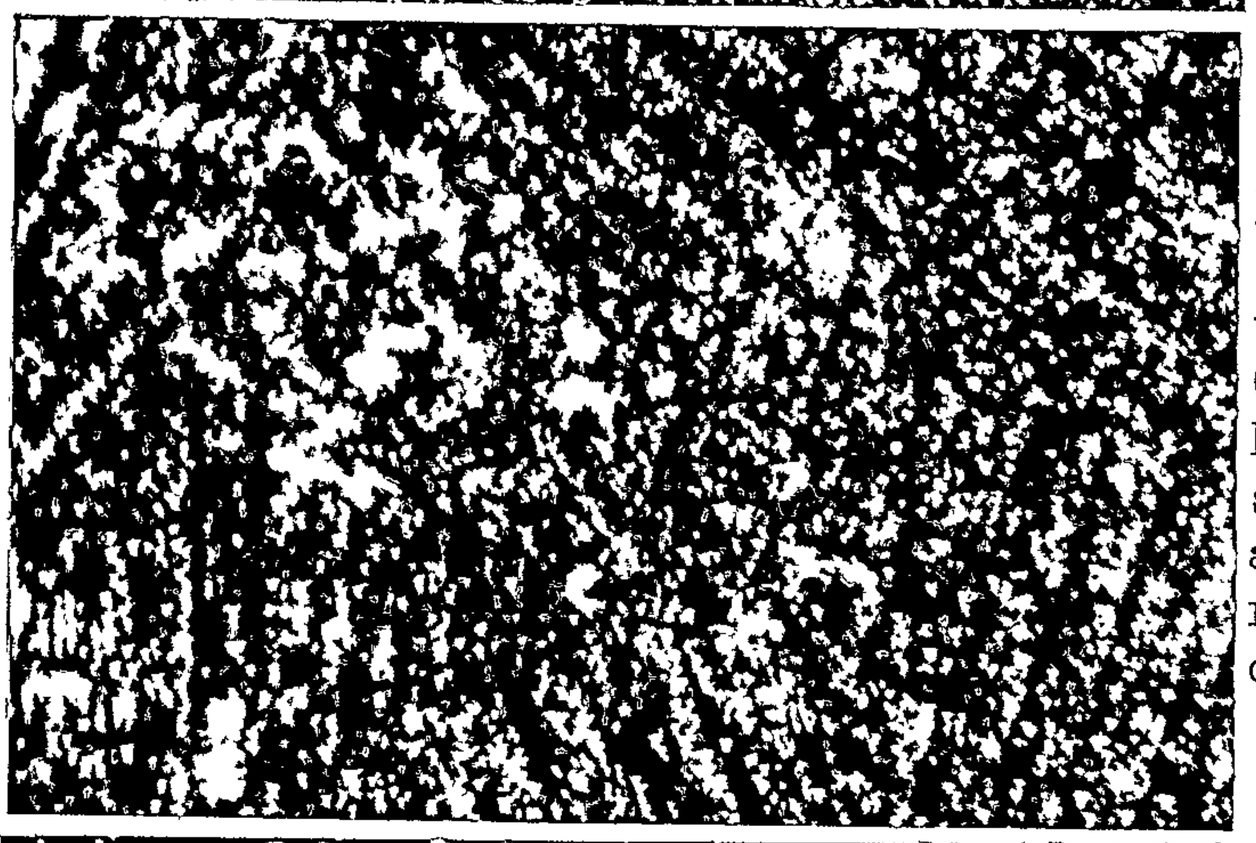

Figure 10.28f
Photomicrograph of a Microbond NP^2 specimen electrolytically etched under the etching conditions C,3,III. Specimen coded No. 1. Tensile bond strength strength = 4.98 MPa. Some areas of composite resin retained after bond testing can be seen (X 168).

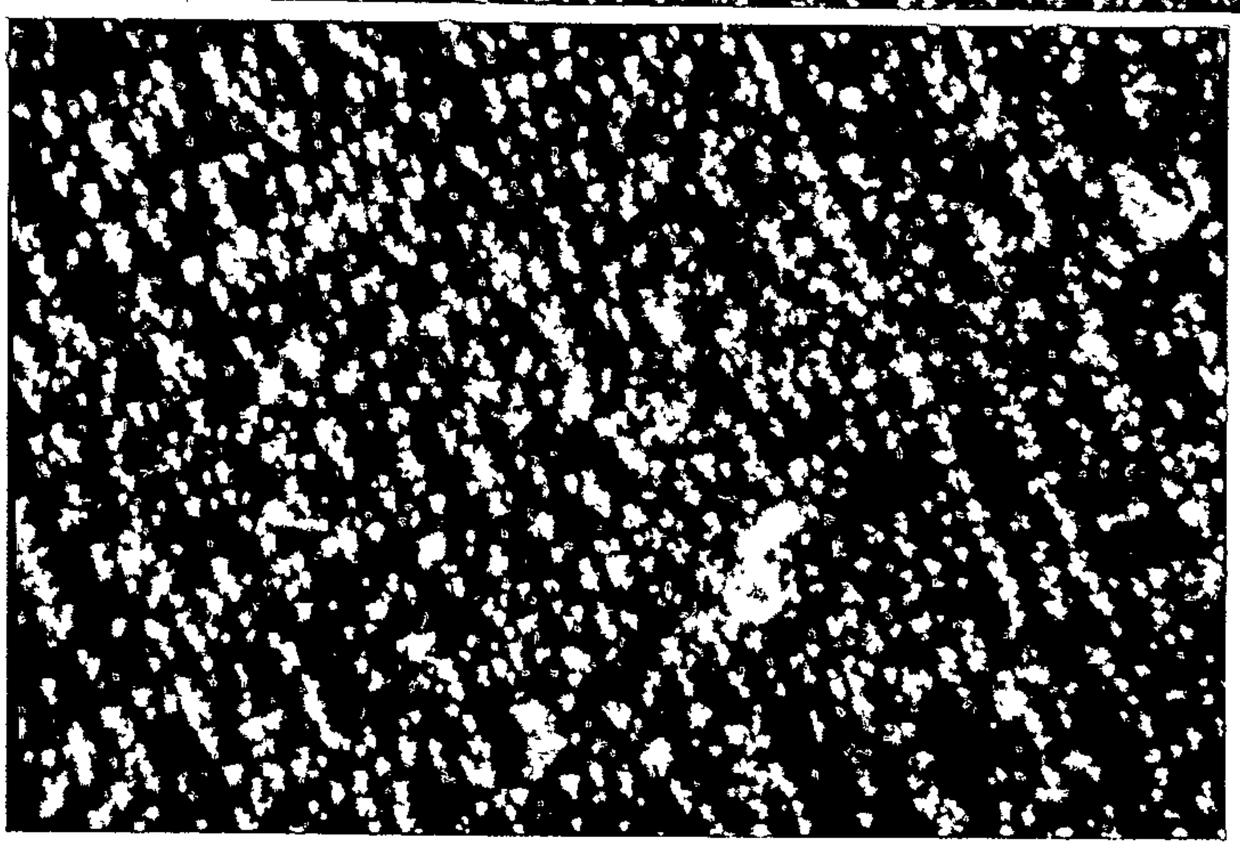

Figure 10.28g
Photomicrograph of a Microbond NP^2 specimen from the same group mentioned in Figure 10.28f. This specimen failed to survive thermal-cycling and no retained composite resin can be seen (X 168).

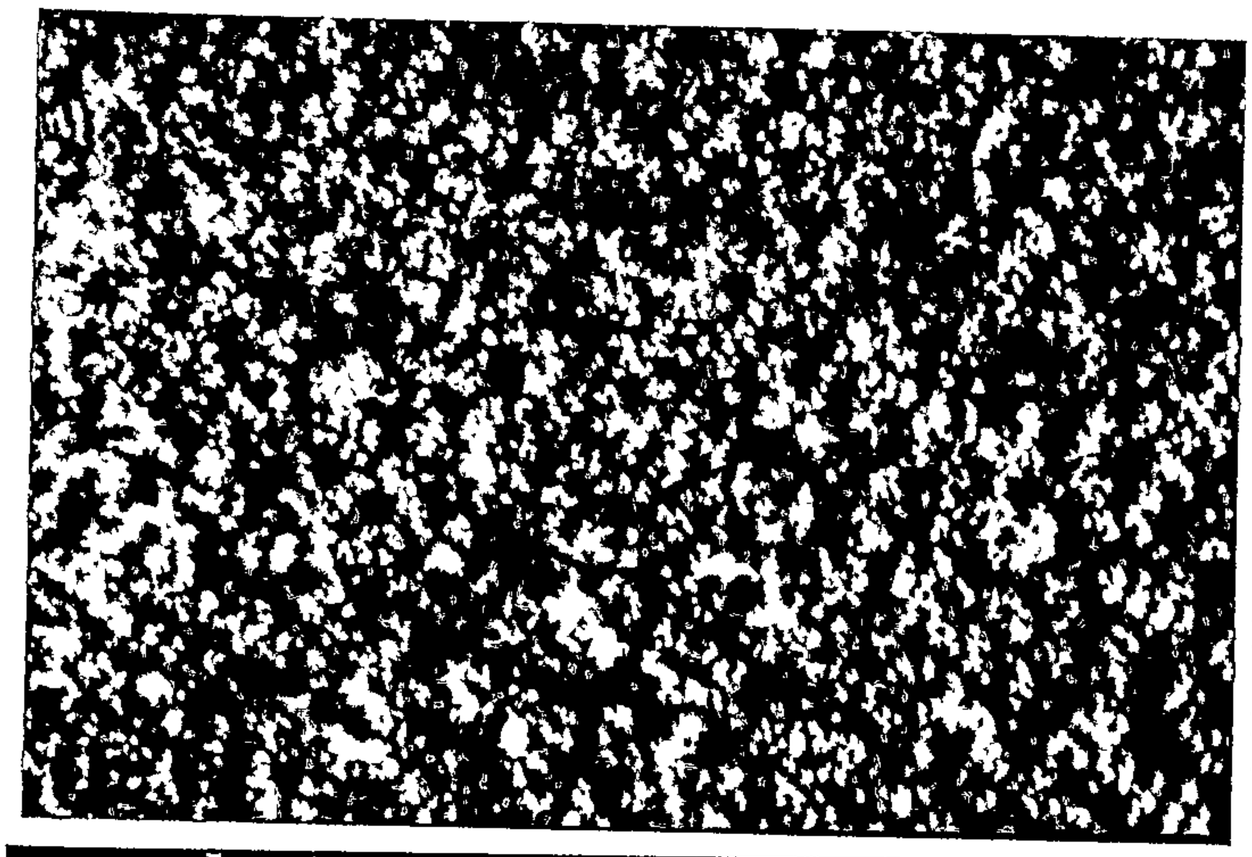

Figure 10.29
Photomicrograph of a Microbond NP^2 specimen electrolytically etched under the etching conditions B,2,II. This is the same specimen as that depicted in Figure 10.27 but subsequent to bond testing. Areas of composite resin can be seen surrounding the retained oxide layer. The tensile bond strength = 5.53 MPa (X 168).

Figure 10.30a
Photomicrograph of an electrolytically etched Rexillium III specimen subsequent to bond testing. This was the only specimen of Rexillium II that failed close to the etched-metal surface. A large area of retained composite resin can be seen indicating a combined cohesive and interface failure (X 34).

Figure 10.30b
Photomicrograph of the surface of the column of composite resin originally bonded to the Rexillium III specimen depicted in Figure 10.30a subsequent to bond testing (X 34).

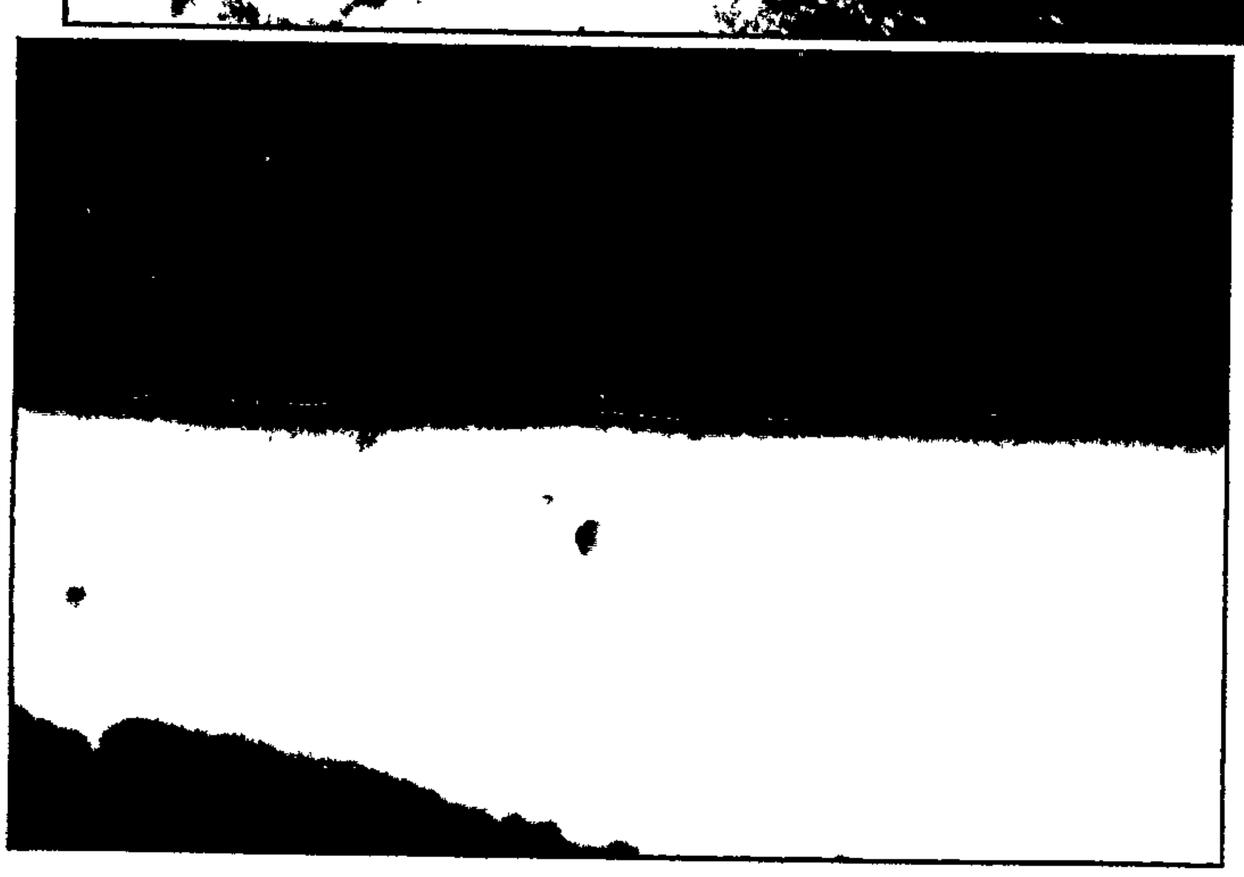

Figure 10.31
Photomicrograph of a cross-section of a column of composite resin subsequent to bond testing and removed from its retaining metal tube. A very thin layer of unfilled bonding resin can be seen covering the top of the white cement (X 168).

Figure 10.32a
Photomicrograph of the bonding surface of a column of composite resin subsequent to bond testing showing an air bubble inclusion (X 34)

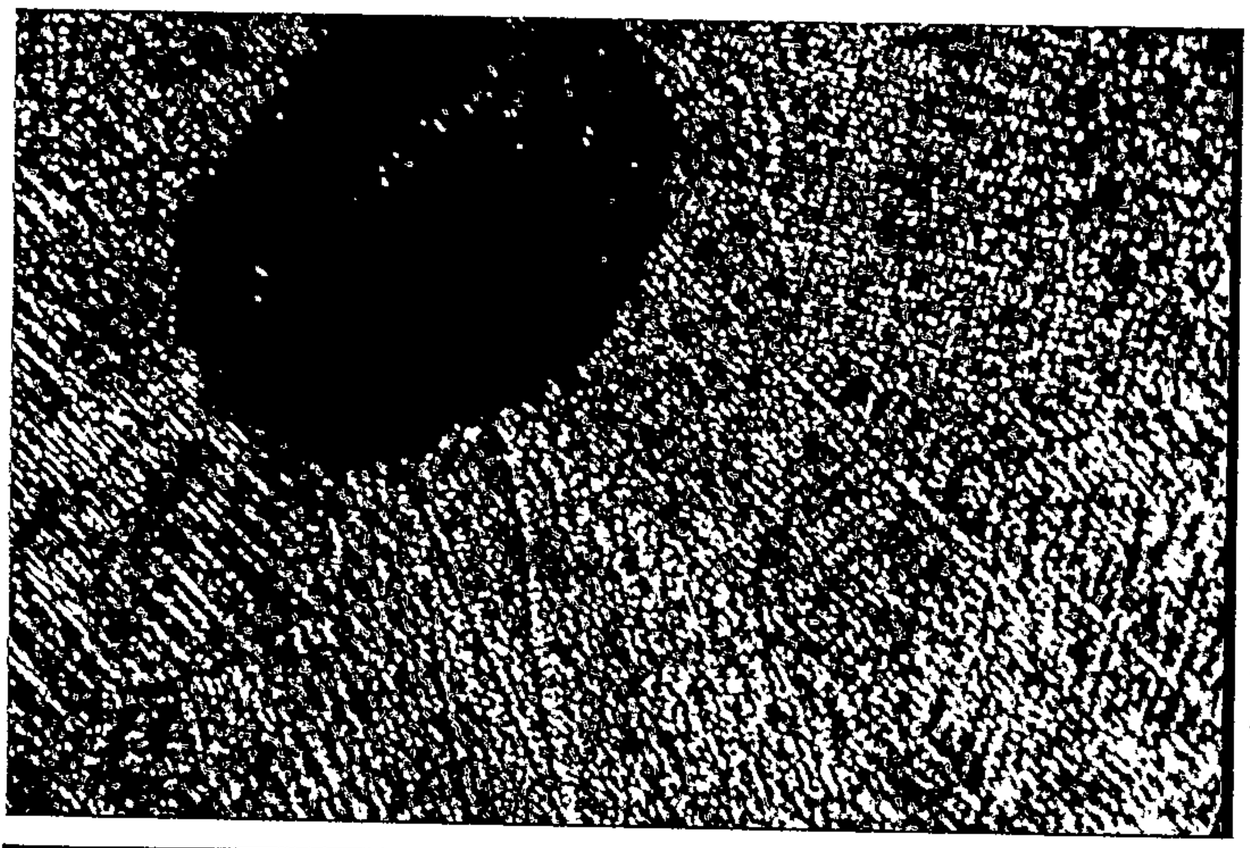

Figure 10.32b
Photomicrograph of the electrolytically etched metal surface of the Microbond NP^2 specimen previously bonded to the composite resin column depicted in Figure 10.32a. An area of retained composite resin corresponding to the floor of the air bubble can be seen. Tensile bond strength = 8.71 MPa (X 50).

Figure 10.33a
Photomicrograph of the bonding surface of a column of composite resin showing the lack of porosity (X 34).

Figure 10.33b
Photomicrograph of the column of composite resin depicted in Figure 10.33a at higher magnification. Note the fine criss-cross pattern corresponding to the dendritic morphology of the electrolytically etched metal surface to which it was bonded (X 168).

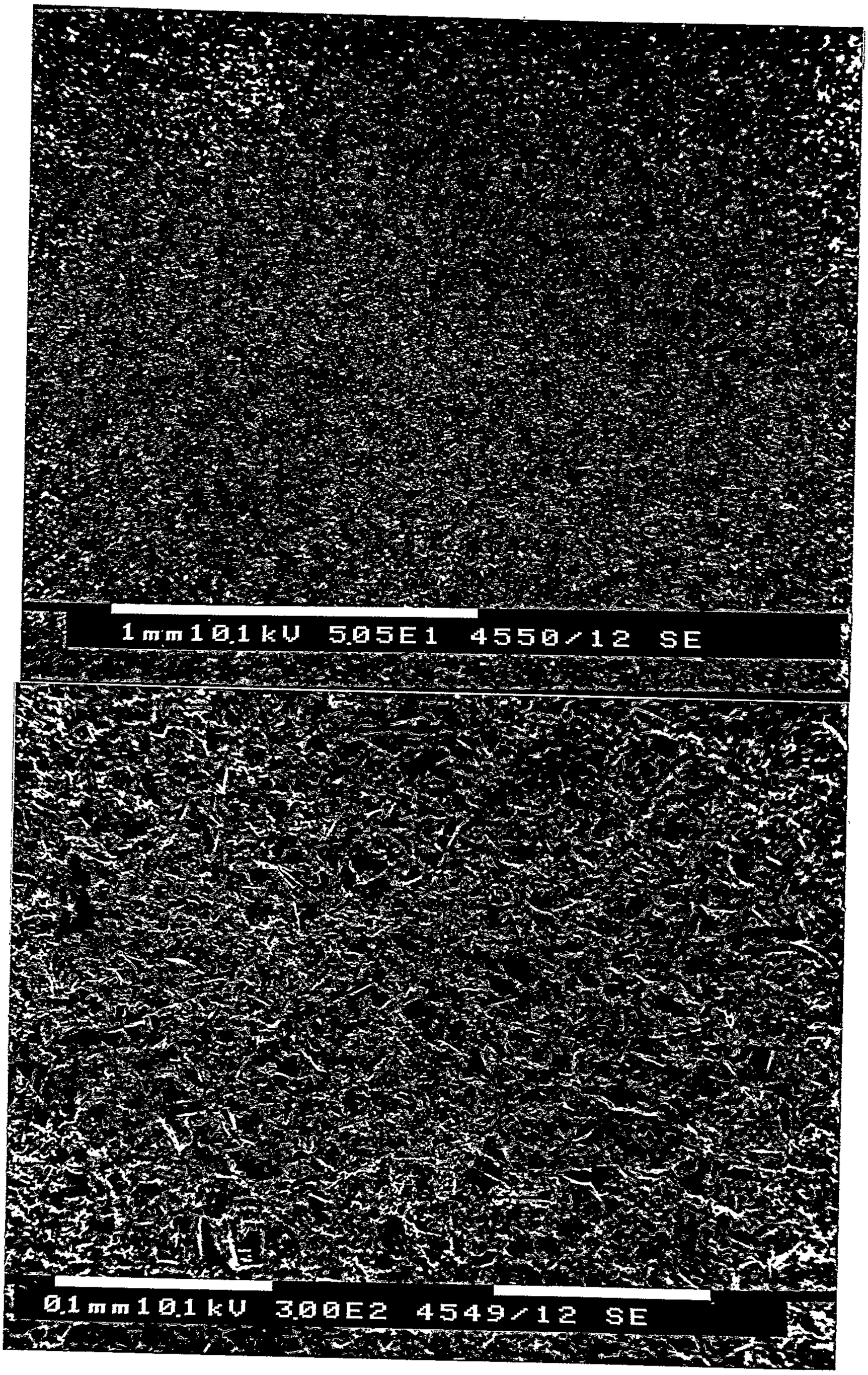

10.34a
(X 50)

10.34b
(X 300)

Figure 10.34a,b
SEM of a Microbond NP^2 specimen after sandblasting with 50μm aluminium oxide particles.

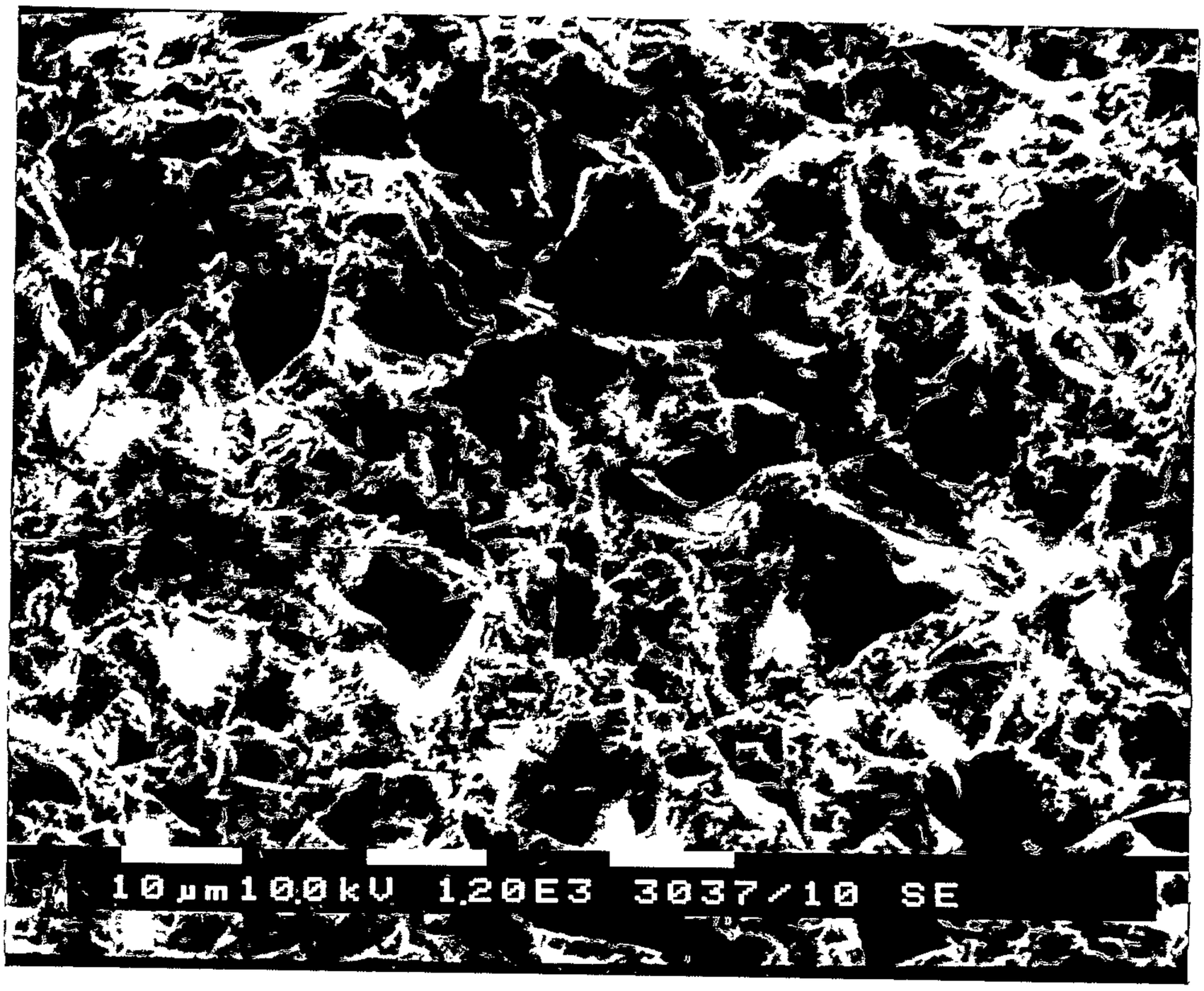

Figure 10.34c
SEM of a Microbond NP^2 specimen after sandblasting with 50µm aluminium oxide particles (X 1200).

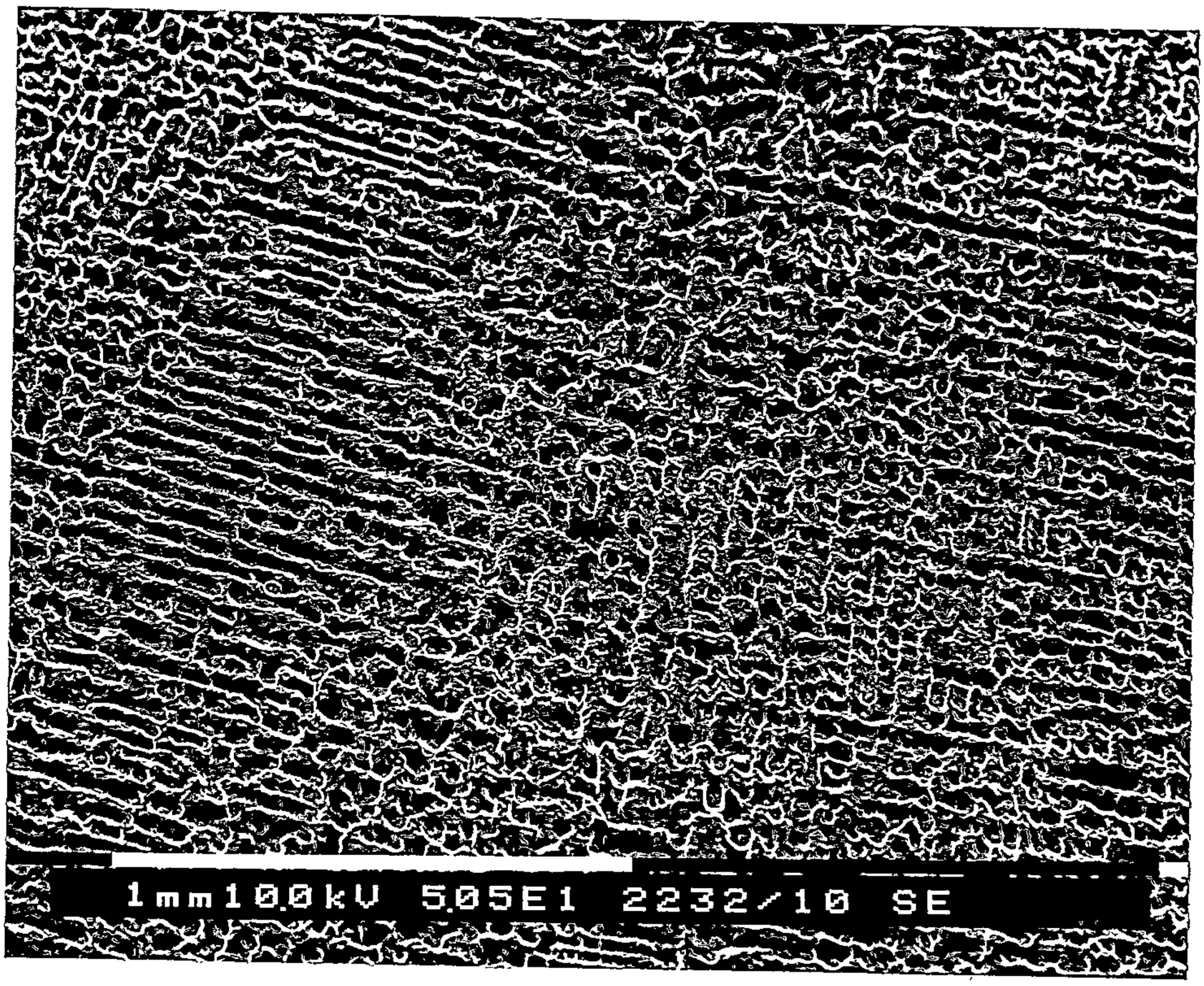

Figure 10.35a
SEM of a Microbond NP^2 specimen electrolytically etched under the manufacturer's recommended etching conditions (B,2,II; Table 10.4) (X 50).

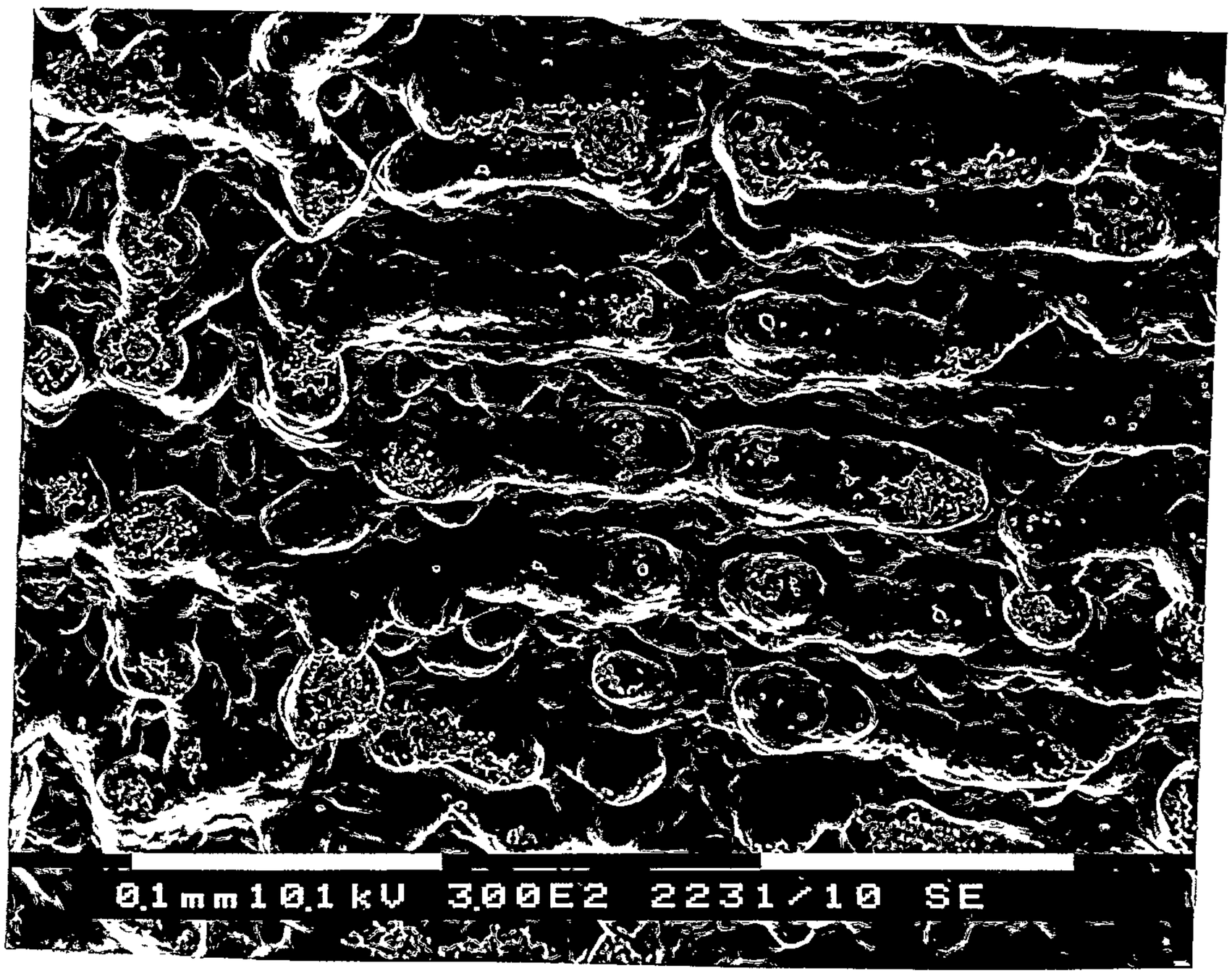

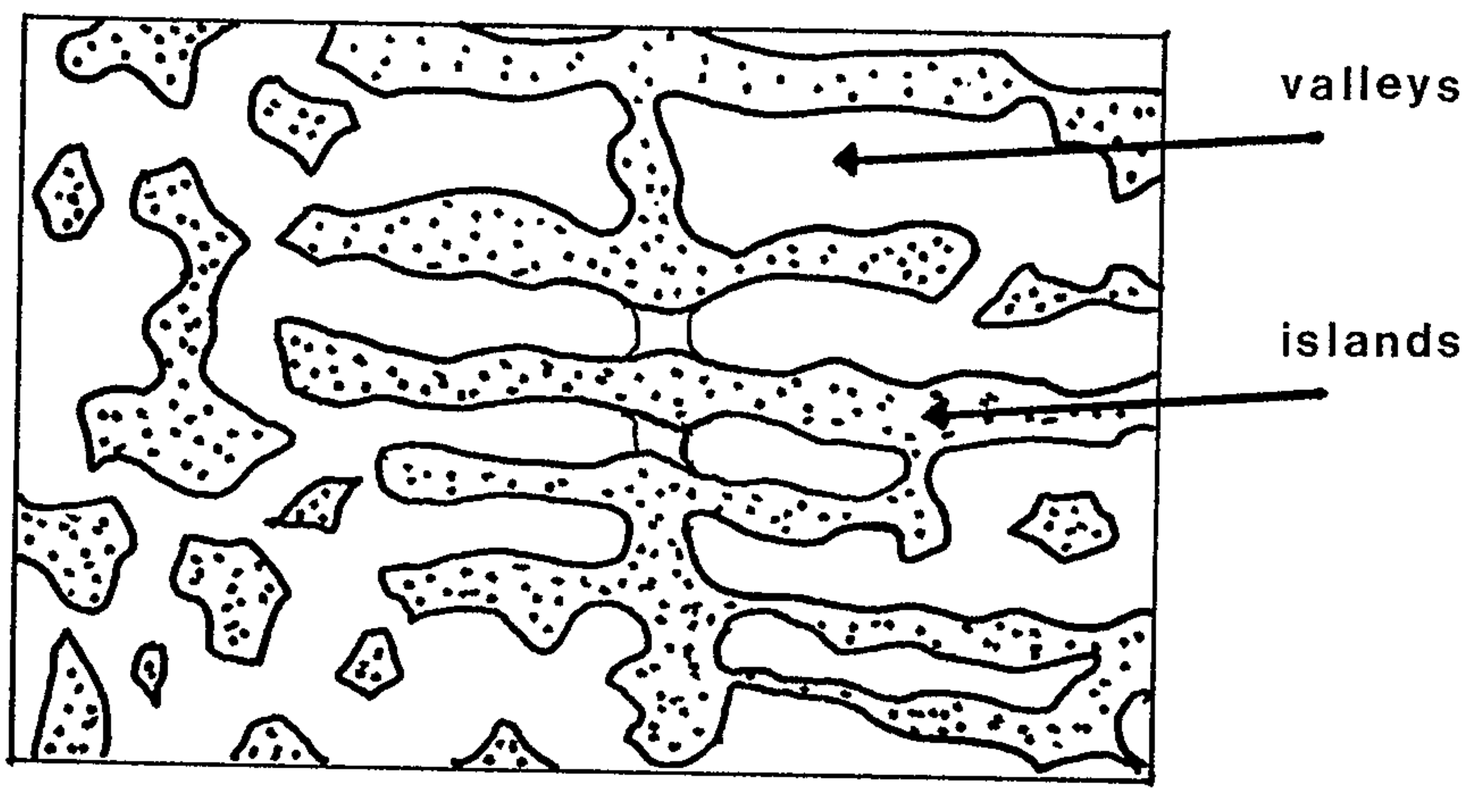

Figure 10.35b
SEM of the Microbond NP^2 specimen depicted in Figure 10.35a with a diagrammatic representation of the main topographical features. Flattened peaks, or islands (see diagram) surrounded by rounded valleys can be seen (X 300).

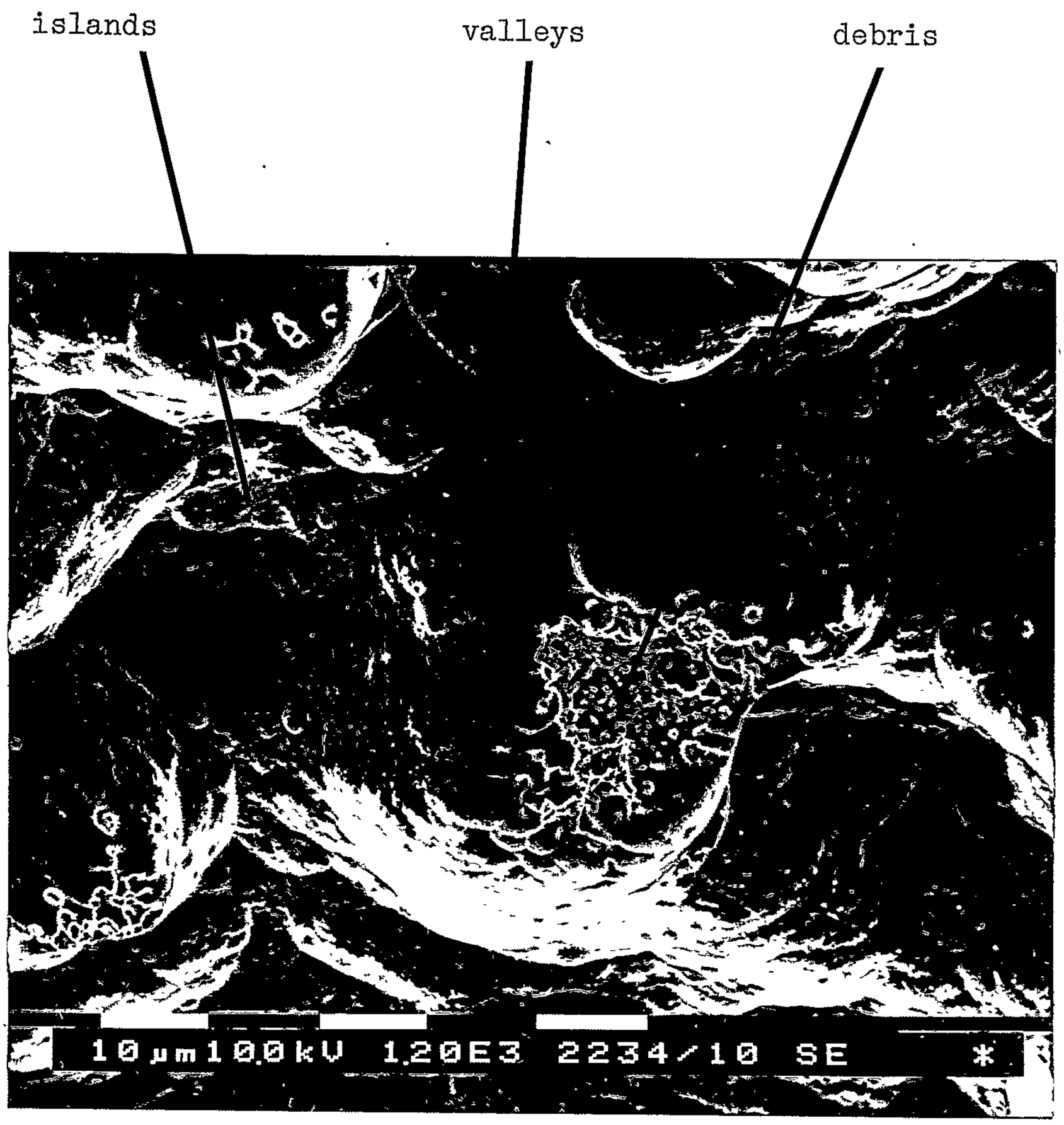

Figure 10.35c
SEM , at higher magnification, of the Microbond NP^2 specimen depicted in Figure 10.35b (X1200). Granular protrusions, or <u>debris</u>, can be seen.

10.35d
(X 2500)

10.35e
(X 5000)

Figure 10.35d,e

SEM of a Microbond NP^2 specimen electrolytically etched under the manufacturer's recommended etching conditions (B,2,II; Table 10.4) showing an area of debris at high magnification.

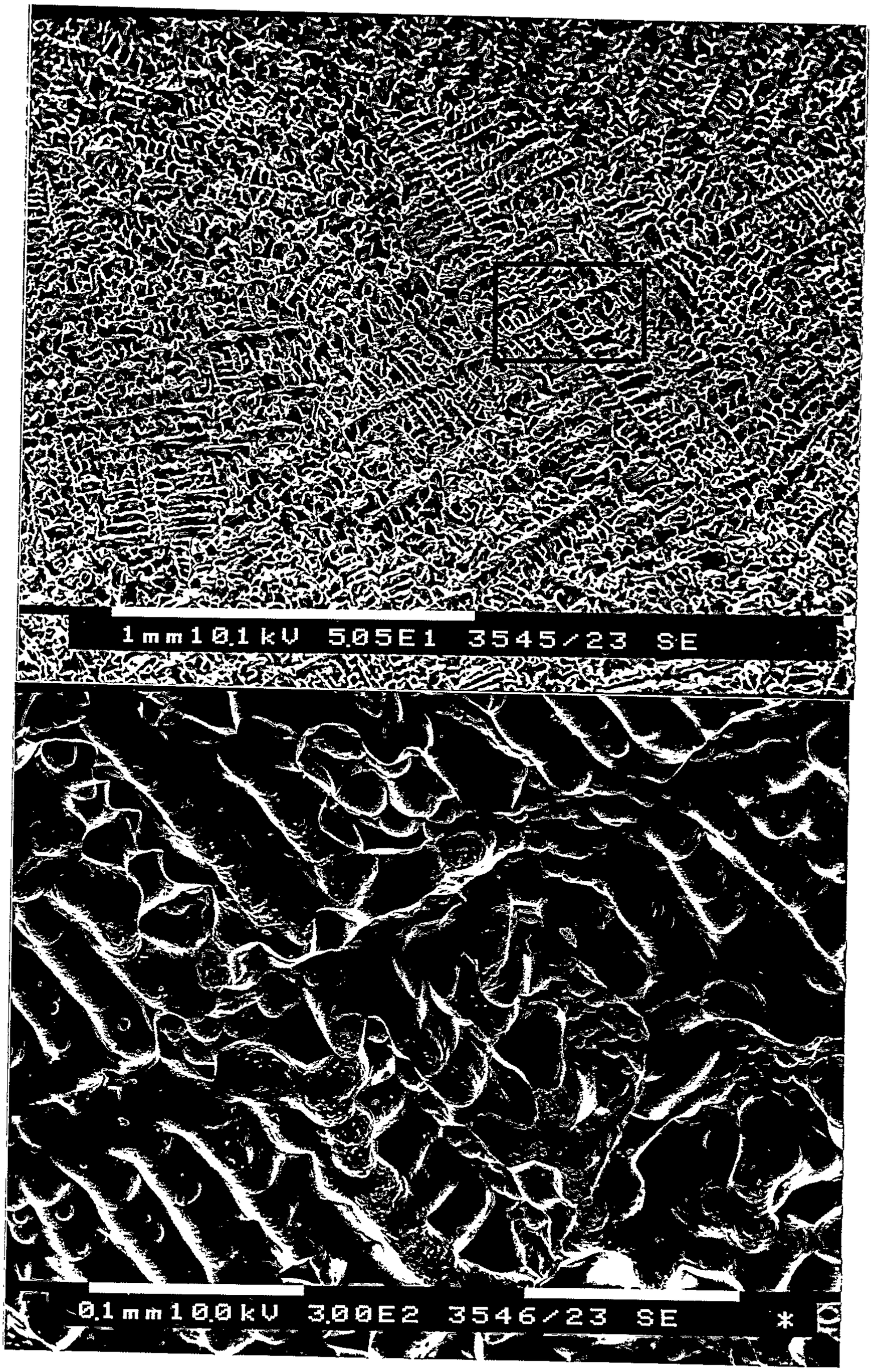

10.36a
(X 50)

10.36b
(X 300)

Figure 10.36.a,b
SEM of a Microbond NP^2 specimen electrolytically etched under the manufacturer's recommended etching conditions (B,2,II; Table 10.4). Figure 10.36b depicts the area outlined in Figure 10.37a.

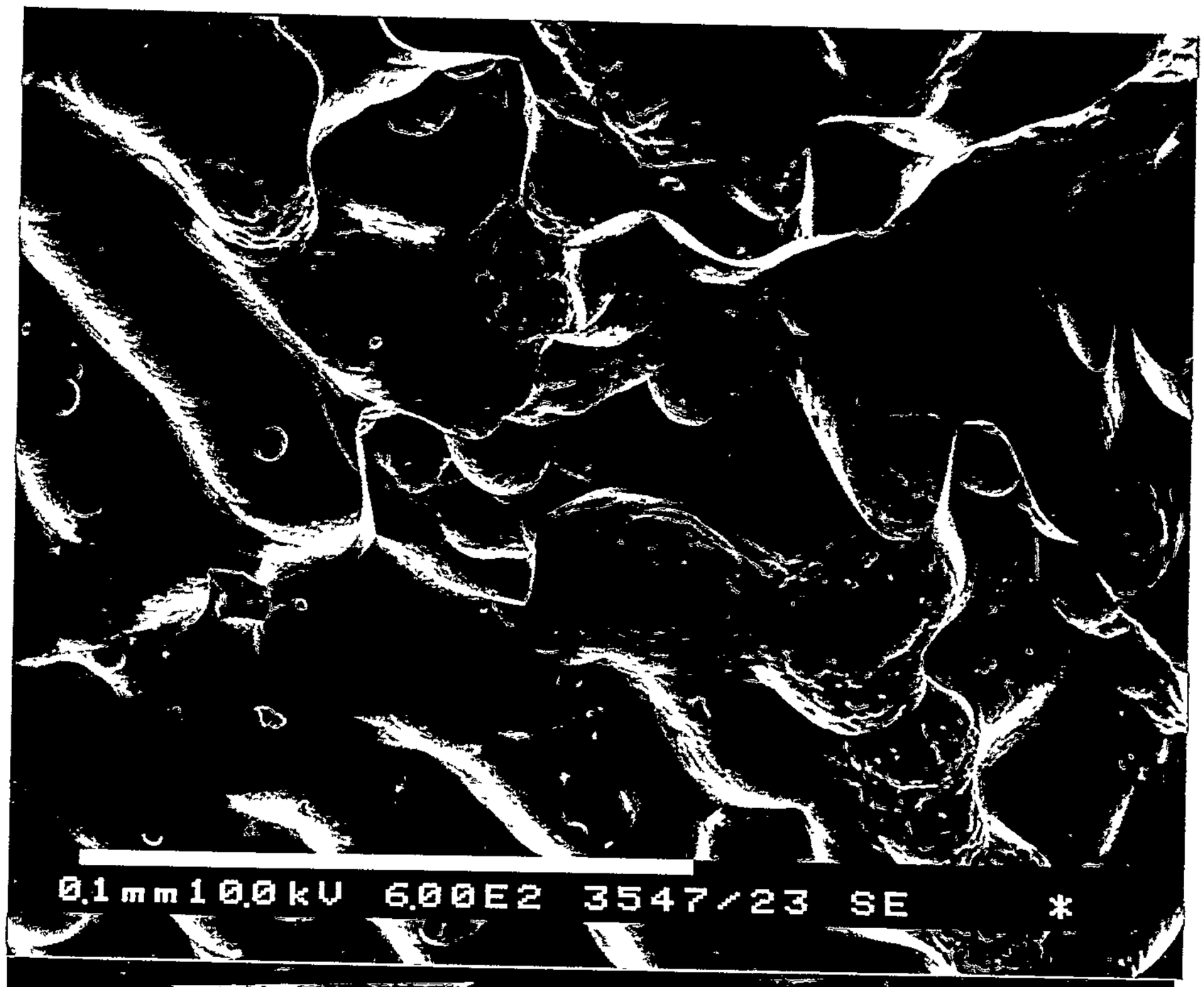

10.36c
(X 600)

10.36d
(X 1200)

Figure 10.36c,d
SEM of the Microbond NP^2 specimen depicted in Figure 10.36a,b showing, at higher magnification, the area outlined in Figure 10.36a.

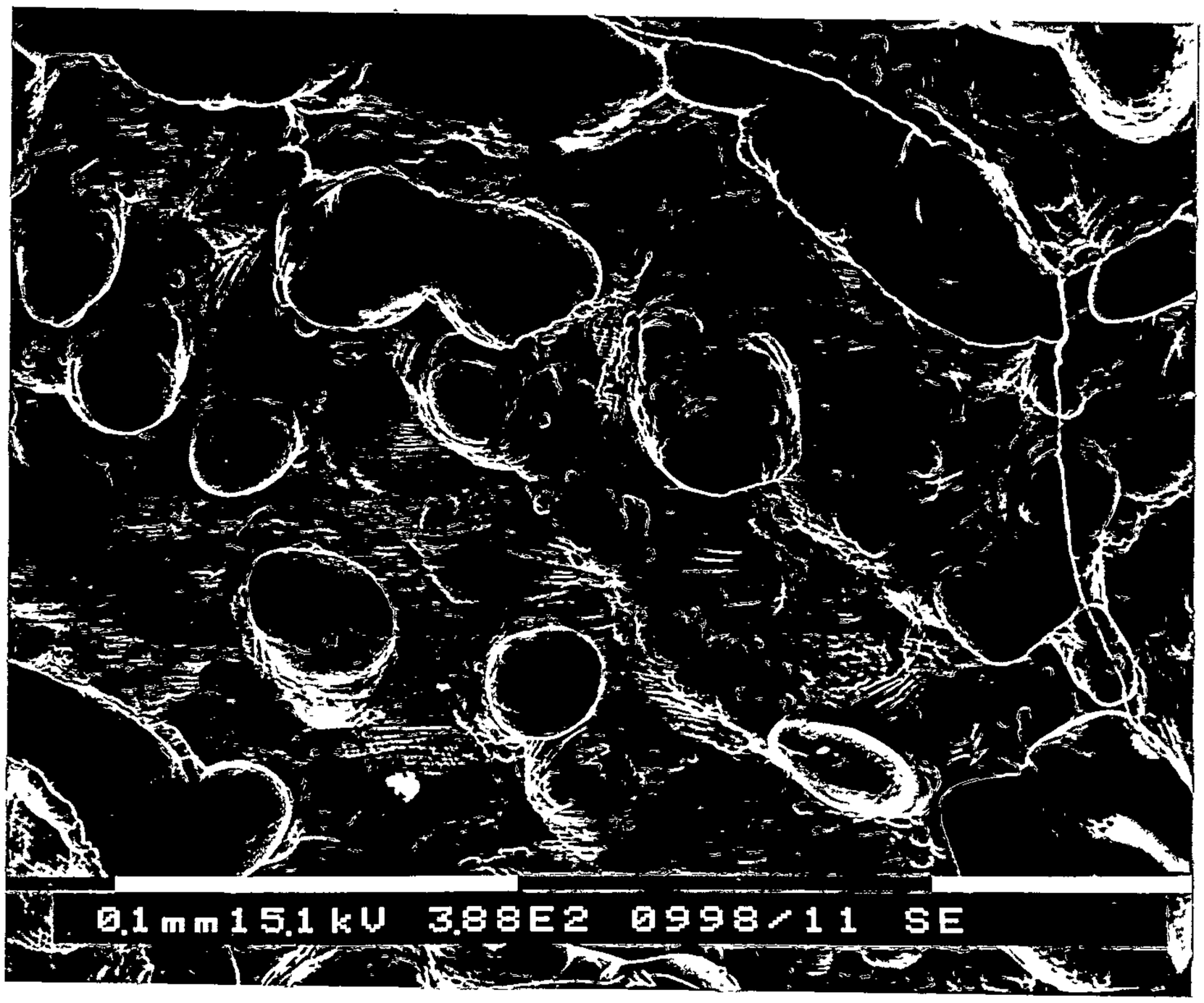

Figure 10.37
SEM of an electrolytically etched Microbond NP^2 specimen showing large islands with scratch marks thought to be marks left by the aluminium oxide particles used to sandblast the specimen prior to etching.

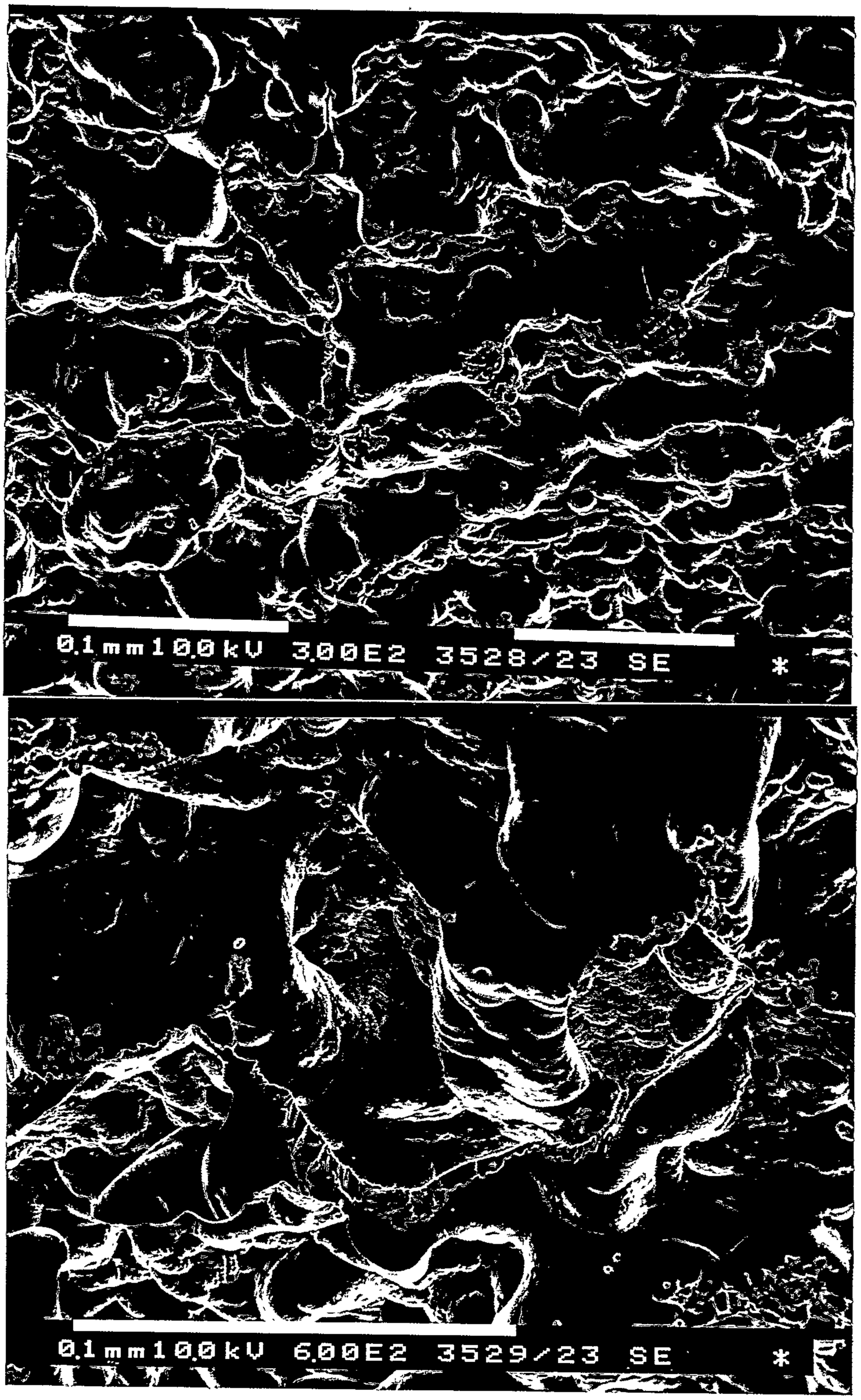

10.38a
(X 300)

10.38b
(X 600)

Figure 10.38a,b

SEM of an electrolytically etched Microbond NP^2 specimen showing the ribbon-like band thought to be a grain boundary.

Figure 10.38c
SEM of the Microbond NP^2 specimen depicted in 10.38a,b at higher magnification showing the ribbon-like band (X1200).

10.38d
(X 287)

10.38e
(X 1200)

Figure 10.38d,e
SEM of another Microbond NP^2 specimen showing the ribbon-like band thought to be a grain boundary.

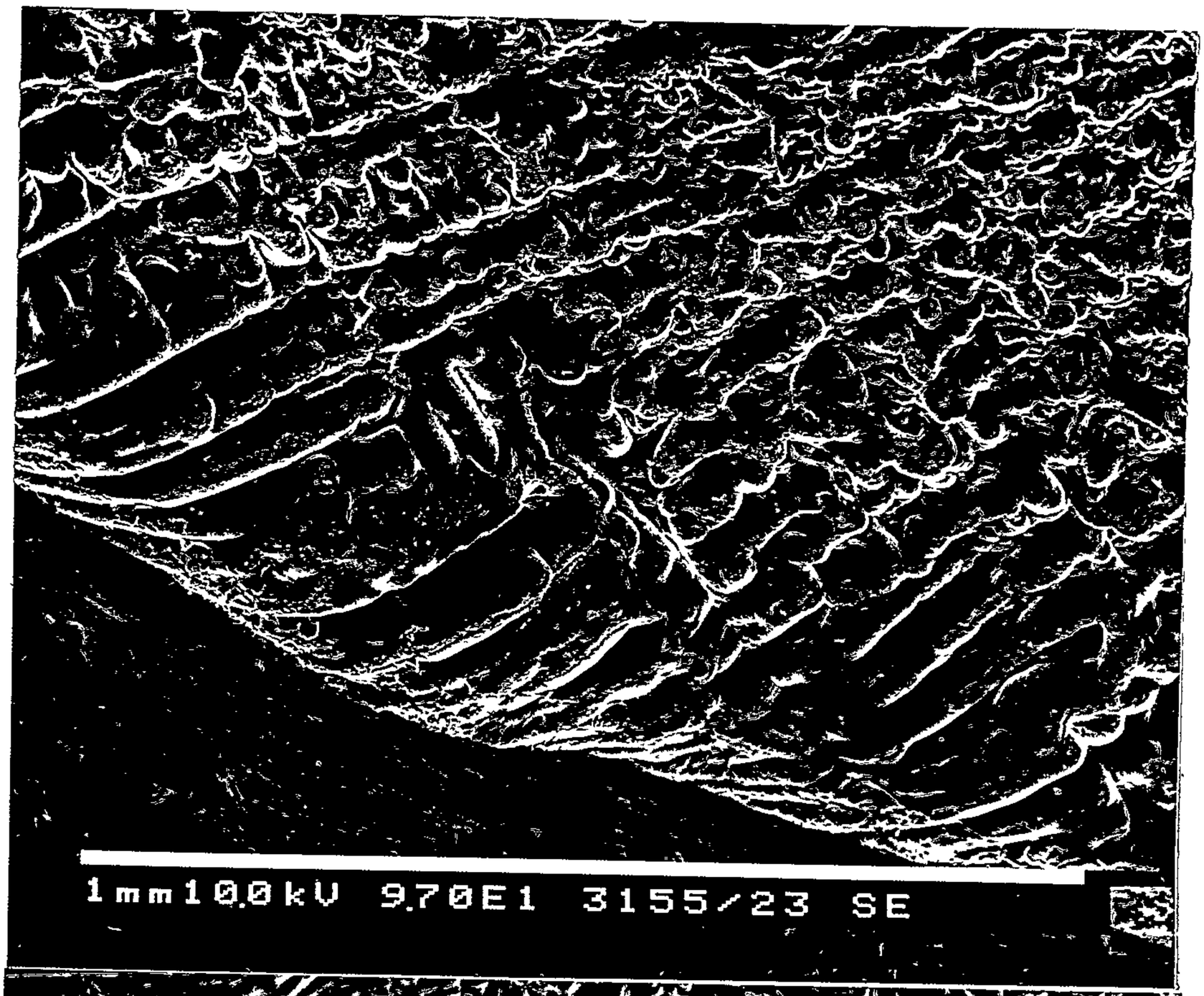

10.39a
(X 97)

10.39b
(X 71)

Figure 10.39a,b
SEM of the edges of two electrolytically etched Microbond NP^2 specimens showing the ditched area at the periphery of the specimens which has a smoother surface than that of the more central areas.

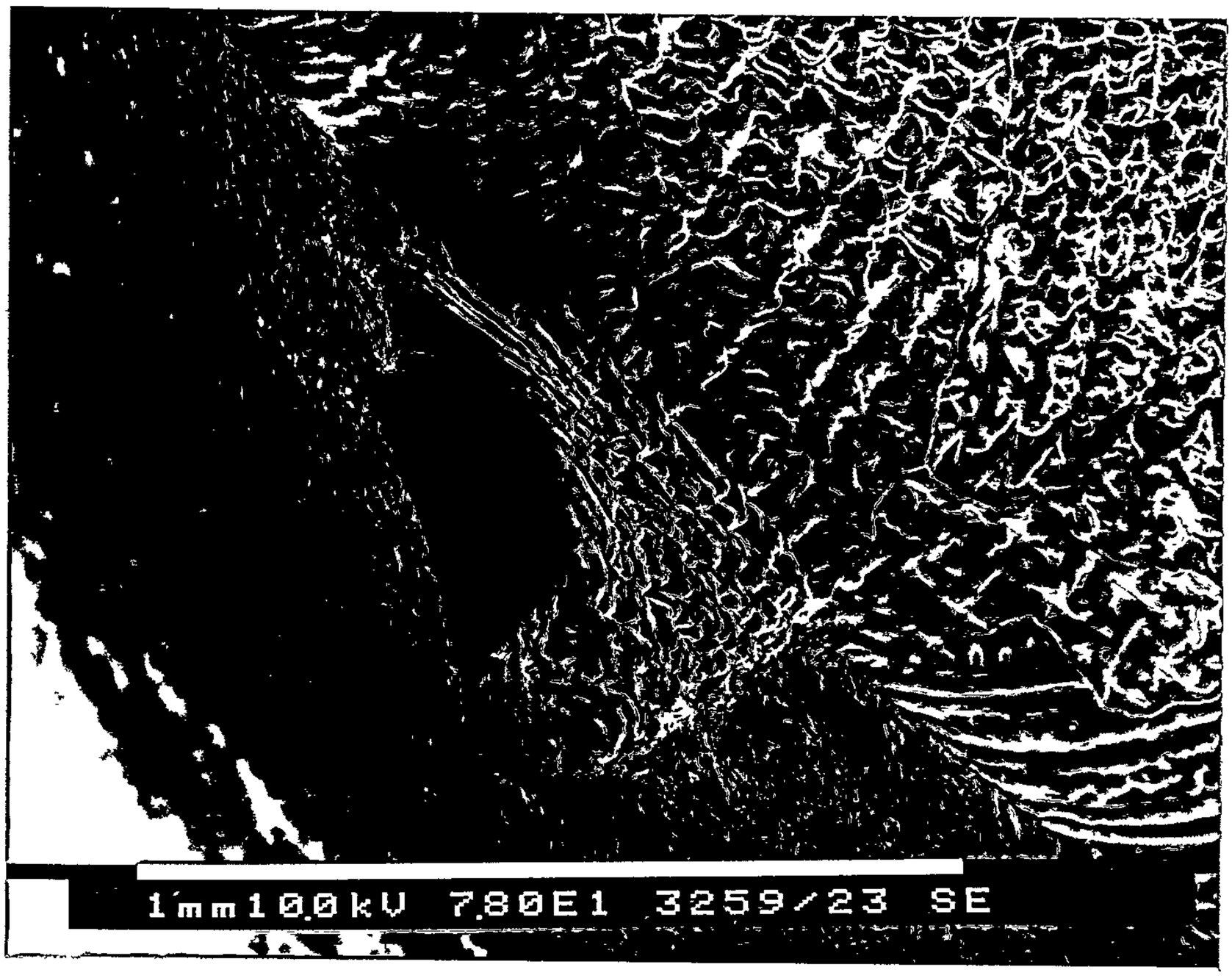

Figure 10.39c
SEM of the edge of an electrolytically etched Microbond NP^2 specimen showing the ditching at the periphery and an area not completely masked during the etching procedure (X 70).

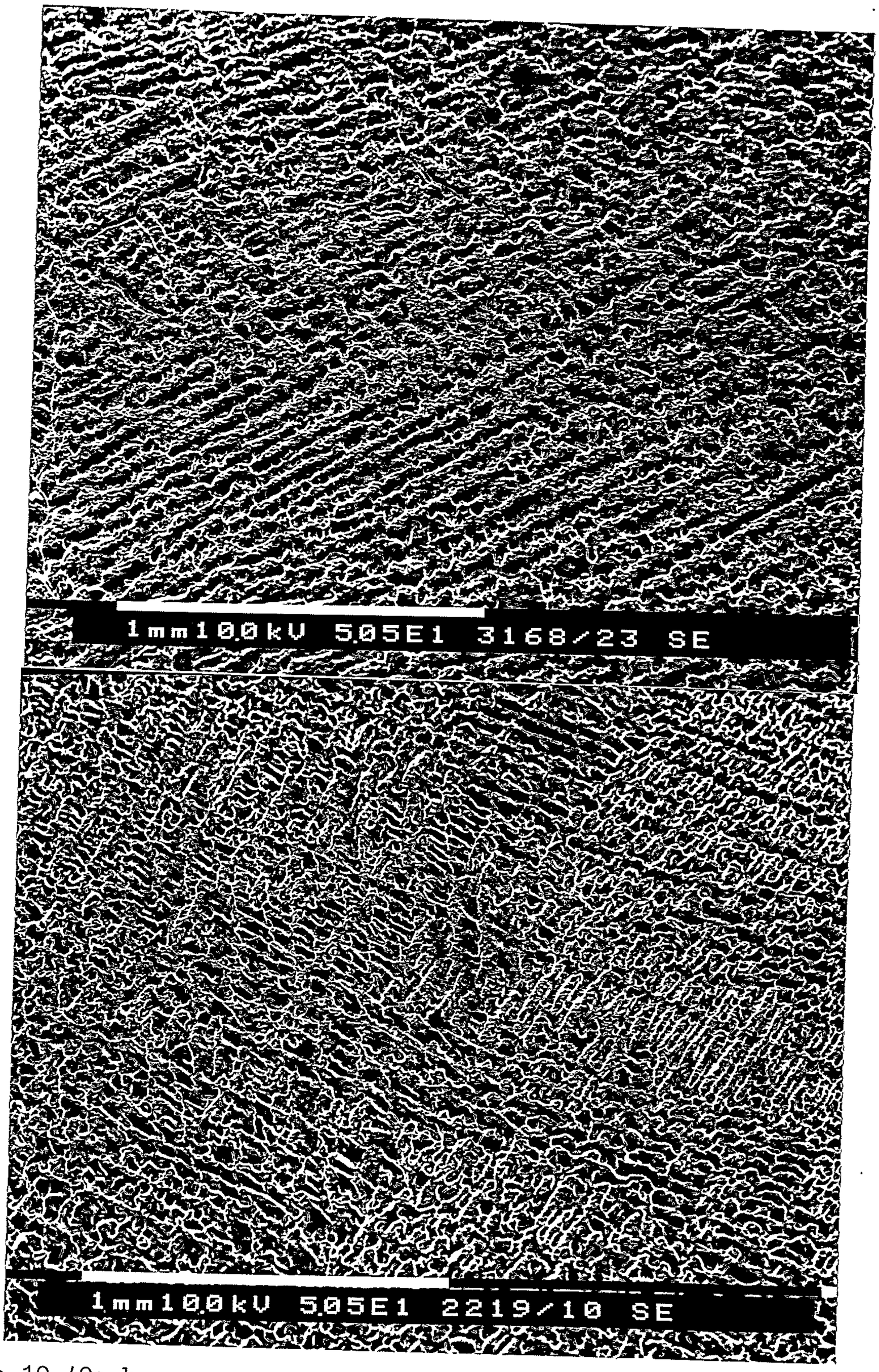

10.40a
(X 50)

10.40b
(X 50)

Figure 10.40a,b

SEM of a Microbond NP^2 specimen electrolytically etched under the etching conditions A,1,II (10.40a) and B,2,II (10.40b). Note the essential similarities of the surface topography at this magnification.

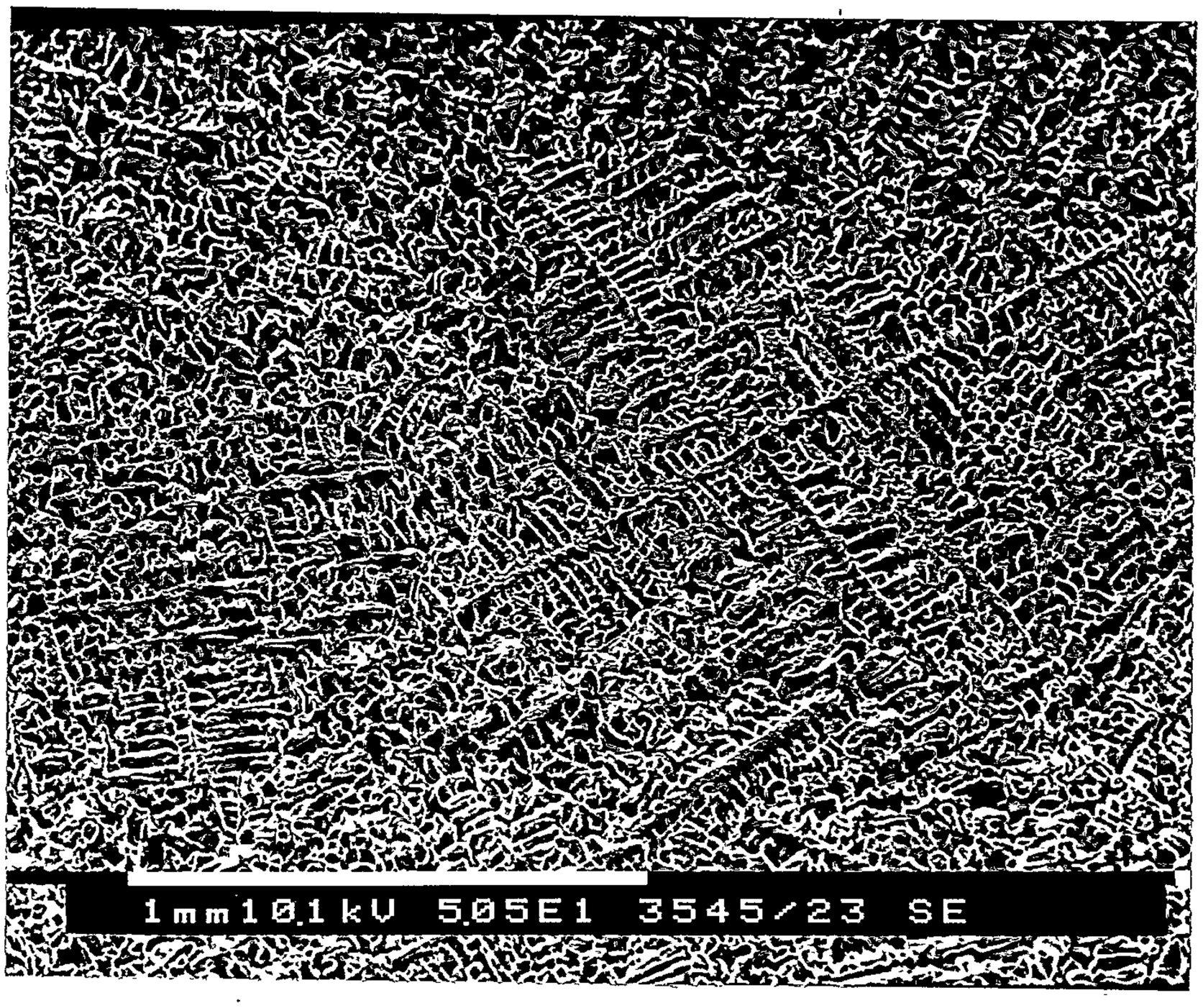

Figure 10.40c

SEM of a Microbond NP^2 specimen electrolytically etched under the etching conditions C,3,III (X 50). The surface topography at this magnification is similar the that of the specimens in Figures 10. 40a,b.

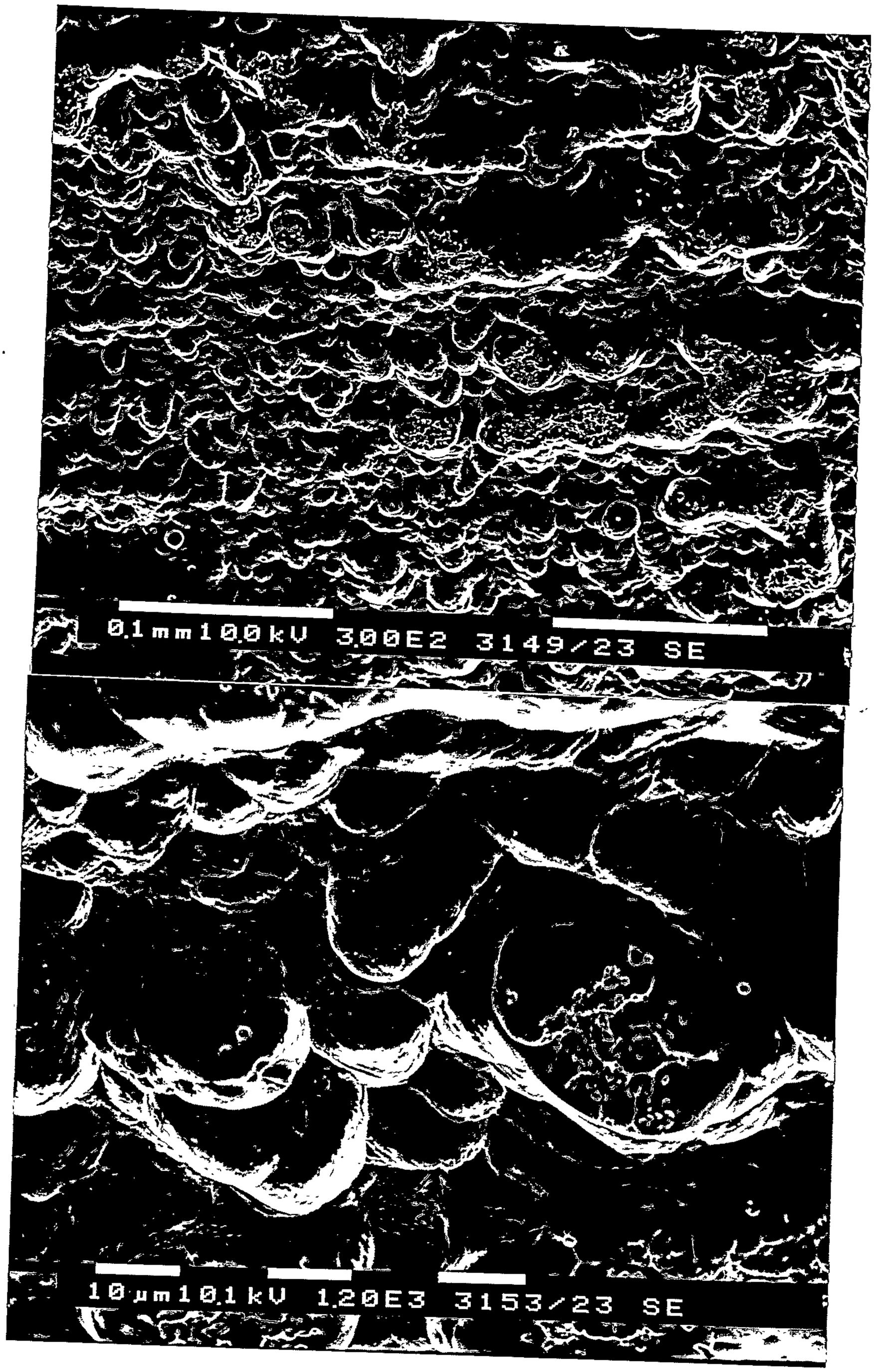

10.41a
(X 300)

10.41b
(X 1200)

Figure 10.41a,b
SEM of a Microbond NP^2 specimen electrolytically etched under the etching conditions A,1,II. This specimen was coded No. 1 in the group of five specimens.

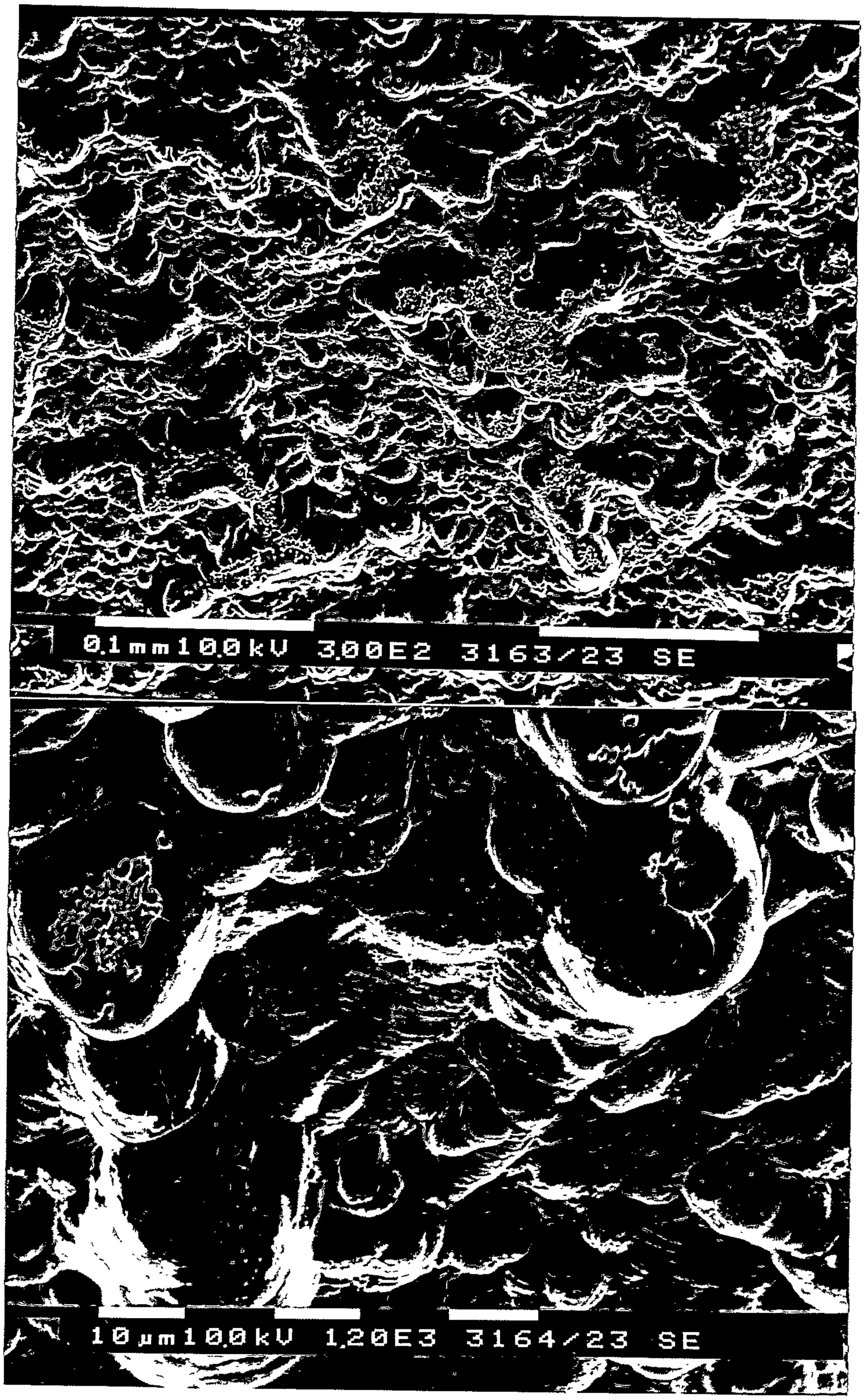

10.42a
(X 300)

10.42b
(X 1200)

Figure 10.42a,b
SEM of a Microbond NP^2 specimen electrolytically etched under the etching conditions A,1,II. This specimen was coded No. 3 in the group of five specimens.

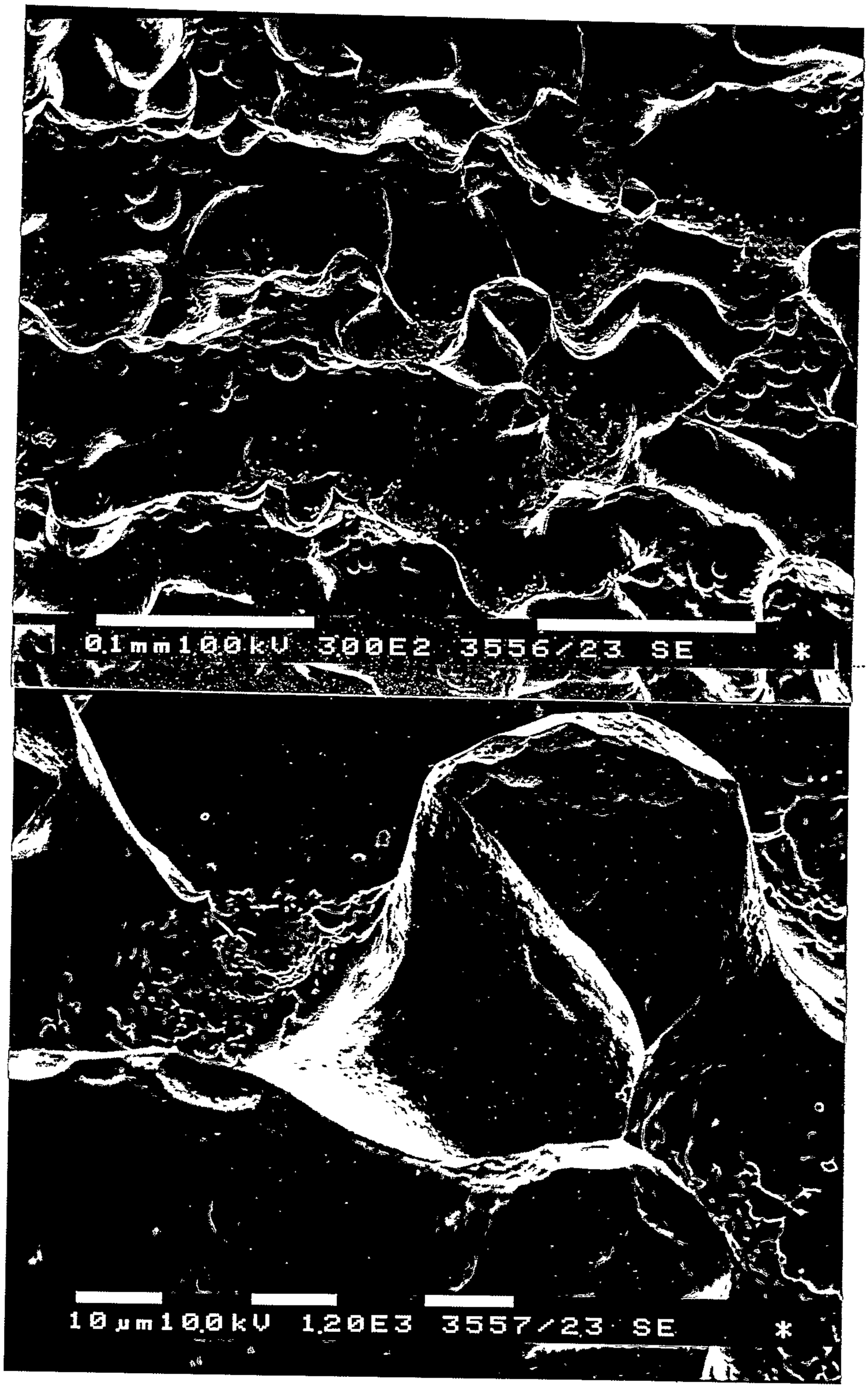

10.43a
(X 300)

10.43b
(X 1200)

Figure 10.43a,b
SEM of a Microbond NP^2 specimen electrolytically etched under the etching conditions C,3,III. This specimen was coded No. 4 in the group of five specimens.

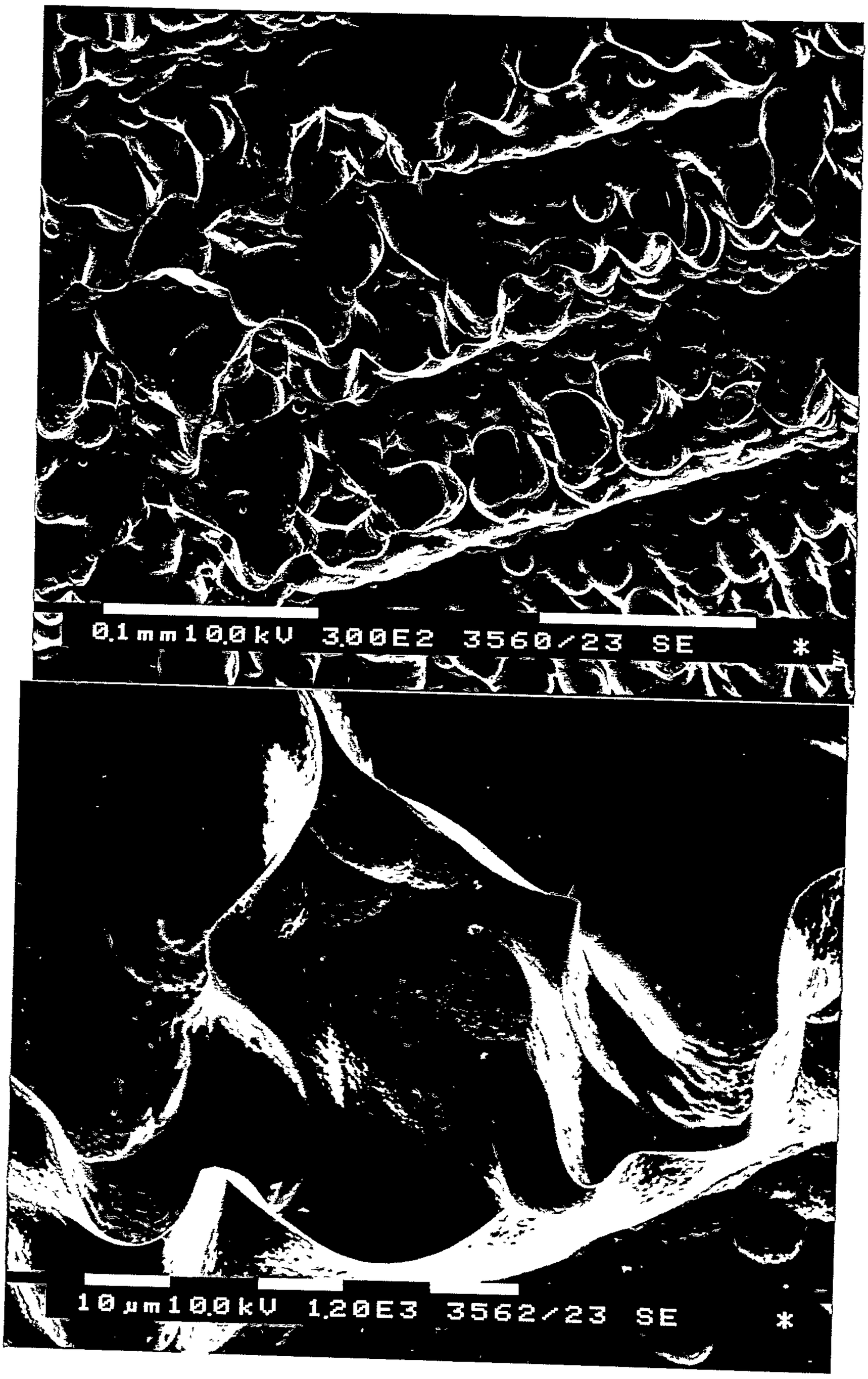

10.44a
(X 300)

10.44b
(X 1200)

Figure 10.44a,b
SEM of a Microbond NP^2 specimen electrolytically etched under the etching conditions C,3,III. This specimen was coded No. 5 in the group of five specimens.

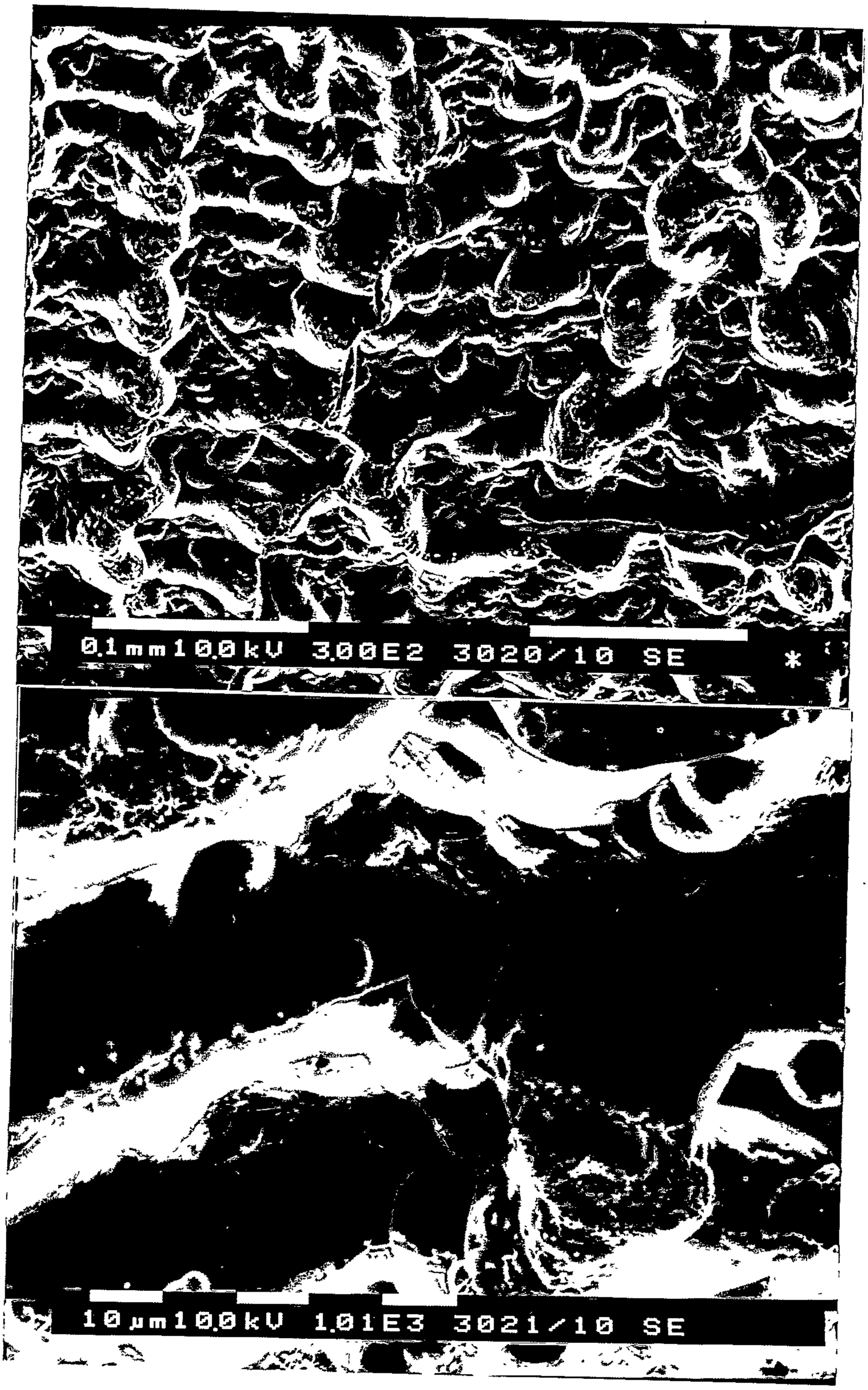

10.45a
(X 300)

10.45b
(X 1000)

Figure 10.45a,b
SEM of a specimen of Microbond NP^2 electrolytically etched under the etching conditions A,1,III (decreased current density, decreased etching solution concentration, increased etching time).

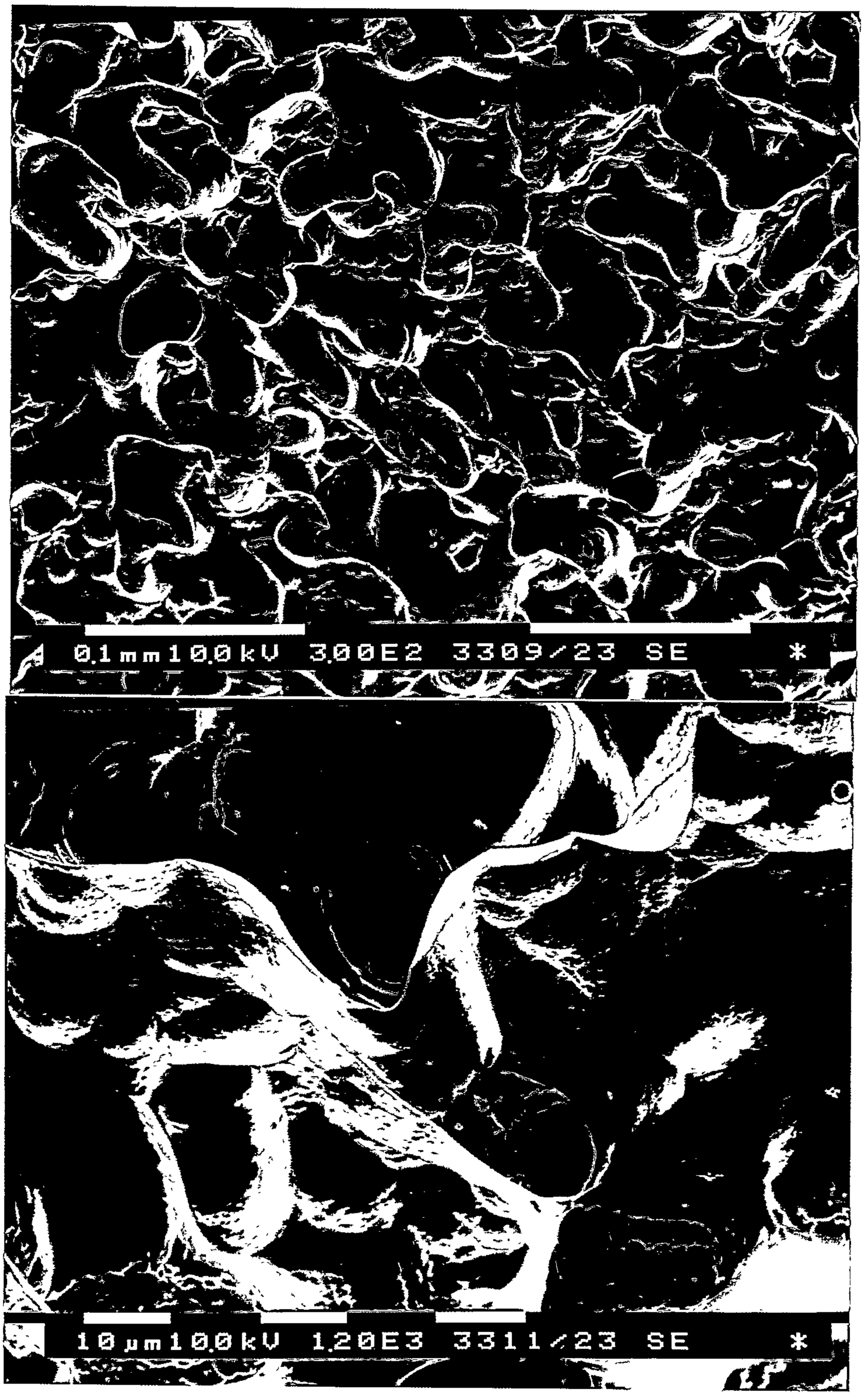

10.46a
(X 300)

10.46b
(X 1200)

Figure 10.46a,b
SEM of a Microbond NP^2 specimen electrolytically etched under the etching conditions A,2,III (recommended current density, decreased etching sólution concentration, increased etching time).

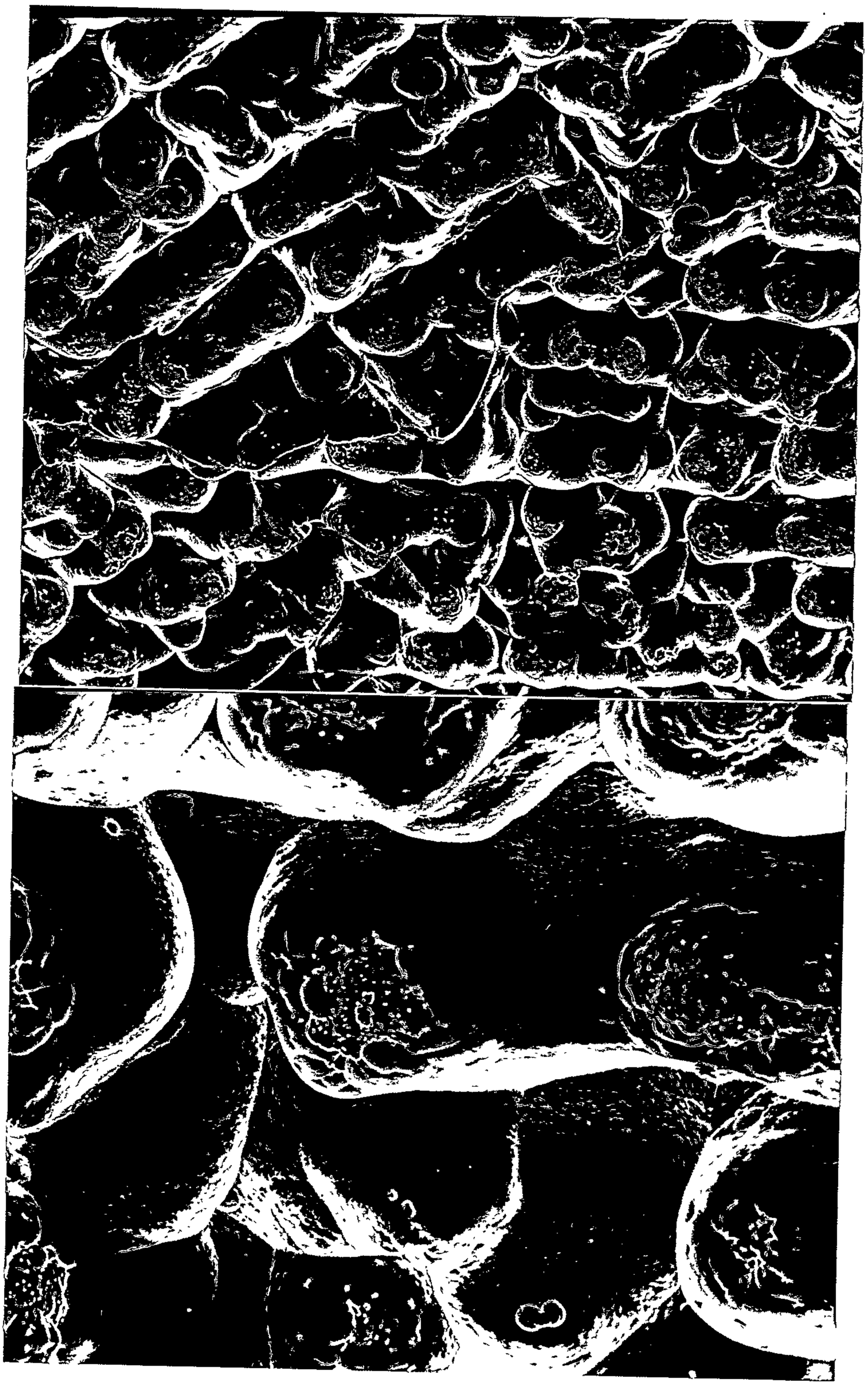

10.47a
(X 300)

10.47b
(X 1200)

Figure 10.47a,b
SEM of a Microbond NP^2 specimen electrolytically etched under the etching conditionsA,3,III (increased current density, decreased etching solution concentration, increased etching time).

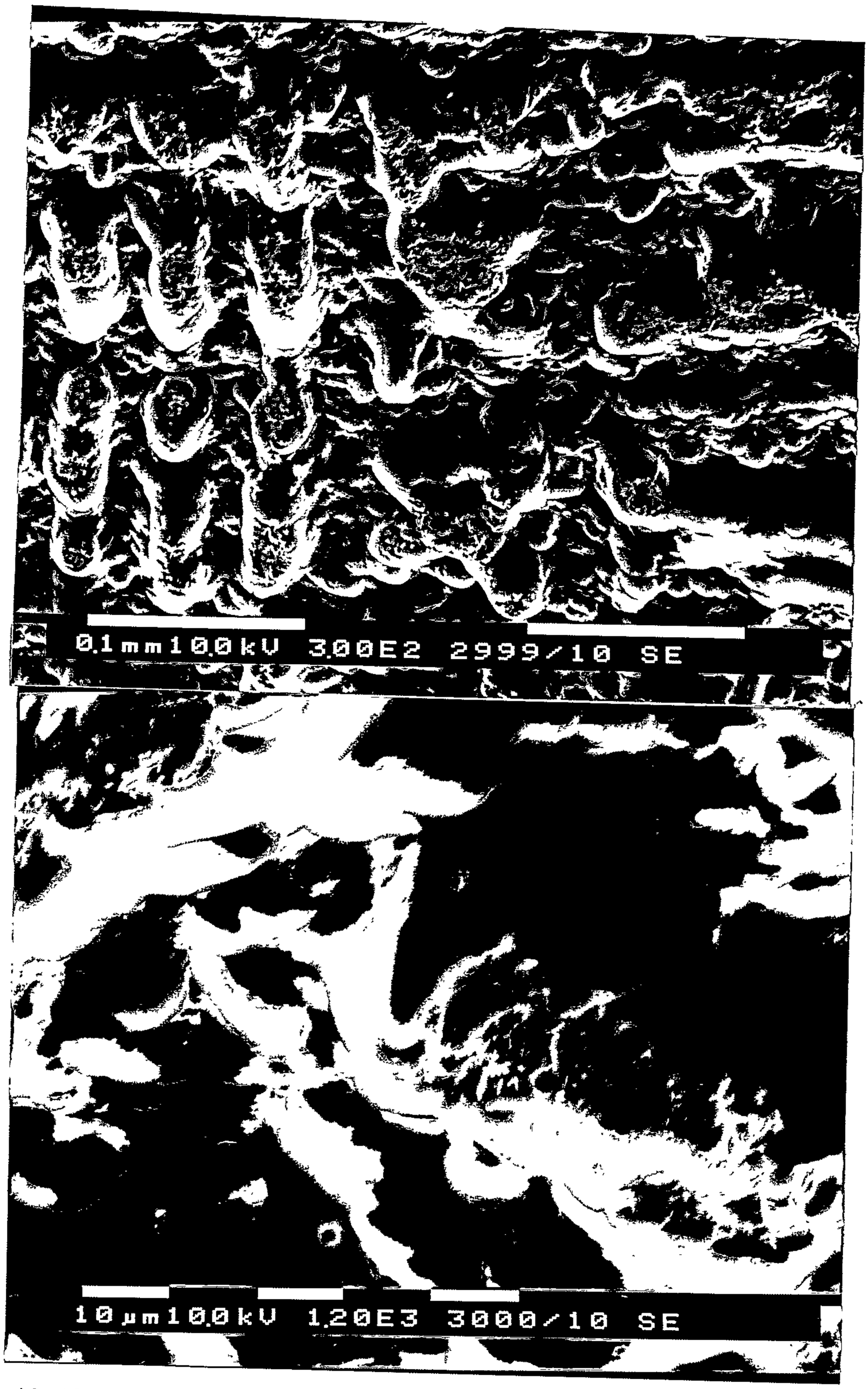

10.48a
(X300)

10.48b
(X 1200)

Figure 10.48a,b
SEM of a Microbond NP^2 specimen electrolytically etched under the etching conditions B,1,II (decreased current density, recommended etching solution concentration and etching time).

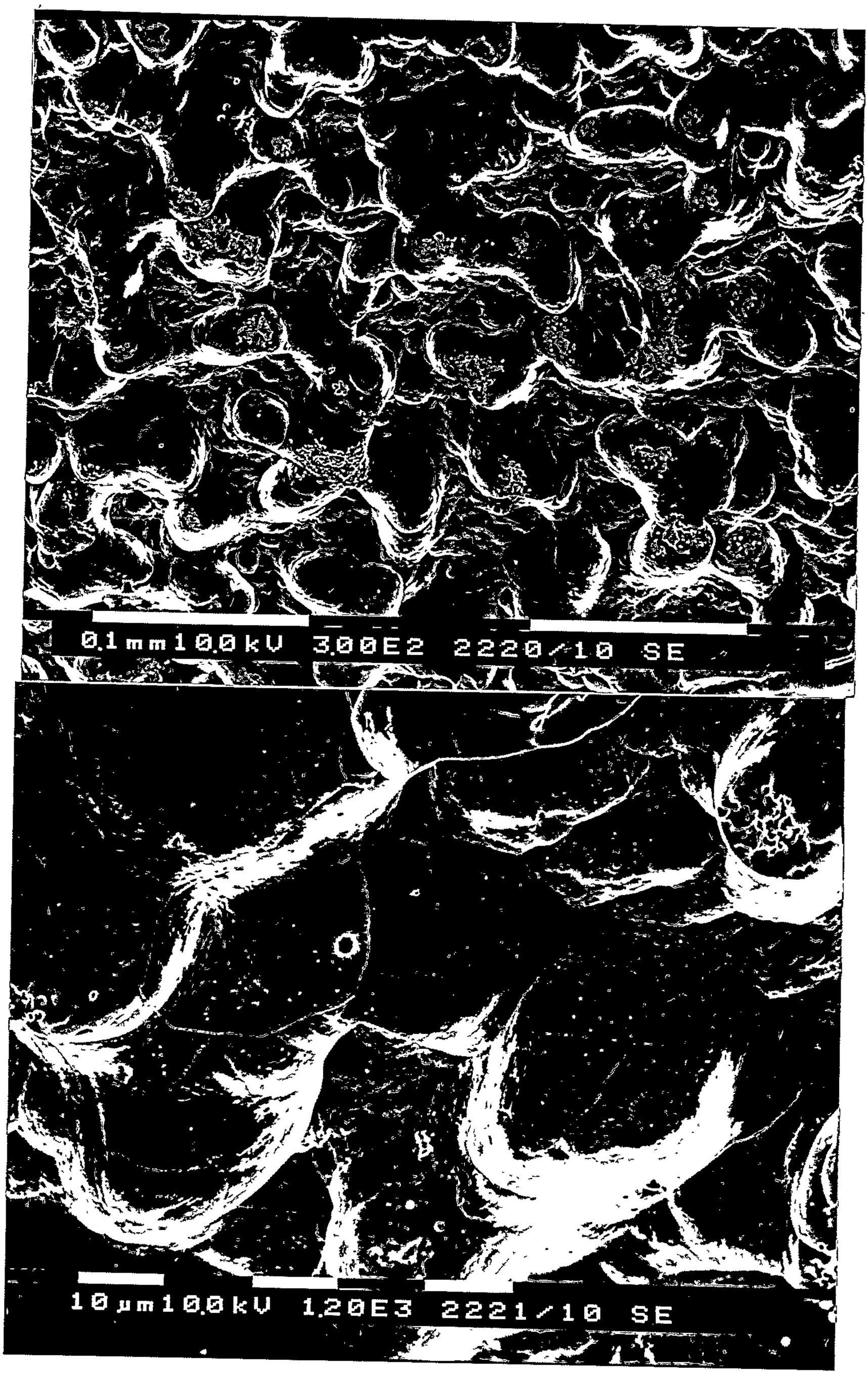

10.49a
(X 300)

10.49b
(X 1200)

Figure 10.49a,b
SEM of a Microbond NP^2 specimen electrolytically etched under the etching conditions B,2,II (recommended current density, etching solution concentration and etching time).

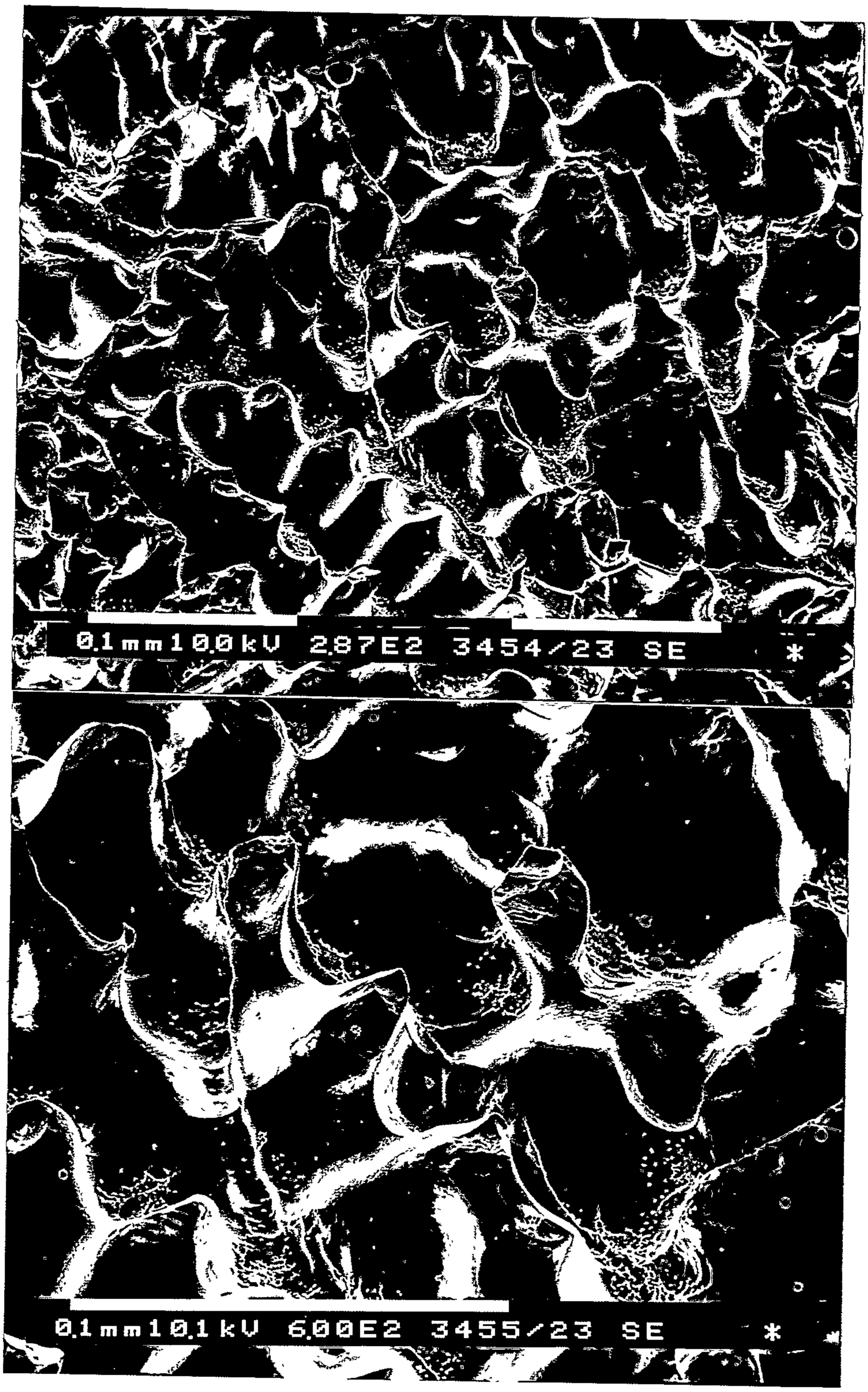

10.50a
(X 287)

10.50b
(X 600)

Figure 10.50 a,b
SEM of a Microbond NP^2 specimen electrolytically etched under the etching conditions B,3,II (increased current density, recommended etching solution concentration and etching time).

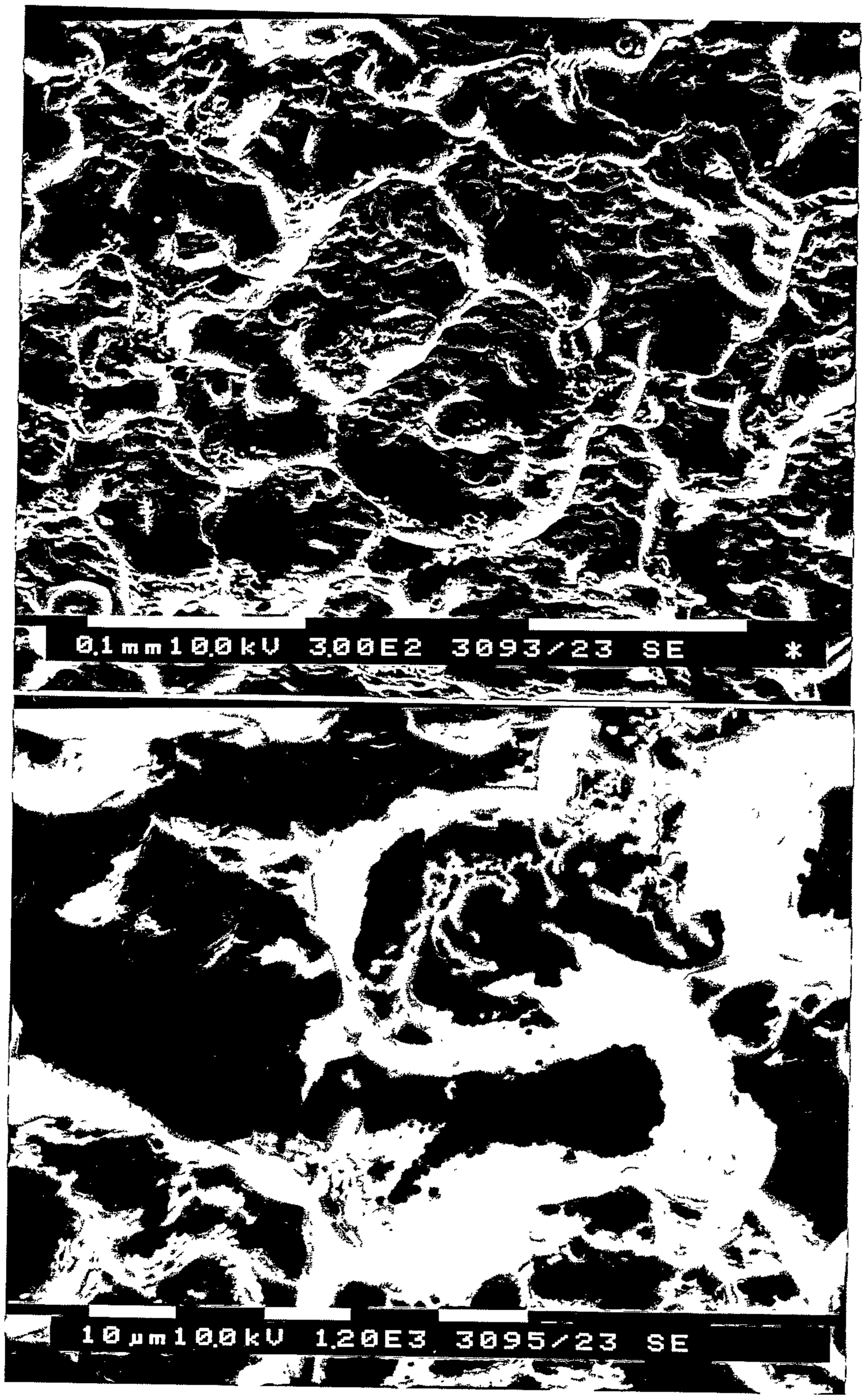

10.51a
(X 300)

10.51b
(X 1200)

Figure 10.51a,b
SEM of a Microbond NP^2 specimen electrolytically etched under the etching conditions C,1,I (decreased current density, increased etching solution concentration, decreased etching time).

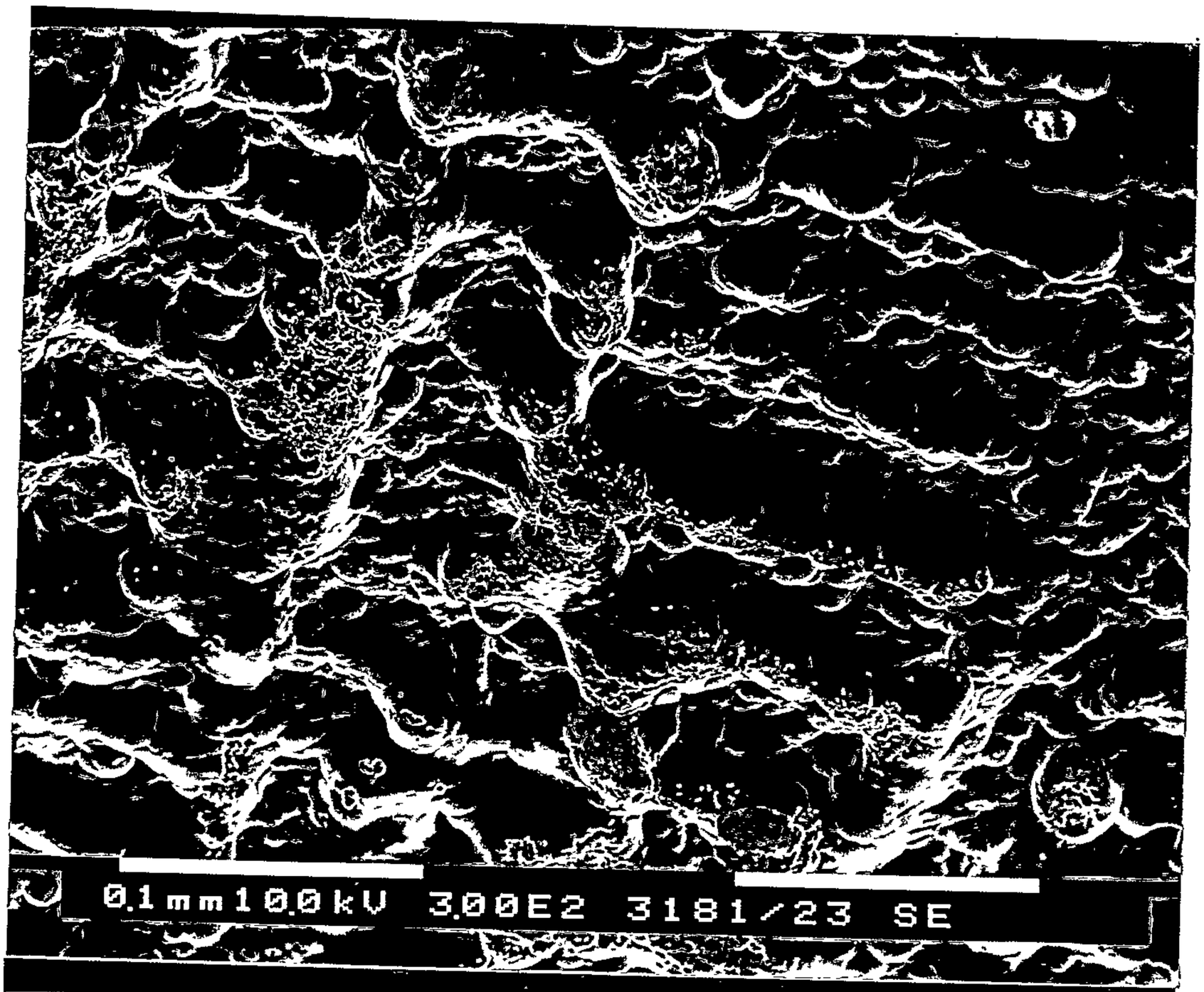

10.52a
(X 300)

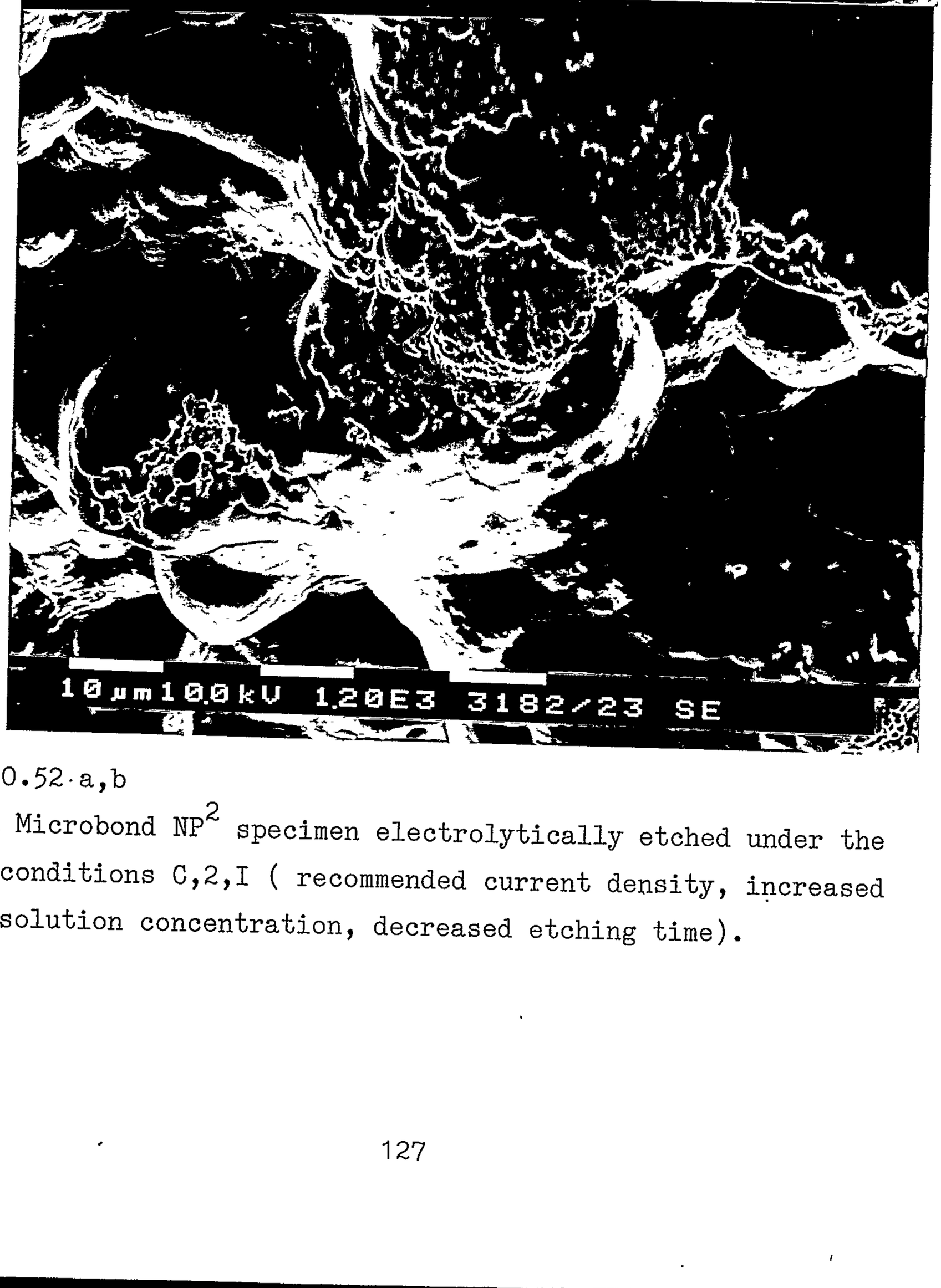

10.52b
(X 1200)

Figure 10.52.a,b
SEM of a Microbond NP^2 specimen electrolytically etched under the etching conditions C,2,I (recommended current density, increased etching solution concentration, decreased etching time).

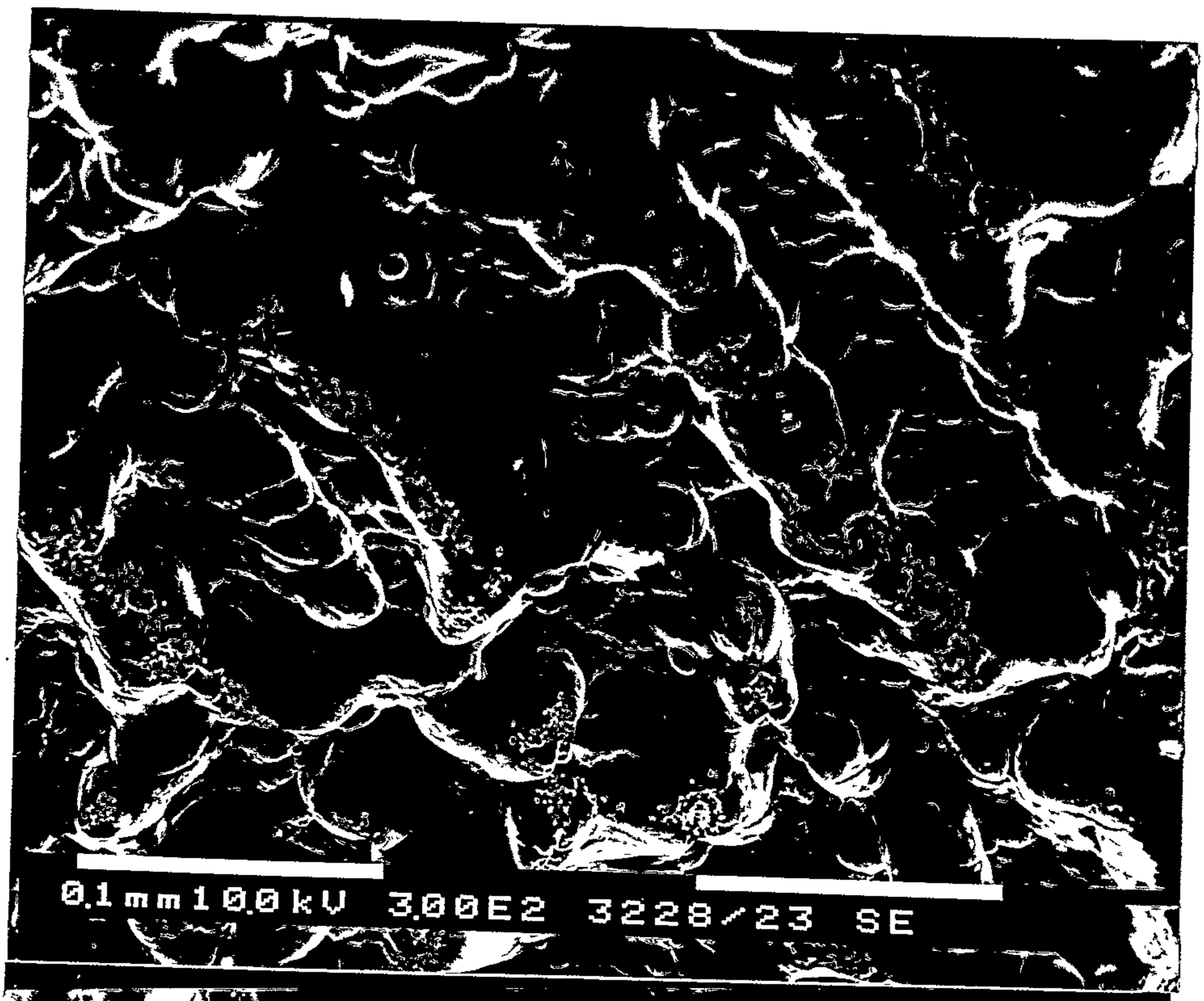

10.53a
(X 300)

10.53b
(X 1200)

Figure 10.53 a,b
SEM of a Microbond NP^2 specimen electrolytically etched under the etching conditions C,3,I (increased current density,increased etching solution concentration, decreased etching time).

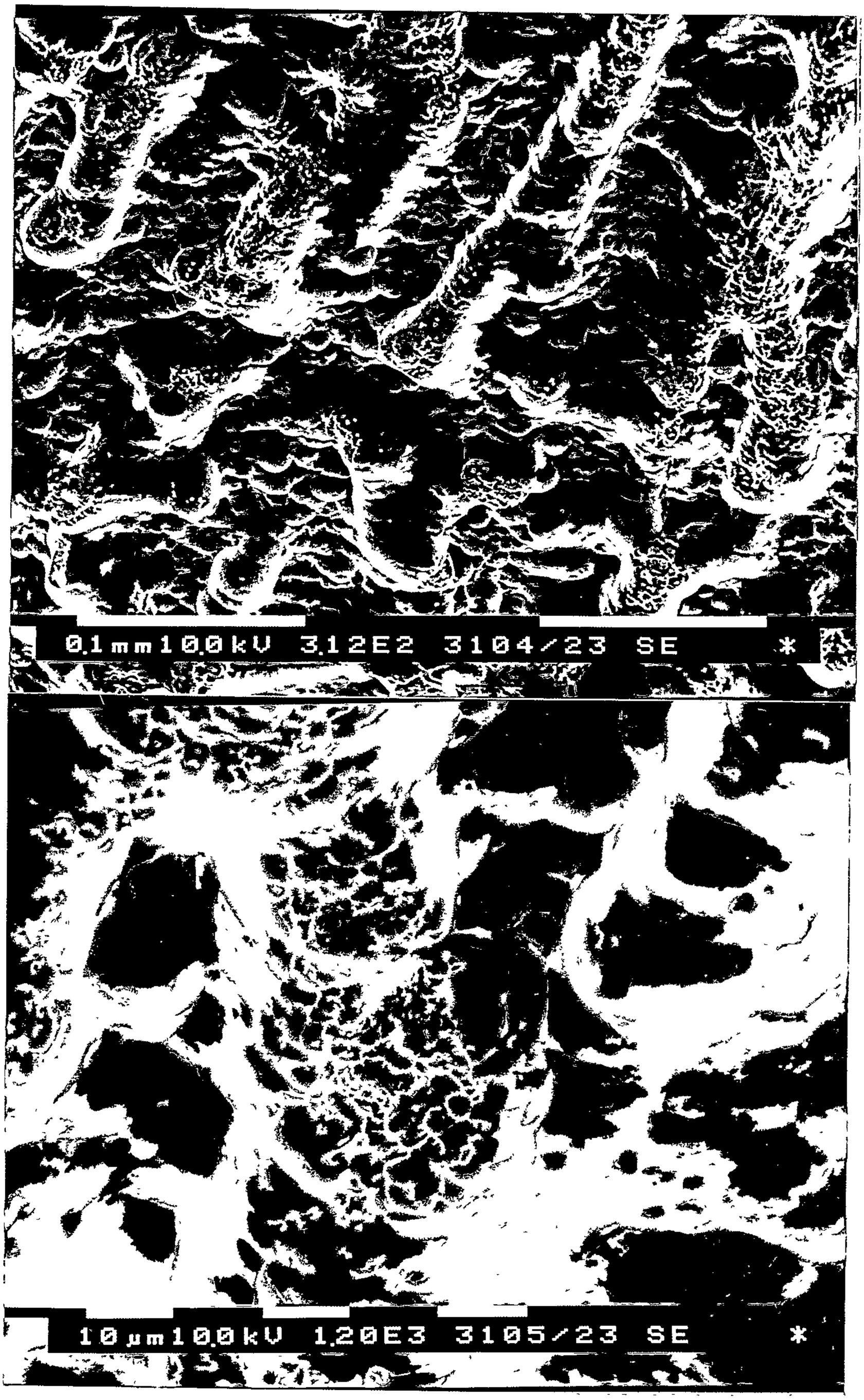

10.54a
(X 300)

(X 1200)

Figure 10.54 a,b
SEM of a Microbond NP^2 specimen electrolytically etched under the etching conditions C,1,I (decreased etching time, increased etching solution concentration, decreased current density).

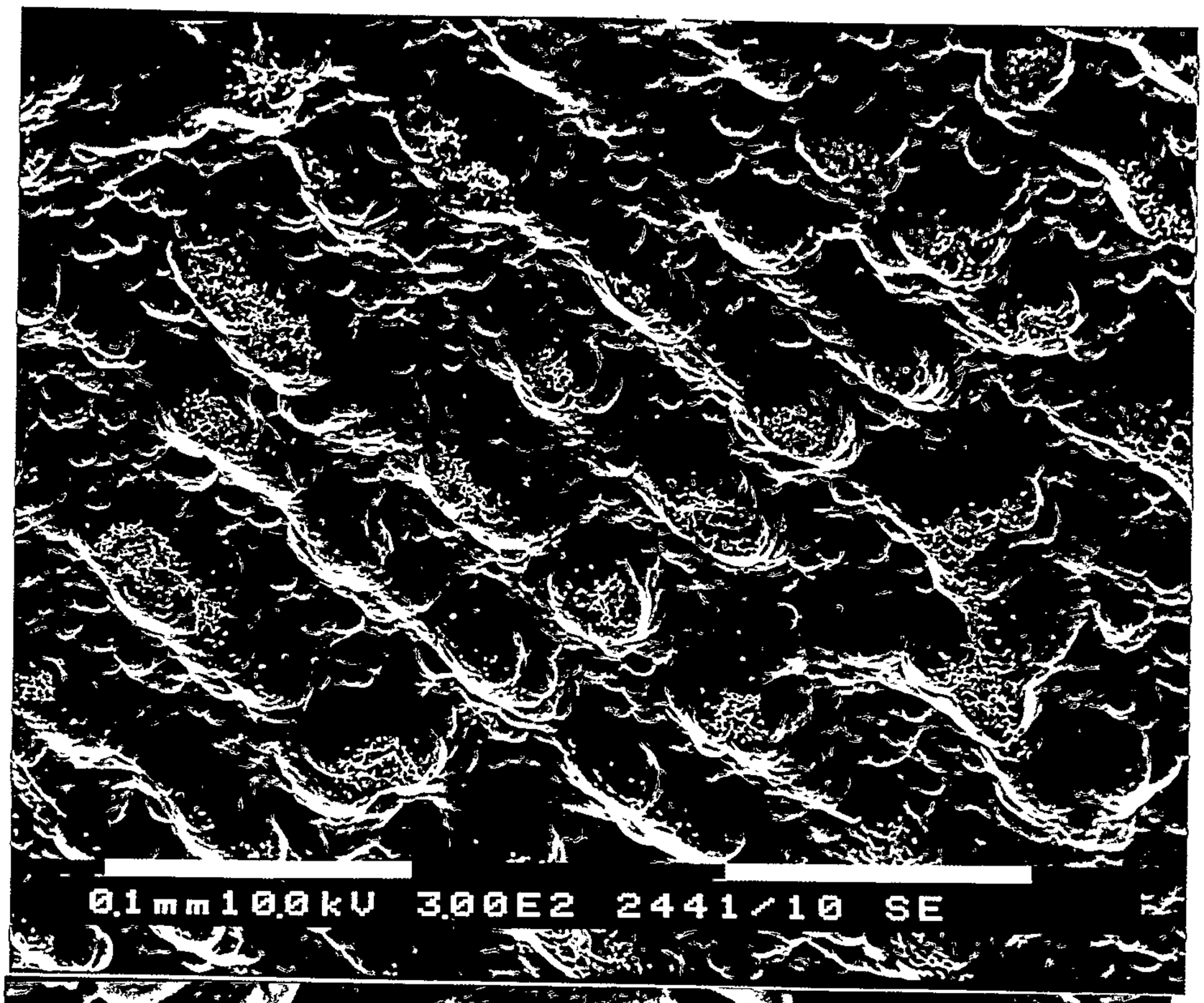

10.55a
(X 300)

10.55b
(X 1200)

Figure 10.55 a,b
SEM of a Microbond NP^2 specimen electrolytically etched under the etching conditions C,1,II (recommended etching time, increased etching solution concentration, decreased current density).

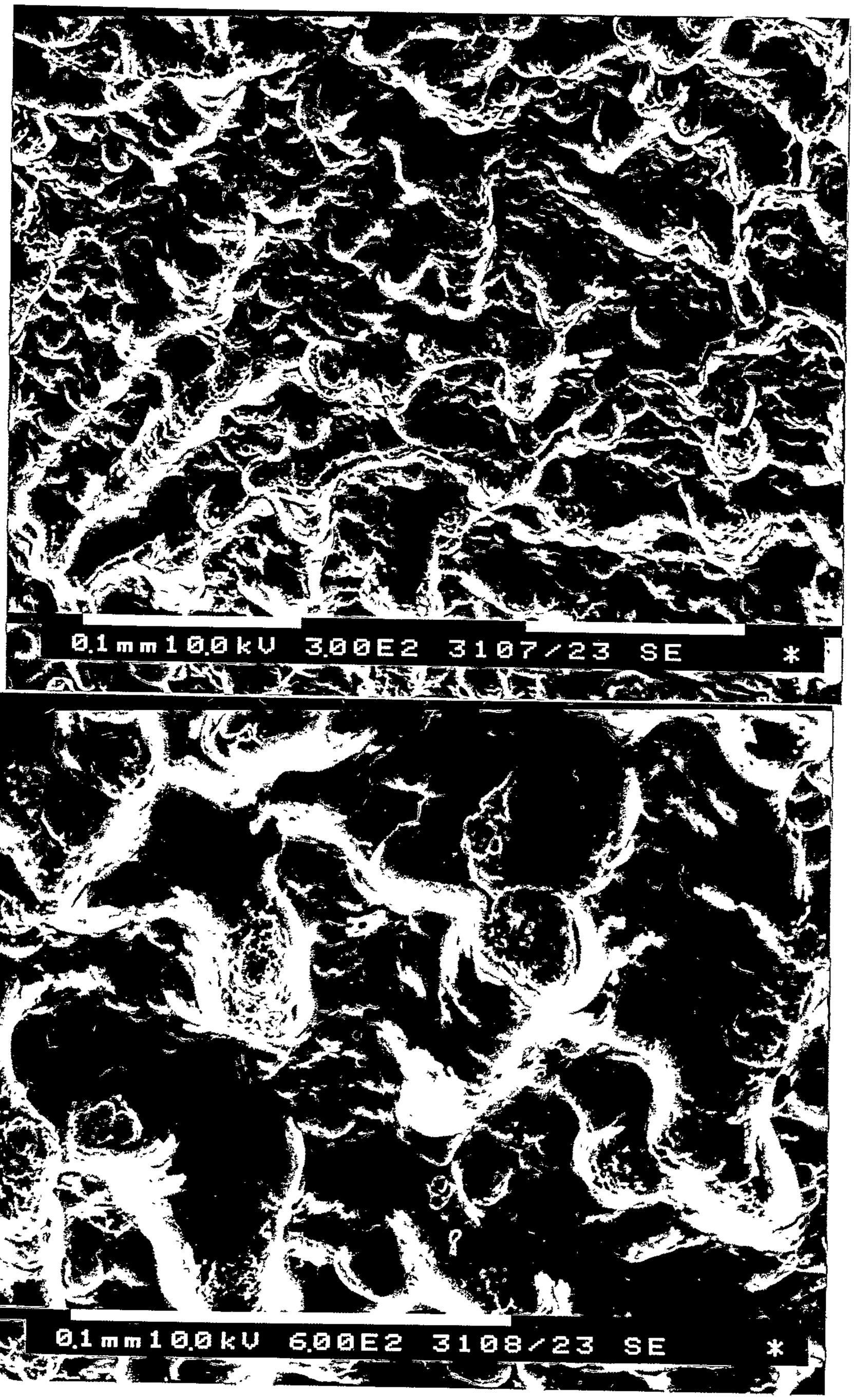

10.56a
(X 300)

10.56b
(X 1200)

Figure 10.56 a,b
SEM of a Microbond NP^2 specimen electrolytically etched under the etching conditions C,1,II (increased etching time, increased etching solution concentration, decreased current density).

10.57a
(X 300)

10.57b
(X 1200)

Figure 10.57 a,b
SEM of a Microbond NP^2 specimen electrolytically etched under the etching conditions B,2,I decreased etching time, recommended current density and etching solution concentration).

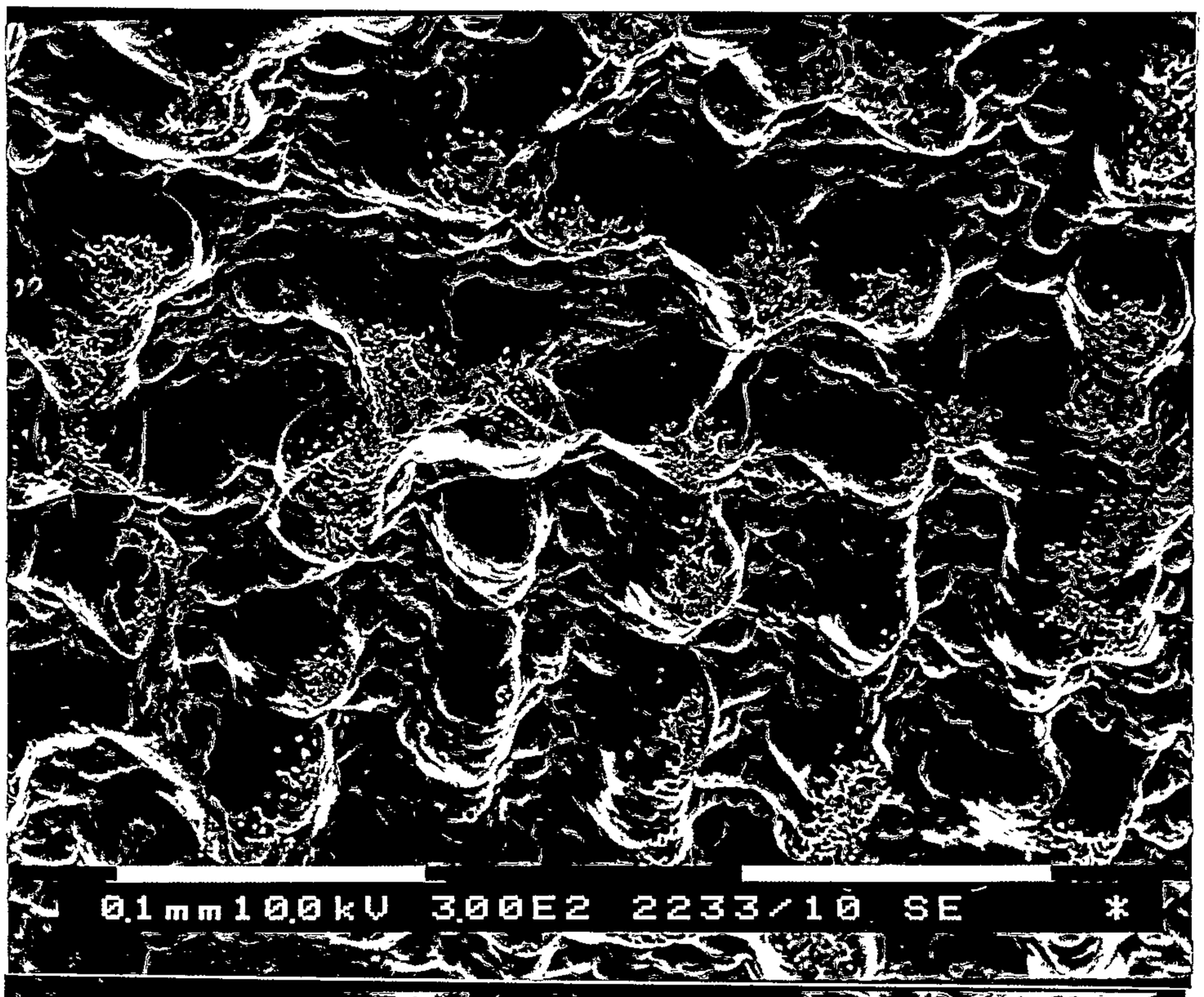

10.58a
(X 300)

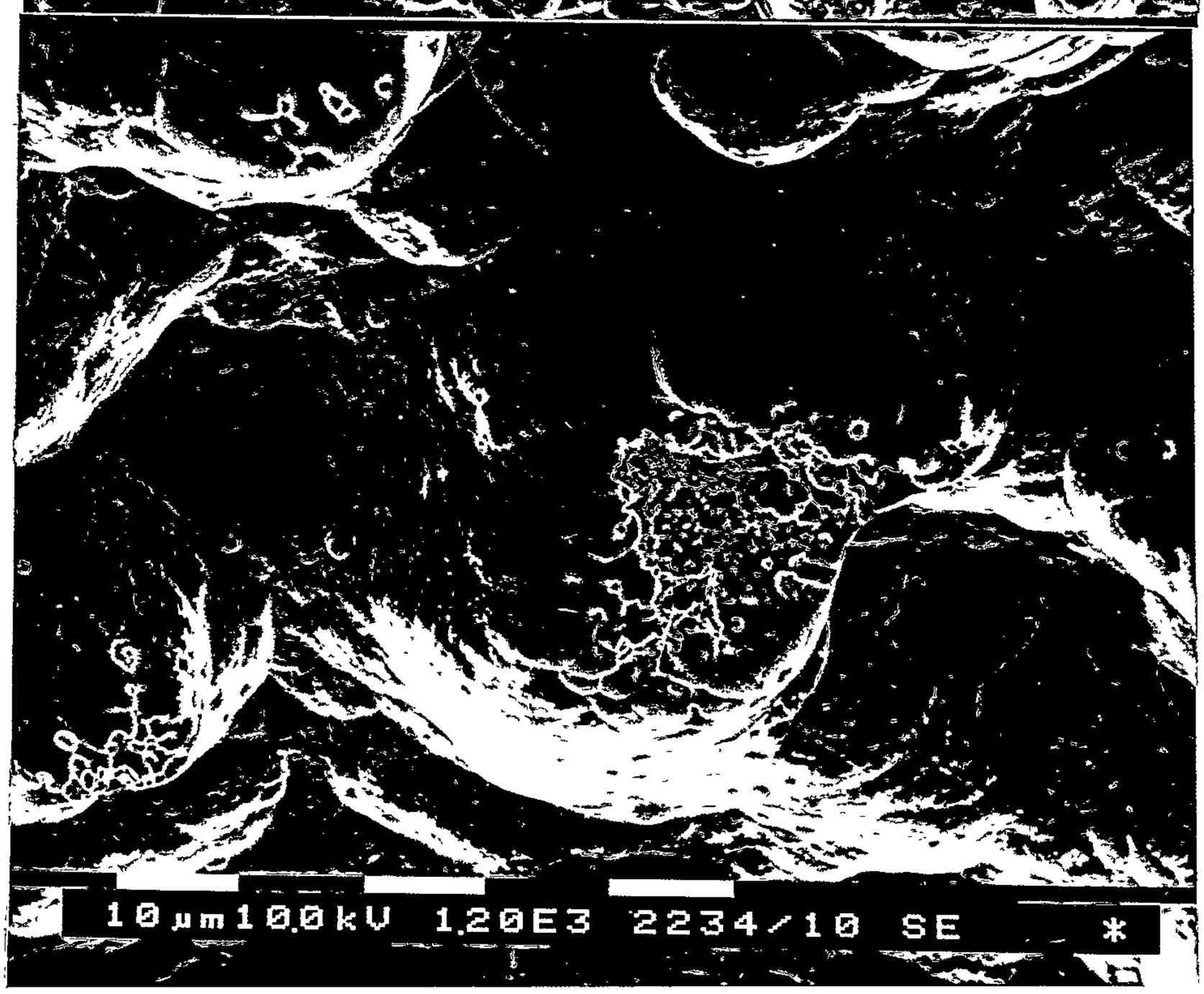

10.58b
(X 1200)

Figure 10.58 a,b
SEM of a Microbond NP^2 specimen electrolytically etched under the etching conditions B,2,II (recommended etching time, recommended current density and etching solution concentration).

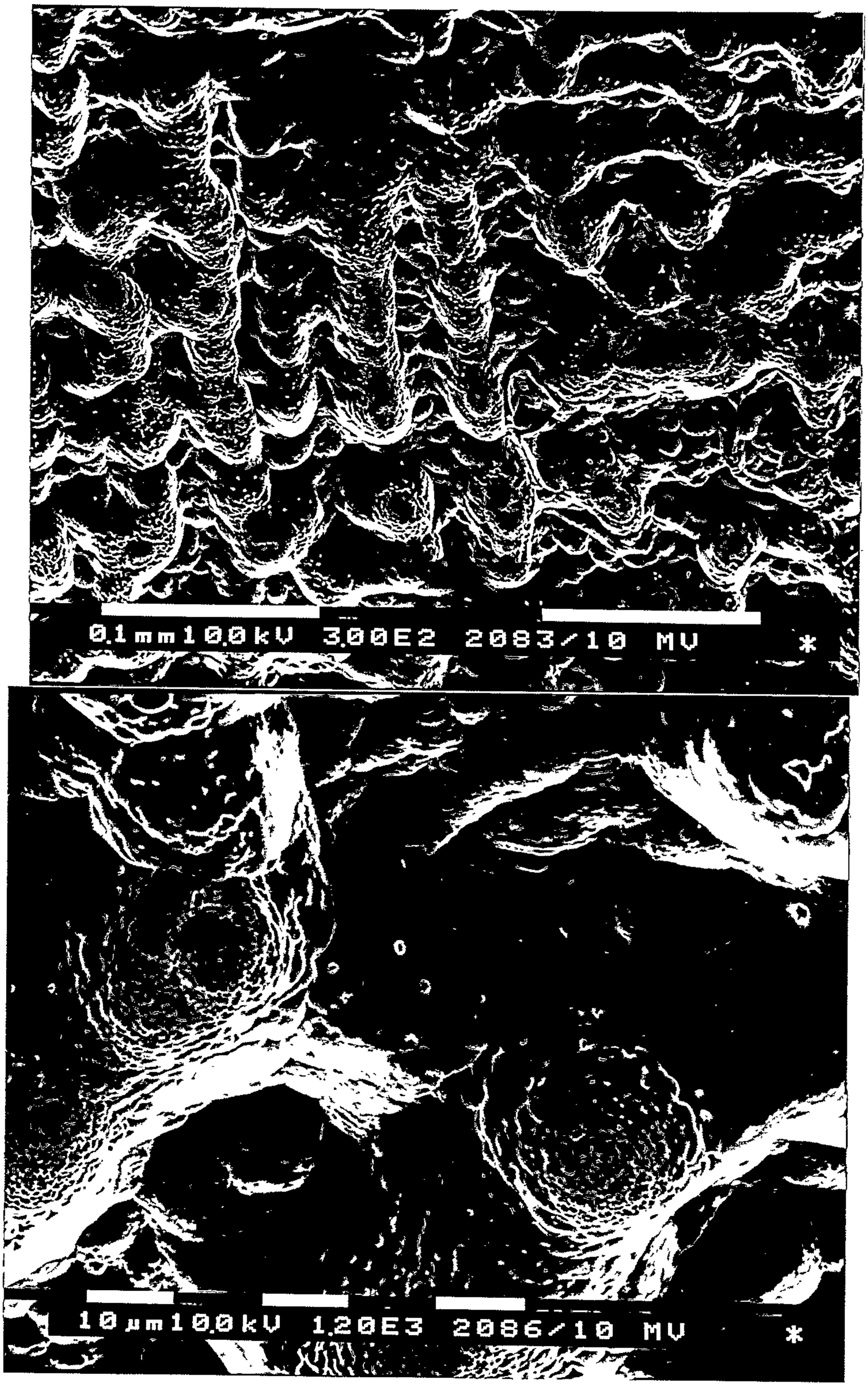

10.59a
(X 300)

10.59b
(X 1200)

Figure 10.59 a,b
SEM of aMicrobond NP^2 specimen electrolytically etched under the etching conditions B,2,III (increased etching time, recommended current density and etching solution concentration).

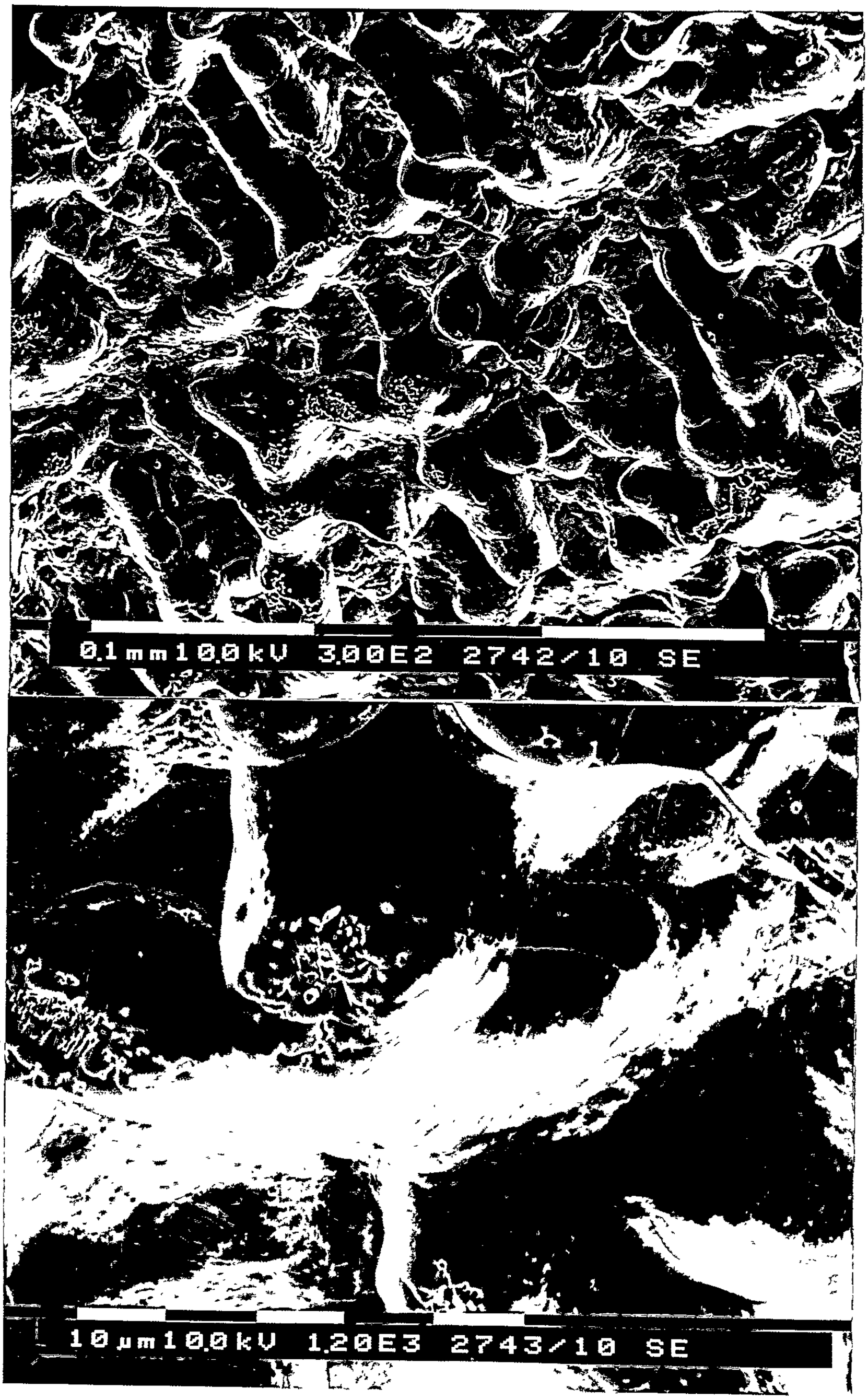

10.60a
(X 300)

10.60b
(X 1200)

Figure 10.60 a,b
SEM of a Microbond NP^2 specimen electrolytically etched under the etching conditions A,3,I (decreased etching time, decreased etching solution concentration, increased current density).

10.61a
(X 300)

10.61b
(X 1200)

Figure 10.61 a,b:
SEM of a Microbond NP^2 specimen electrolytically etched under the etching conditions A,3,II (recommended etching time, decreased etching solution concentration, increased current density).

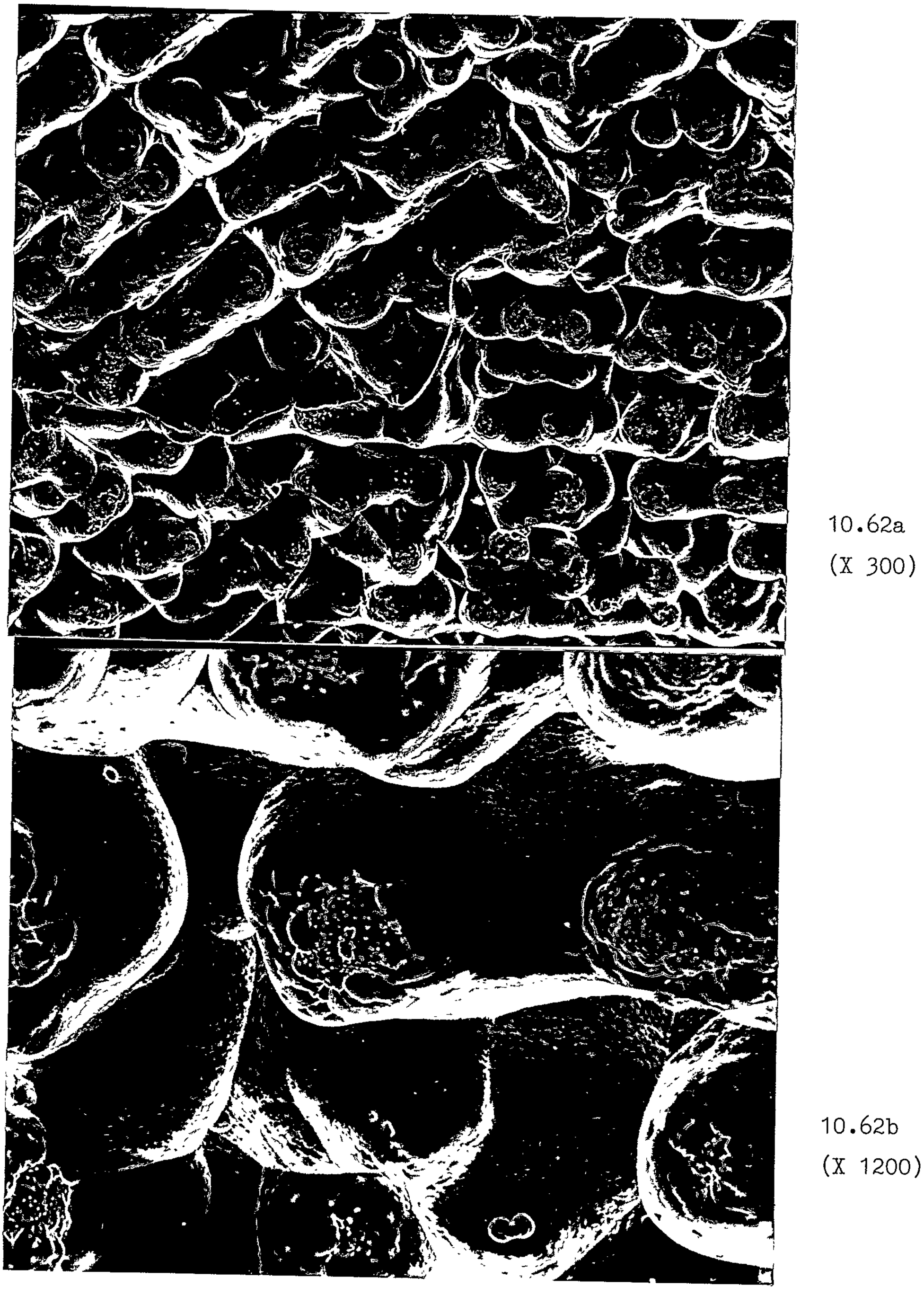

10.62a
(X 300)

10.62b
(X 1200)

Figure 10.62 a,b
SEM of a Microbond NP^2 specimen electrolytically etched under the etching conditions A,3,III (increased etching time, decreased etching solution concentration, increased current density).

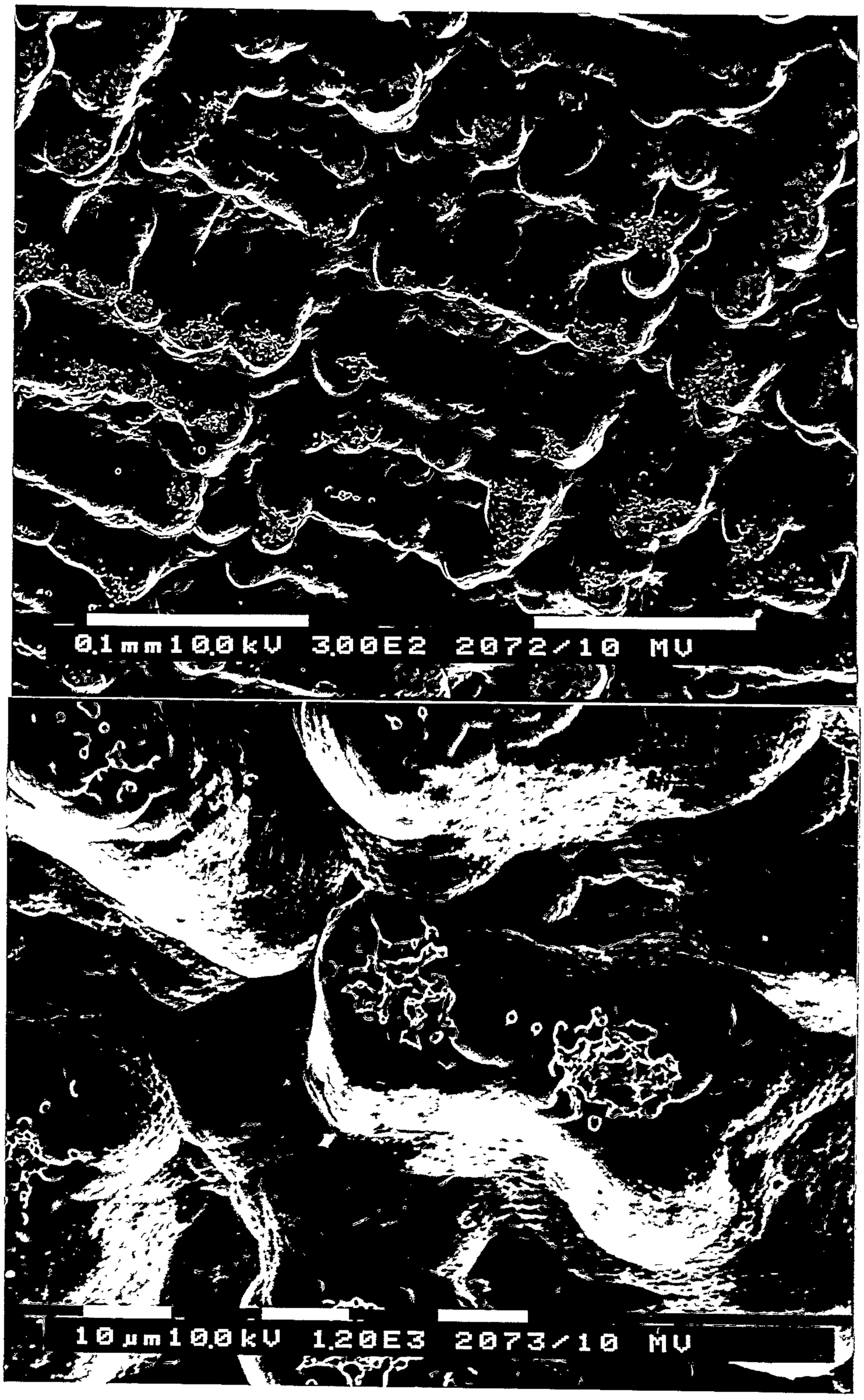

10.63a
(X 300)

10.63b
(X 1200)

Figure 10.63 a,b
SEM of a Microbond NP^2 specimen electrolytically etched under the etching conditions B,3,I. (decreased etching time, recommended etching solution concentration, increased current density).

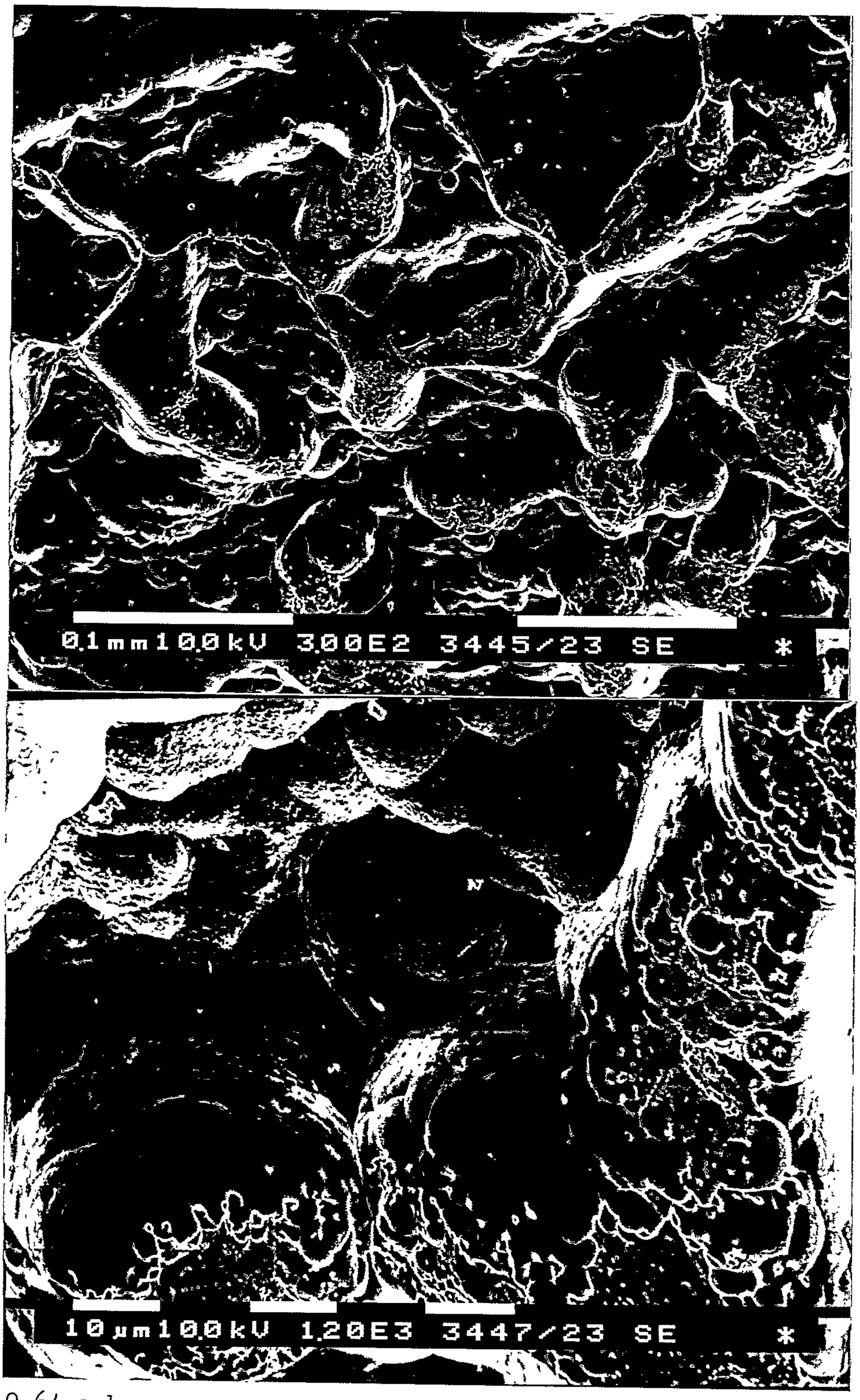

10.64a
(X 300)

10.64b
(X 600)

Figure 10.64 a,b

SEM of a Microbond NP^2 specimen electrolytically etched under the etching conditions B,3,II (recommended etching time, recommended etching solution concentration, increased current density).

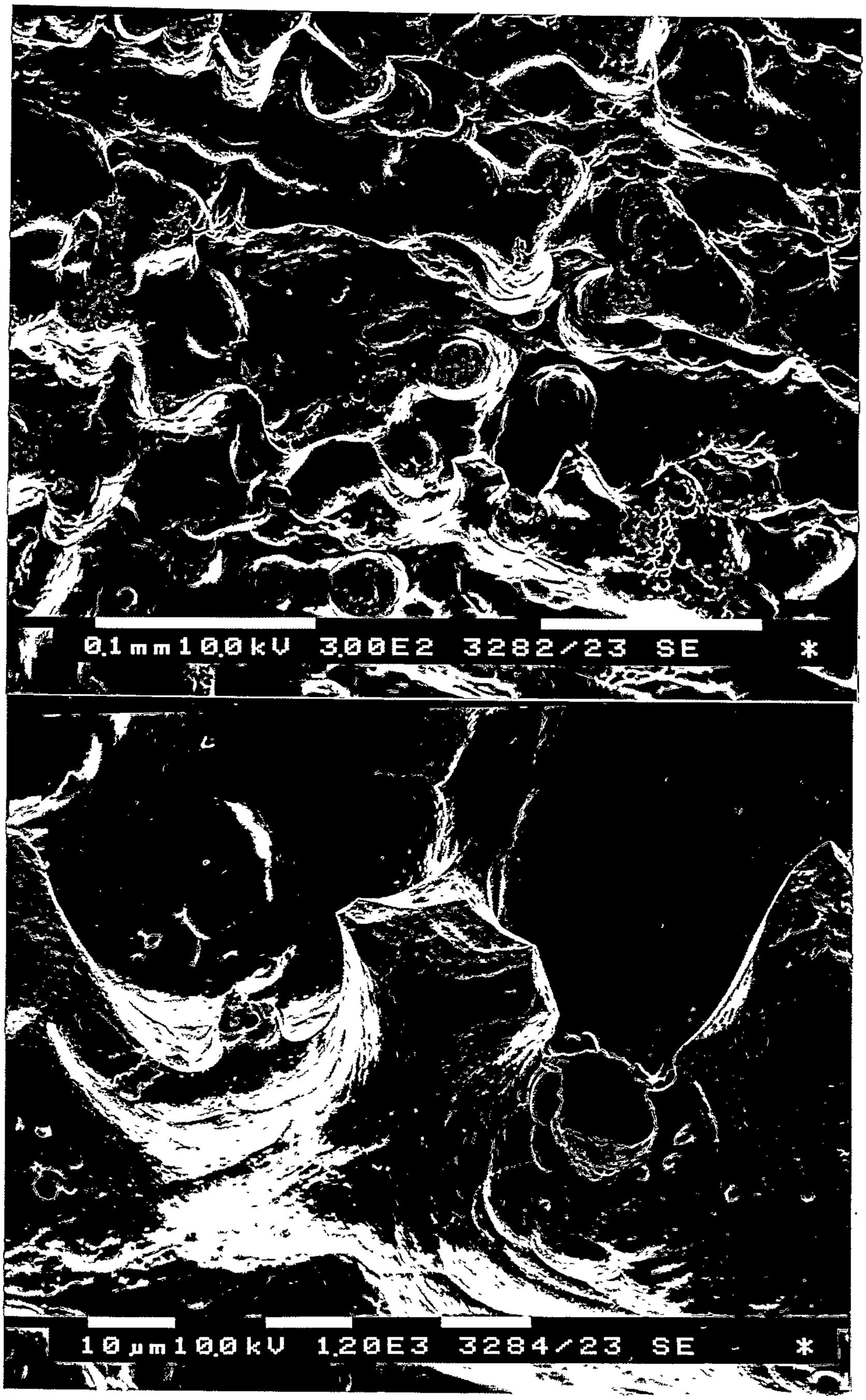

10.65.a
(X 300)

10.65b
(X 1200)

Figure 10.65 a,b
SEM of a Microbond NP^2 specimen electrolytically etched under the etching conditions B,3,III (increased etching time, recommended etching solution concentration, increased current density).

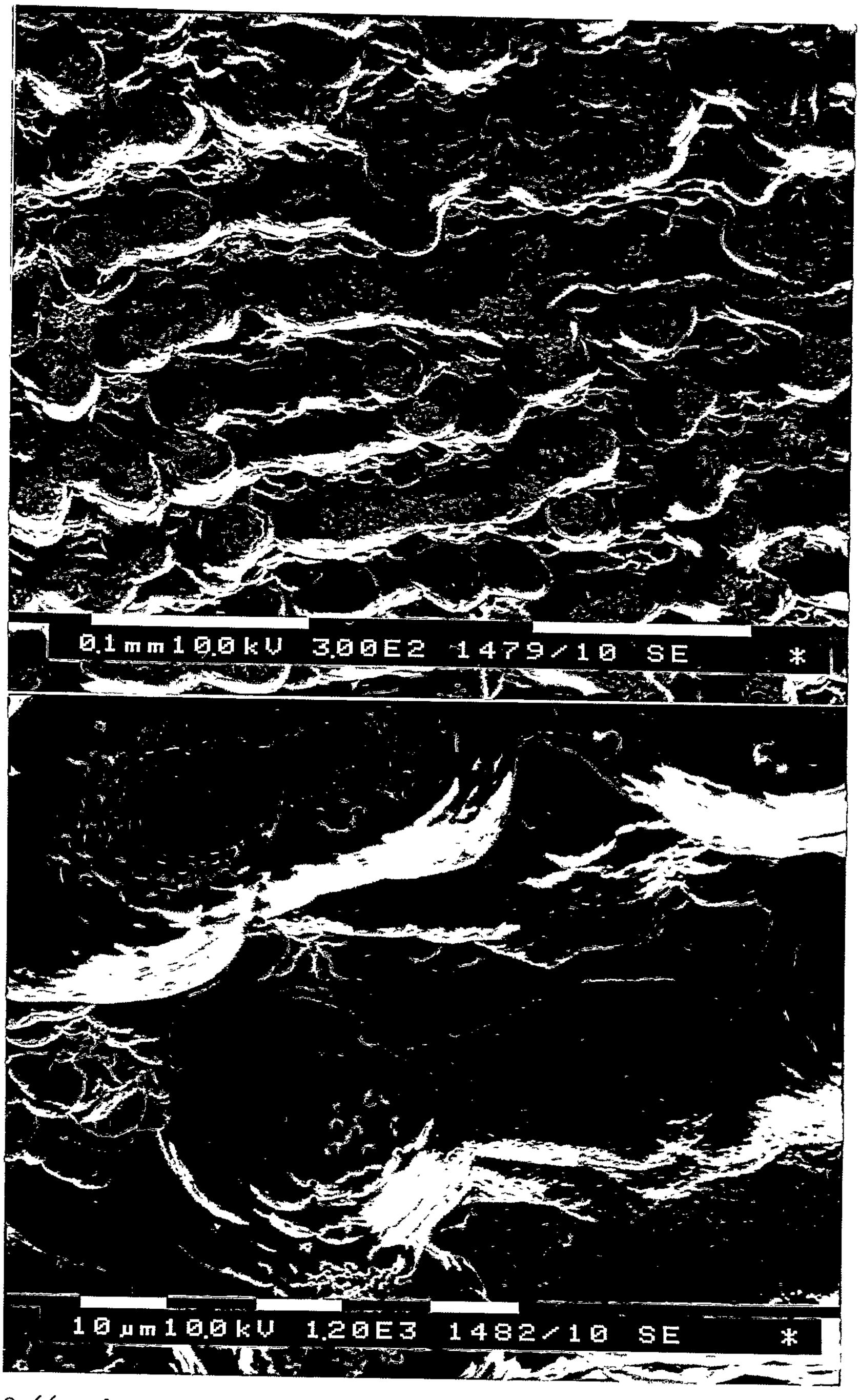

10.66a
(X 300)

10.66b
(X 1200)

Figure 10.66 a,b
SEM of a Microbond NP^2 specimen electrolytically etched under the etching conditions A,1,I (decreased etching solution concentration, decreased current density, decreased etching time).

10.67a
(X 300)

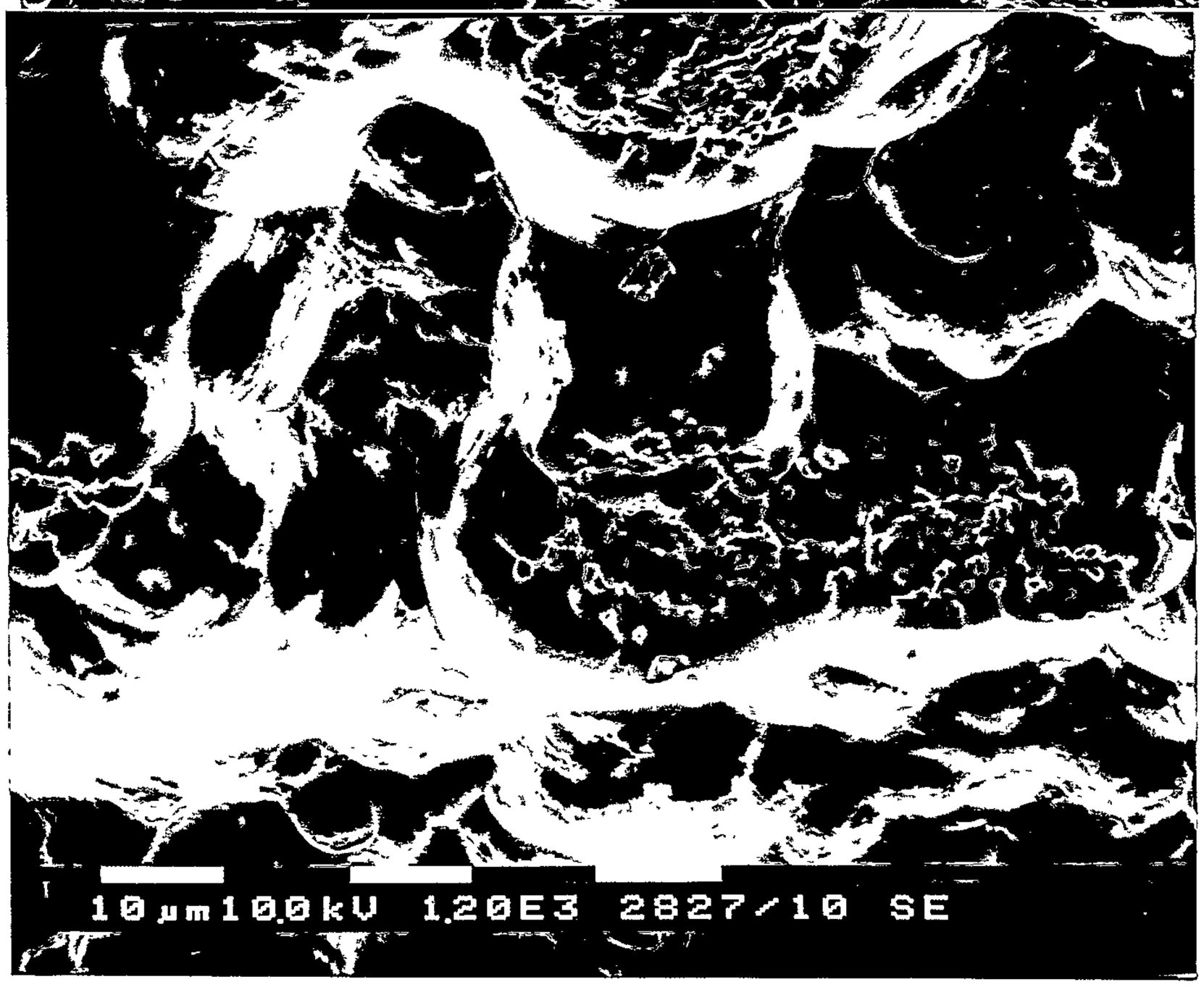

10.67b
(X 1200)

igure 10.67 a,b

M of a Microbond NP^2 specimen electrolytically etched under the ching conditions B,1,I (recommended etching solution concentration, creased etching time, decreased current density).

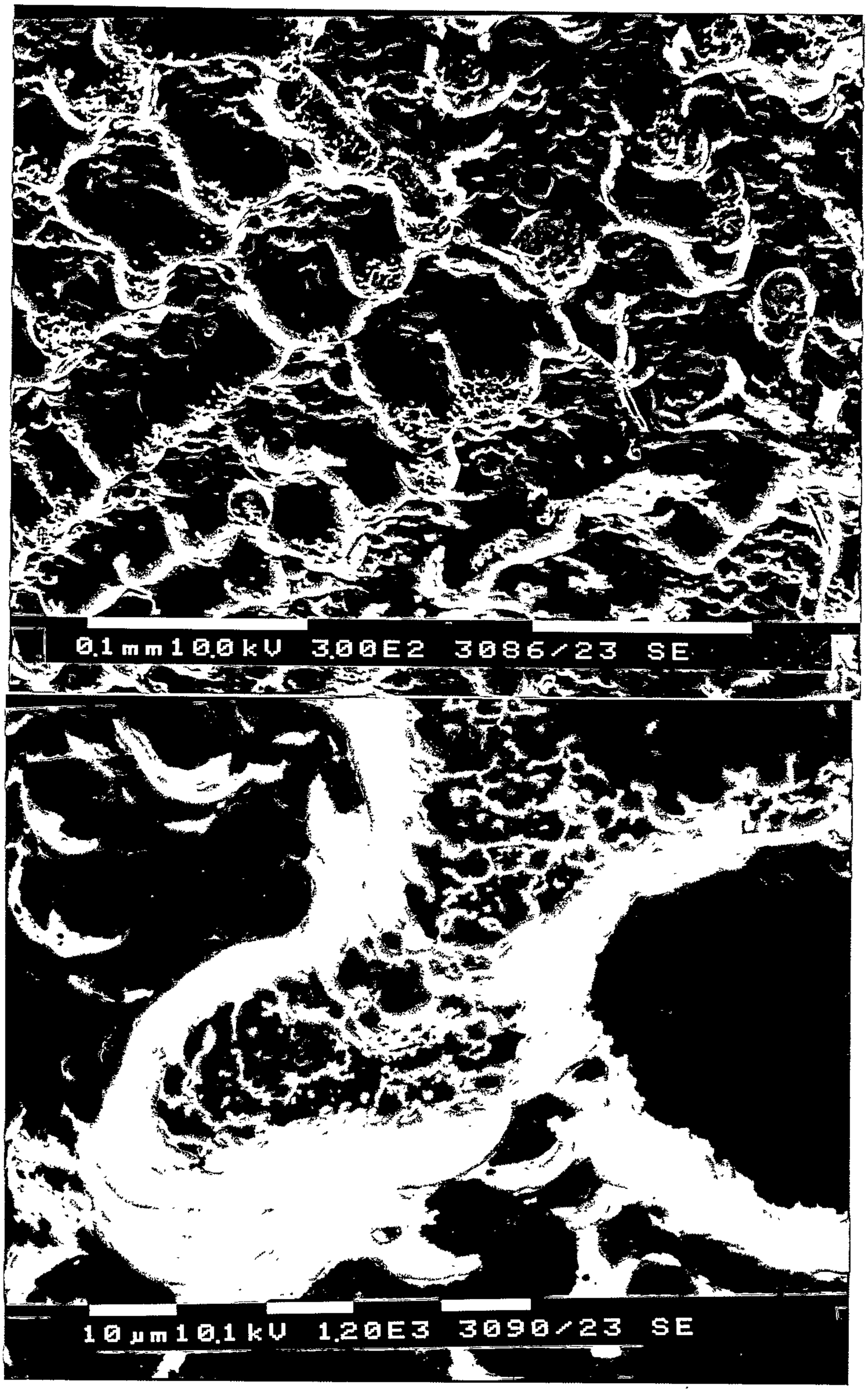

10.68a
(X 300)

10.68b
(X 1200)

igure 10.68 a,b
EM of a Microbond NP^2 specimen electrolytically etched under the
ching conditions C,1,I (increased etching solution concentration,
creased current density, decreased etching time).

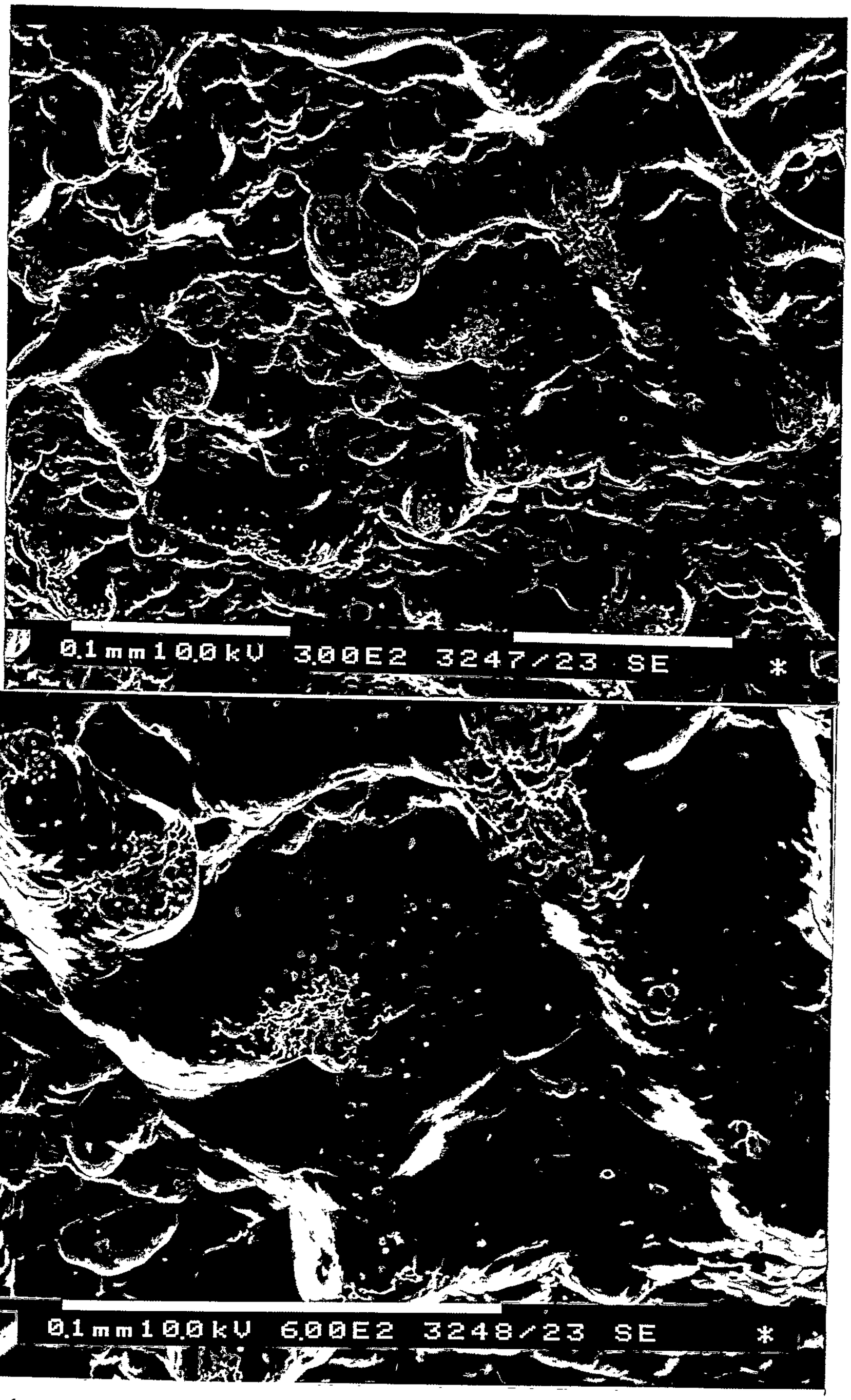

10.69a
(X 300)

10.69b
(X 600)

Figure 10.69 a,b
SEM of a Microbond NP^2 specimen electrolytically etched under the etching conditions A,2,II (decreased etching solution concentration, recommended current density and etching time).

10,70a
(X 300)

10.70b
(X 1200)

igure 10.70 a,b
EM of a Microbond NP^2 specimen electrolytically etched under the
tching conditions B,2,II (recommended etching solution concentration,
rrent density and etching time).

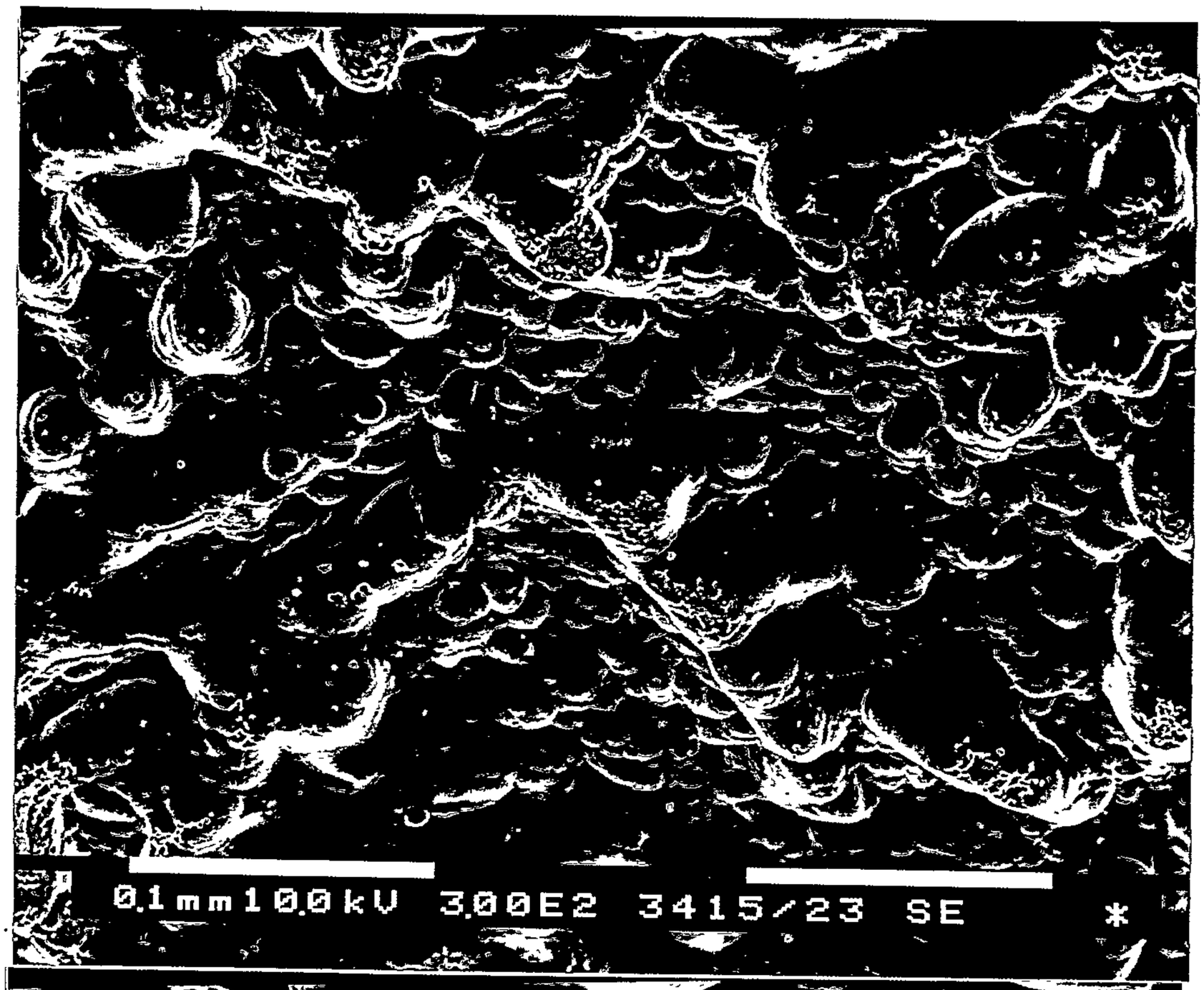

10.71a
(X 300)

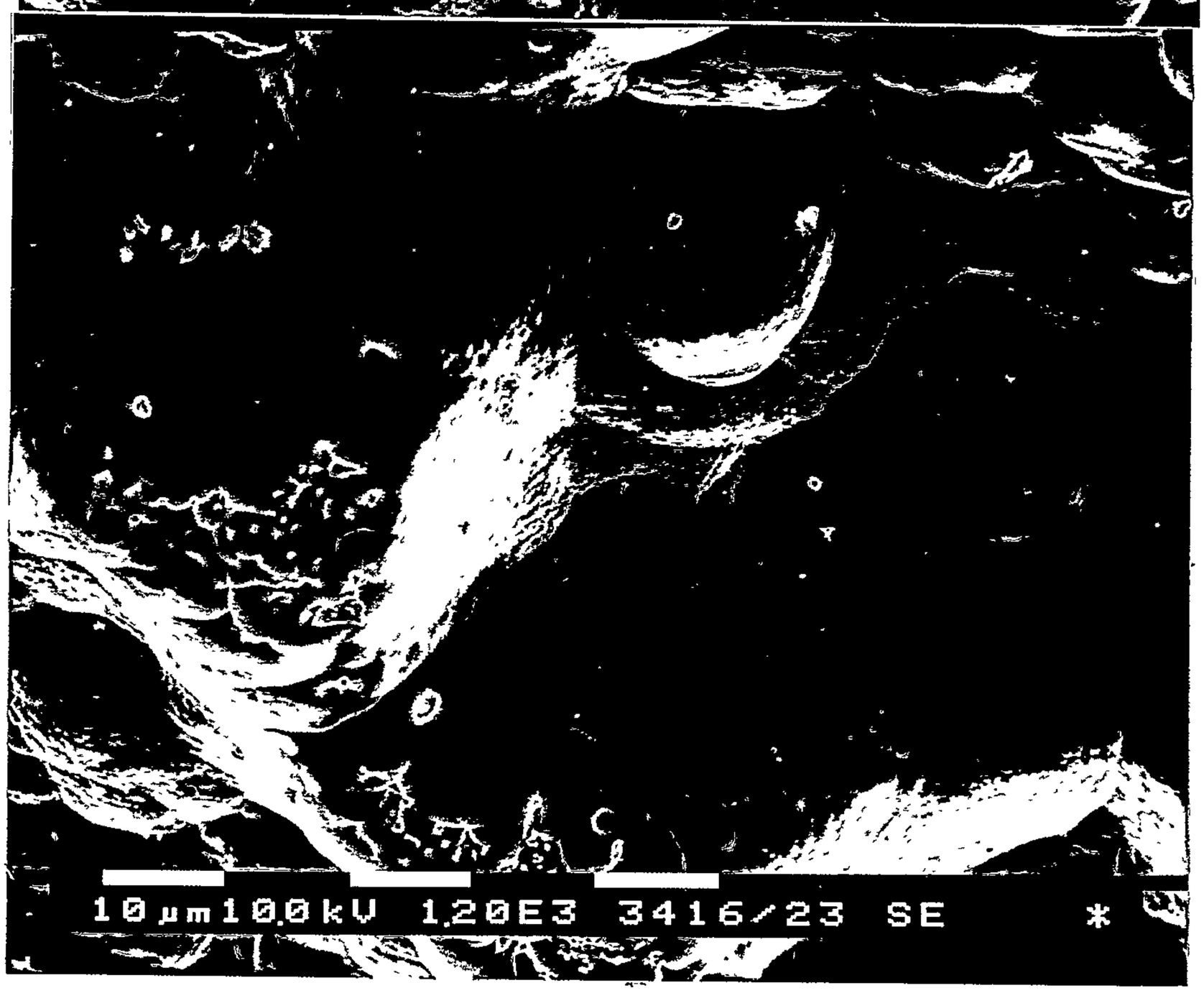

10.71b

ure 10.71 a,b
of a Microbond NP^2 specimen electrolytically etched under the
ing conditions C,2,II (increased etching solution concentration,
mmended current density and etching time).

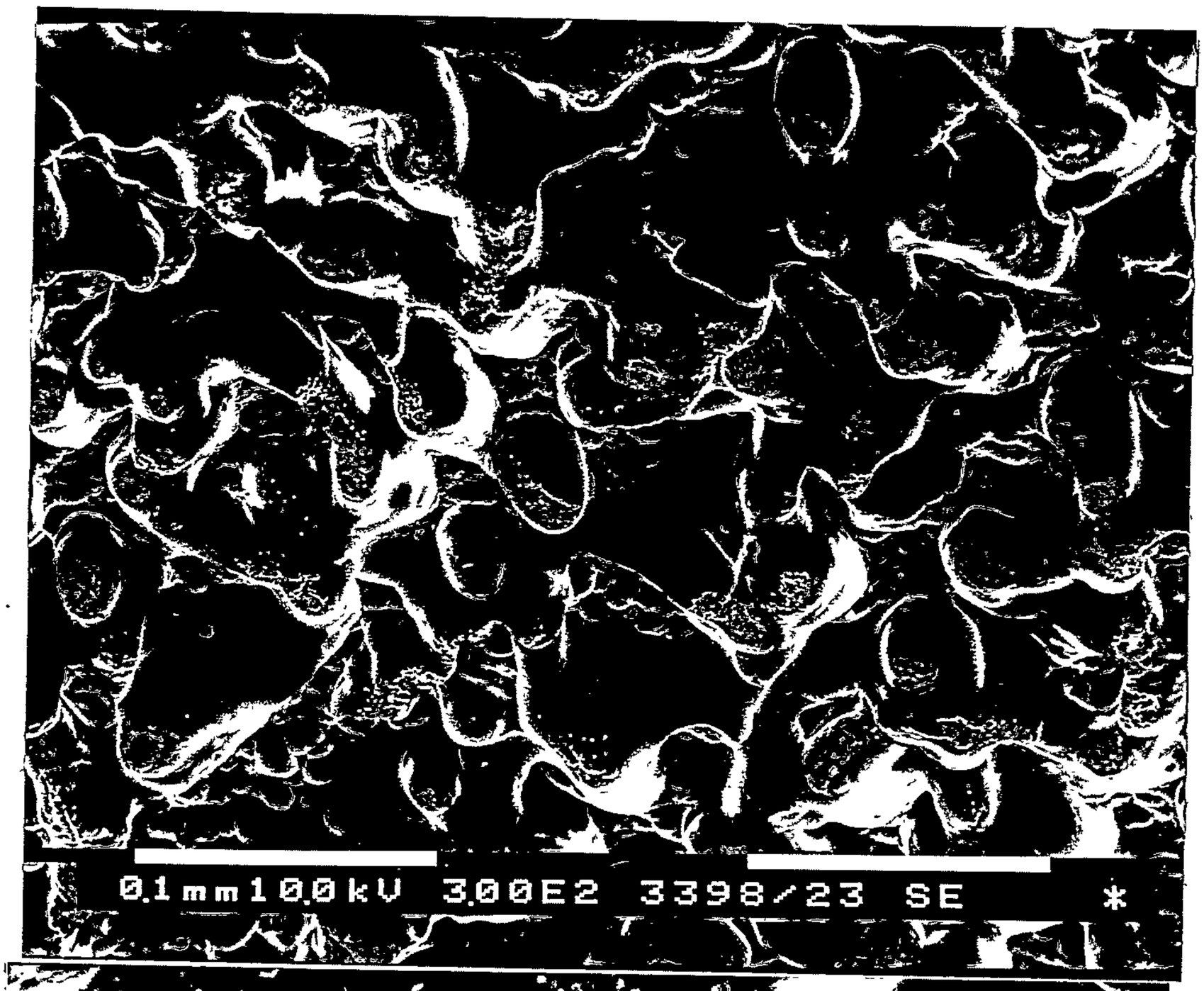

10.72a
(X 300)

10.72b
(X 1200)

Figure 10.72 a,b
SEM of a Microbond NP^2 specimen electrolytically etched under the etching conditions A,3,II (decreased etching solution concentration, increased current density, recommended etching time).

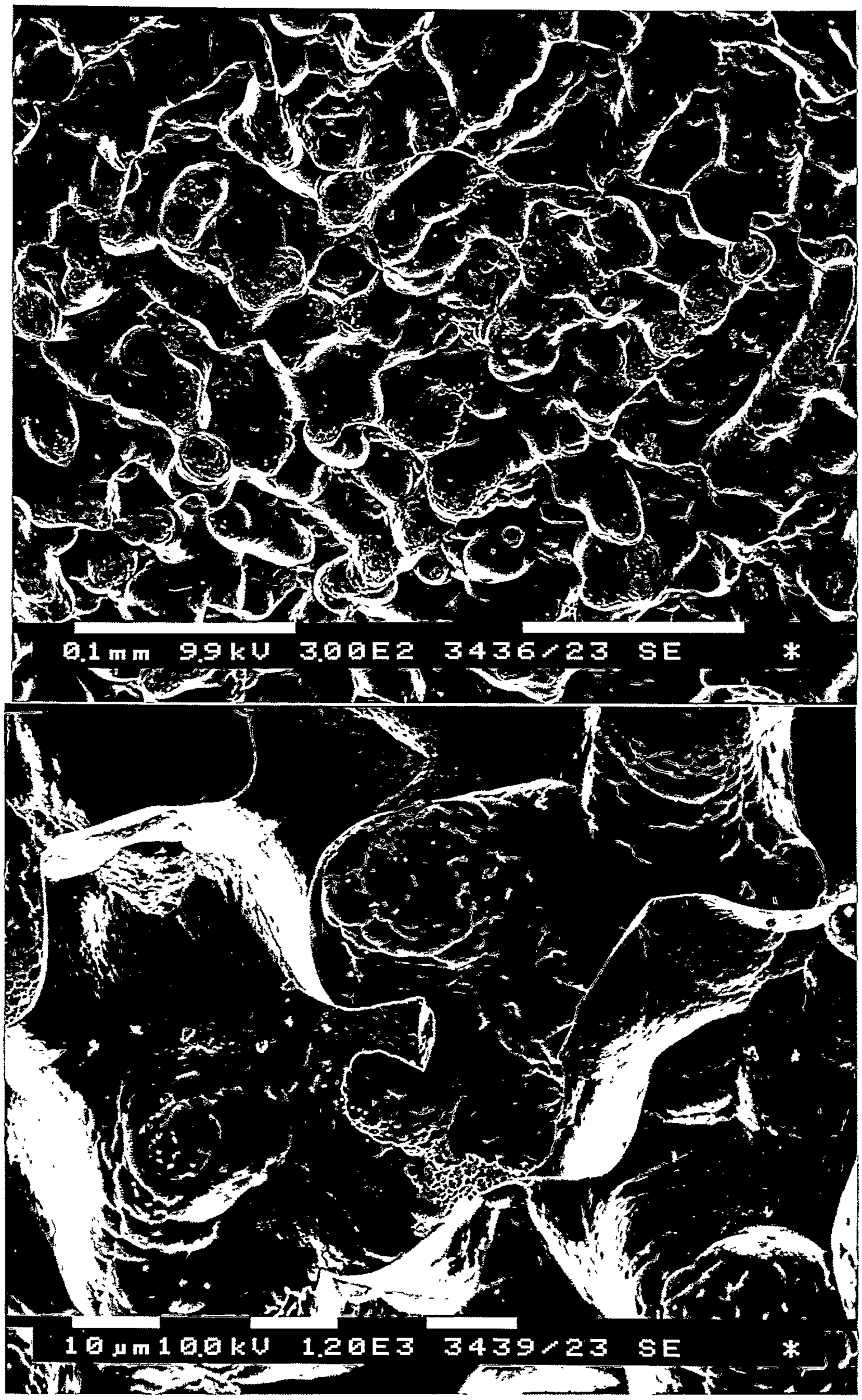

10.73a
(X 300)

10.73b
(X 1200)

Figure 10.73 a,b
SEM of a Microbond NP^2 specimen electrolytically etched under the etching conditions B,3,II (recommended etching solution concentration, increased current density, recommended etching time).

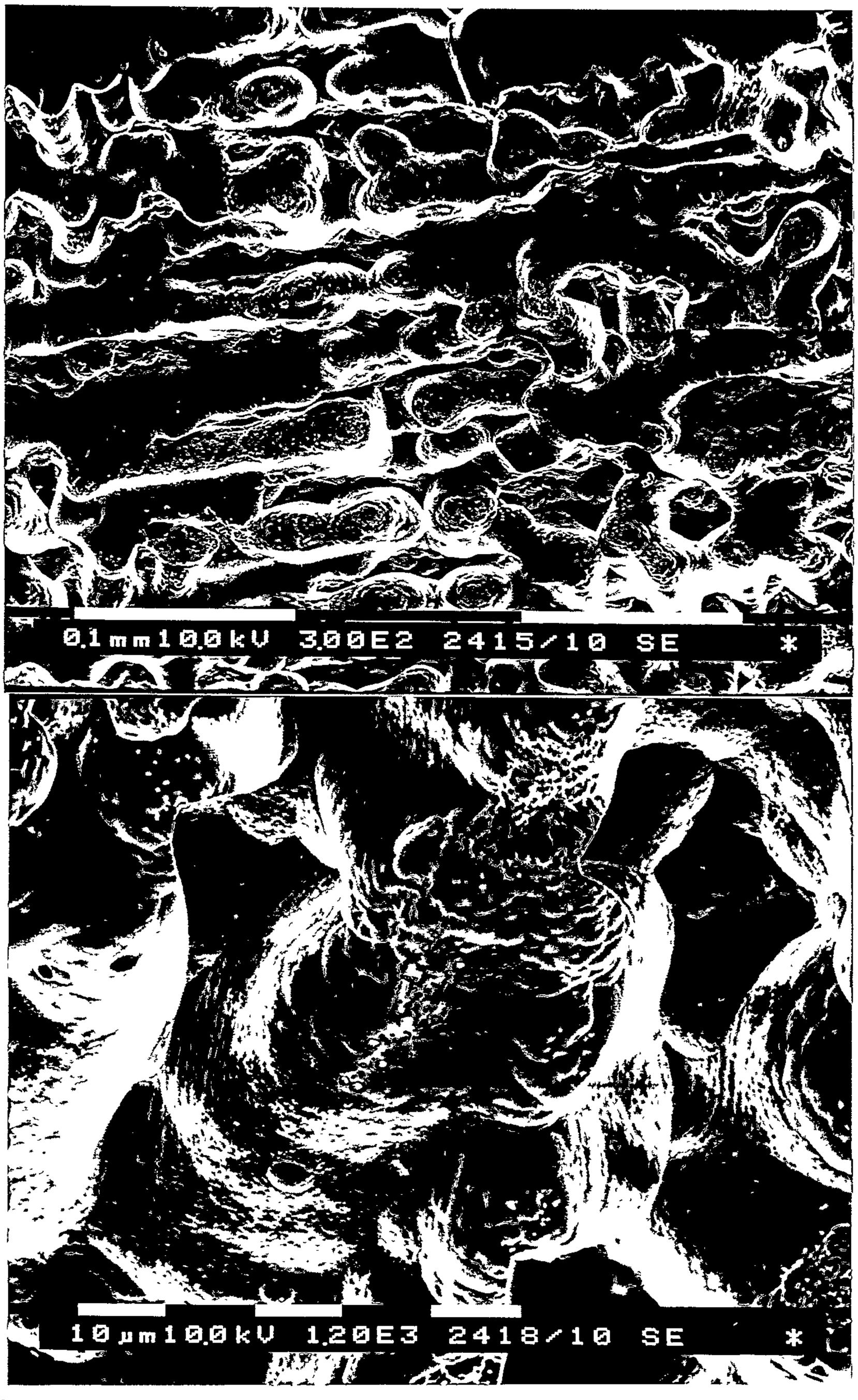

10.74a
(X 300)

10.74b
(X 1200)

Figure 10.74 a,b
SEM of a Microbond NP^2 specimen electrolytically etched under the etching conditions C,3,II (increased etching solution concentration, increased current density, recommended etching time).

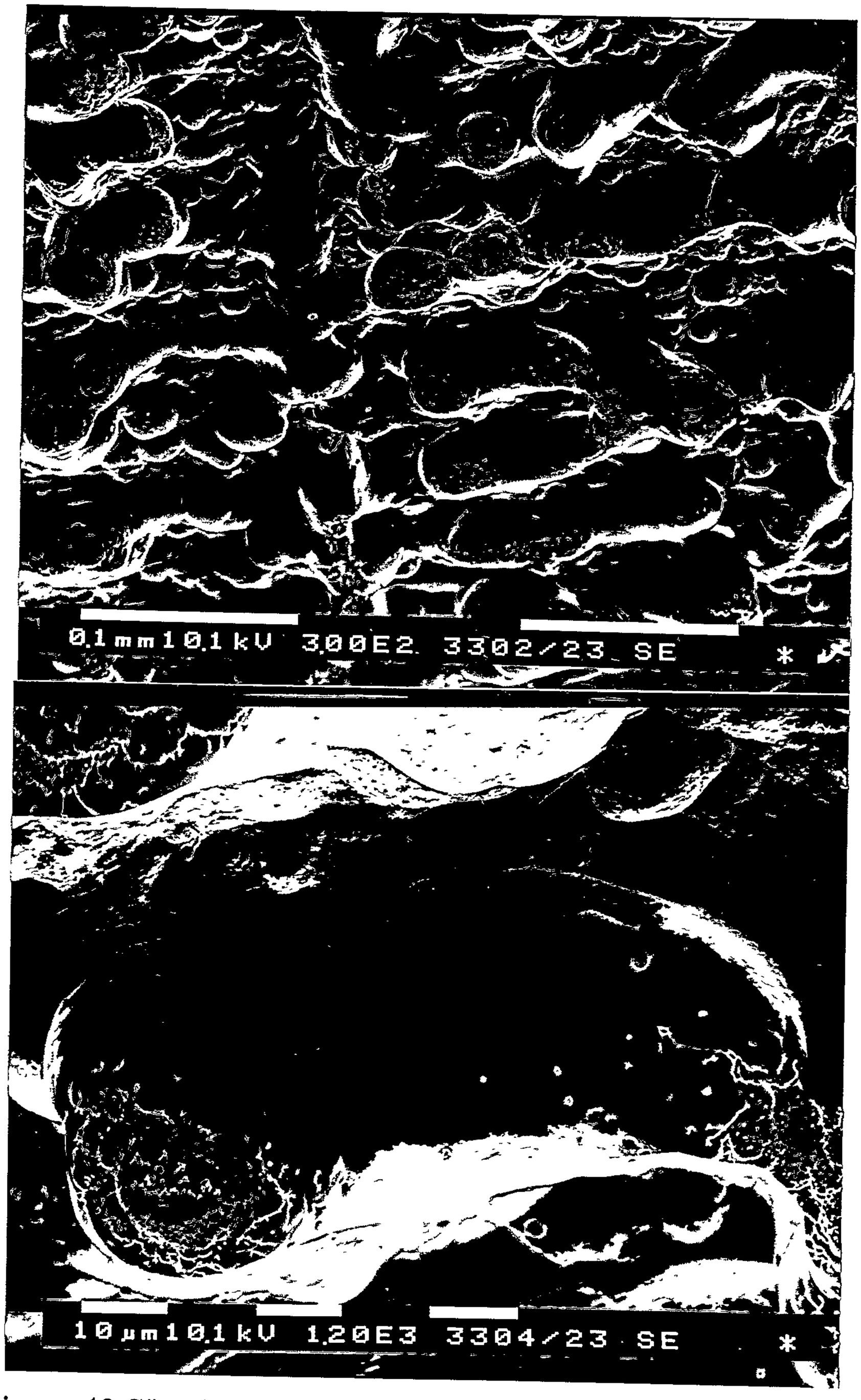

10.75a
(X 300)

10.75b
(X 1200)

Figure 10.75 a,b
SEM of a Microbond NP^2 specimen electrolytically etched under the etching conditions A,2,III. Specimen coded No. 2. This specimen did not survive thermal-cycling.

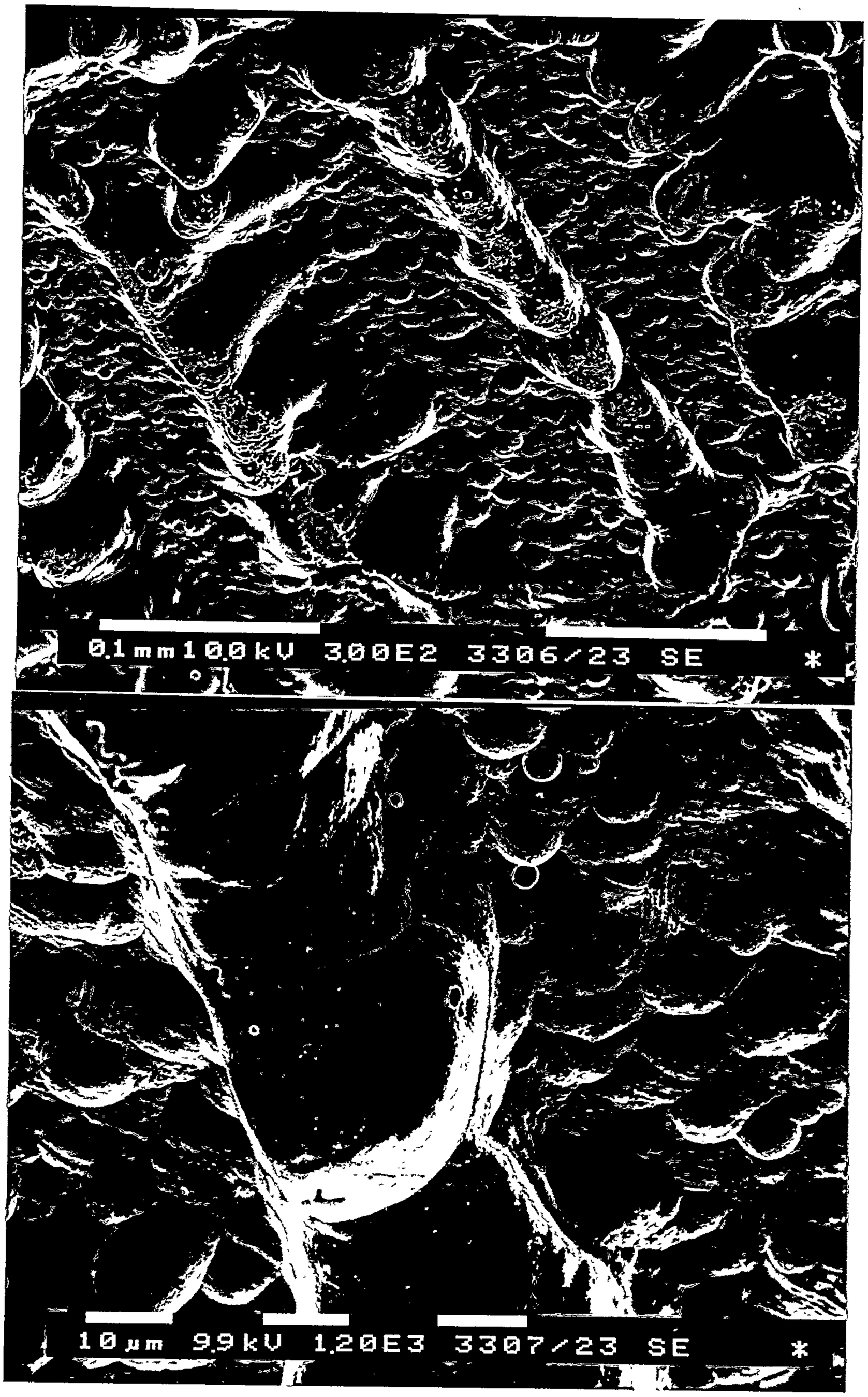

10.76a
(X 300)

10.76b
(X 1200)

Figure 10.76 a,b
SEM of a Microbond NP^2 specimen electrolytically etched under the same etching conditions as the specimen depicted in Figure 10.75a,b, (A,2,III). Specimen coded No. 3. This specimen did not survive thermal-cycling.

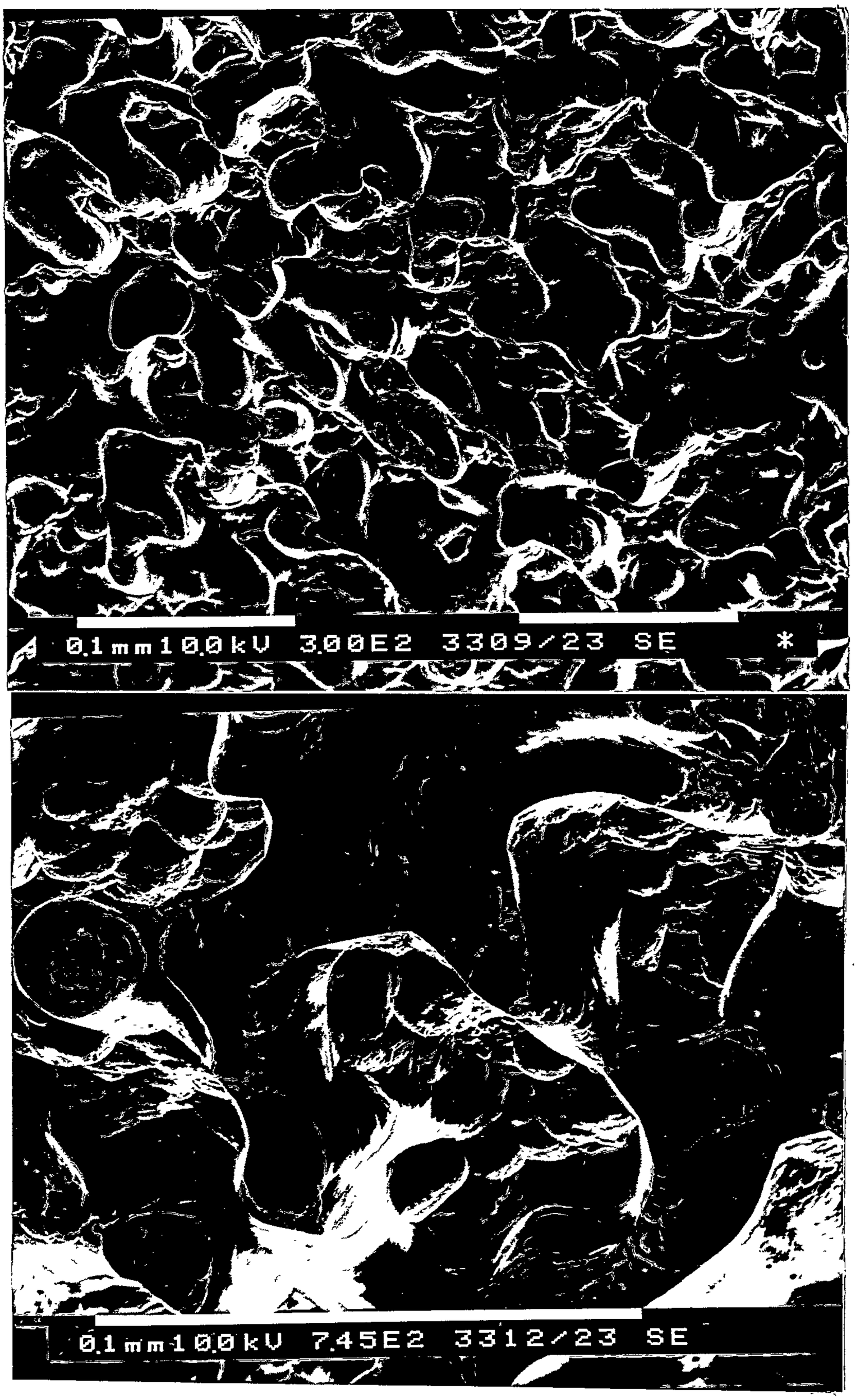

10.77a
(X 300)

10.77b
(X 1200)

Figure 10.77 a,b
SEM of a Microbond NP^2 specimen etched under the etching conditions A,2,III. Specimen coded No. 4. Tensile bond strength = 9.85MPa

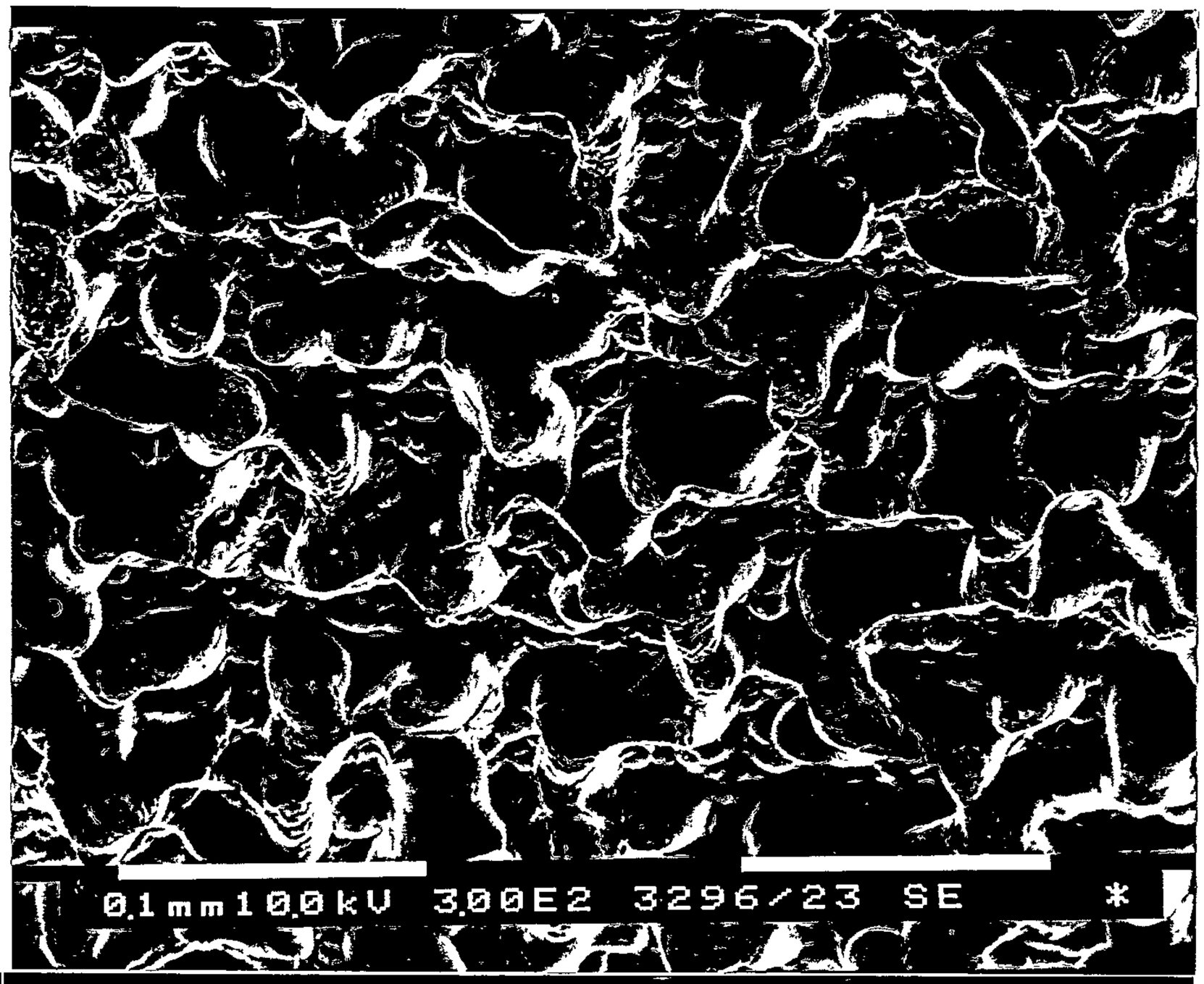

10.78a
(X 300)

10.78b
(X 1200)

Figure 10.78 a;b
SEM of a Microbond NP^2 specimen electrolytically etched under the etching conditions A,2,III. Specimen coded No. 1. Tensile bond strength = 4.98 MPa.

10.79a
(X 300)

10.79b
(X 1150)

Figure 10.79 a,b
SEM of a Microbond NP^2 specimen electrolytically etched under the etching conditions A,2,III. Specimen coded No. 5. This specimen exhibited two, quite different, areas with neither area showing obvious undercut areas (see also over page). Tensile bond strength = 9.40 MPa.

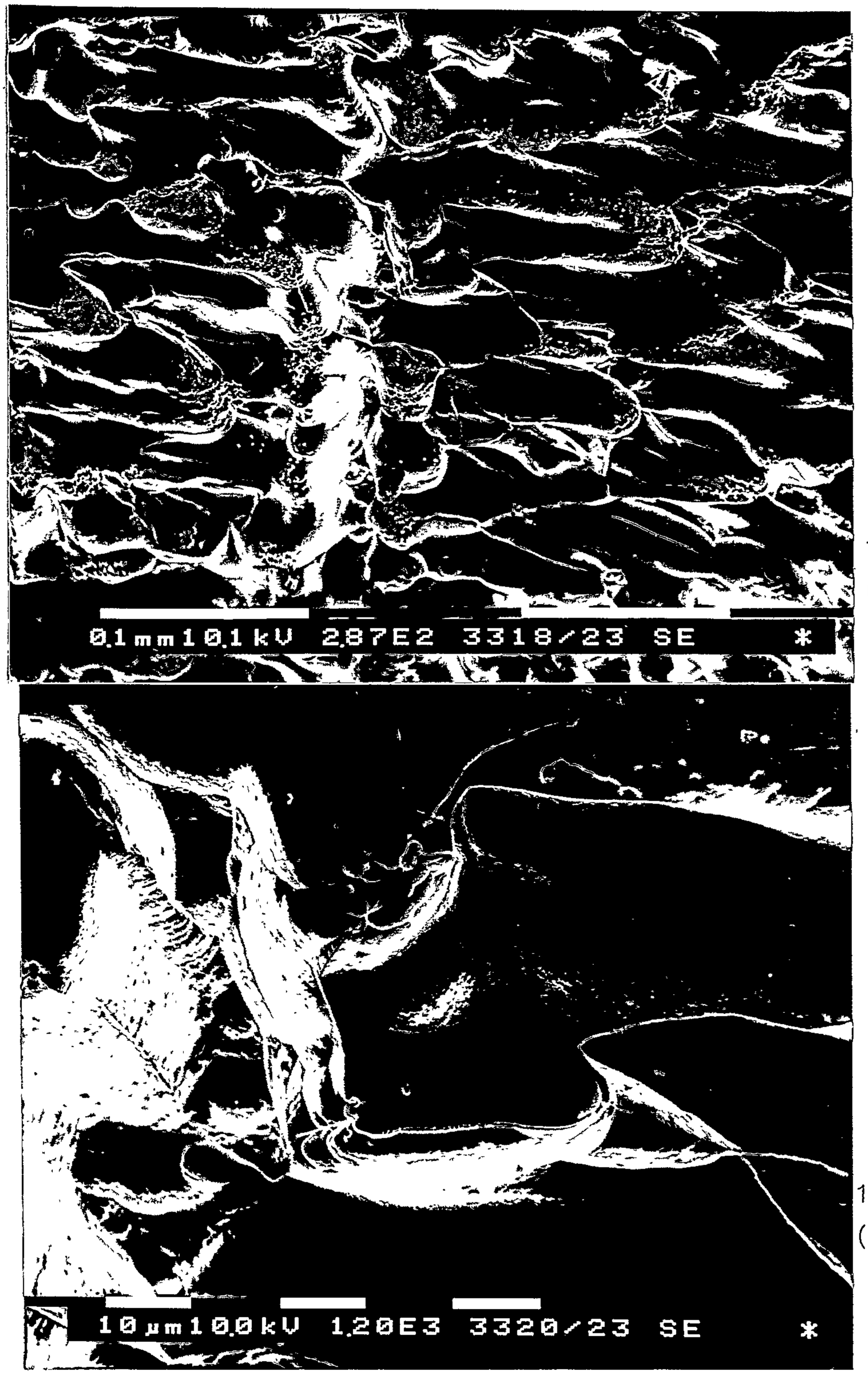

10.79c
(X 287)

10.79d
(X 1200)

Figure 10.79 c,d
SEM of the Microbond NP^2 specimen depicted in Figure 10.79 a,b.
Note the different surface topography compared to Figure
10.79 a,b.

10.80a
(X 300)

10.80b
(X 1200)

Figure 10.80 a,b
SEM of a Microbond NP^2 specimen electrolytically etched under the etching conditions B,3,I. Specimen coded No.5. Tensile bond strength = 7.05 MPa.

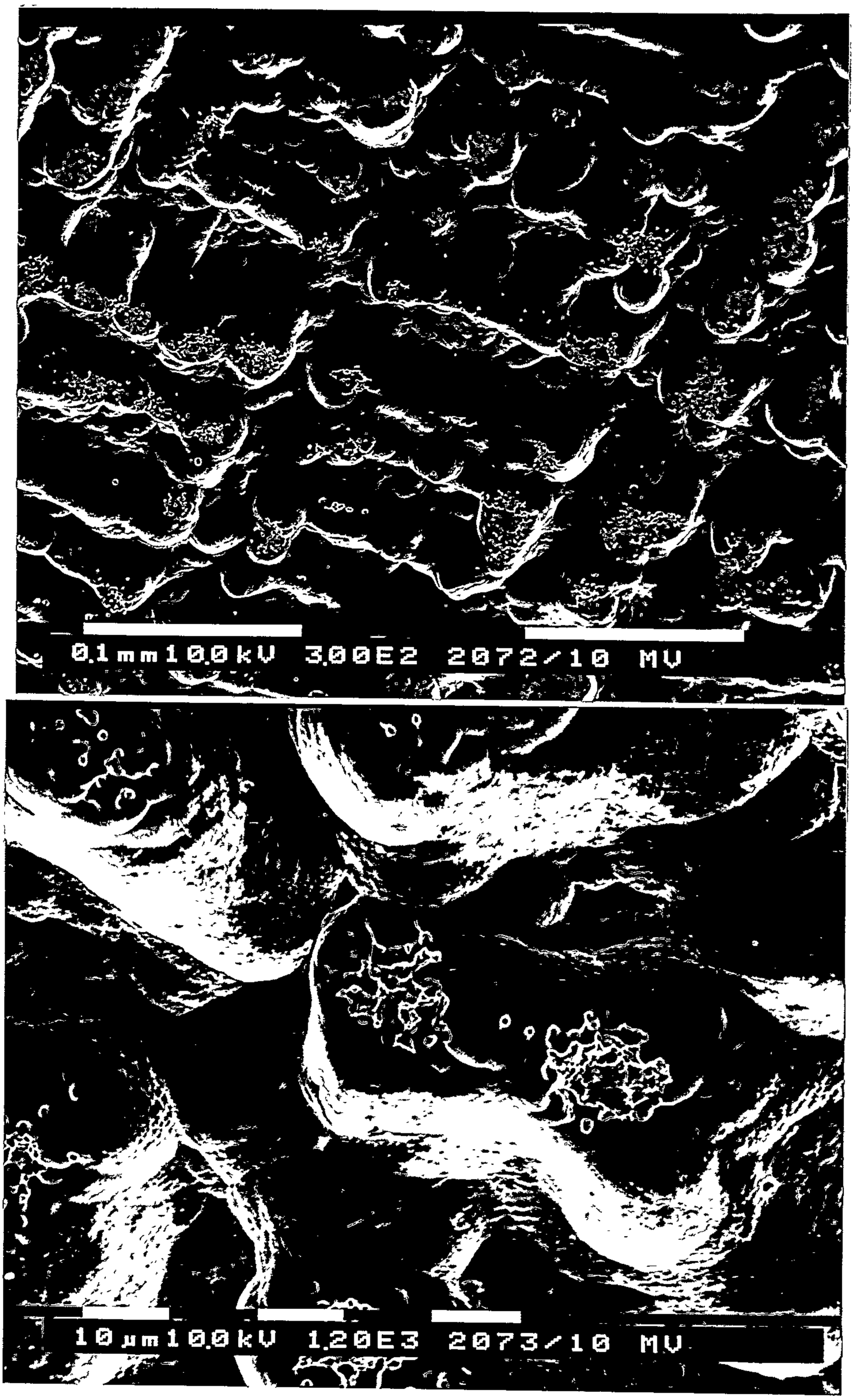

10.81a
(X 300)

10.81b
(X 1200)

Figure 10.81 a,b
SEM of a Microbond NP^2 specimen electrolytically etched under the same etching conditions as the specimen depicted in Figure 10.80 a,b (B,3,I). Specimen coded No. 2. This specimen did not survive thermal-cycling.

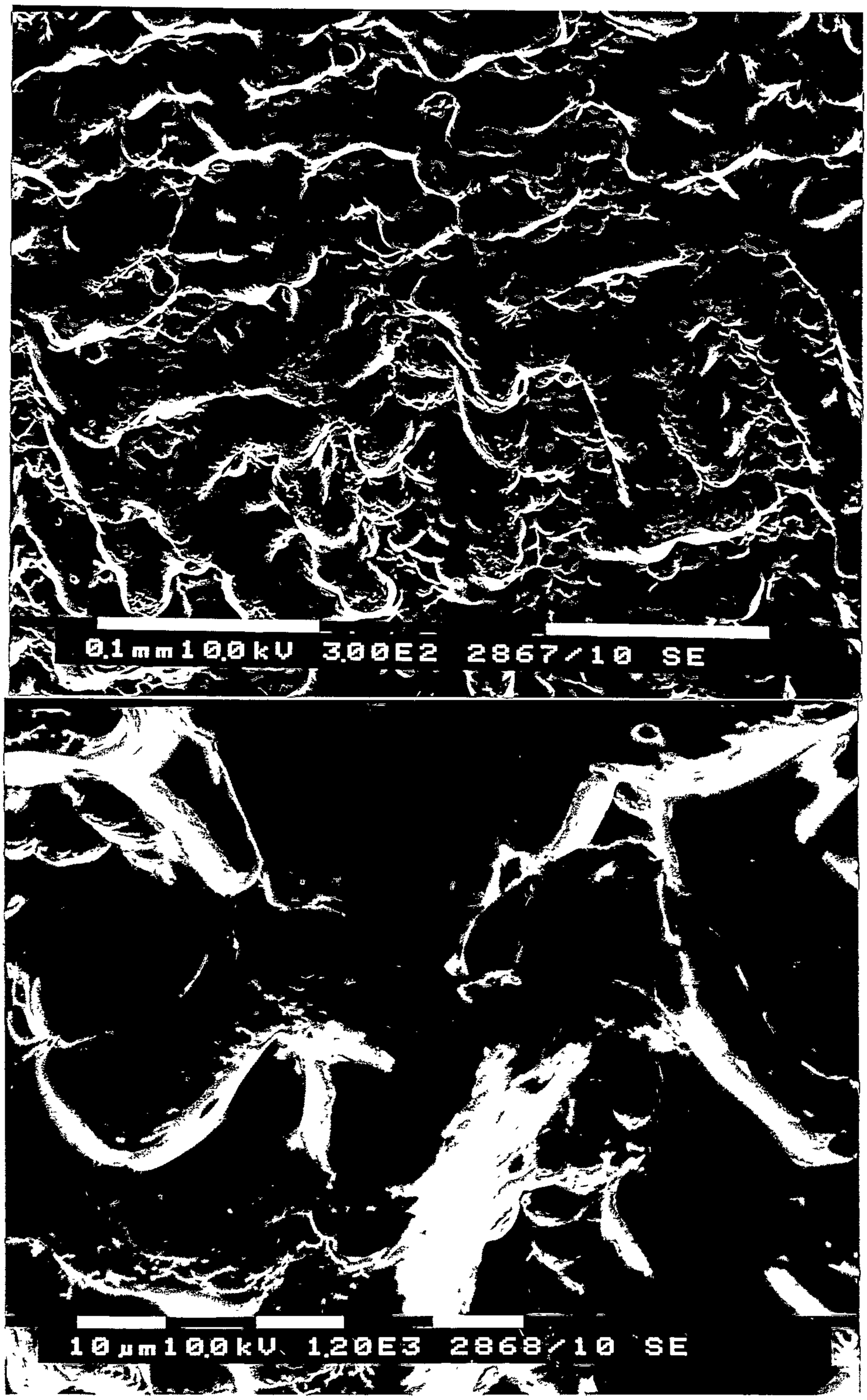

10.82a
(X 300)

10.82b
(X 1200)

Figure 10.82 a,b
SEM of a Microbond NP^2 specimen electrolytically etched under the etching conditions B,2,I. Specimen coded No.5. Tensile bond strength = 11.61 MPa.

10.83a
(X 300)

10.83b
(X 1200)

Figure 10.83 a,b
SEM of a Microbond NP^2 specimen electrolytically etched under the same etching conditions as the specimen depicted in Figure 10.82 a,b (B,2,I). Specimen coded No.1. This specimen did not survive thermal-cycling.

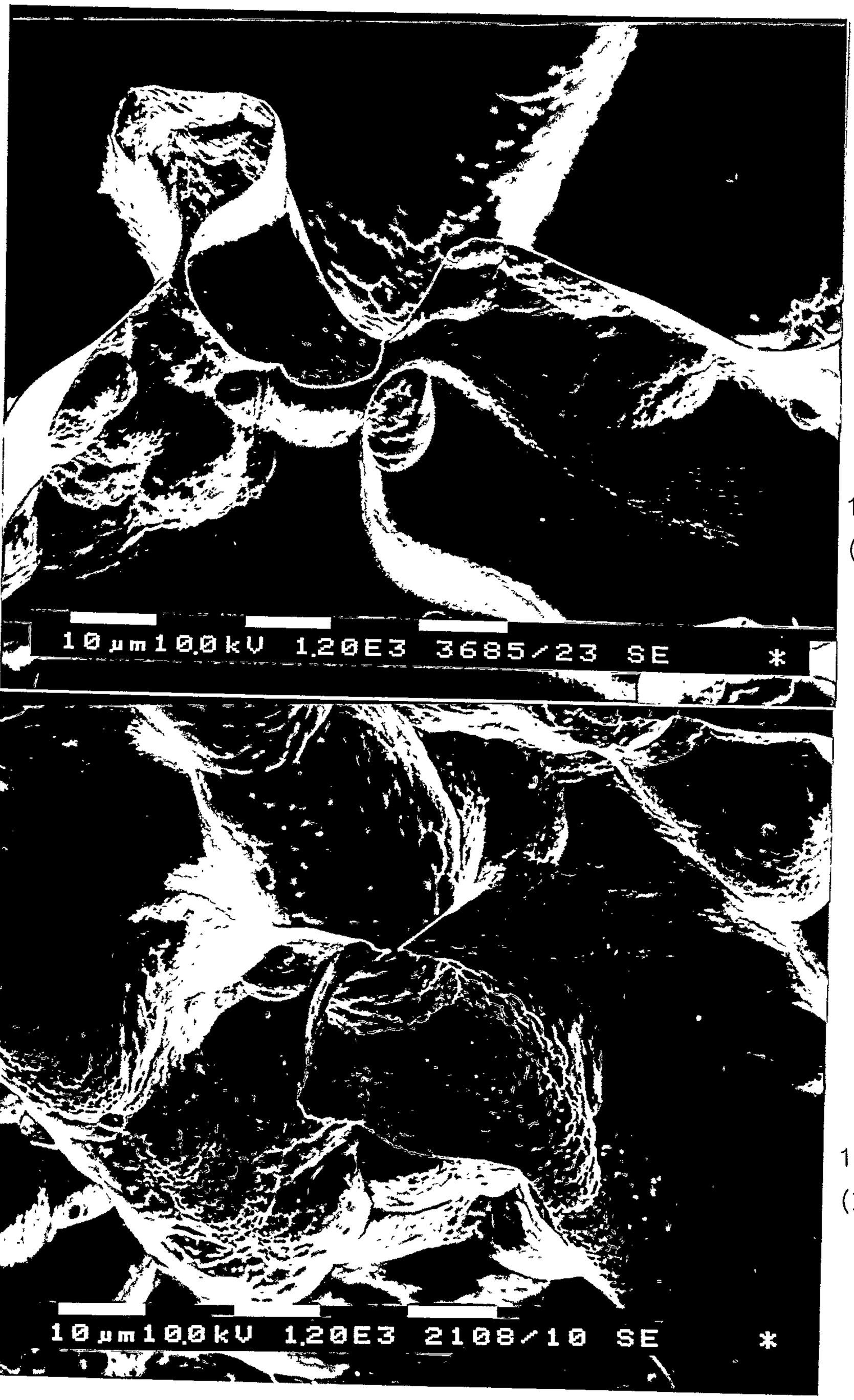

10.84a
(X 1200)

10.84b
(X 1200)

Figure 10.84 a,b
SEM of two Microbond NP^2 specimens electrolytically etched under the etching conditions A,3,III (Figure 10.84a) and B,2,III (Figure 10.84b) showing clear undercut areas . These surface formations were not commonly seen.

Figure 10.84c
SEM of a Microbond NP^2 specimen electrolytically etched under the etching conditions B,3,II. This specimen, similar to those depicted in Figure 10.84 a,b , shows an undercut area which was an unusual finding (X 1200).

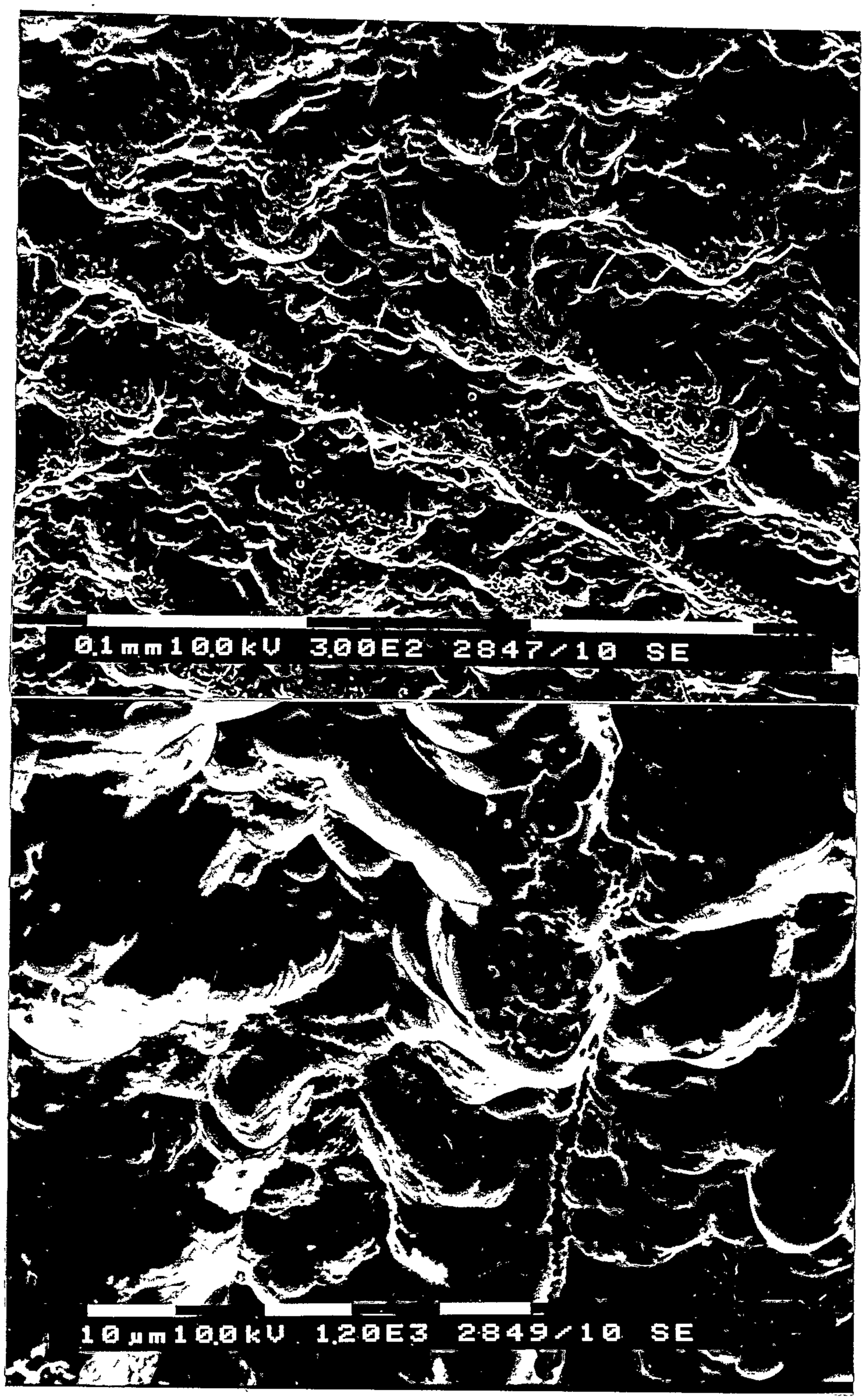

10.85a
(X 300)

10.85b
(X 1200)

Figure 10.85 a,b
SEM of a Microbond NP^2 specimen electrolytically etched under the etching conditions B,1,I where all five specimens in the group failed to survive thermal-cycling.

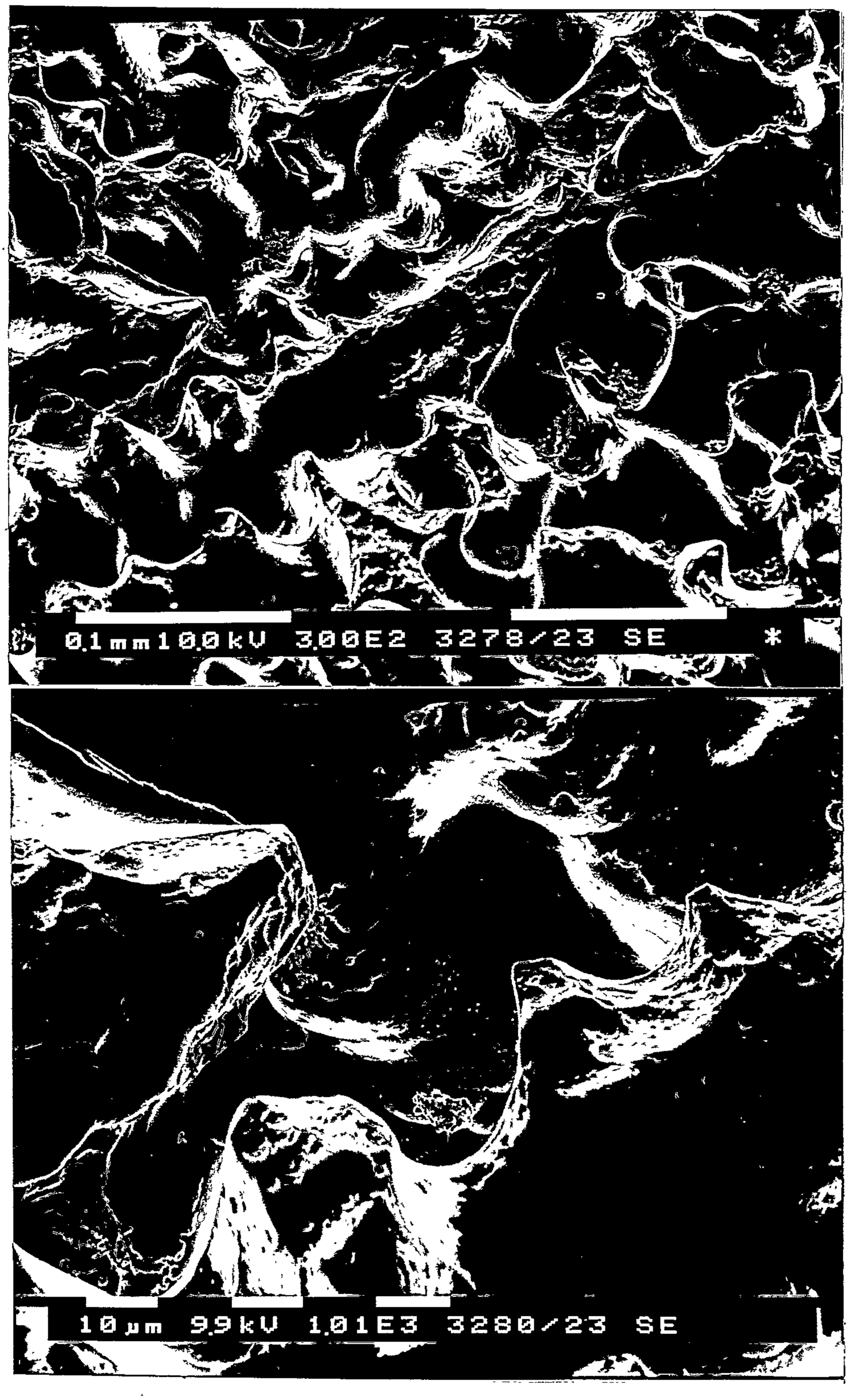

10.86a
(X 300)

10.86b
(X 1010)

Figure 10.86 a,b
SEM of a Microbond NP^2 specimen electrolytically etched under the etching conditions B,3,III where three out of five specimens in the group survived thermal-cycling. This specimen provided a tensile bond strength of 6.91 MPa.

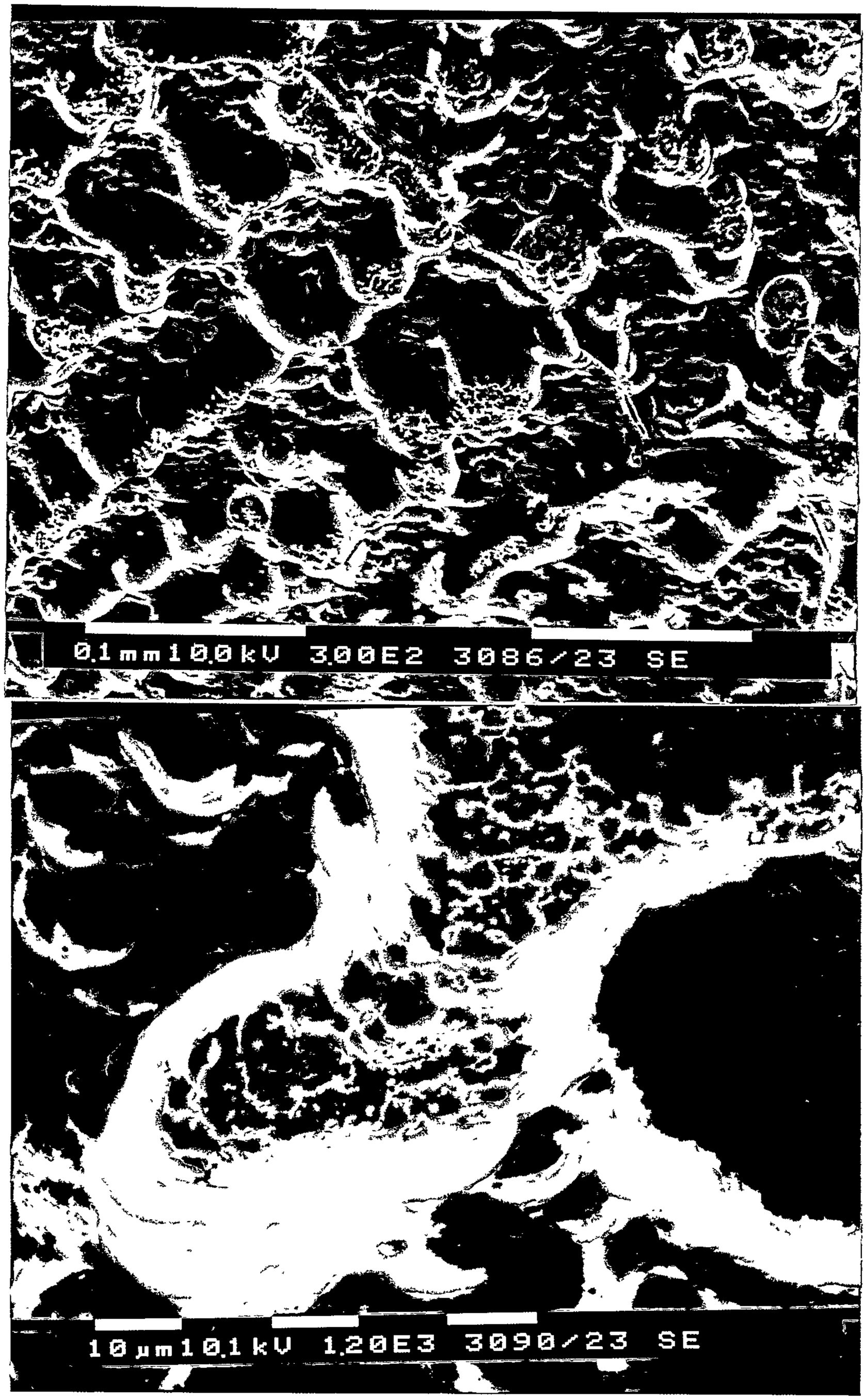

10.87a
(X 300)

10.87b
(X 1200)

Figure 10.87 a,b
SEM of a Microbond NP^2 specimen electrolytically etched under the etching conditions C,1,I in which all the specimens in the group failed thermal-cycling.

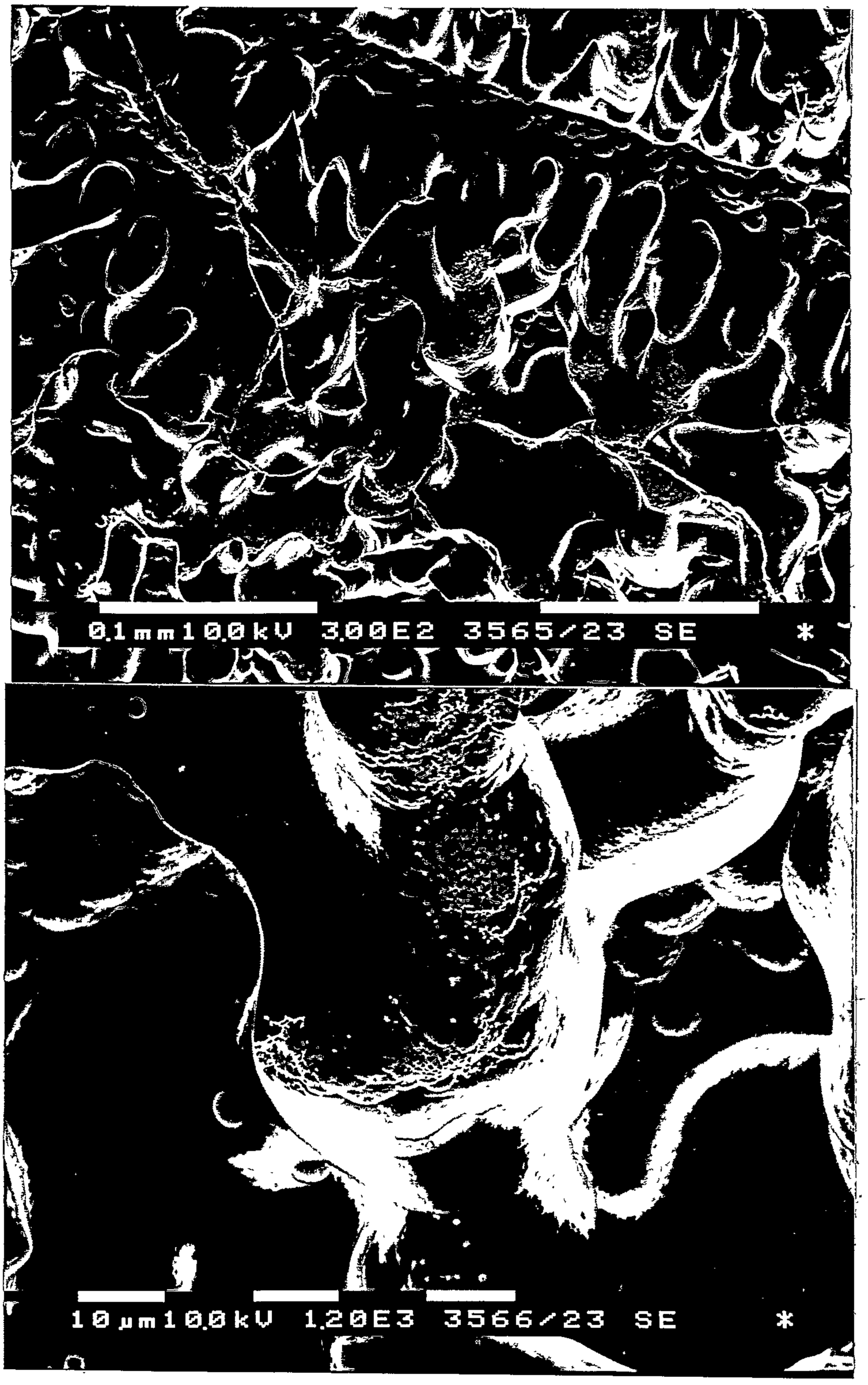

10.88a
(X 300)

10.88b
(X 1200)

Figure 10.88 a,b
SEM of a Microbond NP^2 specimen electrolytically etched under the etching conditions C,3,III in which all five specimens in the group survived thermal-cycling. This specimen provided a tensile bond strength of 8.21 MPa.

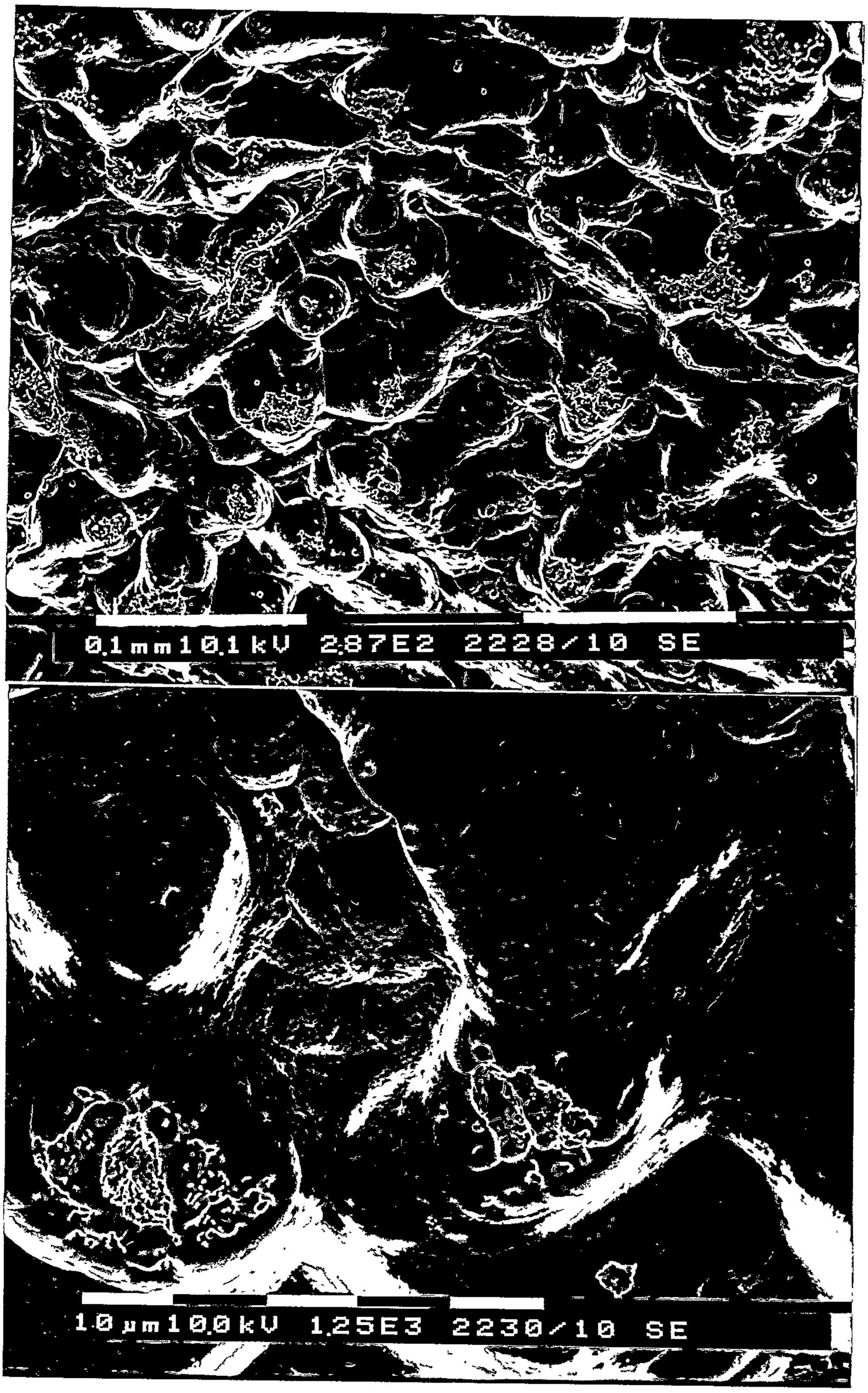

10.89a
(X 287)

10.89b
(X 1250)

Figure 10.89 a,b
SEM of a Microbond NP^2 specimen electrolytically etched under the etching conditions B,2,II. Specimen coded No. 3.

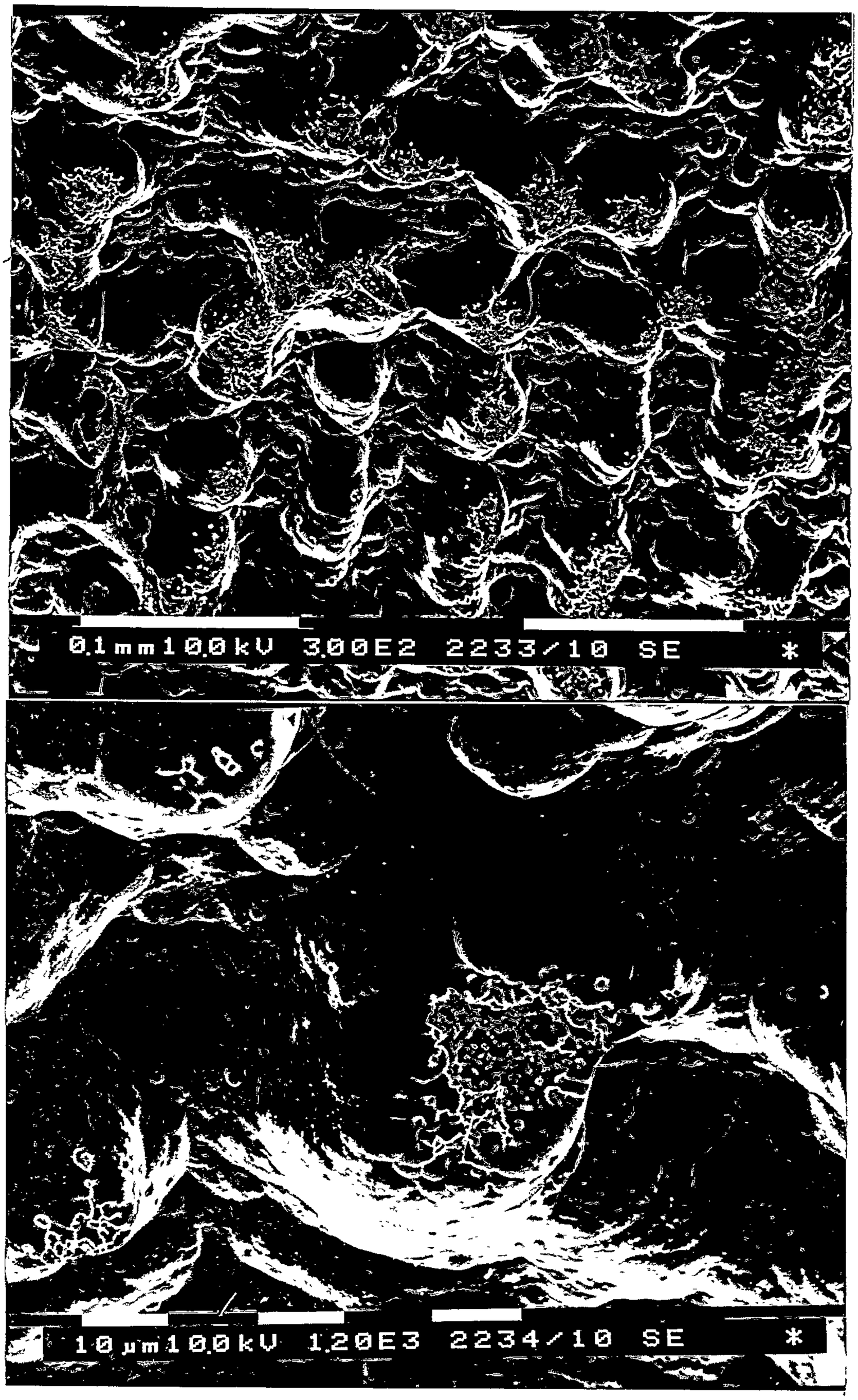

10.90a
(X 300)

10.90b
(X 1200)

Figure 10.90 a,b
SEM of a Microbond NP^2 specimen electrolytically etched under the etching conditions B,2,II. .Specimen coded No. 4.

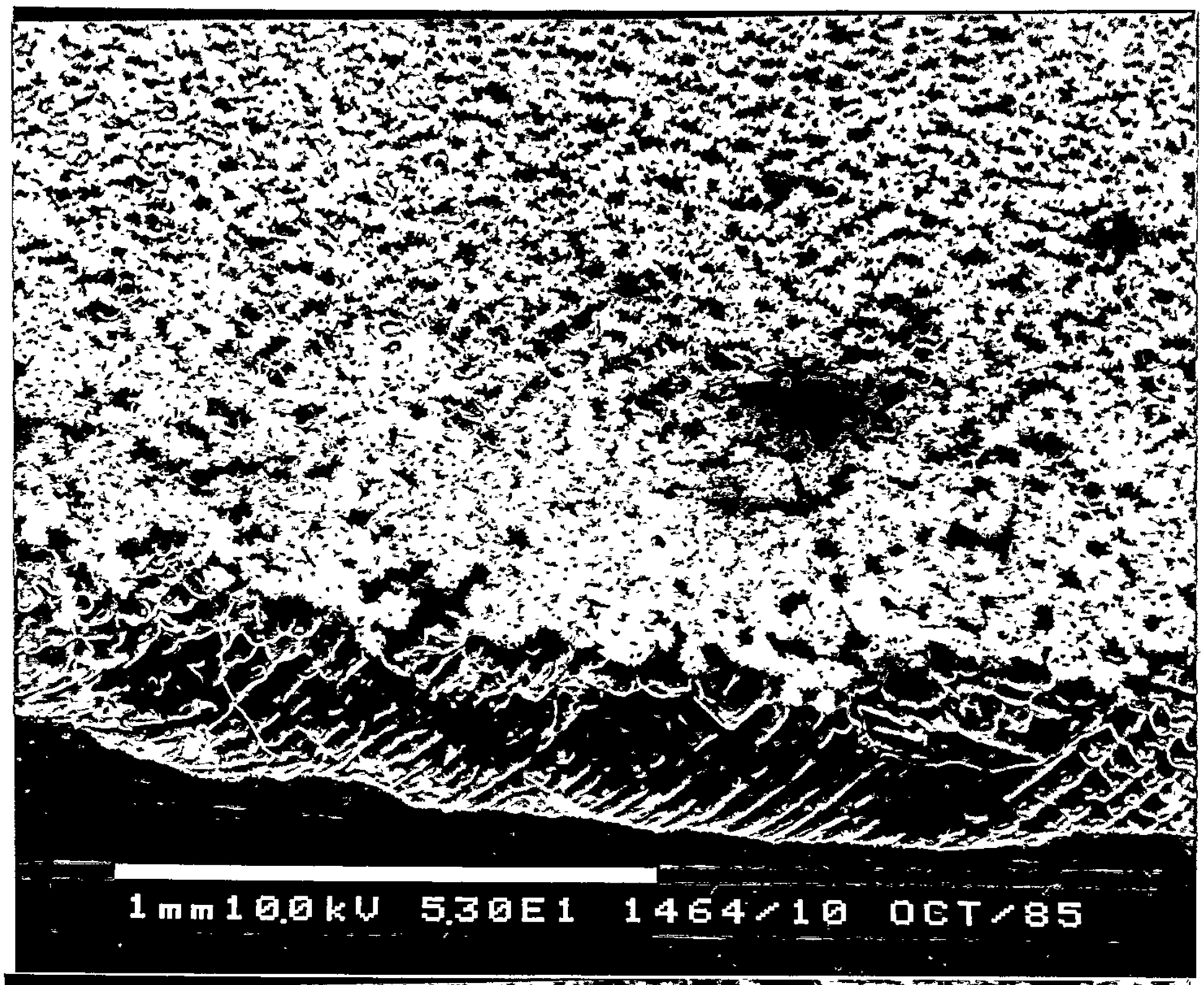

10.91a
(X 53)

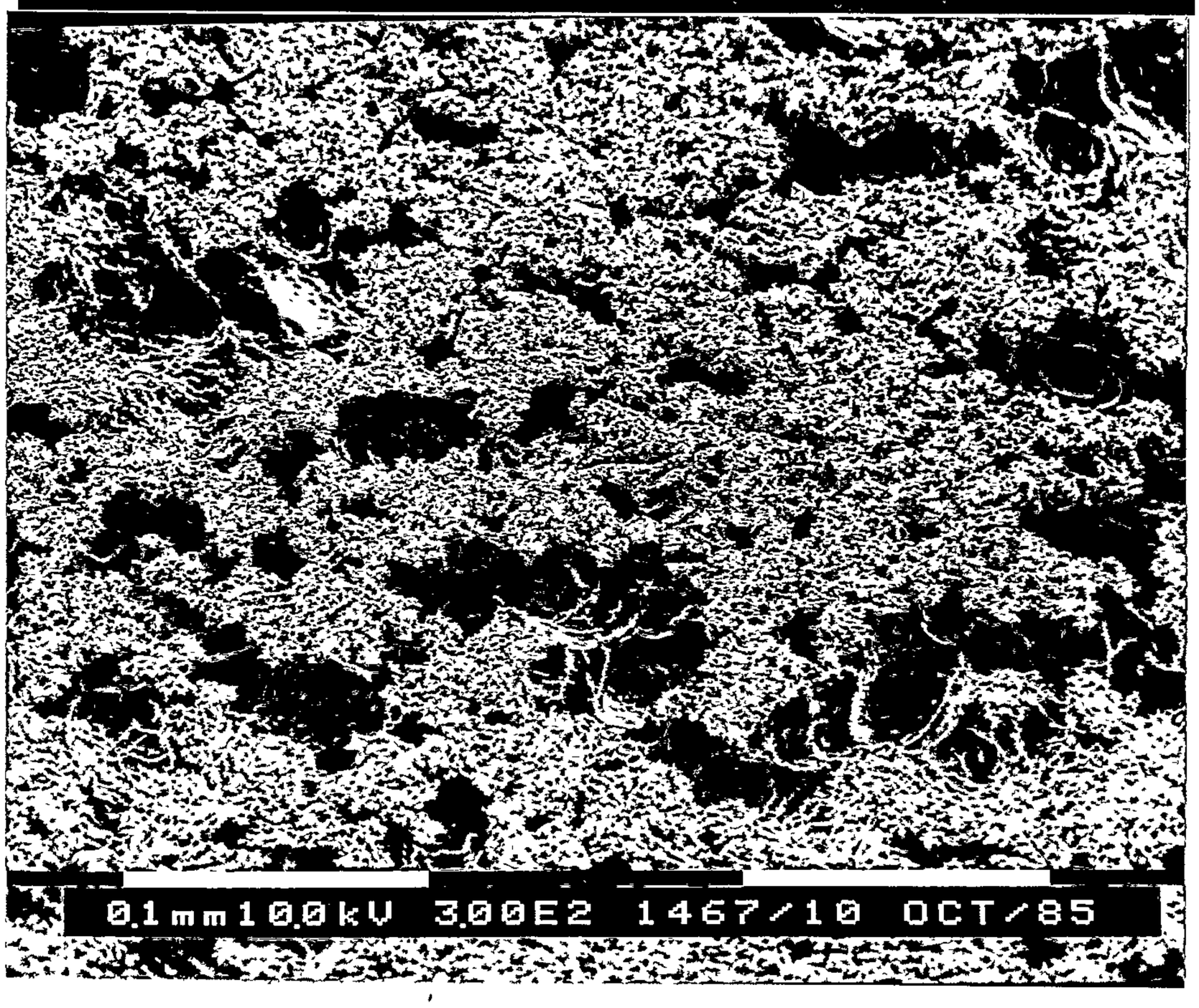

10.91b
(X 300)

Figure 10.91 a,b
SEM of a Microbond NP^2 specimen electrolytically etched under the etching conditions A,1,I. This specimen was etched immediately after it had been subjected to a simulated porcelain firing. A membranous layer can be seen with evidence of an etched metal-surface underneath.

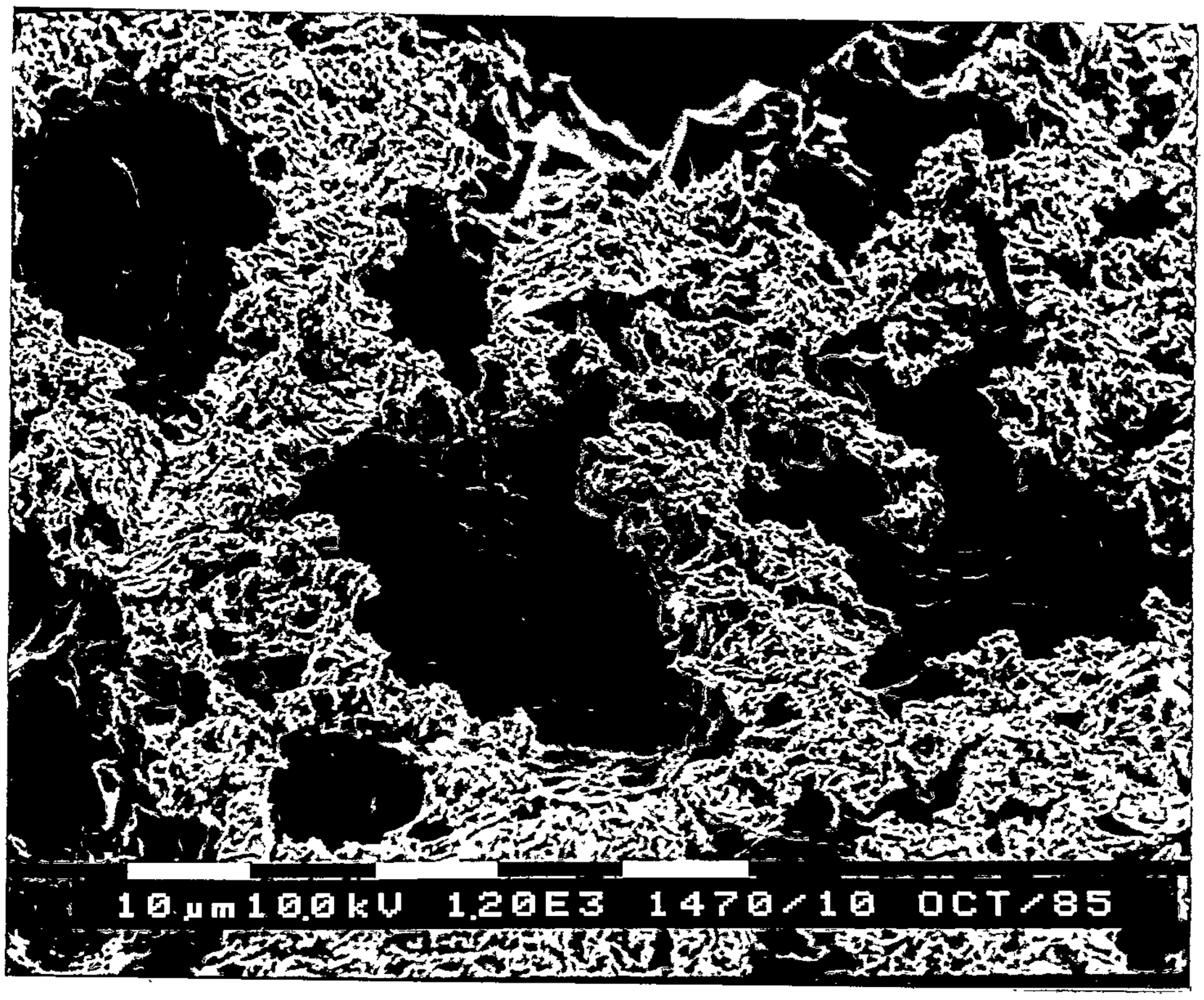

Figure 10.91c
SEM of the Microbond NP^2 specimen depicted in Figure 10.91 a,b at higher magnification (X 1200).

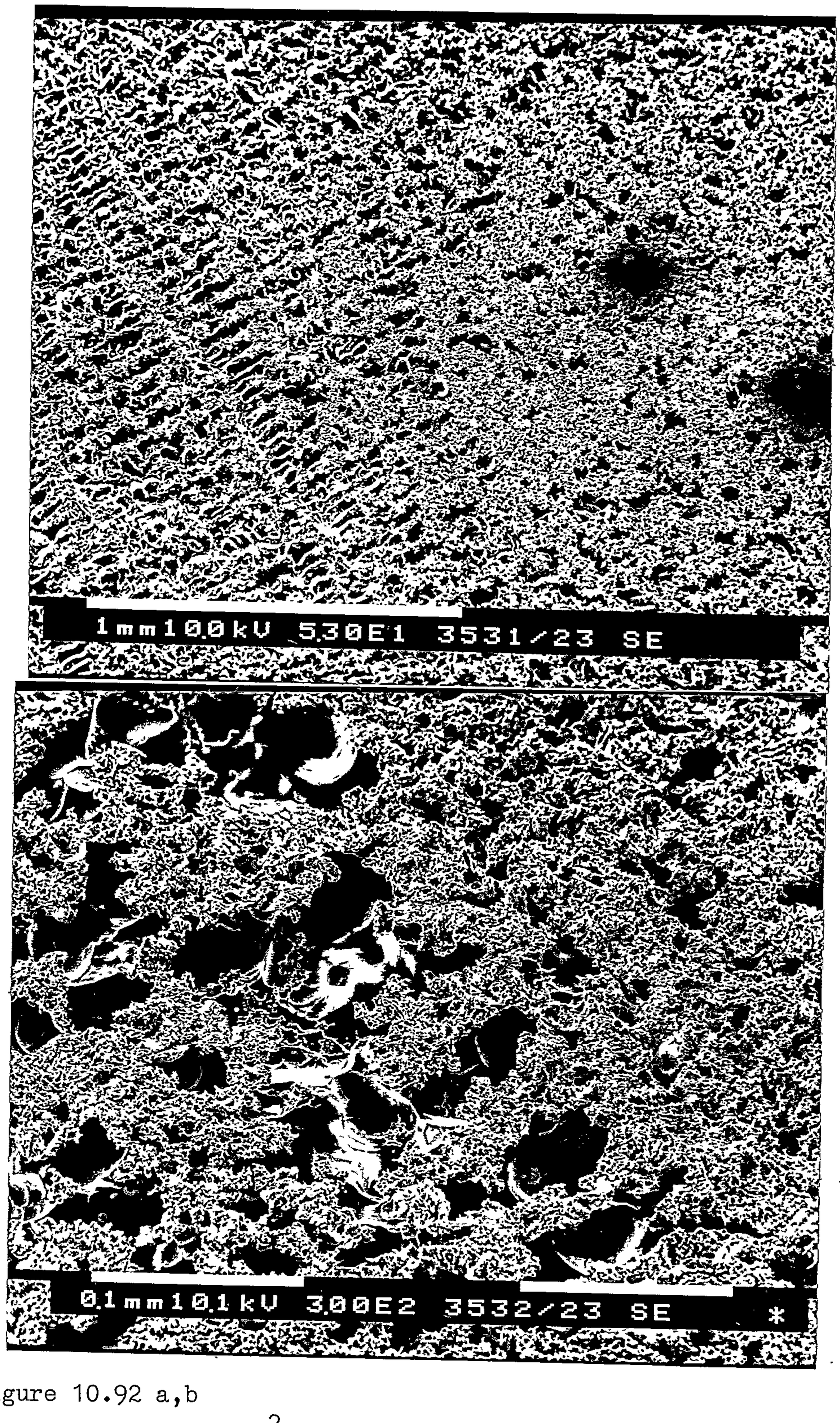

10.92a
(X 53)

10.92b
(X 300)

Figure 10.92 a,b
SEM of a Microbond NP^2 specimen electrolytically etched under the etching conditions B,2,II immediately after the specimen had been subjected to a simulated porcelain firing. A membranous layer can be seen similar to that on the specimen depicted in Figure 10.91 a,b,c.

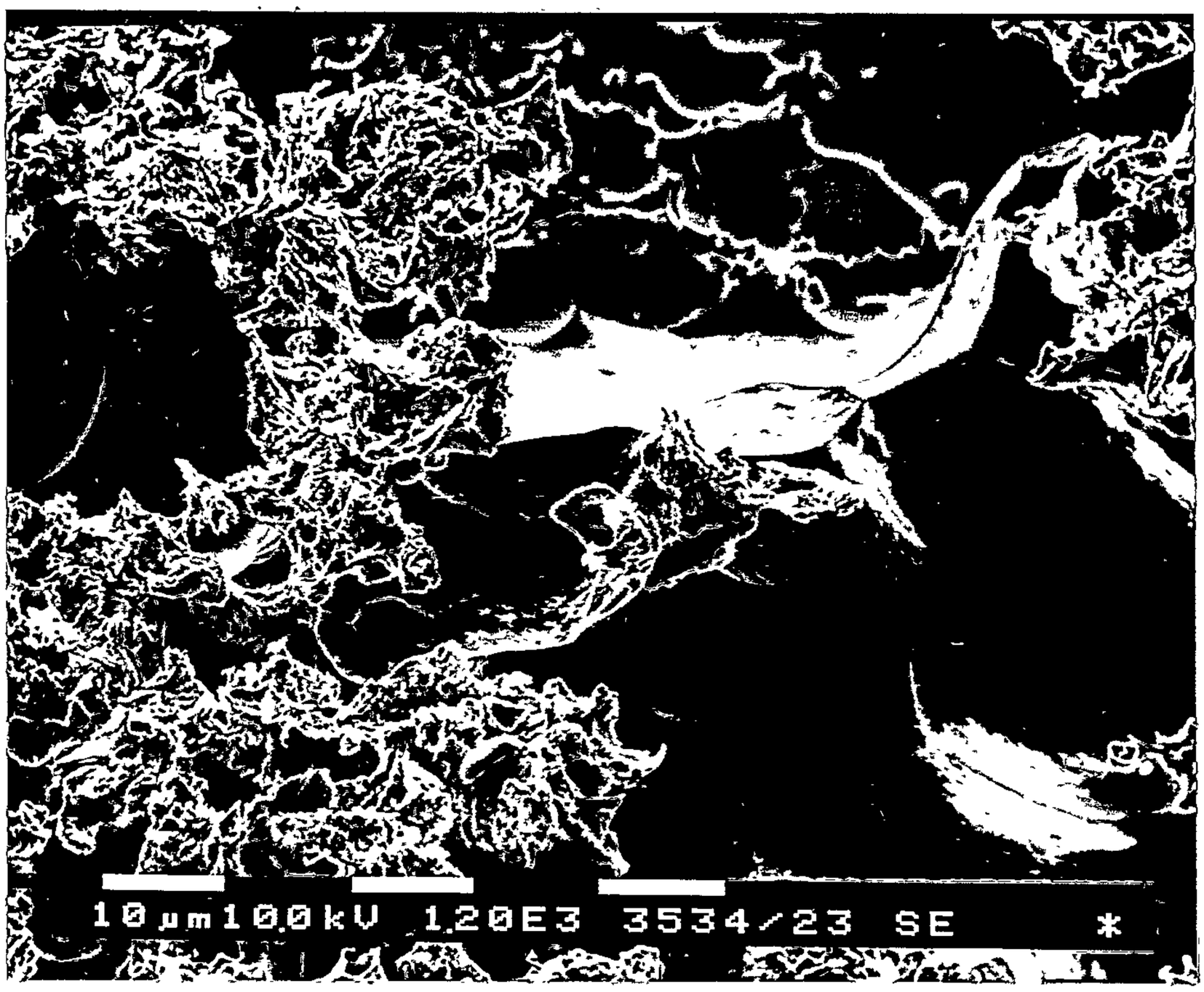

Figure 10.92 c
SEM of the Microbond NP^2 specimen depicted in Figure 10.92 a,b at higher magnification (X 1200).

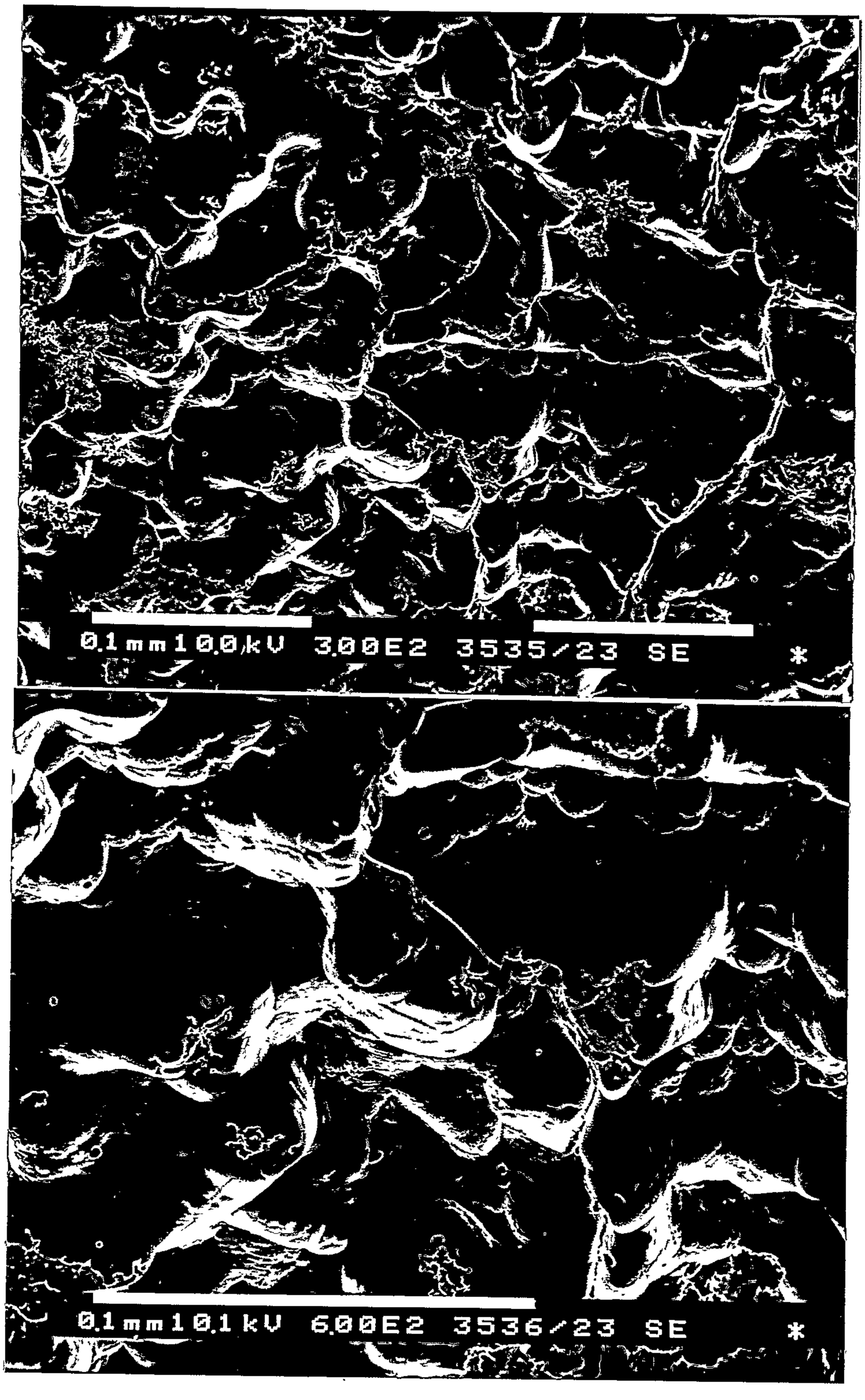

10.93a.
(X 300)

10.93b
(X 600)

Figure 10.93 a,b
SEM of another area of the Microbond NP^2 specimen depicted in Figure 10.92. No membranous layer can be seen.

10.94a
(X 287)

10.94b

FIgure 10.94 a,b
SEM of the Microbond NP^2 specimen depicted in Figure 10.93 and electrolytically etched under the same etching conditions (B,2,II) but without the simulated porcelain firing just prior to the etching procedure.

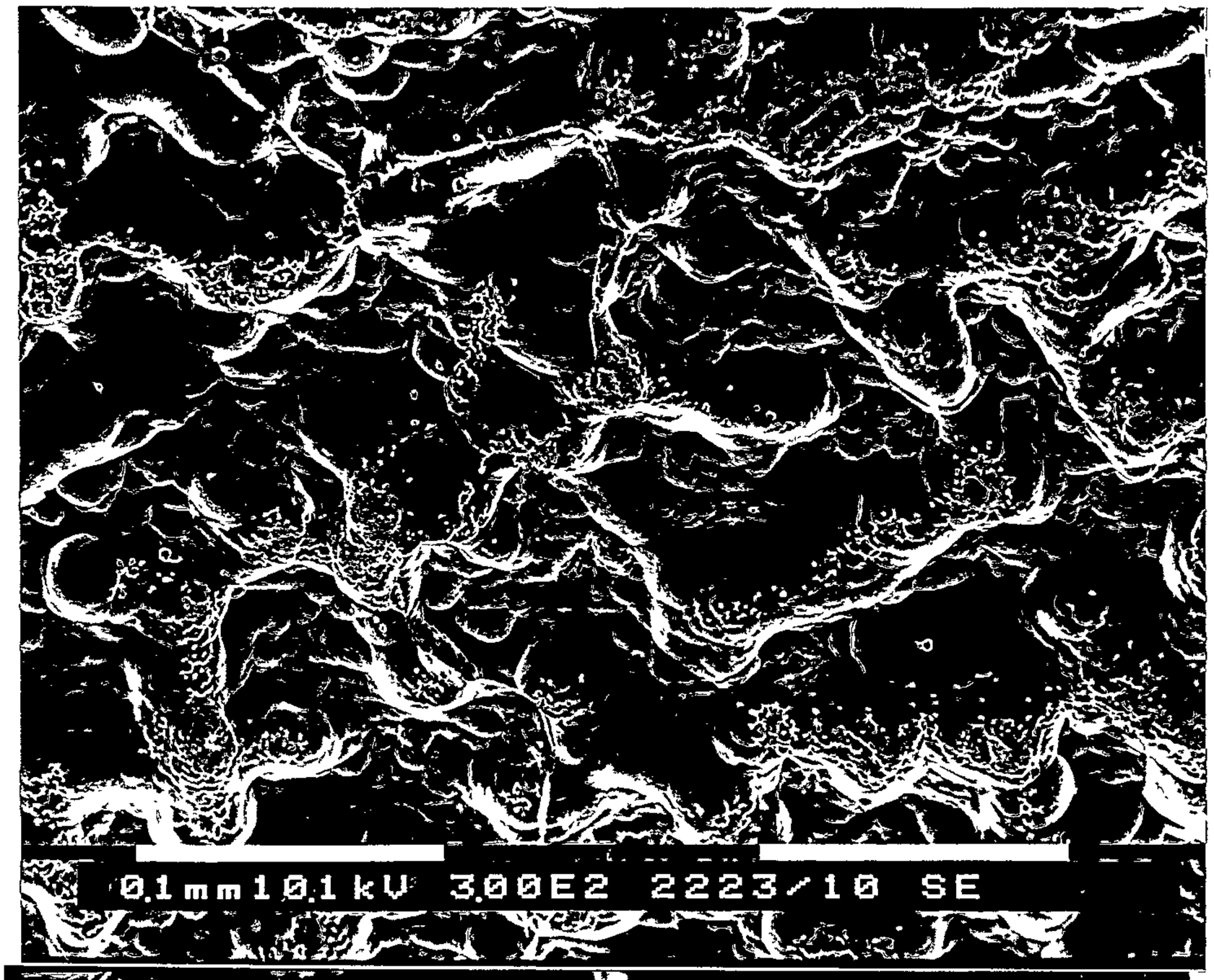

10.95a
(X 300)

10.95b
(X 1200)

Figure 10.95 a,b
SEM of a Microbond NP^2 specimen electrolytically etched under the etching conditions B,2,II for the second time. Specimen coded No.1. Tensile bond strength = 4.84 MPa.

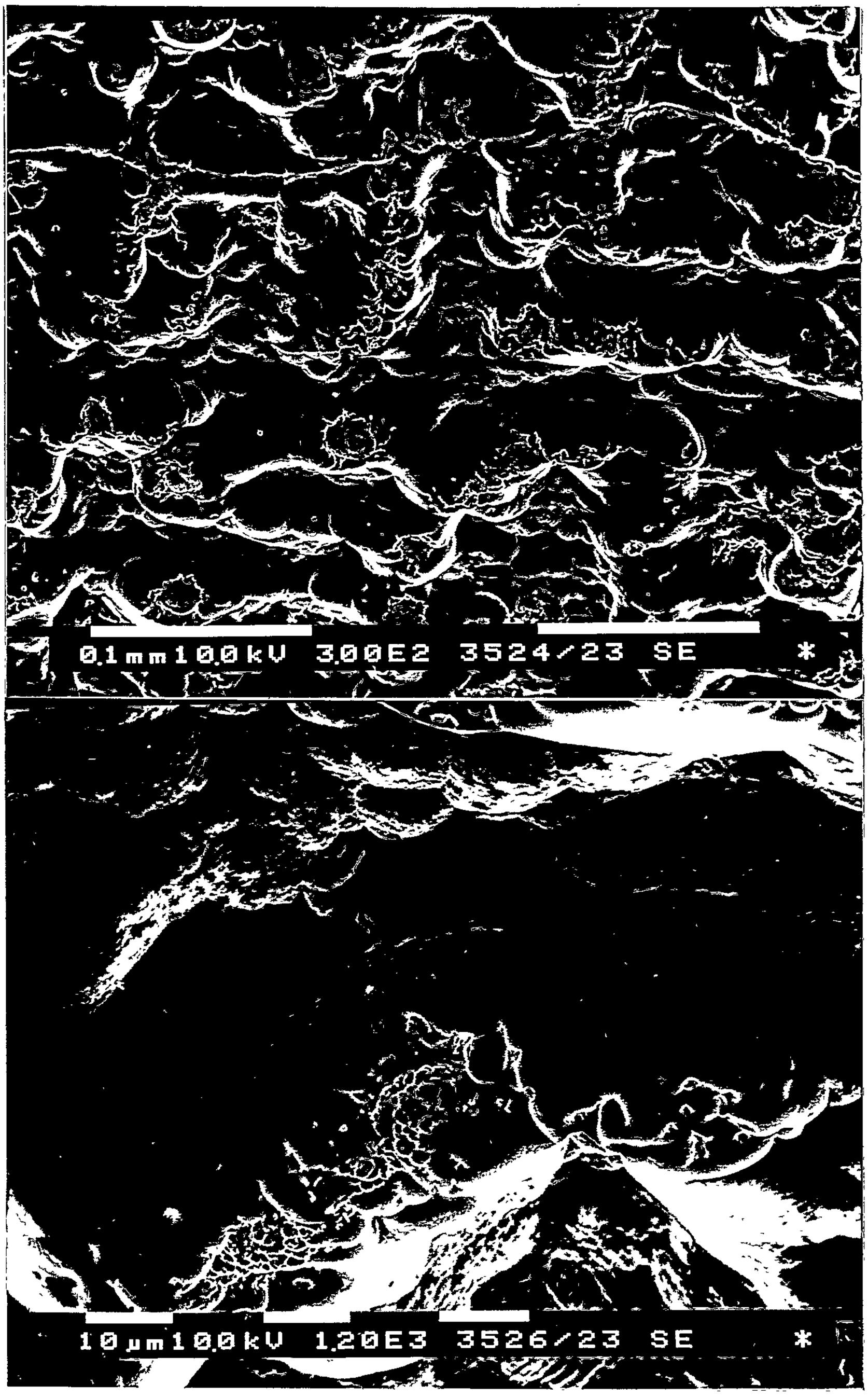

10.96a
(X 300)

10.96b

Figure 10.96 a,b
SEM of the Microbond NP^2 specimen depicted in Figure 10.95 and electrolytically etched under the same etching conditions, but for the third time. No obvious differences can be seen. This specimen failed to survive thermal-cycling.

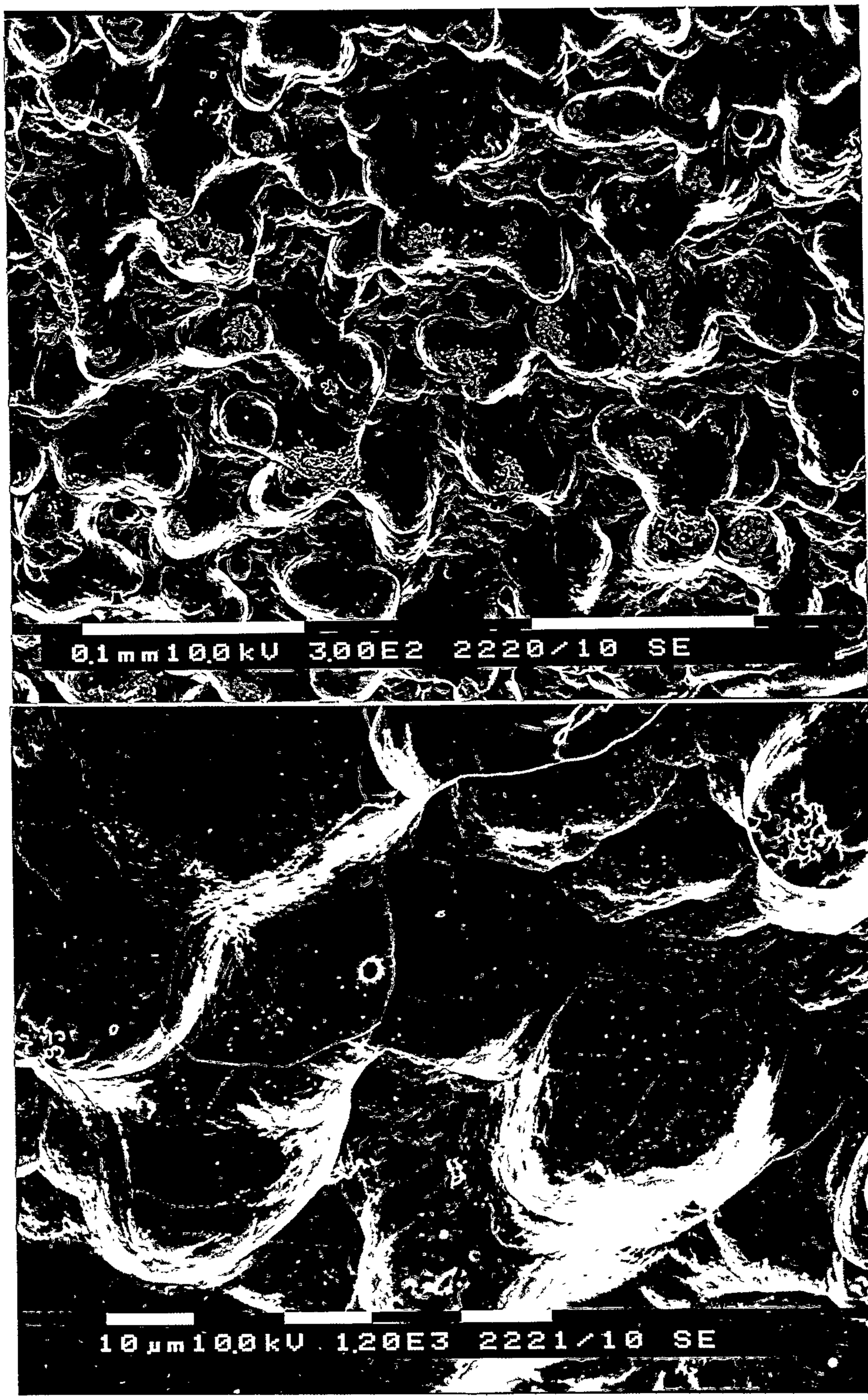

10.97a
(X 300)

10.97b
(X 1200)

Figure 10.97 a,b
SEM of a Microbond NP^2 specimen electrolytically etched under the etching conditions B,2,II for the second time. Specimen coded No. 2. This specimen failed to survive thermal-cycling.

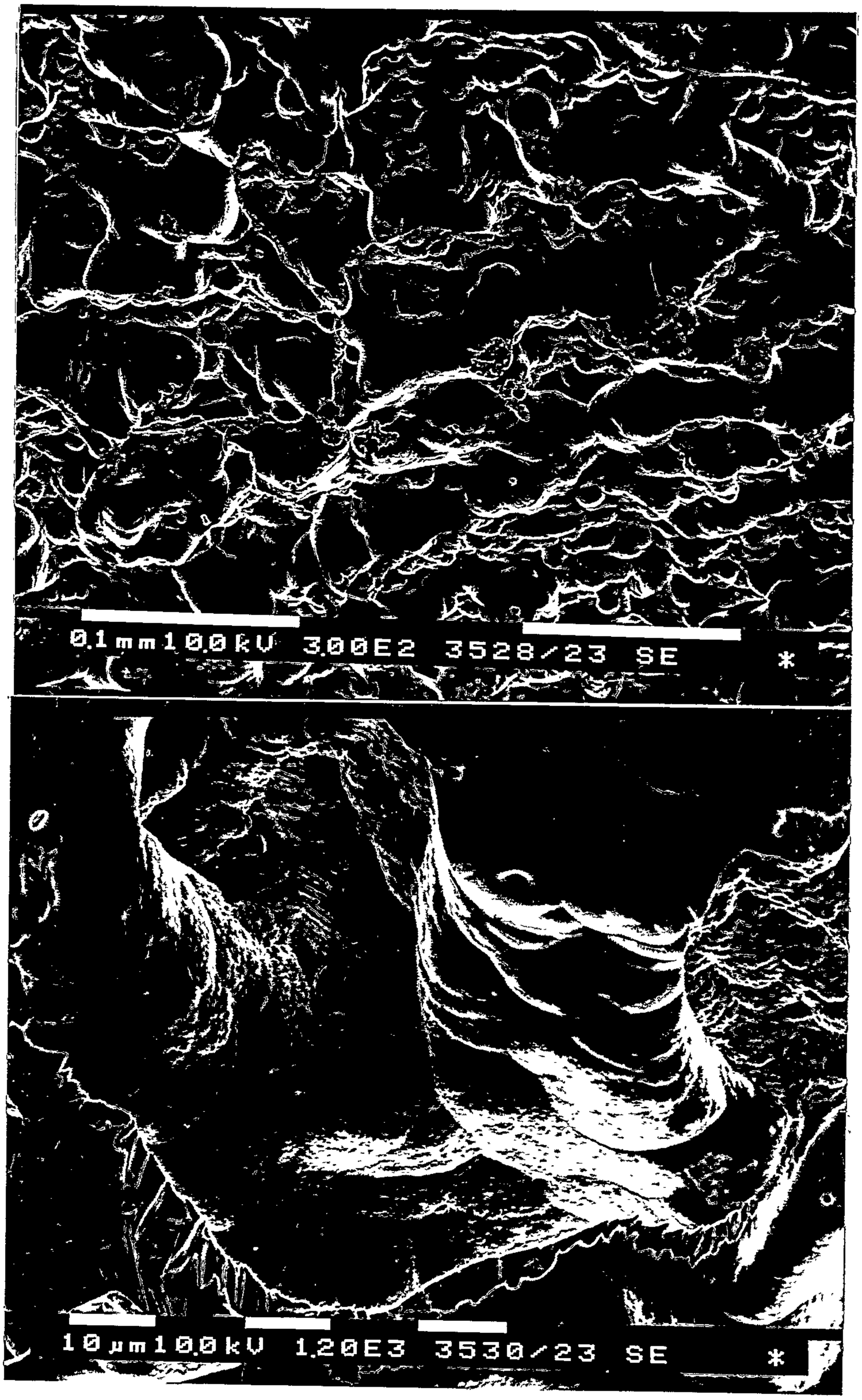

10.98a
(X 300)

10.98b
(X 1200)

Figure 10.98 a,b
SEM of the same Microbond NP^2 specimen depicted in Figure 10.97 and electrolytically etched under the same conditions (B,2,II), but for the third time. Deeper valleys can be seen on this specimen with an indication of some slight undercut. Tensile bond strength = 2.07 MPa.

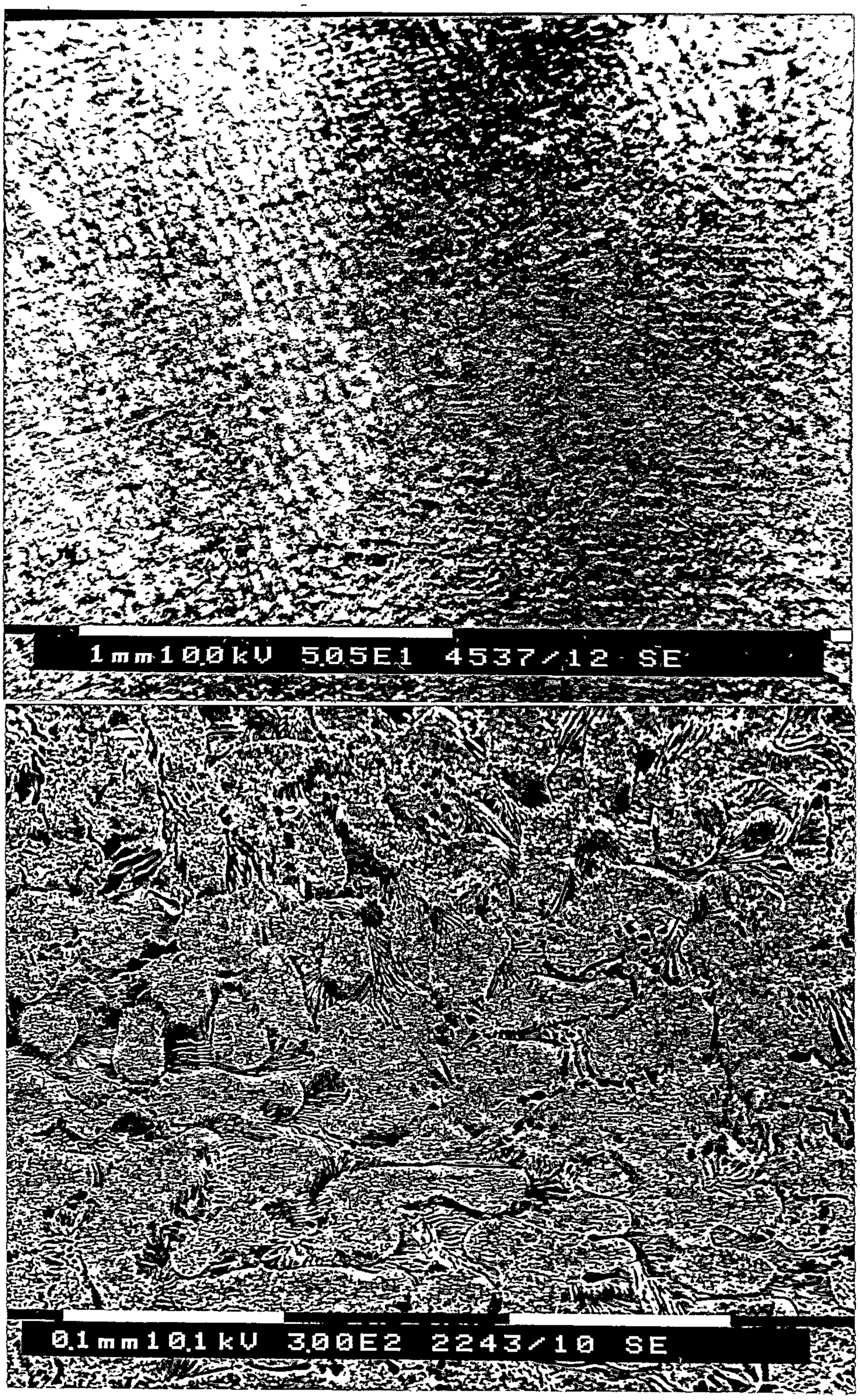

10.99a
(X 50)

10.99b
(X 300)

Figure 10.99 a,b
SEM of the Rexillium III specimen electrolytically etched under the manufacturer's recommended etching conditions (third etch).

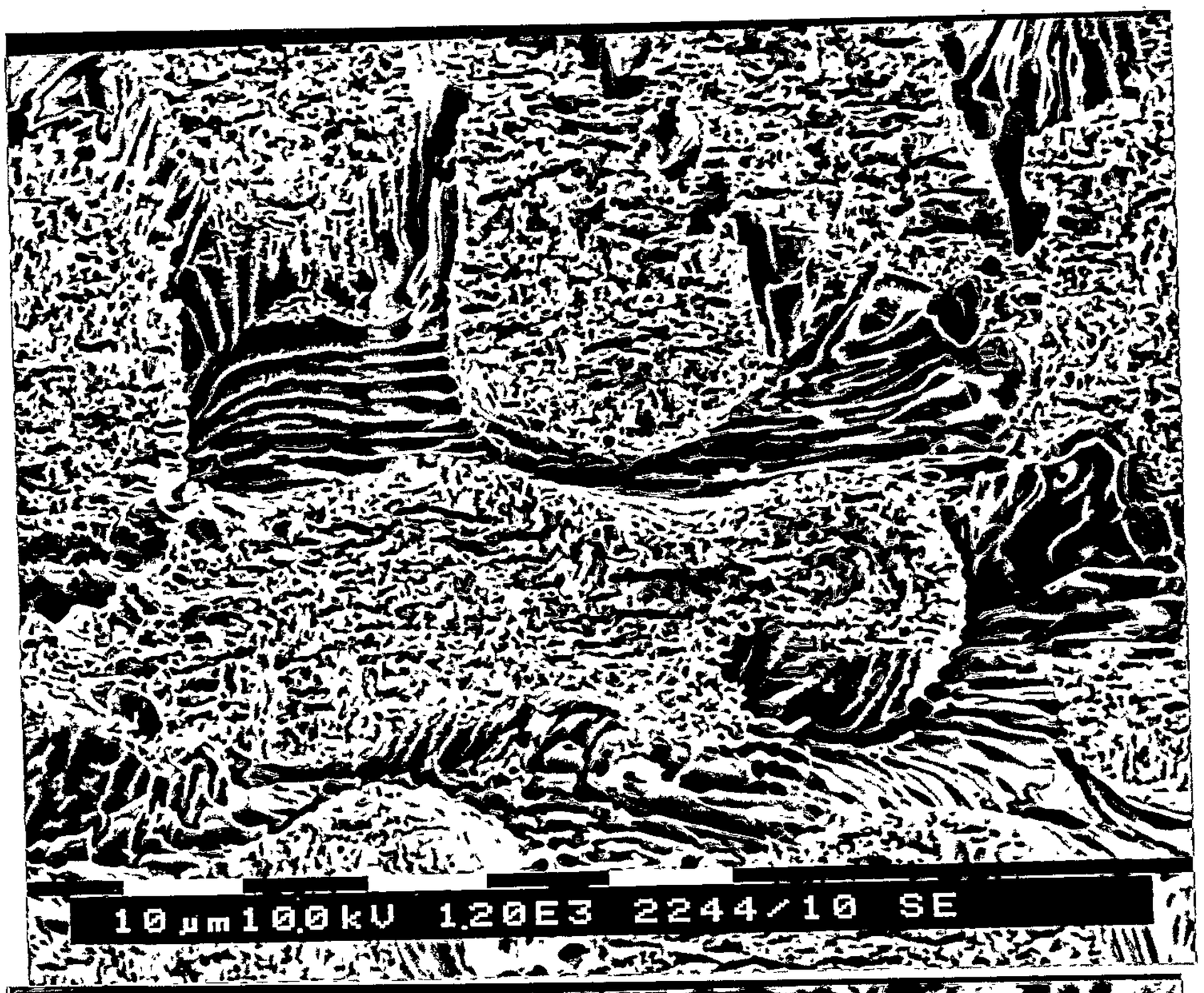

10.99c
(X 1200)

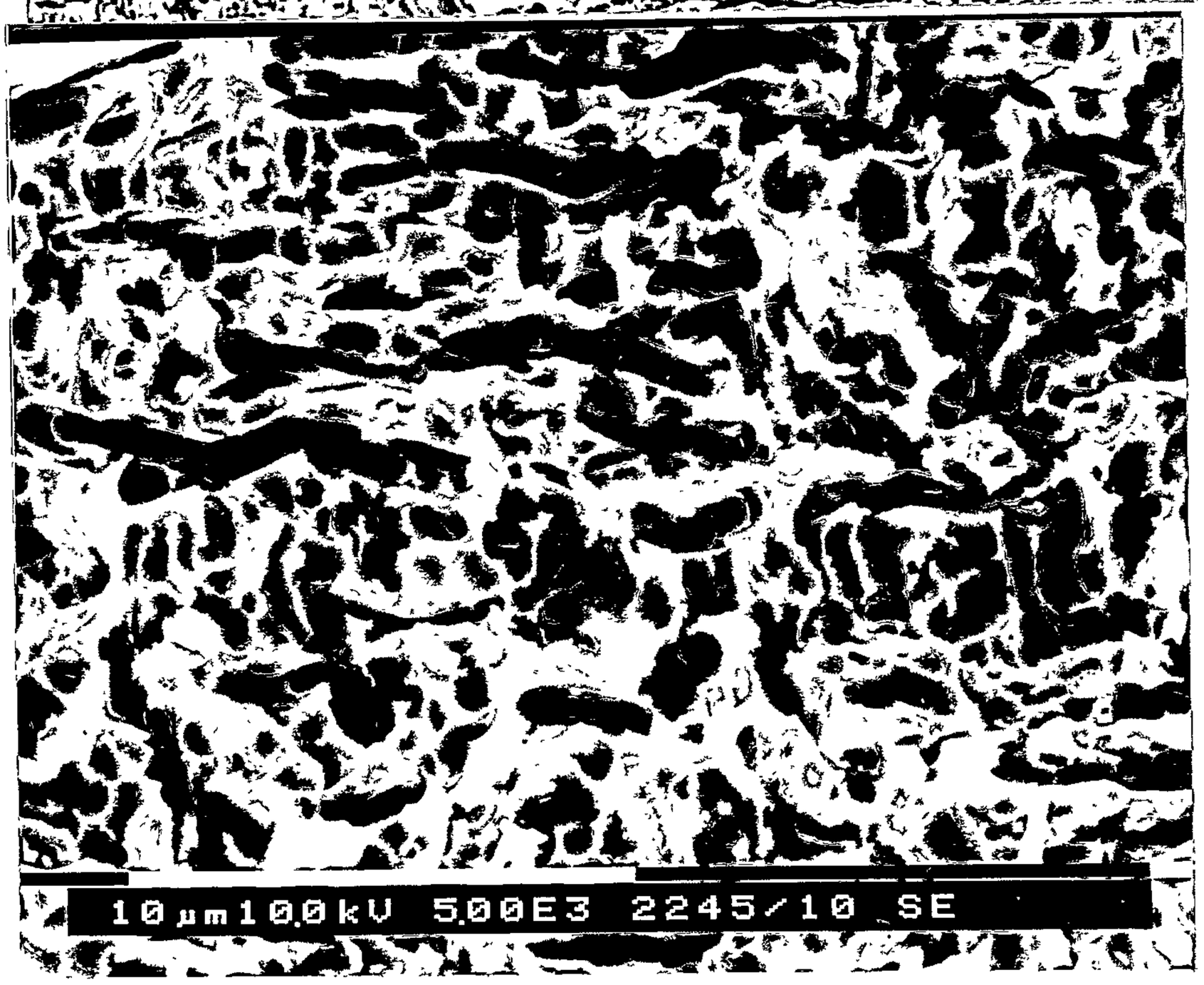

10.99d
(X 5000)

Figure 10.99 c,d
SEM of the Rexillium III specimen depicted in Figure 10.99 a,b at higher magnification.

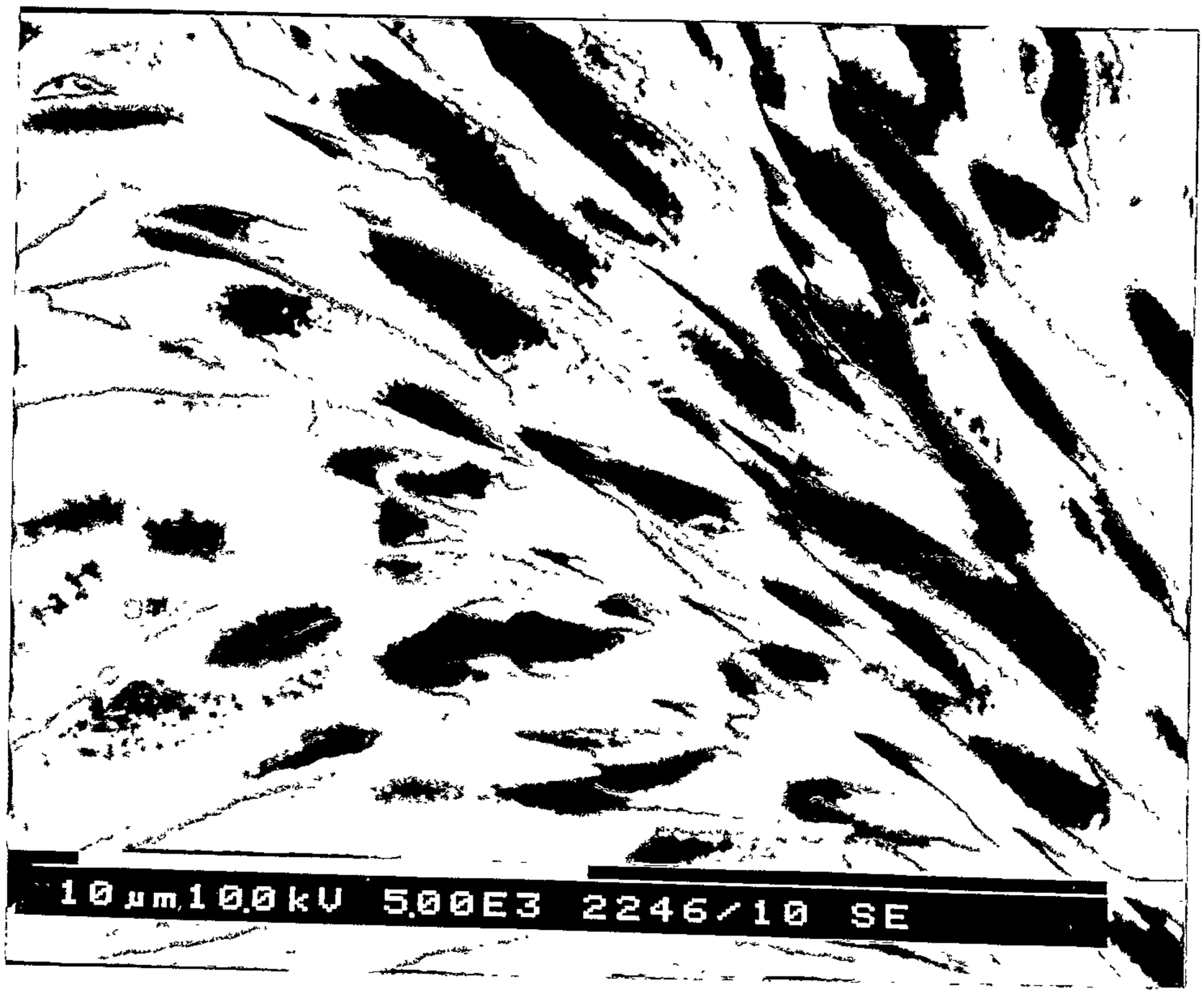

Figure 10.99e
SEM of the Rexillium III specimen depicted in Figure 10.99 a,b, and 10.99 c,d (X 5000).

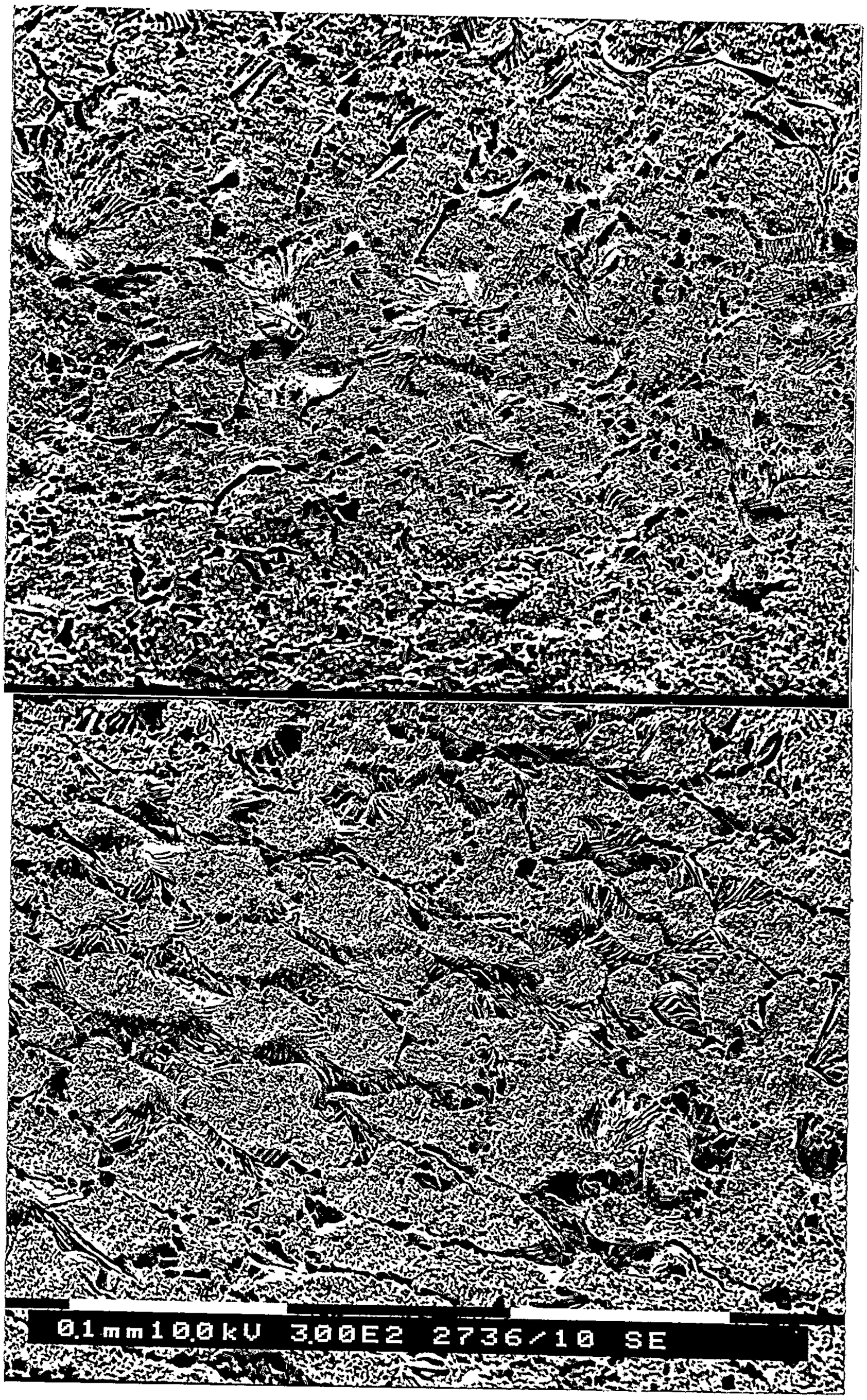

10.100a
(X 300)

10.100b
(X 300)

Figure 10.100 a,b
SEM of the Rexillium III specimen electrolytically etched under the recommended etching conditions. Figure 10.100a shows the second etch and Figure 10.100b shows the fifth etch. The surface topography is very similar on both examples.

10.101a
(X 1200)

10.101b
(X 1200)

Figure 10.101 a,b
SEM of the Rexillium III specimen electrolytically etched under the recommended etching conditions. Figure 10.101a shows the second etch and Figure 10.101b shows the fifth etch. The surface topography is very similar on both examples

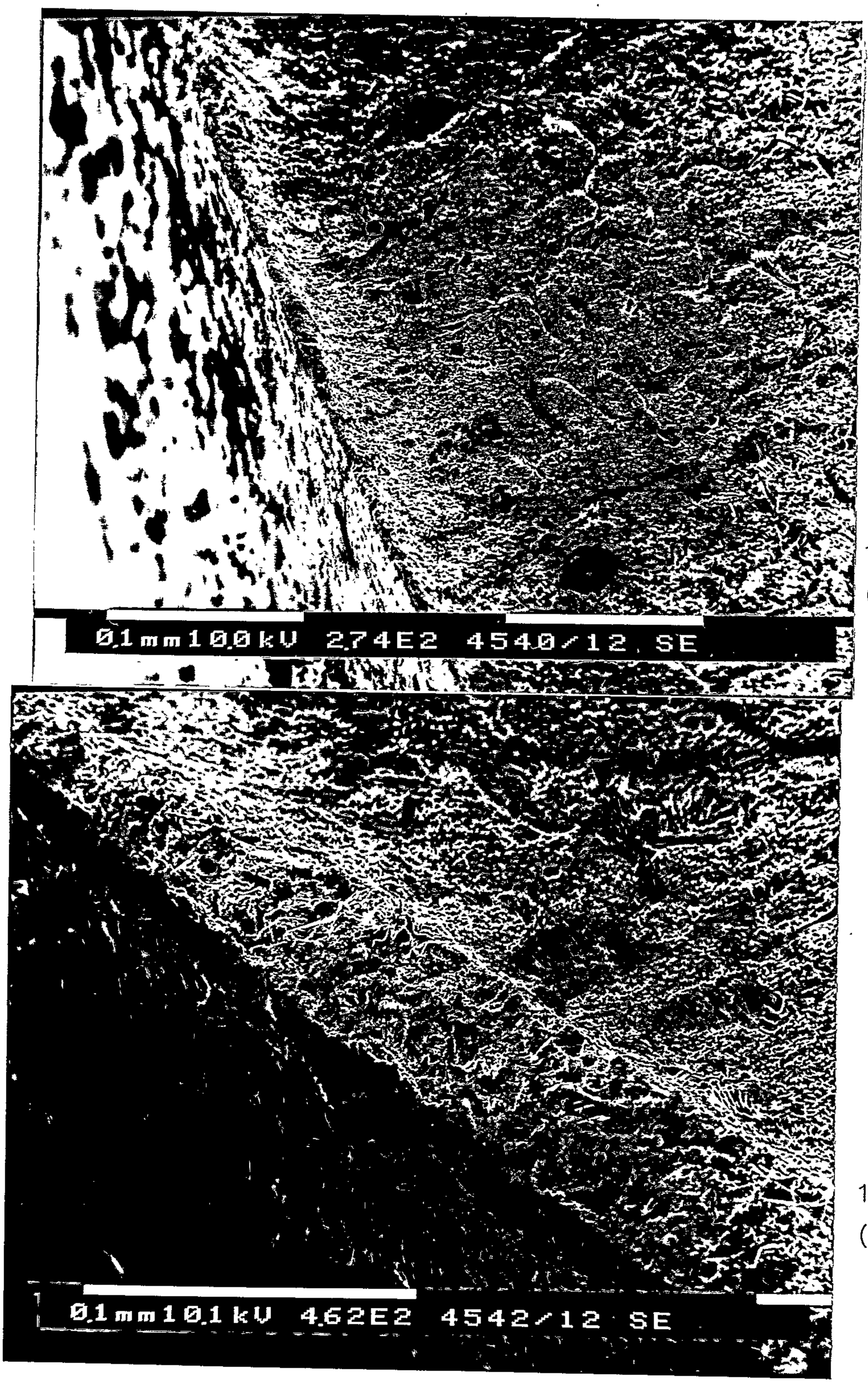

10.102a
(X 274)

10.102b
(X 462)

Figure 10.102 a,b
SEM of the Rexillium III specimen showing the periphery of the electrolytically etched surface from two different etches. Note the lack of peripheral ditching seen on the specimens of Microbond NP^2 (Figure 10.39).

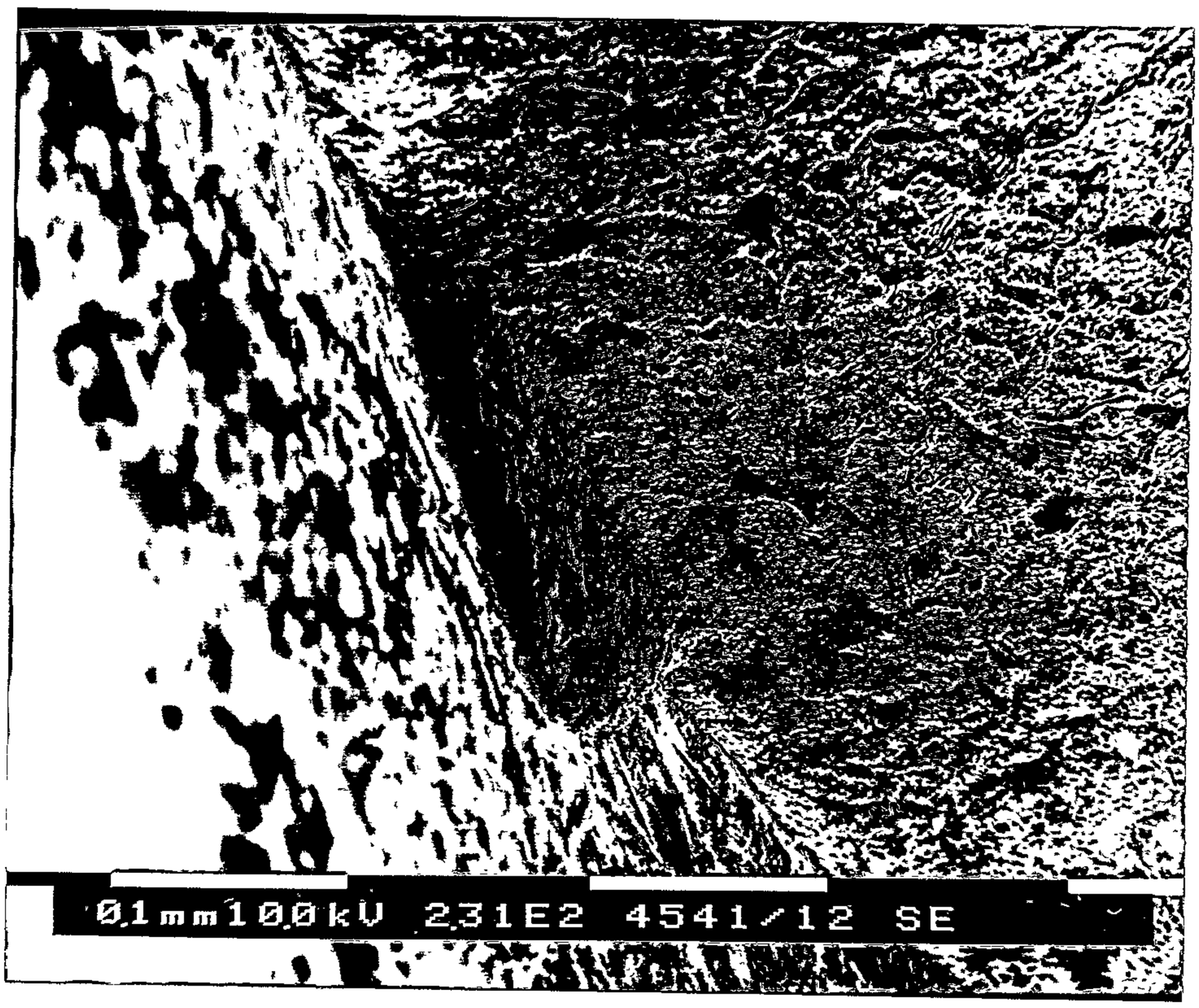

Figure 10.102c

SEM of the Rexillium III specimen showing the periphery of the specimen and an area that has not been completely masked during the etching process (X 287). A similar area was seen on some Microbond NP^2 specimens (Figure 10.39c).

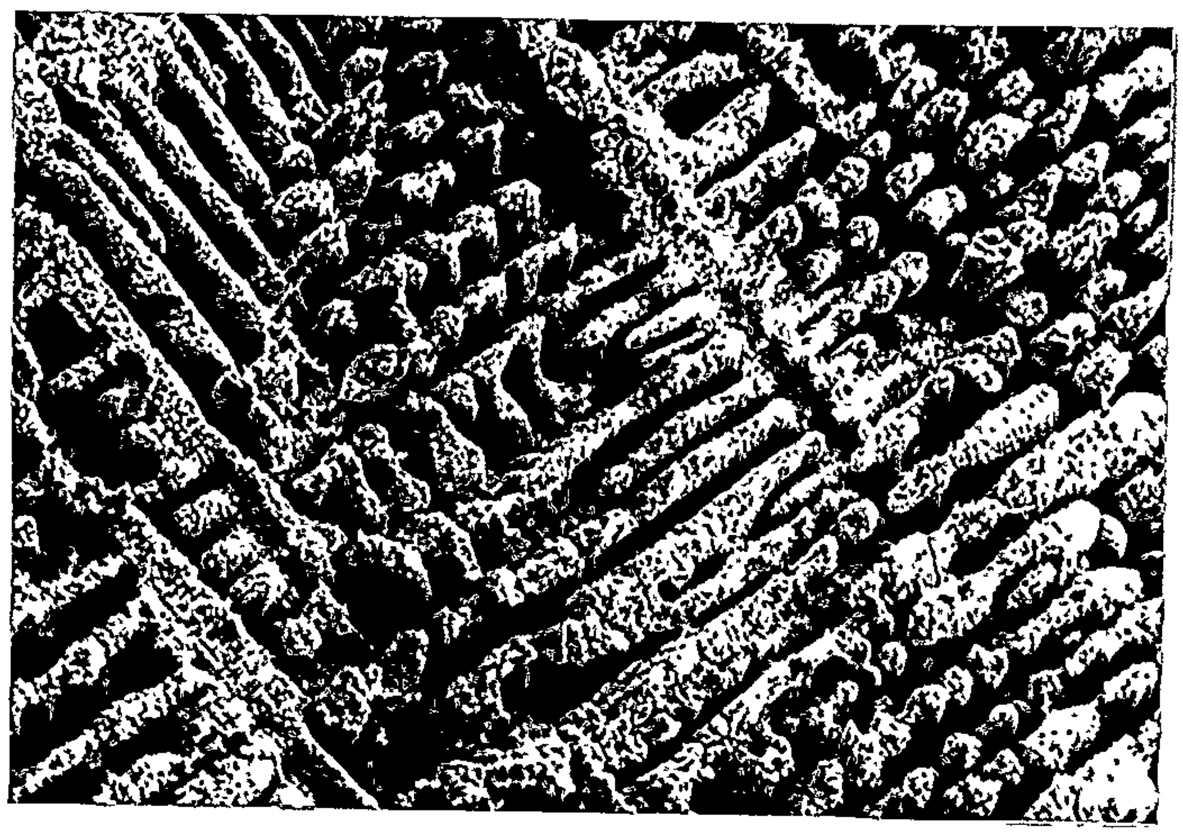

Figure 10. 103a
SEM of Rexillium III alloy electrolytically etched under the manufacturer's recommended etching conditions as published by Simonsen et al (1983) (X 500). The surface configuration is not similar to that observed on the Rexillium III specimen used in this study.

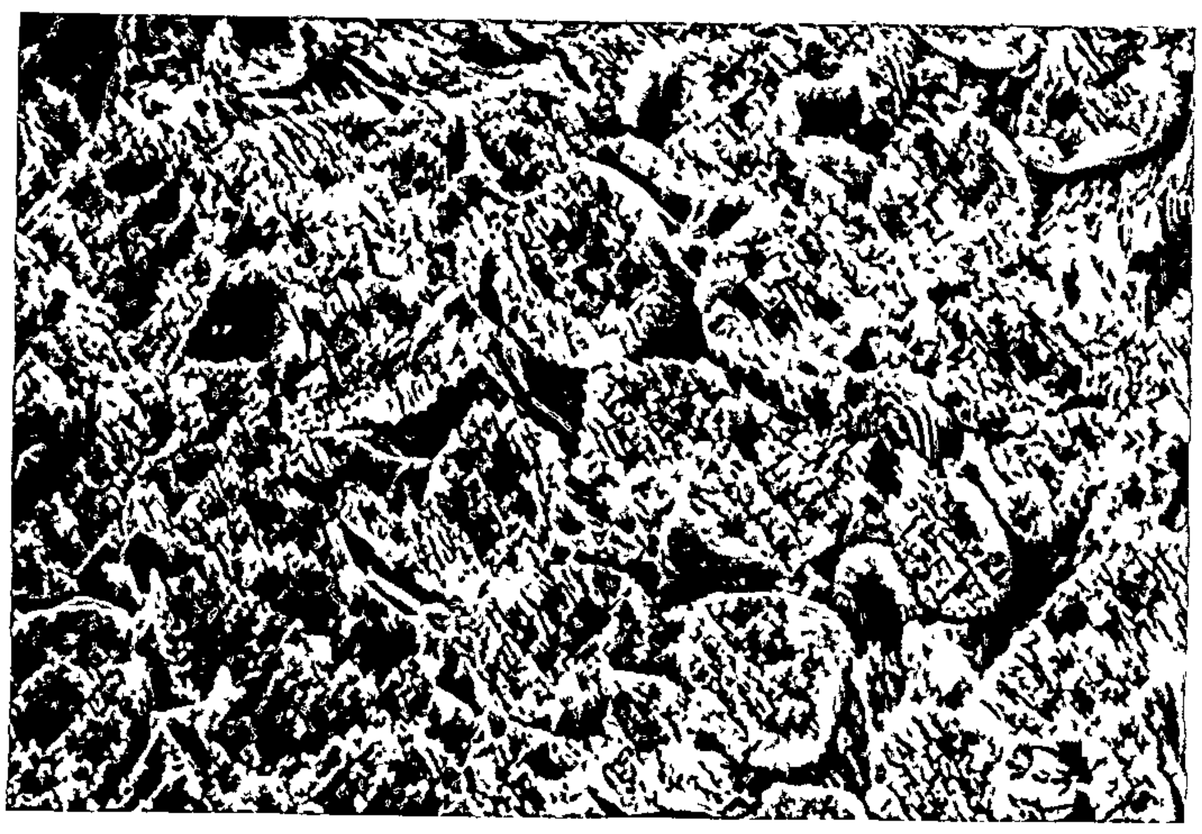

Figure 10.104
SEM of re-cast Rexillium III alloy electrolytically etched under the manufacturer's recommended etching conditions as published by Simonsen et al (1983) (X 2000). The surface configuration of this specimen is similar to that observed on the Rexillium III specimen used in this study (Figures 10.99-10.102).

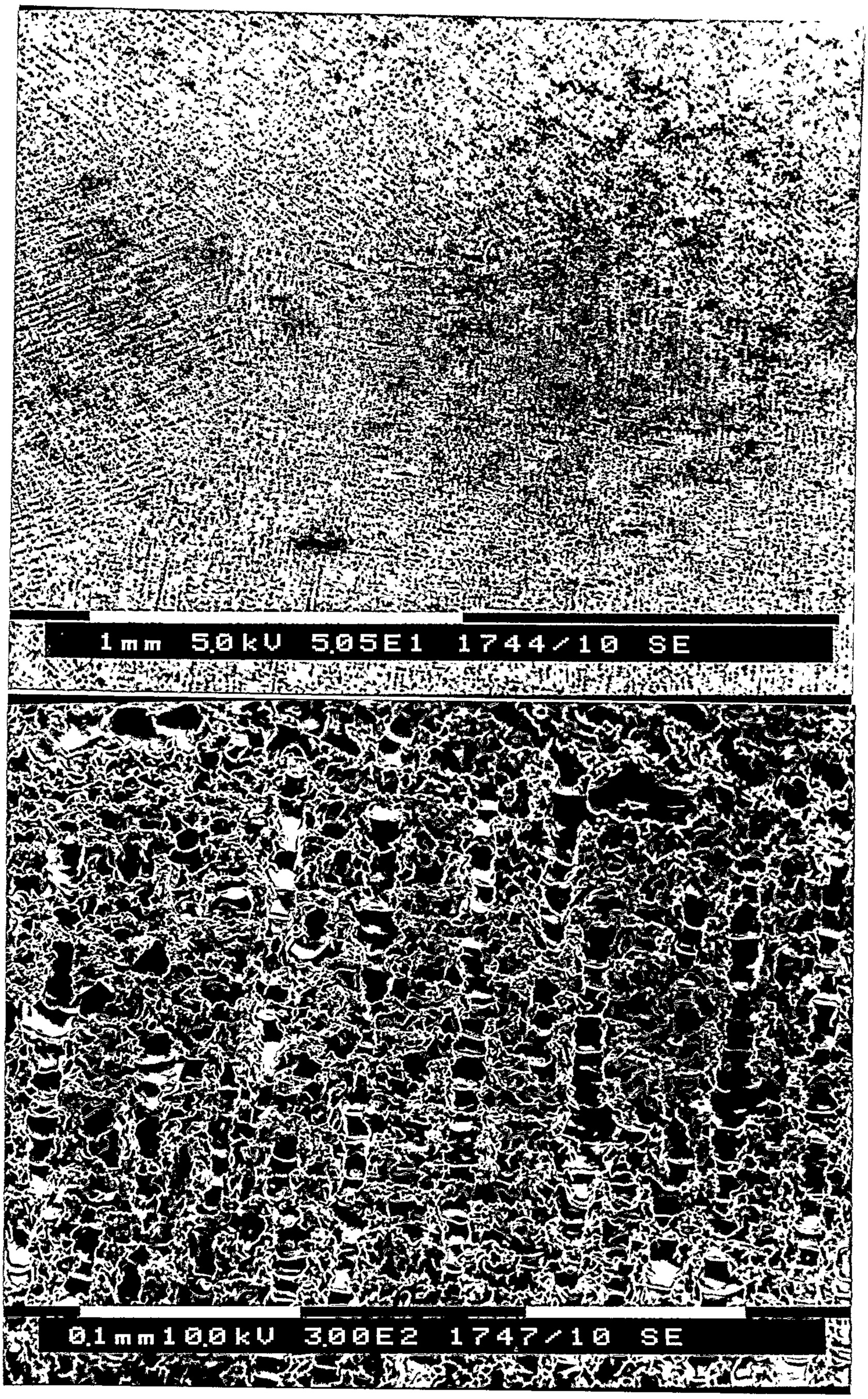

10.105a
(X 50)

10.105b
(X 300)

Figure 105 a,b
SEM of a specimen of Biobond II alloy electrolytically etched under the manufacturer's recommended etching conditions.

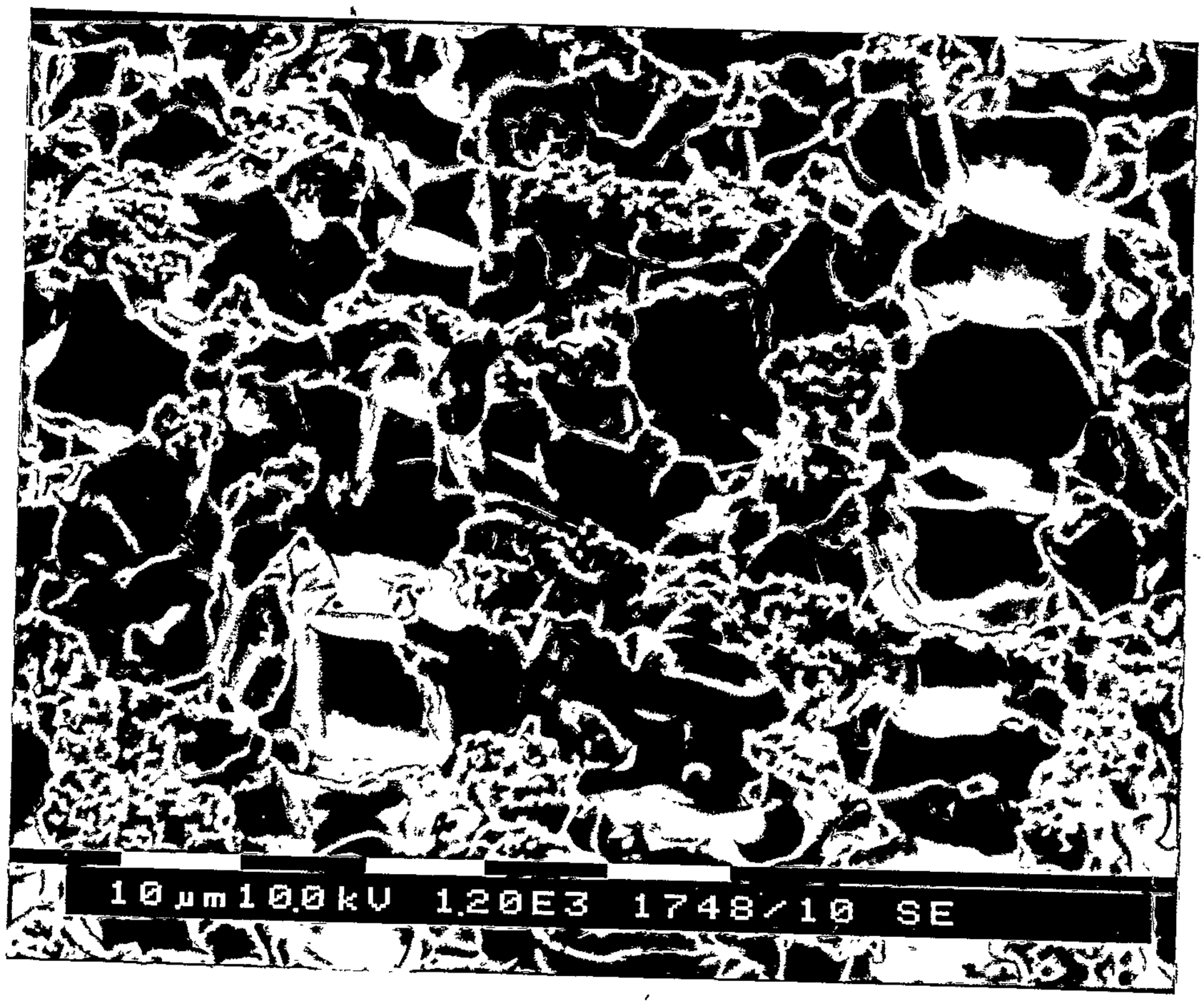

Figure 10.105c -
SEM of the specimen of Biobond II alloy depicted in Figure 10.105 a,b at higher magnification (X 1200).

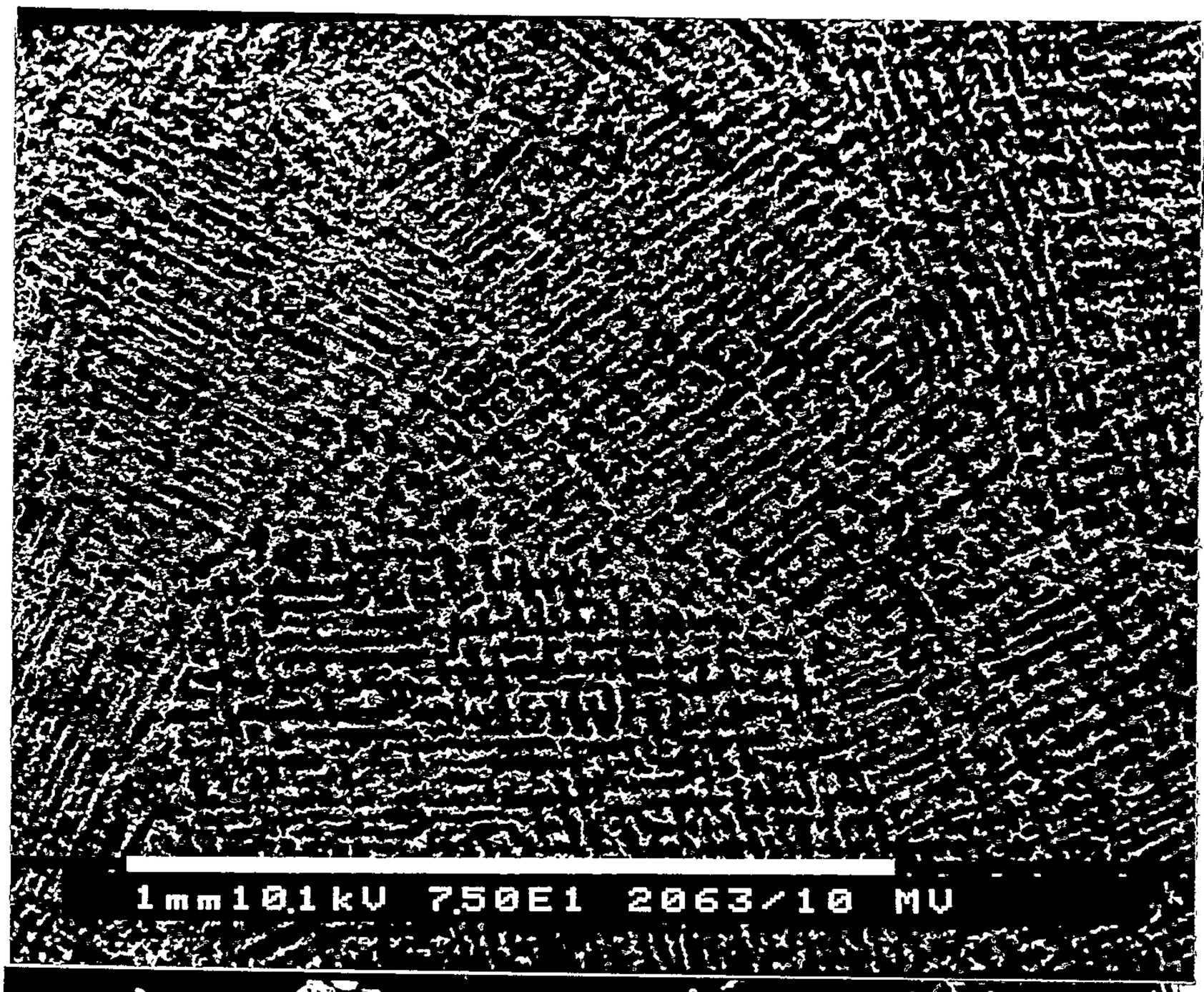

10.106a
(X 75)

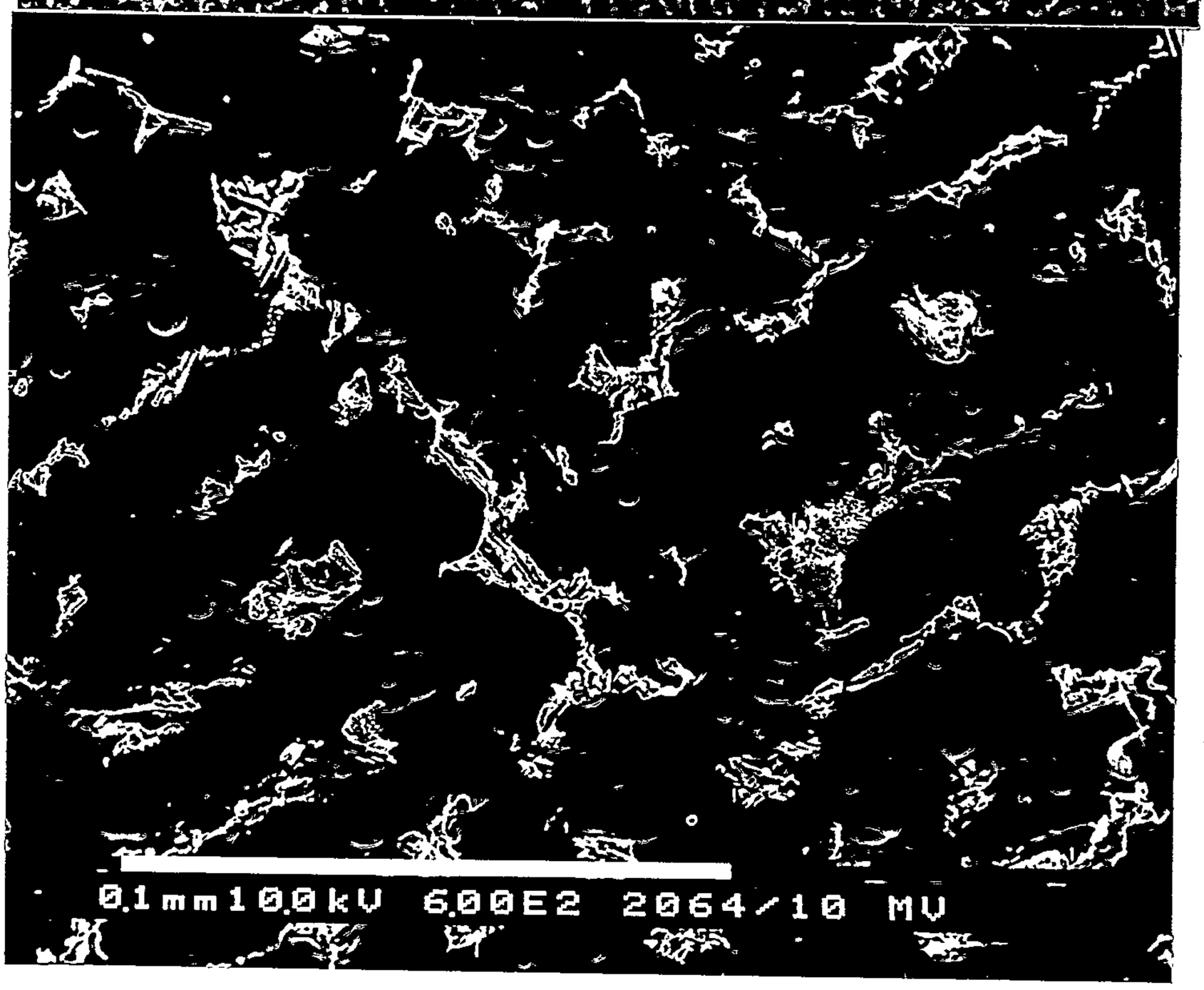

10.106b
(X 600)

Figure 10.106 a,b
SEM of a specimen of the alloy Durabond electrolytically etched under the manufacturer's etching conditions. There is a total lack of mechanically retentive surfice configurations.

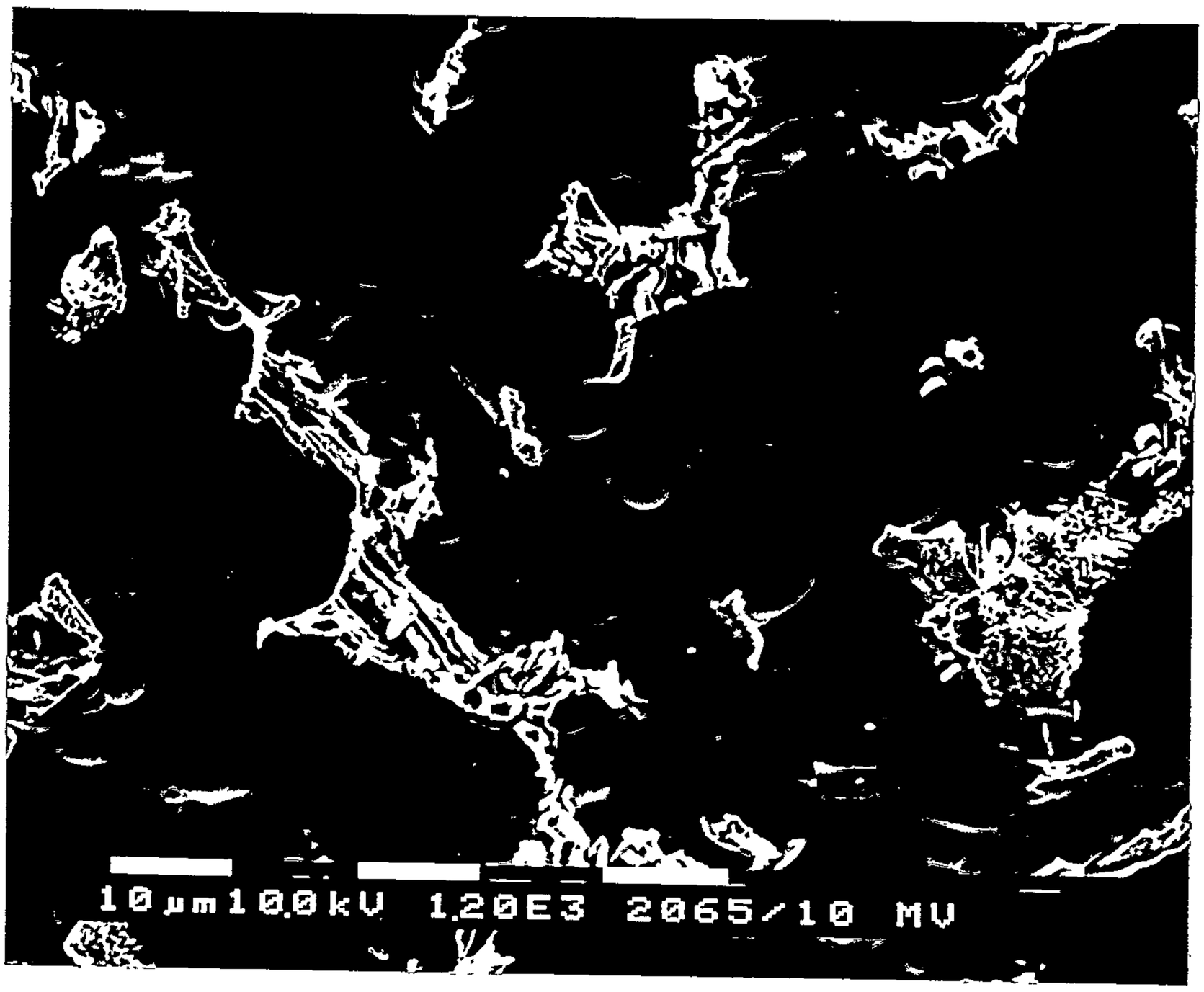

Figure 10.106c
SEM of the Durabond specimen depicted in Figure 10.106 a,b at higher magnification (X 1200).

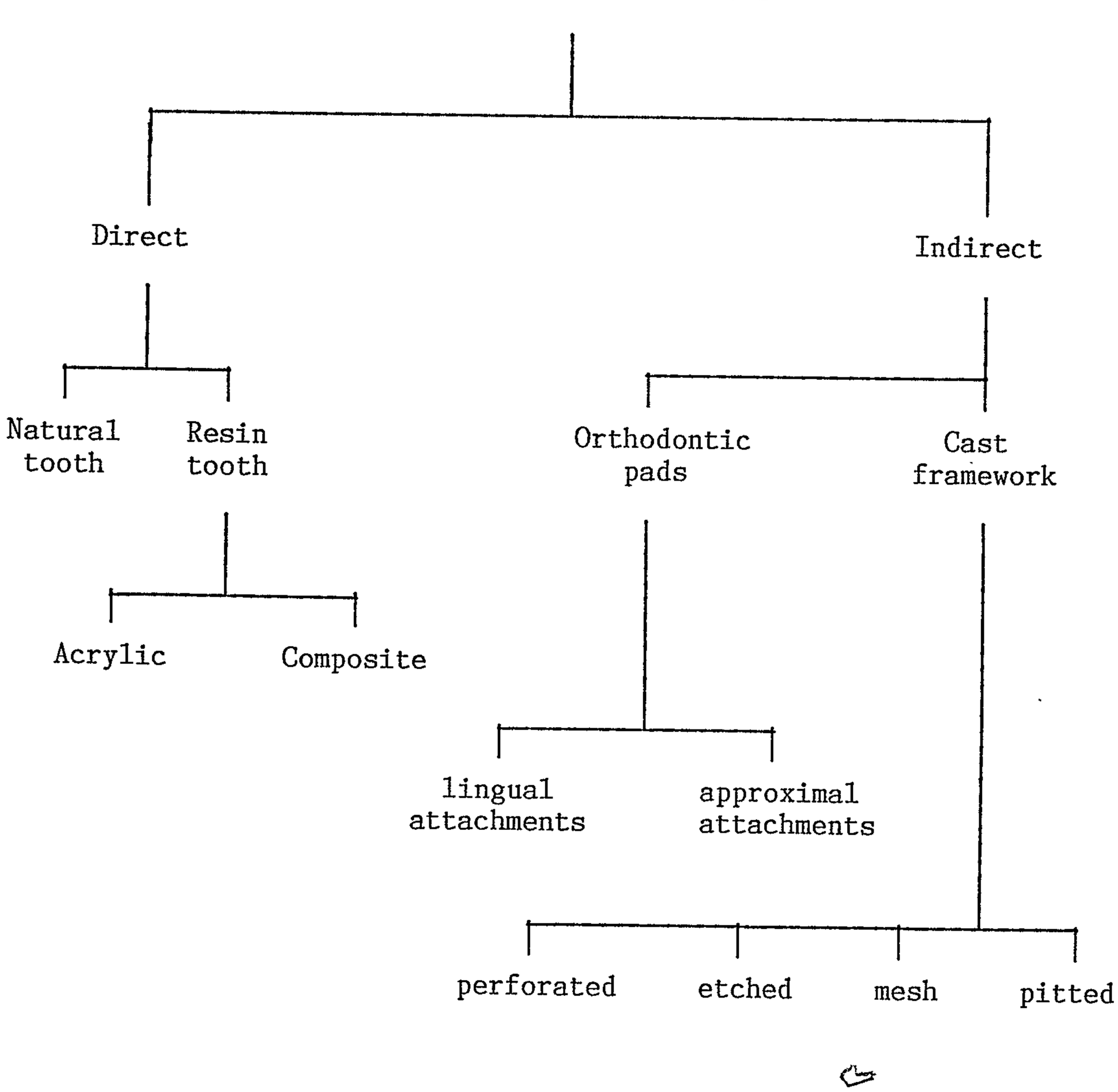

Figure 11.1: A classification of resin bonded bridges. (from Tay, 1986)

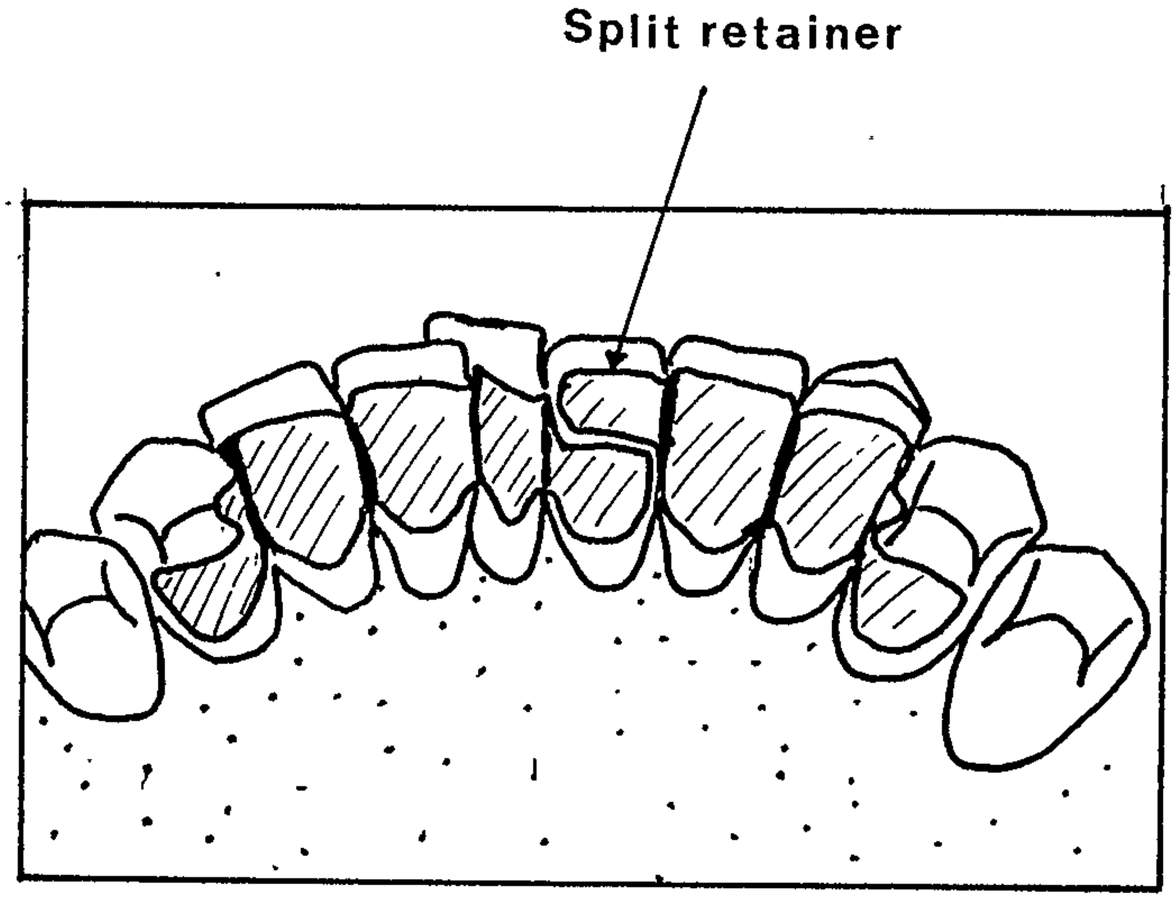

Figure 11.2
Diagrammatic representation of split retainer design for a cast-metal resin bonded periodontal splint (from Rosthchild, 1985).

UNIVERSITY
OF LEEDS
DENTAL LIBRARY